POLITECNICO DI MILANO

Facoltà di Ingegneria dei Processi Industriali

Corso di Laurea Specialistica in Ingegneria Elettrica

Dipartimento di Elettrotecnica

EXPENSION VAR PLANNING IN A MESHED/MIXED AC/DC NETWORK:

The Celtic Offshore Grid

Relatore: Prof. ALBERTO BERIZZI

Correlatori: Ing. CRISTIAN BOVO

Ing. ANDREA MANSOLDO

Tesi di Laurea Specialistica di:
MICHELA SORANNO
Matr. 732662

Anno Accademico 2011-2012

CONTENTS

ASTRATTO IN ITALIANO

Data l'importanza che cui la produzione di eolico offshore si è affermato sul panorama non solo europeo ma mondiale, grazie a buone prestazioni tecniche e competitività economica, è emerso sempre più insistente il bisogno di sfruttare al meglio questa preziosa risorsa. Fra i paesi europei soprattutto del nord, questo tema trova ampio campo di discussione, anche considerando un'ottica futura di collegamento unico dei molteplici parchi offshore che sono destinati a sorgere negli anni a venire. L'Irlanda, dal canto suo, sta elaborando analisi di pianificazione della rete con cui annettere le nuove unità generatrici offshore che sarebbero collocate prevalentemente nel mare d'Irlanda. Dagli studi fin qui effettuati tramite un programma di ottimizzazione economica per lo sviluppo della rete, avente lo scopo di selezionare fra una vasta lista di candidati quei collegamenti ottimali nel rispetto di vincoli tecnici, è emerso come la rete si sviluppi secondo una struttura magliata sia per la parte AC, con cui vengono effettuati i collegamenti tra i più vicini parchi offshore e la costa, sia per la parte HVDC che è quella con cui si coprono grandi distanze, quali ad esempio quelle che intercorrono fra l'Irlanda e la Gran Bretagna. Una rete così costituita, necessita di ulteriori studi dal punto di vista del reattivo, vista la presenza di numerosi cavi in AC e dei convertitori per la tecnologia HVDC. Il seguente lavoro di tesi si colloca a questo livello ed e' incentrato all'elaborazione di un algoritmo di ottimizzazione per far fronte all'esigenza di una pianificazione dell'installazione di reattivo a sostegno della futura espansione di rete. Il modello matematico, che è stato implementato tramite l'uso di un potente software di ottimizzazione, GAMS, è stato testato sia per una rete test e successivamente è stato applicato alla rete reale irlandese.

CHAPTER 1
INTRODUCTION

1.1.Background

The importance of wind power generation has risen along the last years so much to be considered the most important and affordable renewable energy sources with a growing which has been faster than other mainstream technologies in the word. For instance, considering another large-scale technology with relatively low carbon emissions such as the nuclear energy, Fig 1.1 compares the global development of wind energy over the 20 years from 1991 to 2010 with the development of nuclear power capacity from a similar stage of development over the 20 years from 1961 to 1980 (1).

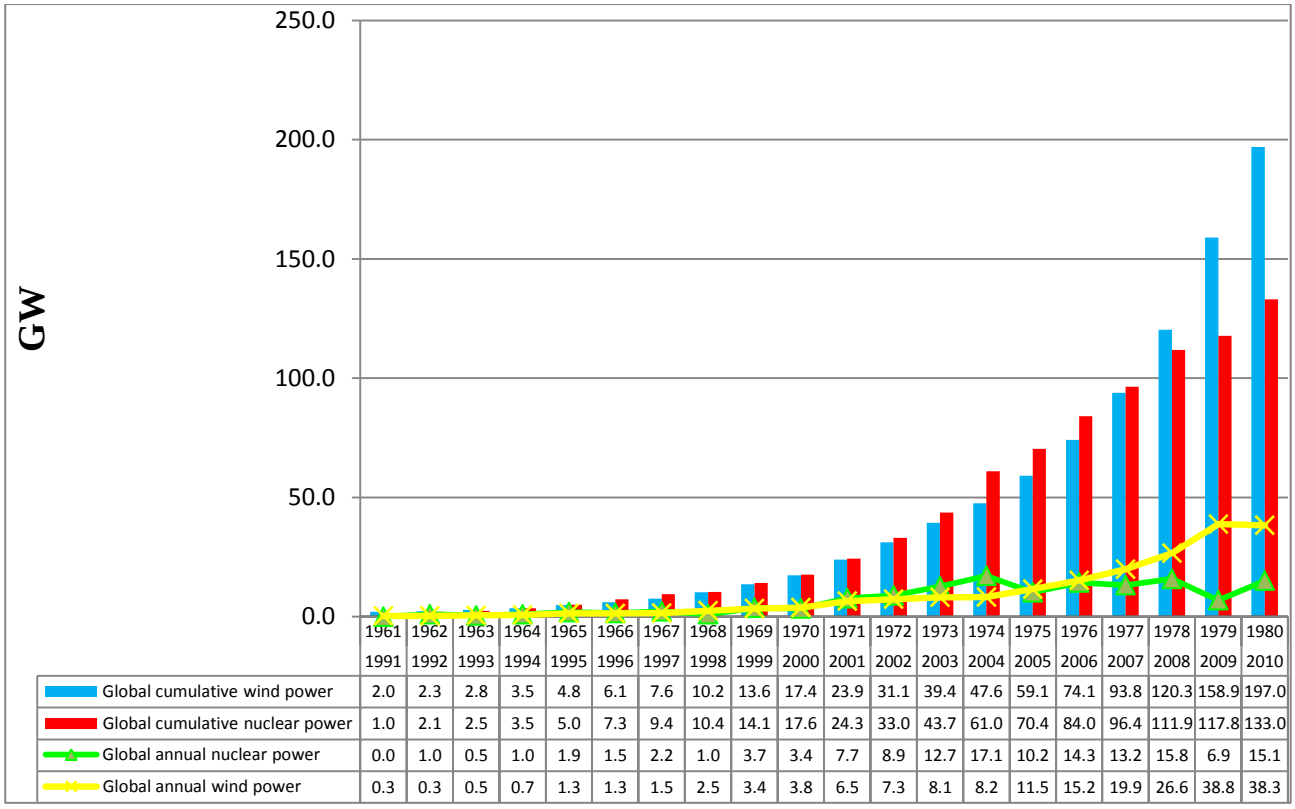

	1961 1991	1962 1992	1963 1993	1964 1994	1965 1995	1966 1996	1967 1997	1968 1998	1969 1999	1970 2000	1971 2001	1972 2002	1973 2003	1974 2004	1975 2005	1976 2006	1977 2007	1978 2008	1979 2009	1980 2010
Global cumulative wind power	2.0	2.3	2.8	3.5	4.8	6.1	7.6	10.2	13.6	17.4	23.9	31.1	39.4	47.6	59.1	74.1	93.8	120.3	158.9	197.0
Global cumulative nuclear power	1.0	2.1	2.5	3.5	5.0	7.3	9.4	10.4	14.1	17.6	24.3	33.0	43.7	61.0	70.4	84.0	96.4	111.9	117.8	133.0
Global annual nuclear power	0.0	1.0	0.5	1.0	1.9	1.5	2.2	1.0	3.7	3.4	7.7	8.9	12.7	17.1	10.2	14.3	13.2	15.8	6.9	15.1
Global annual wind power	0.3	0.3	0.5	0.7	1.3	1.3	1.5	2.5	3.4	3.8	6.5	7.3	8.1	8.2	11.5	15.2	19.9	26.6	38.8	38.3

Fig.1.1 Global wind power development (1991 – 2010) compared to nuclear development (1961-1980)

Because of technical and economical reasons, the onshore strategy has been deployed first with Denmark, Germany and Spain as leading countries (2), followed by UK and Ireland, where potential and wind conditions are among the best in Europe. Due to lack of land resources and some environmental opposition, the wind strategy is now looking at offshore installations since offshore wind farms (OWFs) would save land resources and utilize the more powerful and constant wind energy available on the ocean. Although historically the front-runner in offshore wind was still Denmark, by the end of 2010, with new offshore installations, the UK became the first country to total more than 1 GW of offshore capacity. In Europe the

issue has become important for other northern countries such as The Netherlands and Ireland. The actual state for offshore in the world is reported in Tab.1.1 (1).

	Installed in 2010	Total at end 2010
United Kingdom	458	1,341
Denmark	207	854
Netherlands	0	247
Belgium	165	195
Sweden	0	164
Germany	50	92
Finland	2	26
Ireland	0	25
Total EU	882	2,944
Norway	0	2
China	102	102
Total Word	984	3,048

Tab. 1.1: Offshore wind power (2010)

The deployment of wind resources started in Ireland in early 2000, with the first onshore installation. Through the years, the awareness that Ireland has some of the most favourable offshore wind in Europe as well as excellent tidal and wave conditions has lead to focus on a skilful use of this potential power being able to play a not marginal role in the development of the grid infrastructure required to support the growth of Ireland's power demand. In addition, in the framework for "20-20-20" EU initiative aimed at a lower carbon emission strategy , the installed wind capacity has increased steadily over the past decade, accounting for 4.4% of electricity usage in 2003 up to supply 15% of customer demand today (3). It enables Ireland to progress towards the ambitious target, mandated by the government, of having nearly 40% of the electricity consumption being generated from renewable sources by 2020, the highest goal in Europe, as it is shown in Fig.1.2 for only the contribute given by the wind.

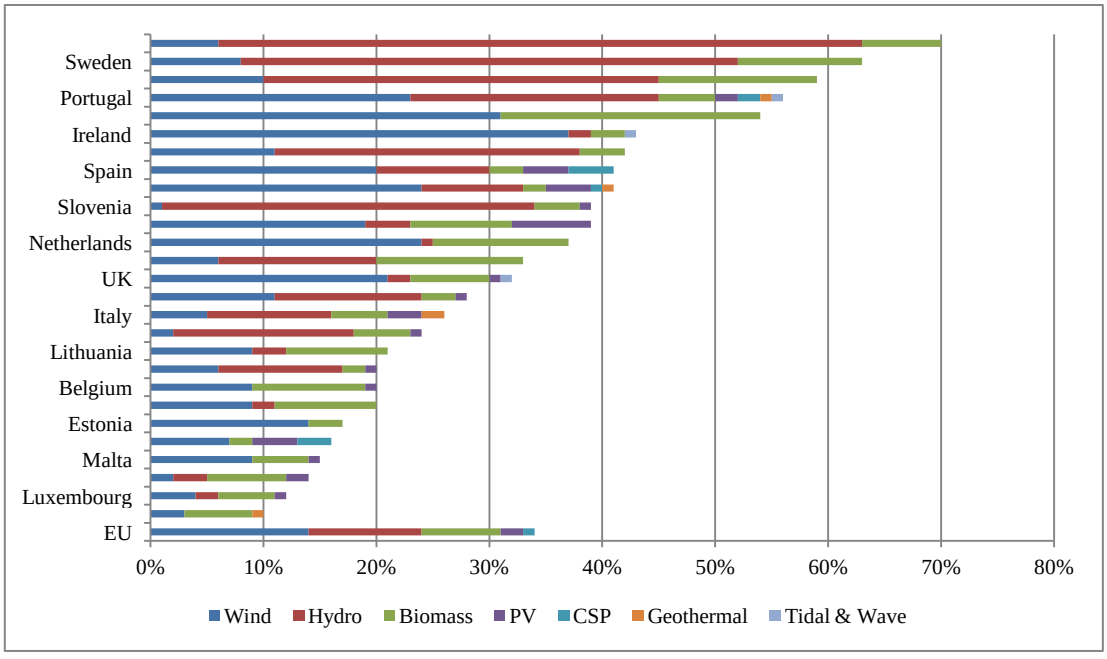

Fig.2.2 Global wind power development (1991 – 2010) compared to nuclear development (1961-1980)

Where in Fig.1.3 has been put in evidence the wind item for Ireland:

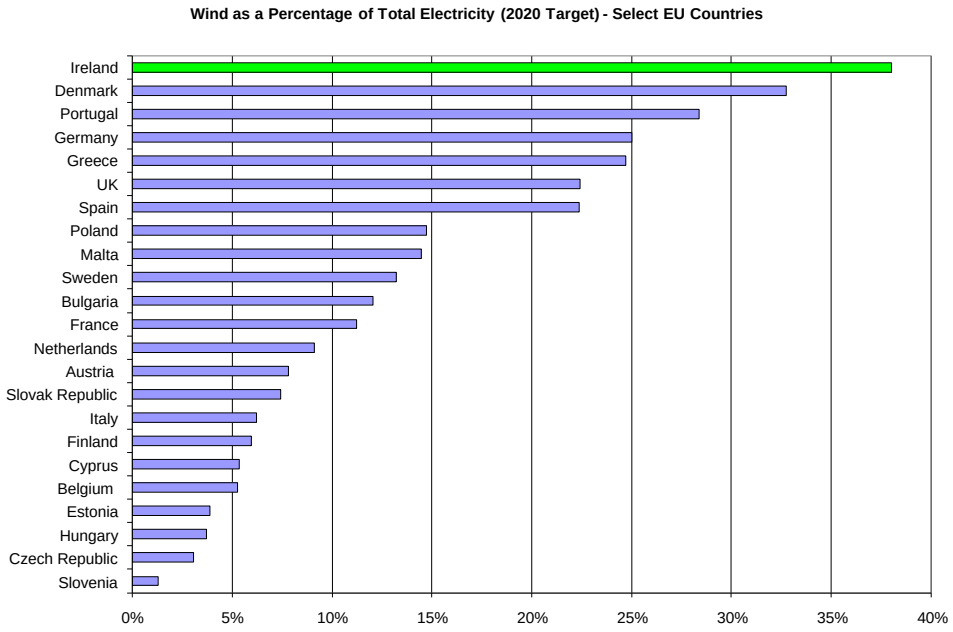

Fig.1.3: Ireland's Renewable Policy Target

1.2.Scope of Work

Some recent studies performed in Eirgrid (4) to set out the appropriate architecture for a future offshore grid have already been undertaken, considering possible development of the Irish Grid all over a twenty years period. An Expansion Strategy has been developed with indication of both the grid structure and the Transmission Technologies to be used. The most relevant result is that the more cost-effective way to deliver the Onshore/Offshore wind for Ireland is by a meshed network composed of both AC and DC technologies, using Extruded as well as Mass Impregnated submarine cables. This allows to better cope with reliability, utilisation of the infrastructure and transmission flexibility at planning and operation stage. A summary of the findings is described in Chapter 2. This has provided the starting point for further considerations which aim at reinforcing the long-term planning analysis and developing optimised off-shore grid strategies.

Looking at the future, the large use of HVAC Cables, and LCC (Line Commutated Conversion) and VSC (Voltage Source Conversion) technologies, has stressed the importance of extending the long term expansion planning to the var support. Coping adequately with the problem of the voltage security assessment in a Long Term Expansion Planning, will constitute the purpose of this work; it will try to go deeply into the reactive analysis when dealing with a meshed AC/DC grid, being characterized by offshore wind-parks connected to the onshore grid by means of submarine high voltage cable routes. It requires proper var planning due to the large amount of cables that may make worse voltage problems, owing to respect transmission capability for any wind conditions. Furthermore, the use of VSC technology allows for a synergy between using HVDC power transfer and a local compensation on AC side.

The relative short distances and the meshed structure make it not straightforward either technically or economically to understand whether AC or DC technology is optimum for this purpose. The differences between these two technologies are discussed fully in Chapter 3.

In Chapter 4 modeling and solving an Optimal Reactive Power Flow, is discussed, considering the available technical literature. This allows investigating optimal sitting and sizing of shunt reactors and capacitors along the grid, considering also different var support methodology, as well as taking into account the control capabilities of the AC and HVDC transmission technologies.

The work has been developed into two stages:

In the first one, carried out by Politecnico of Milan, a Reactive Optimisation Power Flow (ORPF) Algorithm has been set up for the investigation of the var Planning resources. The mathematical model, which is described in Chapter 6, is considering only the steady state and var supply has studied in order to enhance power systems pre-contingency and post-contingency voltage security subject to technical and economic constraints. The algorithm has been developed by using a preliminary test system made by an AC/HVDC meshed grid. Both VSC and LCC HVDC models have been introduced.

The software adopted to formulate and solve the optimization problem is the high level modeling system GAMS and the implementation of the model together with the features of different solvers is formulated in Appendix A.

The second part has been developed at EirGrid, the Transmission System Operator (TSO) of the Republic of Ireland. It has consisted in running multiple scenarios resulting from the preliminary Expansion Planning Strategy described in the Eirgrid Executive report (4). Each solution has been submitted to the ORPF algorithm in order to set up a var planning policy aiming at minimizing an objective functions made by investment costs for reactive compensation, real losses and reliability costs.

In particular, some specific Mixed AC/DC case have been considered to investigate synergies between var supports and VSC installations as well as LCC. At this stage, the Algorithm shows the need of DC centralised coordinated control in a kind of smart HV grid planning concept to minimise investment while maintaining reliability and economic performances. These will be considered on Chapter 5, alongside the other components of which the grid is composed.

The results of application of the method for the Test System are presented in Chapter 7, whereas those for the All Ireland Transmission System operated by EIRGIRD in Chapter 8.

CHAPTER 2
THE IRISH SCENARIO

2.1. The backbone of the Irish electricity system

The High Voltage transmission system in the Republic of Ireland (ROI), owned by Eirgrid, is 6,500 km in length. It consists of a meshed network of high voltage lines and cables at 400 kV, 275 kV, 220 kV,110 kV and substations. Its management and operating requires 'smart' control and monitoring systems, which enable power to be transported in bulk and high quality from generators to areas of demand in order to make the generation of electricity exactly match demand instantaneously throughout the day and night. On the other side, the Northern Ireland (NI) transmission network is operated by SONI (System Operator for Northern Ireland) and comprises approximately 2,100 km of circuits, including 400 km of 275kV double circuit lines and 1,700 km of 110kV double and single circuit lines, which link Northern Ireland's three principal power stations and external connectors to 30 main sub-stations across Northern Ireland. It is connected to Scotland via the high voltage direct current Moyle Interconnector.
The peak demand was 5,090 MW for the ROI and 1,777MW for NI in winter 2010, due to increased heating load as Ireland experienced some of the coldest temperatures recorded in the last 50 years, whilst the minimum demand reached 2,200 MW for ROI and 1100MW for NI. The total generation capacity can be divided into three categories: fully, partially and non dispatchable. The first one gives about 9 GW, most of which comes from conventional thermal generation units (oil, coal, peat, gas) but also hydro-pumped storage. The other two groups cover together 2 GW production of which mostly is wind and a minor part is a small scale distributed generation. The grid is shown in Fig.2.1 (next page).

2.2. Wind farms

Nowadays all over Ireland there are approximately 100 onshore wind farms connected to the electricity system throughout the territory as depicted in Fig.2.1 together with other planned farms, that have signed a connection agreement with EirGrid in Ireland, or that received a planning approval in Northern Ireland. The wind generation peak was 1,284 MW on 12th February 2011, with a maximum capacity of 1,466 MW for ROI, while the highest instantaneous wind generation output was 311MW for NI, having a wind farm connected capacity of 335MW.

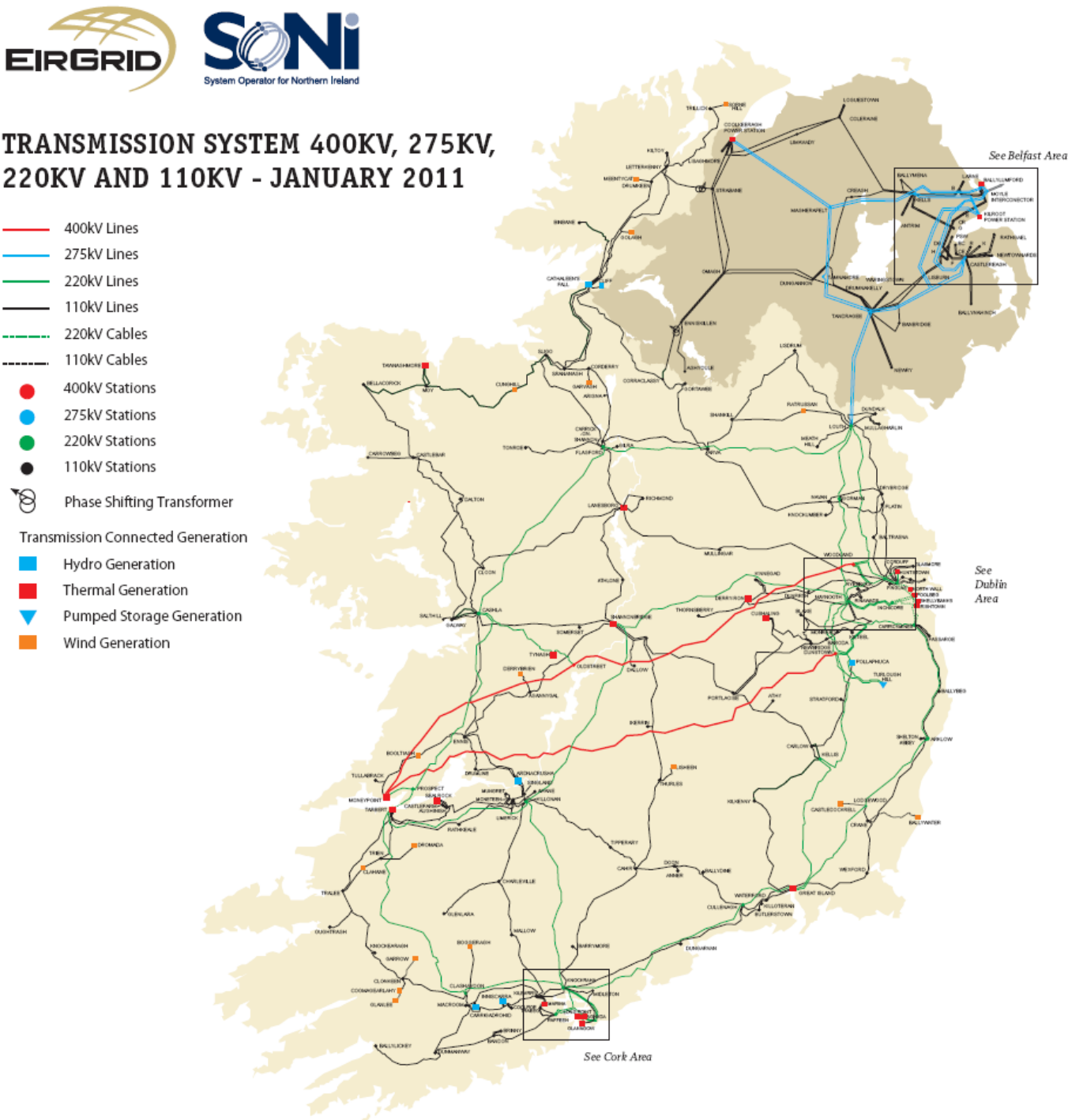

Figure 2.1: Irish Transmission system

Not only new more onshore wind farms in Irish plans, but the prospective by the 2030 to use the more powerful offshore wind valued by Eirgrid studies in MW as shown in the following Fig.2.2, has lead to deal seriously with the relative issues.

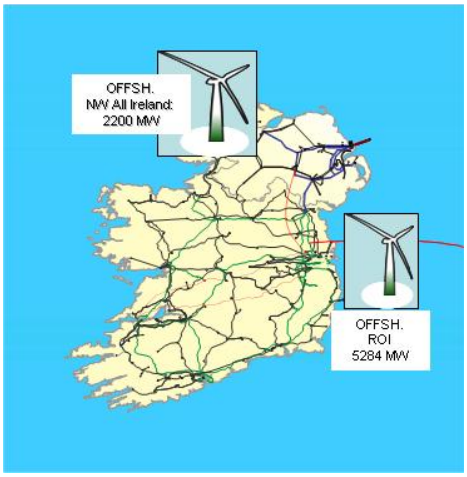

Figure 3.2: Irish Transmission system

2.3. The explanation plan

The need to extend the offshore and onshore grid in order to accommodate the new planned wind farms and to investigate the interaction between offshore and onshore reinforcement, has lead EirGrid in partnership with RSE (the Italian nationally funded research centre for electricity) to develop a software and a new methodology to calculate the most efficient transmission network Expansion Strategy Plan (ESP), which studies a technical/economical investigation of possible grid topologies aiming at transferring onshore energy produced offshore. It is based on the optimization of objective functions made up by several costs:

- the cost of the capital assets i.e. lines, cables and stations,
- the cost of generation production to supply load demand year
- the cost of wind curtailments due by TSO for network constraints
- the cost of load shedding

The investigation was divided into two distinct concepts (Fig.2) both focused on an Irish-only development(PART A) and an interconnected development(PART B). The Irish-only study examined the network from only the Irish transmission network, whilst the interconnected development looked at the potential added benefits, deficits or changes as a result of interconnection to other networks. About that, EirGrid is already on track to deliver the East West Interconnector on schedule, and within budget in 2012. This will connect Ireland to the British Grid for the first time, with potential to buy and sell power. EirGrid has also looked at the case for further subsea links, possibly connecting the national grid to Europe, first of all France. These grid reinforcement will allow Ireland to potentially export renewable energy from its rich wind and ocean energy resources across Europe.

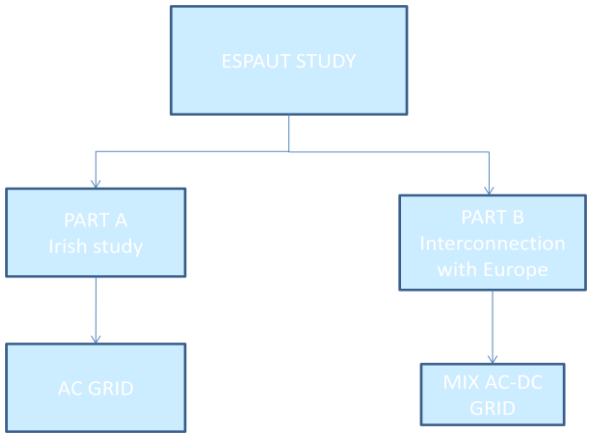

Figure 4.3: Irish Transmission system

As a base case level an offshore wind generation of 3GW has been examined and 5 GW was selected as the first alternative ESP development scenario. Both plans have been developed by adopting steps of three years and a Starting from this point, in order to reflect reality both of them are assumed to have a phased development by a 3 year step and a completion date for all generation by 2030. Consequently not only the final stage of an ESP could be compared, but also steps along the way, according to a two-step methodology as shown below in figure 2.4 and 2.5:

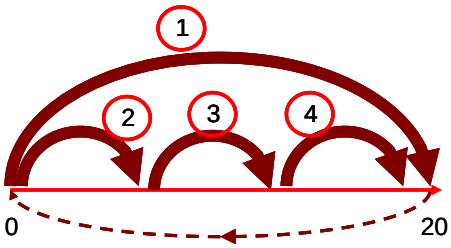

Figure 5.4: Irish Transmission system

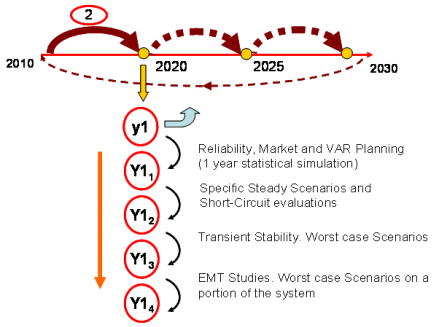

Figure 6.5: Irish Transmission system

In a long term expansion the relevant point is the final years, which has been chosen as the end of the analysis. In combination with this there is a view on the intermediate years with the proper Load/Generation conditions that gives us the perception of the evolution of the expansion. The existing network for each intermediate year is incrementally updated with the expansion results of the previous year, see Figure3. Moreover due to the limited number of Scenarios, the ESPAUT solution is a first screening of the strategic development plan of infrastructures. However the planning process requires further technical/economical investigation, see figure. 8.7. In one year, different scenarios of major importance for the results have been identified according to different conditions of load and generation. The criteria in selecting scenarios have considered limited number of combinations, worst cases, balance with the probability of occurrence and representation of the yearly Energy produced and consumed. In the Table 2.1 the scenarios, the corresponding duration in hours in a year and the relative assumptions for all of them are listed:

Scenarios	ALL IRELAND	GREAT BRITAIN	hours
1	HWind-Low Load	HWind-Low Load	**589**
2	HWind-MedLoad+MedWind-Low Load	HWind-Low Load	**609**
3	HWind-Low Load	HWind-MedLoad+MedWind-Low Load	**385**
4	HWind_MedLoad+MedWind_Low Load	HWind-MedLoad+MedWind-Low Load	**3705**
5	Low High Load	Low High Load	**3473**

Table 2.1: scenario summery and weighting factors

One important combination is High Wind- Low Load because best represents the need of interconnection. Both countries (Ireland and Great Britain) in Low Load conditions can offer an excess of wind energy which might be exported to mainland Europe. On the opposite side there is Low Wind - High Load, which is very frequent when most of the conventional generation has to supply the load. This scenario provides the most onerous case for the expansion to cater for conventional generation. Between these two extreme operating conditions, that are not sufficient to fully represent the yearly behaviour, consulting historic data have been identified some intermediate periods which may occur in particular for windy conditions across Ireland and the UK. This mainly depends on the geographical distribution of the wind resources. Three additional intermediate scenarios have been considered which better integrate the equivalent yearly behaviour:

In Table 2.2, the definition of High, Medium and Low is shown, as well as the probability of each wind and load scenario to occur. This probability of occurrence has been calculated according to available historic wind and load data profiles based on hour.

scaling coefficient	Wind AI+NWSCO	WIND GB	load
high	1	1	1
medium	0.37	0.34	0.58
low	0.11	0.11	0.37
probability	wind AI+NWSCO	WIND GB	load
high	0.14	0.10	0.23
medium	0.58	0.58	0.46
low	0.28	0.32	0.32

Table 2.2: Scaling factors and probability

2.4.Model

The optimum expansion strategy developed in order to connect the offshore wind generation gathering platforms to the All Ireland transmission system is based on a mathematical model which uses the algorithm of branch and bound and chooses, among a set of line and transformer candidates, those that best satisfy the considered optimization function. The Branch and Bound Method is used by the program to provide a solution, given the combinatorial nature of the problem; this method is very effective in reducing the number of combinations to be actually examined. A tree is made, where each node in the tree corresponds to some combination of integer variables which are constrained to be 1 or 0. In the case of this problem the 1 or 0 relates to whether a candidate reinforcement (e.g. an offshore cable circuit) is in or not.

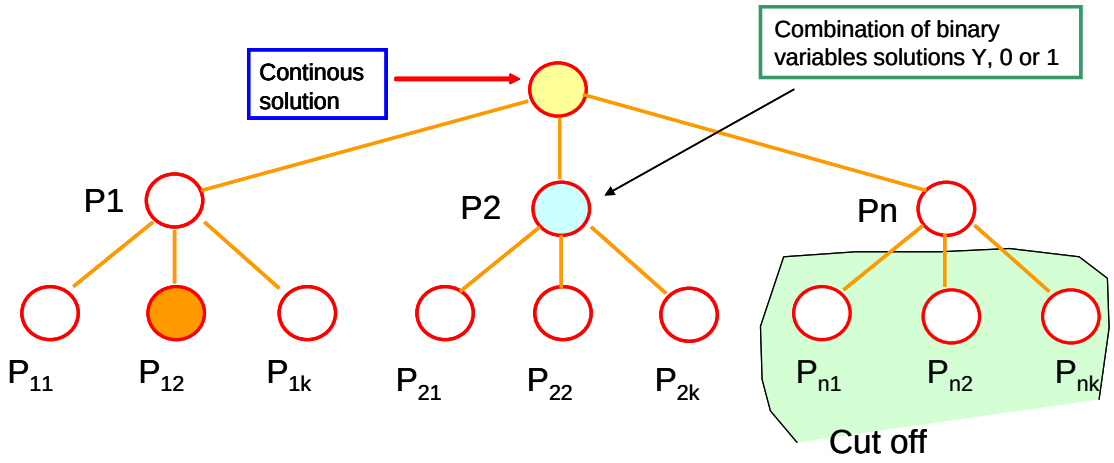

Figure 2.6 Branch and Bound methodology

The number of combination depends on the binary variables to be defined. The program first considers one of the potential solutions to provide a Current Best Solution (CBS). Then one of the combinations of integers is changed (e.g. a circuit removed or added) and the resulting new solution is considered, in so doing the new solution may prove to be optimum and hence a new optimum is obtained. Once, all the integer variables are fixed a Current Best Solution (CBS) is reached, i.e. P_{12}.The program re-dispatches generation in each of its potential solutions to minimise the production cost to permit, which in association with reinforcement and system loss costs provide a final cost for that solution to be compared to the CBS. Other branches are explored starting from the most attractive stage, i.e. P1. If during the process of fixing integer variables a more expensive solution than the CBS is found, i.e. P_n, then the node P_n and al the branches downstream, Pn1, Pn2, P_{nk} are eliminated (Cut off). In the process of proceeding through the tree, the algorithm calculates an Estimated Best Solution (EBS); a tolerance is calculated between EBS and CBS. This provides a reference as to how far the CBS is from the optimum solution. Given that the EBS is only an estimated value, and may not provide to be accurate (i.e. the EBS may not exist), a tolerance level is selected within which the current CBS solution is considered acceptably optimised to terminate the process within a reasonable timeframe.

The program uses the linear power flow approximation(DC Power flow); therefore, losses are neglected in the energy balance equation.

A binary variable Y_{nlnew} has been introduced to represent the presence or the absence of candidate circuits and this has made the model a Mixed Integer linear optimization problem(MILP). Since it is an optimization problem, it consists of an objective function to minimize:

$$OF = operation + investment$$

where OF is the a yearly cost with the following breakdown.

The DC equation is written assuming:

- N_d node numbers,
- M_d branches,
- $R_{i,j}$ line, cable, transformers, HVDC, etc.., (the resistance of the branch connecting node i-th, with node j-th).

The following equation can be found:

The investment cost has been annualized according to CER(Commission for Energy Regulation) and collects the cost of candidate lines or cables $Cost_{nlnew}$, defined as:

$$investment = \sum_{nl_{new}} (Cost_{nlnew} * Y_{nlnew})$$

Since exact losses are neglected, they have been included in the cost definition, assuming an average yearly loading of 40%. Therefore operation costs are composed of four terms which are:

$$operation_{ns} = production_{ns} + LSH_{ns} + Wcurtailment_{ns} + MP_{ns}$$

One unique cost $production$ resumes the yearly cost of producing the electrical energy for supplying the load and the estimated losses:

$$production_{ns} = \sum_{ng} (C1_{ng} * PG_{ng,ns})$$

The The other elements in the objective function considers unhelpful behavior inside the grid to have to take into account with very high cost coefficient CLS_{nn} has been chosen 5000 €/MW, based on Eirgrid practice. For instance one likely aspect may be the total load shedding, valued by the cost function $cols_{ns}$:

$$LSH_{cost,ns} = \sum_{nn} \left(CLS_{nn} * LS_{nn,ns}\right)$$

$Wcurtailment_{ns}$ takes into account the total penalization costs due to violation in respecting production limits in both wind generation areas and in thermal generation areas. The former are calculated below as:

$$Wcurtailment_{ns} = \sum_{areegen} (COSTcurt_{areegen,ns} * Pcurt_{areegen,ns})$$

The penalty values for $COSTcurt_{areegen,ns}$ are related to the different incentive policies for offshore and onshore that are dependant by different countries. This reflects the market price, and notably the price paid for the wind under refit regardless of network constraints. Refit tariff is set up in Ireland and Britain to:

- 60 Euro/MWh onshore
- 140 Euro/MWh offshore
- 220 Euro/MWh for waves
- 150 Euro/MWh for GB Offshore

Finally a penalization is considered for minimum must run units violation constraints in thermal generation areas and the value is the highest because is the last that can be violated .

$$MP_{cost,ns} = \sum_{nareegen} (COST_{areegen,ns} * LOSTP_{areegen,ns})$$

The optimization problem so far described requires to introduce some equality and inequality constraints. First of all, real power balance at each bus is given by:

$$\sum_{ng=G\_N} PG_{ng,ns} = \sum_{nl=froml} T_{nl,ns} - \sum_{nl=tol} T_{nl,ns} + \sum_{nlnew=fromc} T_{NEW\,nlnew,ns} - \sum_{nlnew=toc} T_{NEW\,nlnew,ns} + LOAD - LS_{nn,ns}$$

Where $T_{nl,ns}$ is the real power flow through each existing link calculated as linear function of the nodal phase of its from and to bus via DC power flow equations. In this case, similar equations can be written for the AC grid, assuming however that no losses are present and that voltage is similar to the nominal value in each node

Assuming:

- N number of AC nodes
- M number of AC branches,
- $X_{i,j}$ the longitudinal reactance between node i-th and j-th
- $T_{i,j}$ the active power flow on this branch from I to j, is given by::

$$T_{nl,ns} = \left[\sum_{nn=froml} V_n\right] * \left[\sum_{nn=tol} V_n\right] * \frac{K}{XB} * \left[\sum_{nn=froml} \theta_{nn,ns} - \sum_{nn=tol} \theta_{nn,ns}\right]$$

Where V_i , V_j , ϑ_i , ϑ_j , $K_{i,j}$ are the absolute value of Voltages, the phase angles, at node I and j and the transformer ratio between node I and j respectively.

The same meaning for T_NEWnl,ns connected to each candidate link selected (Y=1)

$$T\_NEWnl,ns = \left[\sum_{nn=fromc} V_n\right] * \left[\sum_{nn=toc} V_n\right] * \frac{K}{XB} * \left[\sum_{nn=fromc} \theta_{nn,ns} - \sum_{nn=toc} \theta_{nn,ns}\right]$$

To have an index of how much active power remains not delivered, an equation for real power balance for both wind area and thermal area generation are written as follow:

$$P_{AREAG_{wareagen,ns}} = \left[\sum_{ng=wareagen} PG_{ng,ns}\right] + Pcurt_{areegen,ns}$$

$$P_{AREAGTH_{thareagen,ns}} = \left[\sum_{ng=thareagen} PG_{ng,ns}\right] + LOSTP_{areegen,ns}$$

Active power flow is null for each candidate link not selected (Y=0), independent of the nodal phase s of its from and to bus obviously match the constrains:

$$TNEW_{nlnew,ns} = 0$$

Taking into account the thermal limits for the links, lower limit and upper limits on real power flows are formulated as inequality constraints:

$$T_{NEW\,nl,ns} \geq T_{min} * \Delta capnew$$

$$T_{NEW_{nl,ns}} \leq T_{max} * \Delta capnew$$

The possibility for each generators in varying its own production is the variable which represents the amount required for supplying the demand according to the equality:

$$\sum_{ng} PG_{ng,ns} = \sum_{nn} (LOAD_{nn} - LS_{nn,ns})$$

This mathematical model has been made running by GAMS (Generic Algebraic Modeling System) using CPLEX solver which has given results by considering the operation of the system in one year both in unperturbed and N-1 conditions. All the control variables taken into account are collected in the table 2.3.

MW forniti dai generatori	$PG_{ng,ns}$
Load shedding	$LS_{nn,ns}$
active power flow through links	$T_{nl,ns}$
active power flow through new links	$T_{NEW\,nlnew,ns}$
voltage phase	$\theta_{nn,ns}$
shift between extreme buses of PST	$SFAS_{nl,ns}$
wind power generation	$P_{AREAG_{nareagen,ns}}$
Wind power missed	$MANCATAP_{AREAG_{nareagen,ns}}$
conventional power generation	$P_{AREAGTH_{nareagen,ns}}$
conventional power missed	$MANCATAP_{AREAGTH}$
Binary variable for candidate links	Y_{nlnew}

Table 2.3:variables

Among all the variables adopted in this model, only two are useful for the further studied on the reactive topic: $PG_{ng,ns}$and Y_{nlnew}. While the resulting value of the former will fill in the data of the nominal power for each generator and will be so used as starting point for the different scenarios in the var planning optimization model for the Eirgrid Grid, the latter is the most useful since has let to depict the future enlargement of the grid as it reported more deeply in the following paragraphs.

2.5.Results for long term expansion: part A

The PART A model considers only Ireland and its interconnection with Britain, dividing the whole network into five areas: Northern Ireland, North West, South West, East, United Kingdom; Europe has been modeled by equivalent generators. This representation is shown in Fig.2.7, where also candidate links are drawn for the base-case scenario, which examines the Expansion Strategy Plan for 5 offshore generation sites producing 3.2GW of generation by 2030.

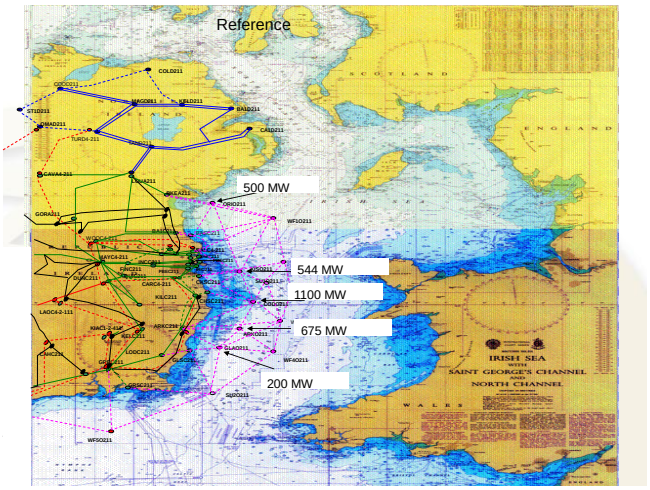

Figure 2.7: Existing Grid (solid lines) and candidate network (broken lines)

The assumed evolution for the power generated by the five offshore wind units along the analyzed period looks like the curve in the Fig. 2.8.

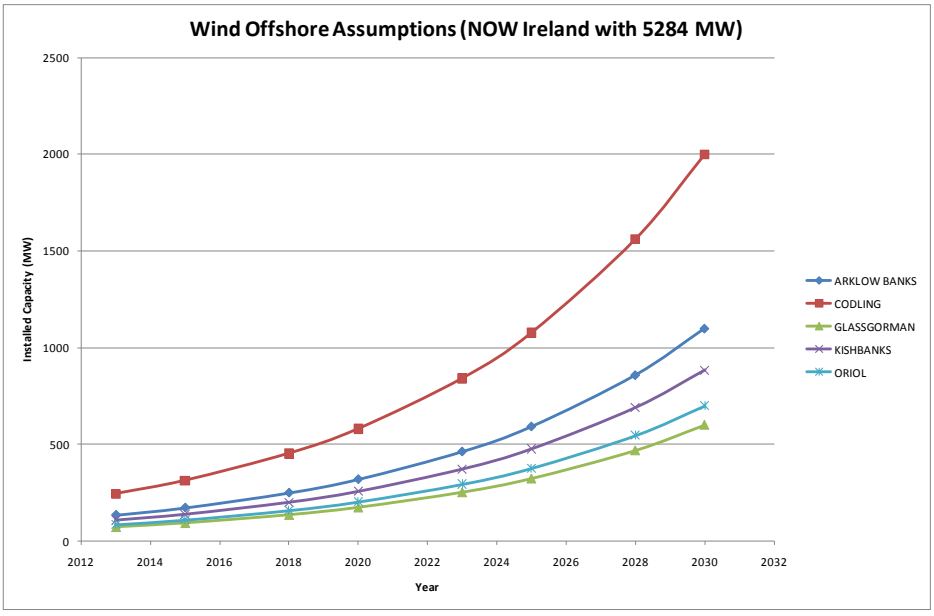

Figure 2.8: assumption offshore wind power

The links chosen by the program as the best are drawn by solid purple line for the year 2020,2025 and 2030.

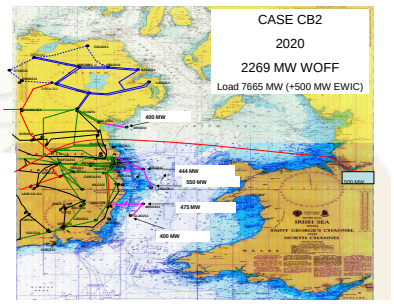

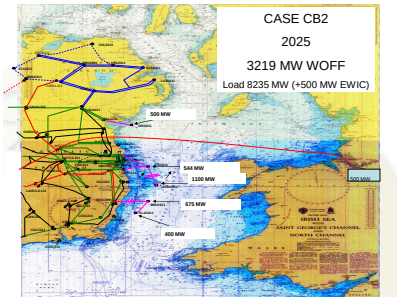

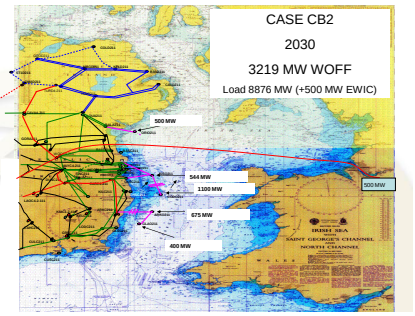

Having higher installed capacity of c.5.2GW of generation by 2030, let to analyse the scenario MID5, keeping from the BASECASE scenario the previous 5 offshore generation sites.

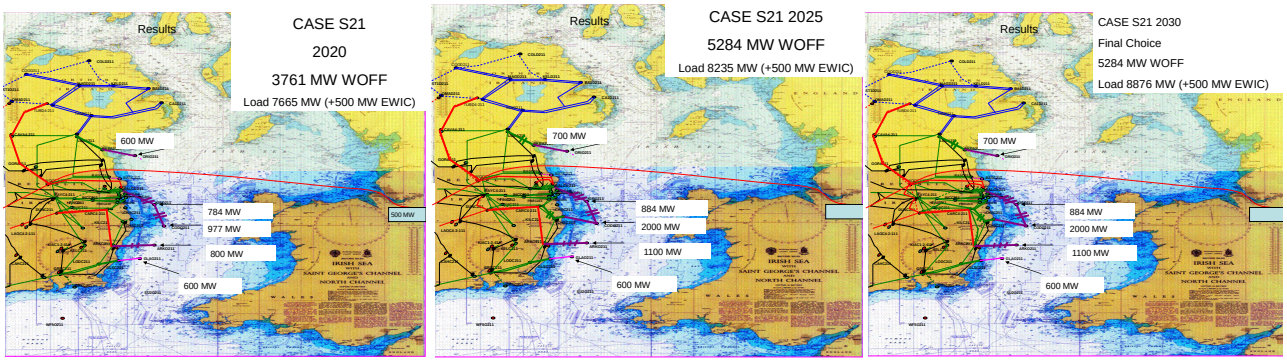

As last variation it has been decides to share the same total amount of offshore wind generation of 5.2GW on ten locations instead of five. The so new scenario Scenario MID10 examines the Expansion Strategy Plan (ESP) for 10 offshore generation sites, 5 of which are defined by the applications received and 5 for geographic variation in a row of further offshore.

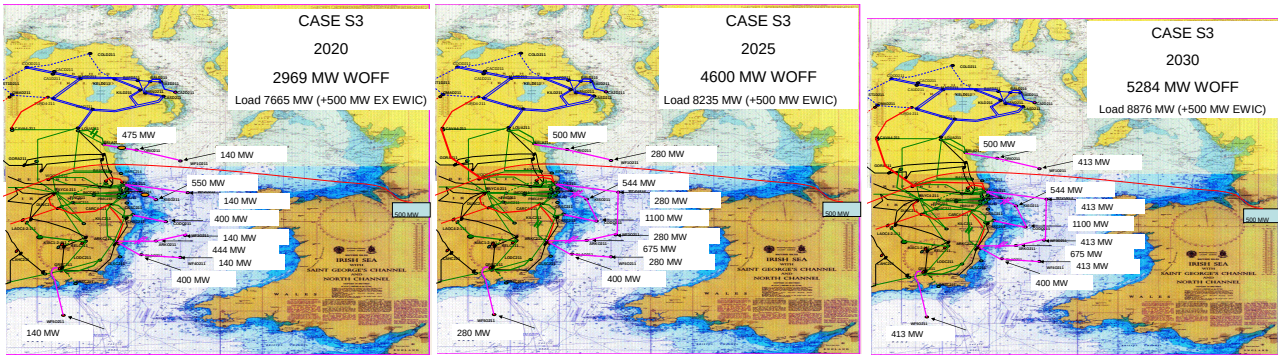

EirGrid/ERSE position was to start from an AC approach concerning the link; consequently the reactive impact on the power system has to be considered carefully and in a large variety of scenarios. Voltage control will be a major issue because of the large extension of the offshore grid and the variability of the wind power resources and therefore of the infrastructure loading. In the following table three different AC circuit have been listed with their relative attributes. It worth to underline the high capacitance value due to the specific need to use compulsory cable for offshore applications.

	R [Ohm/km]	X [Ohm/km]	C [nF/km]	tgd p.u.	S [MVA]
Three Core 220 kV 1000 mm2 Cu	**0.057**	**0.09**	**200**	**1.00E-04**	**320**
Single Core 220 kV 1200 mm2 Cu	**0.046**	**0.07**	**198**	**1.00E-04**	**460**
Single Core 400 kV 1400 mm2 Cu	**0.043**	**0.07**	**216**	**1.00E-04**	**930**

Tabella 2.4: Electrical parameters of transmission offshore alternatives

In some cases a technical limit could be reached suggesting that some offshore reinforcements need to be selected to be DC or embedded DC. Due to the practicalities in the software of processing millions of possible ESPs to find the optimum solution, the base case analysis was provided different sizes of connection limited to only one possible technological cable solution.

EXPANTION OFFSHORE in ROI+GB

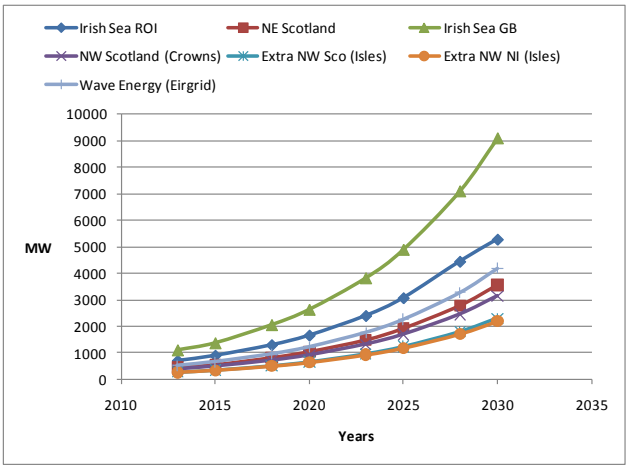

Figure 2.9: EXPANTION OFFSHORE in ROI+GB

2.6. Results for long term expansion: part B

After initial analysis with candidate reinforcements from Ireland the same investigations were repeated only for the MID5 scenario with a new candidate list of reinforcements which include options to develop the offshore network into an interconnected network with other European countries notably Britain and France. The philosophy for the wider offshore candidate reinforcements is identical to Irish only analysis. Existing strategic network plans were used and supplemented with other conceivable potential reinforcement options. In figure 2.10 the list of candidates is geographically shown.

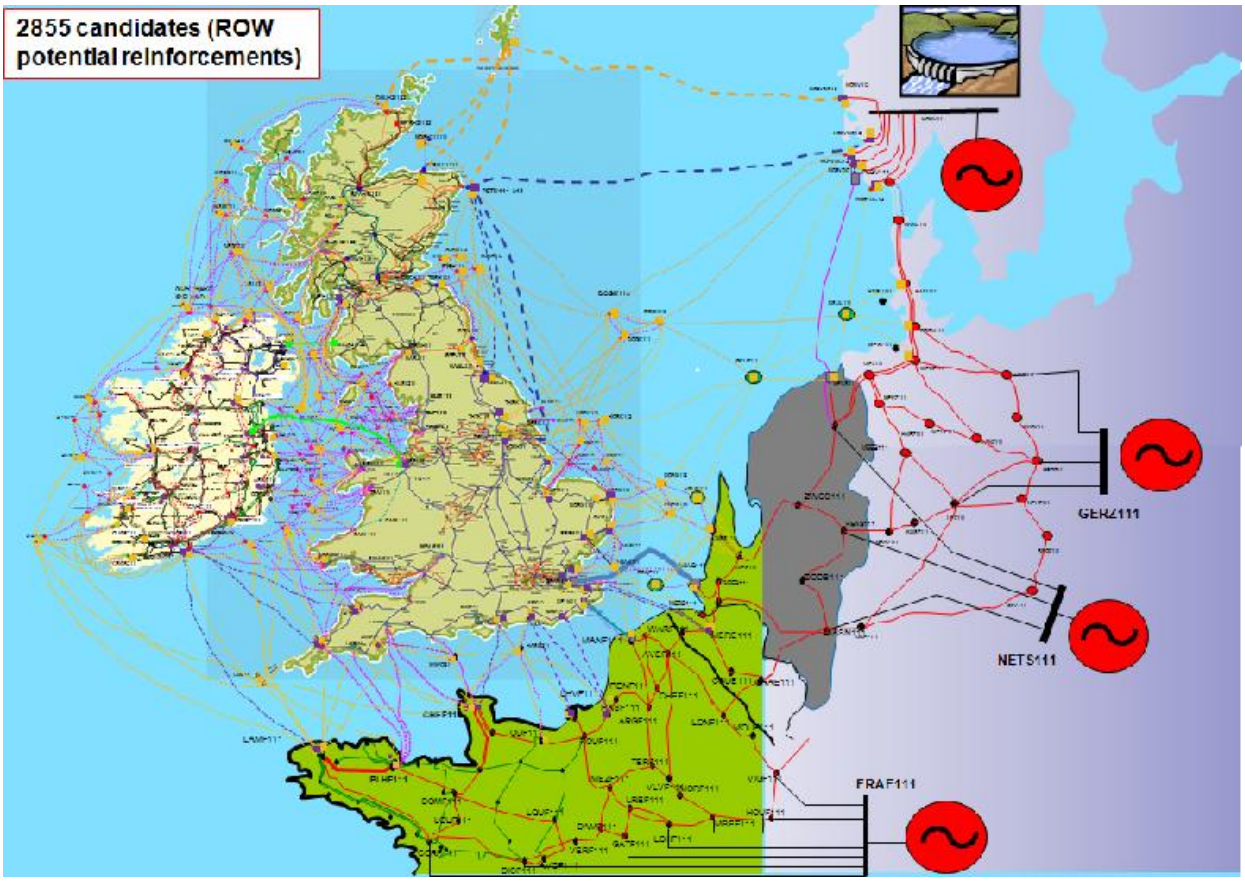

Figure 2.10: Reinforcement per both AC type and DC type

In the figure above the candidate reinforcements are shown for the both the technological studied, with the DC technological reinforcements represented by purple lines for LCC and yellow lines for VSC technology).

In order to do so the existing network model has to been extended to the neighbouring countries and for computation reasons, the load and generation models for mainland European have been formulated by equivalents: four equivalent load/generation nodes have been modelled to account for France, Netherlands and Germany and Norway. The fundamental reason for modelling a wider northern European equivalent network is that exporting/importing power from/to Ireland will have a cascading impact on the need for grid expansion not only in Britain, but also at the British interface with mainland Europe especially in the Channel and the Thames Estuary as well as the North Sea. Therefore it is important for accuracy in the Ireland network expansion to realistically model transmission capacity available onshore in neighbouring countries considering, if any, grid expansion projects elsewhere in Europe.

The criteria of introducing the large amounts of candidate is summerized in Fig.2.11

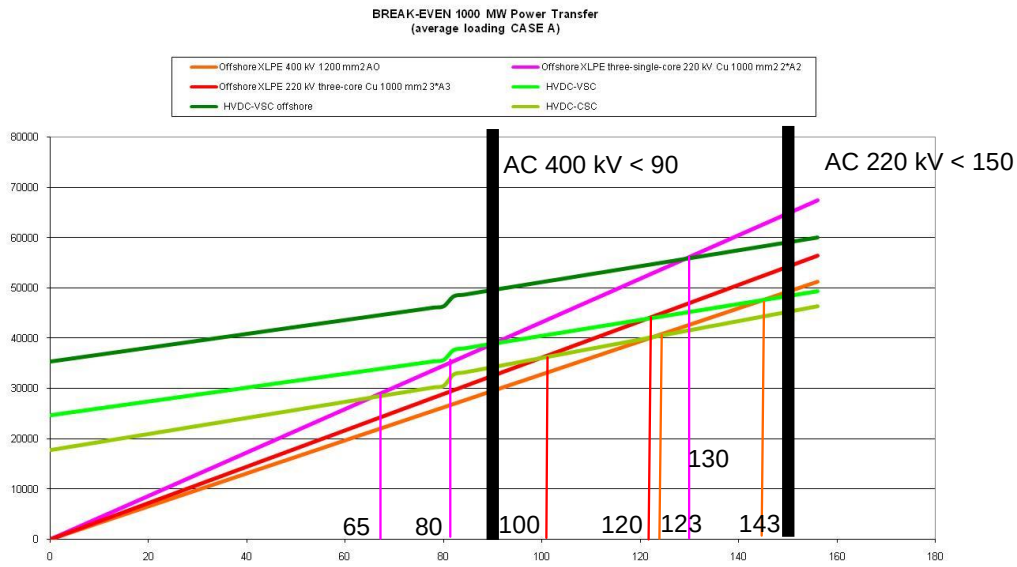

Figure 2.11: Cable break-even distances

For distance shorter than 80-90 km it has been stated to consider an AC 400 kV XLPE and DC VSC solution. Instead for those one longer, a HVDC technology has been assumed;in particular HVDC LCC has been selected only for point to point onshore applications or submarine interconnection with HVDC unites to be installed in mainland. Each HVDC VSC technology has been selected for all offshore connections and any distance. This approach has provided a large set of AC and DC transmission alternatives for the offshore connections, especially in the Irish Sea, where distances are well within the economical breakeven distances of AC application. See Figure 2.12.

This model gives indicative information about the overall interconnected system behaviour, particularly congested areas, preferential exporting routes from Ireland to, Britain and Europe, wind delivered and curtailed, the size of infrastructure expansion plan. Note that the analysis accounts for the British Expansion offshore plan only(reference Crown 3 ODIS).

Figure 2.12: Mixed AC/HVDC meshed candidate grid_Irish Sea Zoom

The ESP has comprised a number of large HVDC circuits as both LCC and VSC technologies. It has been particularly interesting that there have been some parallel DC and AC paths selected for those distances where both technologies are technically viable. This implies that the ESP has selected the higher cost DC technological solution because its power flow capability minimises the need for further network reinforcement (or better use of lower cost generation). Consequently, a mixed solution with both AC and DC circuits proves to be the more profitable. Due to the large distances and the length needed, it also makes a lot of sense that a part of the offshore grid would be better in the form of DC links. The topology is quite interesting, as it shows the HVDC links used as "main roads" whereas the AC links are used as secondary roads. This reduces the amount of offshore infrastructure by several kilometres compared to the just AC links solutions. An important result is that the offshore grid and the onshore network are symbiotic, as the optimisation process finds ways to connect a huge amount of generation offshore without allowing major constraints onshore. In fact, the circuits offshore also help to relieve loaded onshore links. This is not surprising, because scenarios of very low energy wind input were considered and weighted properly in the optimisation process.

This scenario examines the Expansion Strategy Plan (ESP) for 5 offshore generation sites producing about 5GW of generation by 2030. Isles and Wave Energy are not included and Wind curtailment penalty is 10000 Euro/MWh. Following the results obtained for intermediate years until 2030.

In order to minimise the scale of circuits/capacity needed, the offshore network could benefit from power flow controllers which allow a better exploitation of the infrastructure by suitably re-routing power flows on a minimum subset of connections. This potential must be tested at the expansion phase, when the additional infrastructure costs can be included. The application of power flow controllers may results in an overall optimisation benefit reducing network expansion as well as providing further system flexibility to better optimise dispatch of conventional generation.

The controllability may provide enhanced performance to the network and it is of particular interest to verify performance potential at the expansion planning stage. Indeed with purely AC reinforcements the electrical parameters of the routes, existing and the candidate reinforcements could provide a markedly over sized ESP. For instance, a long link to France would represent a very high impedance path as an AC circuit that would impede power transfer through it. Therefore, some extra reinforcements may be decided in order to sufficiently lowered the impedance path and let the power to flow. Furthermore, the variability of some generation resources create multiple power flow patterns, which without power flow control devices may result in an overdesigned network. If it is optimum to do so, a circuit can be loaded to the maximum capacity for any scenario, avoiding extra reinforcements. It is noteworthy that the circuit itself can be much more economic than the corresponding AC model Compared to the pure AC model, the solution is expected more cost effective overall.

The 2015, will be finally the grid system used for the further studies which are the objective of this thesis.

CHAPTER 3
THE OFFSHORE TECHNOLOGY: THE REACTIVE PROBLEM

3.1. Offshore potential

The deployment of offshore generation in Ireland is expected to become increasingly favorable, in the medium /long term. This is a consequence of the increasingly needs of renewable energy demand and of the saturation in space and in potential on shore that the Gate3 [] offer fulfillment. Furthermore, offshore may offer more stable wind condition and a higher capacity factor.

With reference to Fig.3.1 where potential resources are shown along all Island offshore areas, it can be noted how both the west and east coast present areas with wind speed more than 7m/s and depths that may accommodate wind farm.

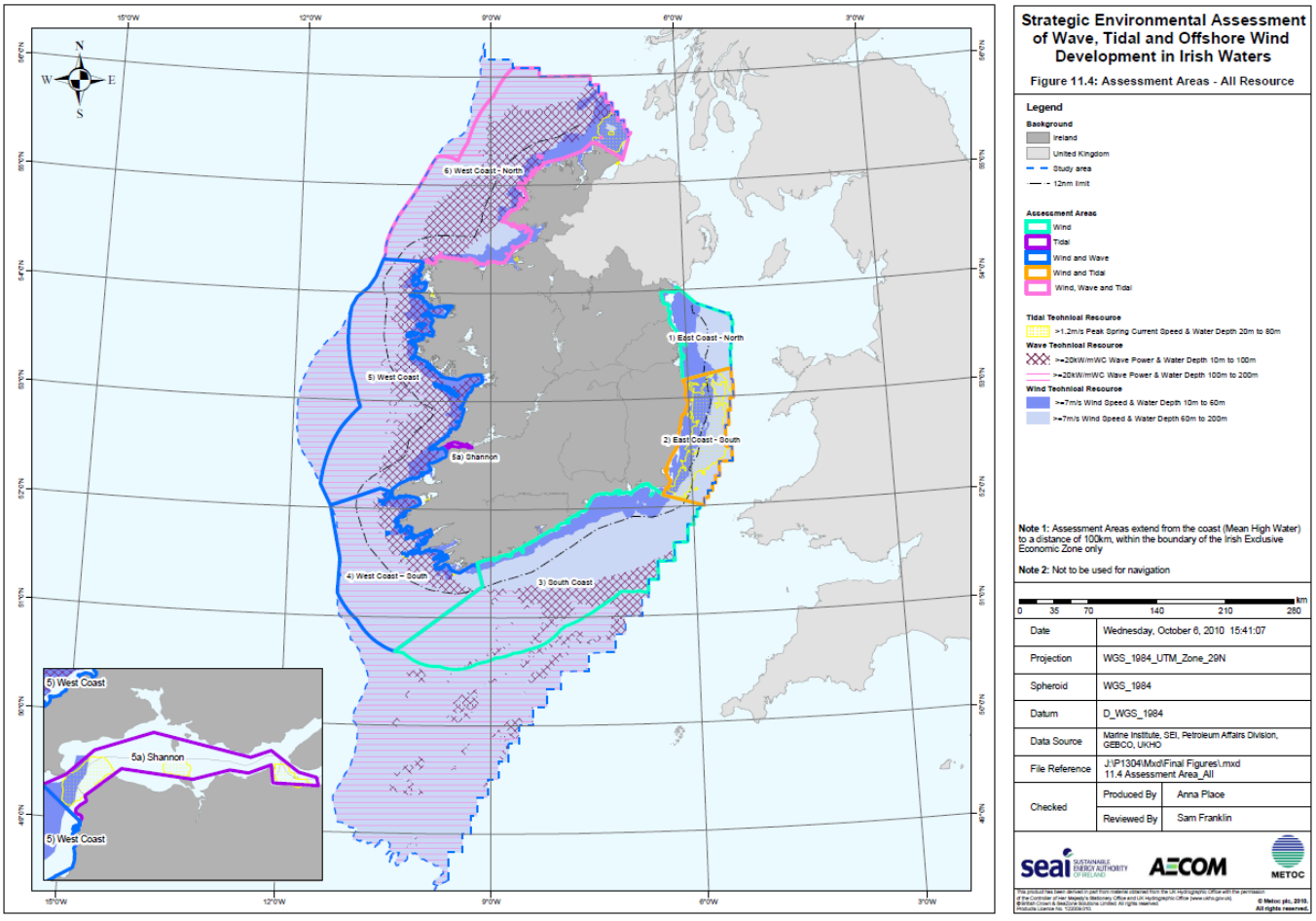

Figure 3.1: Offshore Wind coasts potential

Nevertheless, offshore wind is at an early stage of deployment and many issues make it a major challenge compared to onshore, mainly related to the supply chain to be set up: ports, platforms, installation equipments, as well as the suitable architecture and Transmission technology for connection.

In particular, the Offshore Grid will be dictated by the Cable Technology. Whether DC or AC it has been part of the previous work [Offshore] where a comprehensive Cost/Benefit analysis has indicated some potential Grid structures and associated technologies.

However, based on these results, a further critical technical/economical assessment is necessary to fully verify compliances with the Transmission System Operator(TSO) in the Transmission Planning Criteria (TPC). Of particular concern is the Voltage Control, var planning related resources, following large amount of AC cables together with and increasing variability of wheeling flows to, from and through All Island jurisdictional area.

3.2. Wind variability

The power production of a wind turbine depends significantly on wind speed, which is an uncertain factor and whose probability distribution, when it is not possible to have real data, in general may be considered following the Weibull probability distribution function:

$$f(v) = k\left(\frac{v^{k-1}}{c^k}\right)e^{-\left(\frac{v}{c}\right)^k}, \qquad x \geq 0$$

where *k* is a shape factor that for the ground and in West Europe it may be assumed as 2. The scale factor *c*, instead, can be taken equal to the average speed such as 7.9 m/s. The area below the curve between two values represents the probability. Multiplying this value for the number of hours in one year 8760, will give the number expected of hours related to that wind speed interval:

$$\mathrm{h}(v_1 \leq v \leq v_2) = 8760 \cdot \int_{v_1}^{v_2} f(v)dv$$

Knowing the distribution function, the average speed is calculated in a continuous way as:

$$v_{\mathrm{ave}} = \int_0^{\infty} vf(v)dv$$

Varying the parameter *k* and *c*, other different distribution shapes can be drawn and among them there is the Rayleigh distribution with $k = 2$; and it is widely used when there is little knowledge about the wind features:

$$f(v) = \frac{2v}{c^2}e^{-\left(\frac{v}{c}\right)^2}$$

Although different distributions are considered, there is a unique relationship which expresses the theoretical average power value associated to the wind as a function of its average value of the speed v_{ave}, considering a turbine with an horizontal assis:

$$P_{th} = \frac{1}{2}\rho S v^3$$

The average value of the wind speed becomes:

$$P_{ave} = \frac{1}{2}\rho S(v^3)_{ave}$$

It is worth to underline the cubic dependency on the wind speed, which shows up as the most important factor: therefore an increase of 10% in speed determines a 33% more in power generated. Besides, the factor S which indicates the bigger the section covered by the pales is, the higher the power potentially will be. But the choice of the diameter is highly conditioned by the prices on the market.

In a practical way, it is not more possible to obtain more than a 60%-70% from an undisturbed wind flow because of the vortices effects that there are close to the exiting zone of the pales. This gain is quantified by the power coefficient C_p defined as

$$C_p = \frac{P_{usable}}{P_{th}}$$

In order to face the change in the wind speed, for a turbine it is important to be able to vary the rotation speed Ω (rad/s) since in this way it can maximize the peak power tracking while the wind is changing: this results is obtained working close to values for the tip-speed ratio λ which maximizes the coefficient C_p.

$$\lambda = \frac{\Omega r}{v}$$

Each turbine has a its own curve for $C_p$related to λ. Normally the low value for Ω requires in most cases, the interposition of a gear to make the low speed rotation of the pales compatible with the higher speed required by the generators connected. When the generator has several poles and has a big diameter, the multiplier is not necessary.

Variation of the average power over a period of 20 years are characterized by a standard deviation of about 10 % or less, and this allows a good evaluation of the economic gain for a wind farm. To give a real representation of the variety in generation along the year, it should be convenient to divide the year in group of hours characterized by an almost constant production, being considered as a function of synoptic time i.e seasonal and weekly cycles, neglecting turbulence and diuturnal cycle. This is the approach that will be followed in modeling this part of the system as it will described in chapter 5.

About the generator connection, five types of wind turbine generators are available though the market has largely been dominated by the doubly fed concept (DFIG). This prevalence is due to the Voltage Control capability requirements which the TSO are gradually incorporating in their TPC. Some types, like SCIG (Squirrel Cage Induction Generator), are not able to control reactive power consumption and they have limited voltage quality control, whereas the full converter concepts are quickly gaining a significant in market share. Instead DFIG has as one of its main advantages a good control of power in the stator circuit by small injection of power in the rotor circuit. Moreover, real and reactive power can be controlled independently.

Since for the wind turbines the possibility to change their Ω is fundamental, they are equipped with control and protection systems: the first one acts on rotor speed, turbine orientation, start-up and shutdown. The protection function guards against conditions such as over-speed, generator overload, and even excessive

vibrations. About the integration in the power system, they need of converters that let separate the frequency of the grid from that of the generator, guaranteeing variable speed. Moreover, these modern types of system don't require the multiplier any more, since the converter acts as "electric gear".

3.3. Transmission alternatives

3.3.1. AC technology

The technology choices for an offshore network are in many ways similar to those for an onshore network. However, since the offshore network is mainly used for the connection of generation and to transfer bulk of power to onshore demand, the technological selections for an offshore grid may be markedly different to those of an onshore. Also unlike onshore networks, offshore networks are are unique because they are developed entirely in the sea and therefore cable technology must be used. An investigation on the available technologies for Offshore Transmission considering that costs estimations have been completed as part of the LTEP study, based on a European Average of infrastructure costs.

Subsea cables have been in service from the 1950s worldwide. Advancement in technology made three-core HVAC 150 kV Extruded Cables available for subsea application in recent years, following offshore Wind Farm connections in the North Sea. Today technology is under development for higher HVAC Voltages, 220kV and 400 kV. In particular, three-core configuration can be developed for 220 kV, whereas only single core is likely to be developed for 400 kV. For the Offshore Grid study, it has been assumed that three AC technologies were available at 220 and 400 kV. In figure 3.2, a general configuration of an offshore connection is shown from the gathering platform on shore.

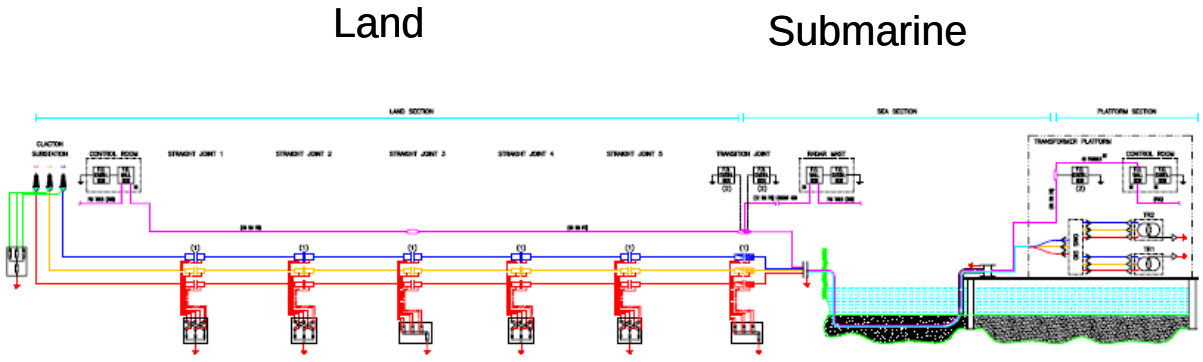

Figure 3.2: Offshore connection

The separation between submarine and land portion needs to be broken out. The gathering platform is equipped with HV/MV transformers and switching devices. Land cable can be laid in cross-bonded configuration of the sheath (as normal practice within Ireland). If the connection is close to the sea, the land cable is usually omitted. DC technology is also being considered for longer distances. In particular the recent development of multilevel Voltage Source Converter (VSC) technology is of interest in particular in a Meshed AC context for the concept of an "Offshore" Supergrid. Furthermore VSC DC technology allows the use of cross-linked polyethylene (XLPE) cables. In this study, land cable sections have been modeled using typical parameters for EirGrid's standard cable types and installation methods (as applicable), and both conventional LCC and VSC has been considered with PPL and XLPE cable respectively.

HVAC 220 kV three-core

At present, all the offshore wind farm connections have been realized using a cable shown in figure 3.3

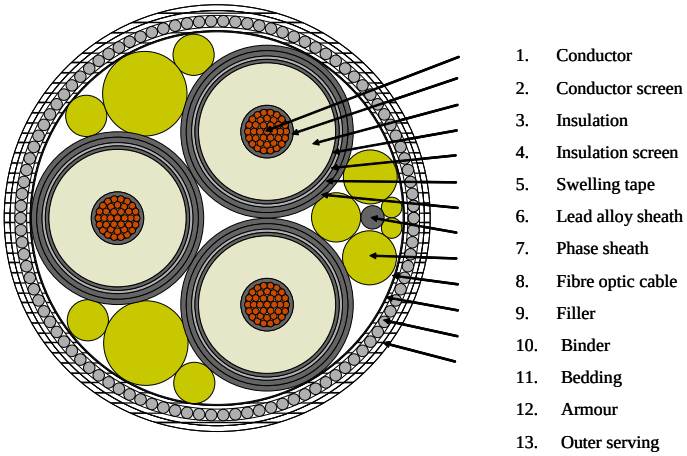

Figure 3.3: Three-core cable

This particular technology allows some cost savings in installation, as in principle only a single cable needs to be laid. The conductor material used is the copper rather than aluminium as the former has a higher rating for a given cross section area. Each cable has a XLPE insulation layer and over it there is an impervious metallic sheath, such as lead to avoid direct contact with water, the so called 'dry design'. At present, the AC technology offshore is predominately at 150 kV although some smaller sections at 220 kV have been installed. At 150 kV, with a 1000 Cu mm^2 section, no more then 180-200 MVA can be transferred on shore. However, by increasing the voltage, the size of the three-core hits the edge of present manufacturer plants and investment are needed to set up the supply cable chain. At present the rating limit for 220 kV is about 320 MVA. Larger core sections, although theoretically possible, but are likely to require enhancements in cable manufacturer factories, which are not expected to be developed. The cable can also provide a fibre optic conductor for signal transmission purposes from the export platform, and has been assumed to provide communications links as applicable for studies. Table 3.1 provides the electric parameters utilized in the studies.

	R Ohm/km	X Ohm/km	C nF/km	tgδ p.u.	S [MVA]
Three core 220 kV 1000 mm2 Cu	**0.057**	**0.09**	**200**	**1.00E-04**	**320**

Table 3.1: Electrical Parameters

Like all the AC cable, this , due to their capacitive nature, requires reactive compensation equipemente to be installed at one or both ends of the cable. As the cable length increasesm the ampunt of capacitve charging current increases and the amount of active power that can be transmitted decreases. The following graogh shows for Ac cable trasnmission how the maximum real power transferred reduces dramatically for longer cable distances :

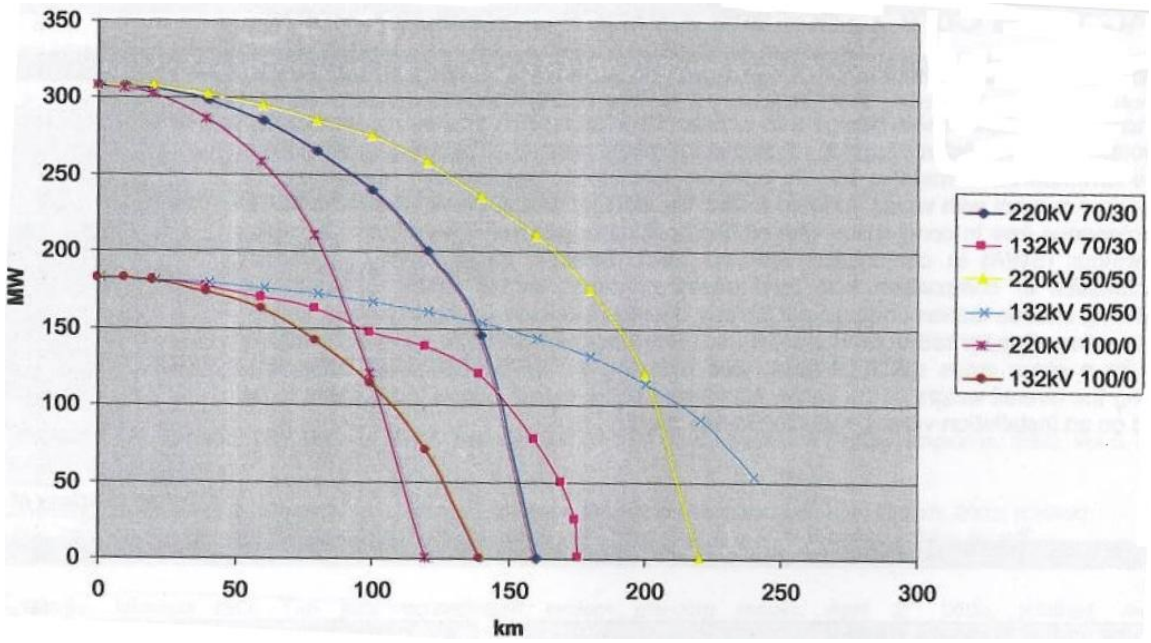

Figure 3.4: Maximum real power transfer in 132kV ans 220kV cables.

In the graph differen scenario have been considered with a 100/0 , 50/50 and 70/30 reactive compensation split between onshore and offshore. It can be seen that the 100/0 is the worst although it is the least expensive as all the reactive compenstionis placed onshore , the weight requirements on the offshore platform are reduced substantially. Another option to increase the capacity of AC transmission cable is to place a third of the reactive compensation half way aloing tha cable on an interstitial offshore platform (33/33/33 scenario). However the costs of this extra platform needs to be carefully considered. For our analysis the best solution has been chosen: a 50/50 compensation.

AC 220 kV single-core

For a larger capacity, a single core arrangement must be used. Cable and accessories are available for this technology. In figure 3.5 an example of the laying is shown.

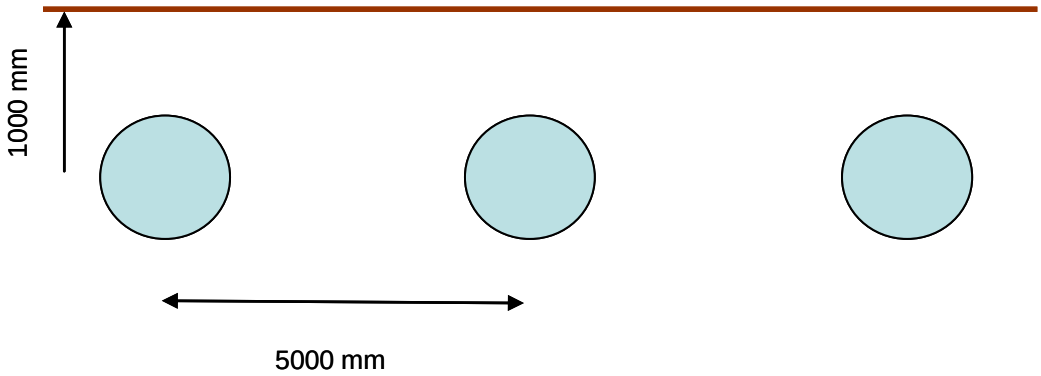

Figure 3.5: Laying Example of Single core

Generally, the cable is placed undergrounded at a depth of about 1m at the bottom of the sea, to protect against anchor strikes. The single core phase are laying at least 50 m apart each other in order to avoid any potential damage during installation of subsequent phases. The general armor cable is shown in Figure 3.6.

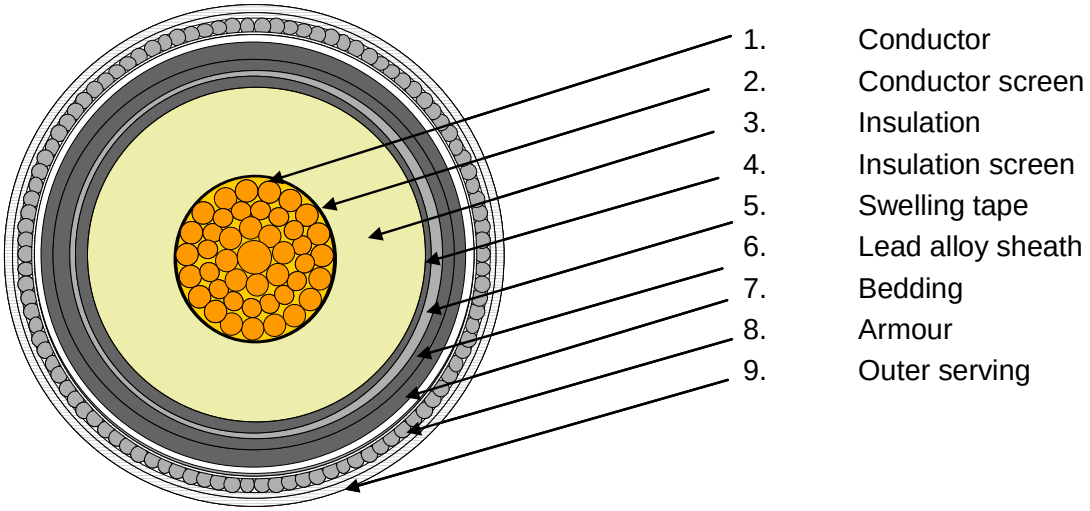

Figure 3.6: Cross Section of Subsea Single core

This is generally a more expensive solution, because of the cable manufacture and installation complexity. However, a higher transfer capacity can be obtained. In table 3.2 the electrical parameters are shown.

	R Ohm/km	X Ohm/km	C nF/km	tgδ p.u.	S [MVA]
Single core 220 kV 1200 mm2 Cu	**0.046**	**0.07**	**198**	**1.00E-04**	**460**

Table 3.2: Electrical Parameters for 220 kV Single Core

AC 400 kV single-core

The 400kv solution is similar to the AC 220kv solution. It is worth noticing that the technology is under development at present for accessories and the solution will be viable in the near future. The electrical parameters used in the studies are shown in Table 3.3.

	R Ohm/km	X Ohm/km	C nF/km	tgδ p.u.	S [MVA]
Single core 400 kV 1400 mm2 Cu	**0.043**	**0.07**	**216**	**1.00E-04**	**930**

Table 3.3: Electrical Parameters for 400 kV Single Core

HVAC transformers

Transformers are required offshore to step up the wind turbine array collection voltage to the high voltages required for efficient long distance power transmission. Increasingly the voltage, reduces the amount of current required to give the same power flow, which reduces the size and hence cost of the conductor required and also reduces power losses in the conductors. Onshore transformers are required if the offshore network is operating at a different voltage to the onshore interface point. Transformers usually are equipped with ON Load Tap Changers (OLTC) to allow the voltage ratio to be varied to keep network voltages within limits. These devices are usually the heavies items of plant on an offshore substation and would normally be situated in the centre of the platform. Transformers ratings need to allow for apparent power (MVA) comprising both the real power (MW) and the reactive power (MVar) provided by wind turbines and reactive compensation as well as reactive power requirement of cables.

Transformer HV terminal can be connected directly to the HV gas insulated switchgear (GIS). This allows efficient use of space on the offshore platform. The GIS is used for switching electrical circuits under both fault and normal operating conditions . One benefits of using GIS it its compact size compared to air insulated switchgear (AIS), which makes it ideal for offshore applications. In addition , the GIS operating components are fully encapsulated offering significant protection in harsher environments such as offshore and coastal installations. One of the disadvantages of using GIS is that the SF6 gas used to provide insulation is one of the most potent greenhouse.

3.3.2. DC technology

DC technology has been proven technically viable since the 50s, using the Line Commutated Technology (LCC), which uses thyristor valve converters, whose commutation is carried out by the ac system voltage, to transfer bulks of power over HVDC system interconnection with a good technical capability, combined with low operating losses. On the other side, HVDC units were very expensive and break-even points with AC only happened around 100 km for submarine. Applications, mostly point-to-point and technology, have been used in very specific cases, like interconnections between un-synchronized countries, compulsory use of long distance cables or to provide controllable power flows between different nodes in a single synchronous AC system . Instead their installation on offshore platforms is difficult because of the extra equipment they required to operate, i.e. switched capacitors banks and harmonic filters. Oil filled and PPL cables have been used as cable transmission technology. They are available up to 600 kV. In recent years advancement in the technology has produced Voltage Source Converter technology (VSC), which uses insulated gate bipolar transistors (IGBT) and gate turn-off thyristors (GTO). The launching of initiatives to develop offshore grids has boosted the possibilities for this technology as it appears attractive in principle to design a DC meshed system in a multi-terminal arrangements. VSC does not need a generating source at both ends of the circuit (unlike LCC) and therefore is the obvious choice for DC circuits required to energize offshore stations. VSC can use the same XLPE cable technology as power can be reversed by reversing the current instead of the voltage, thanks to the controllability of the valves in both operations on and off: that makes VSC function as independent voltage source and it allows the real and reactive power flow to be controlled independently.Since that, VSC can perform black start against offshore AC electrical islands. Moreover, this technology is 40-60% smaller that LCC. At present, DC XLPE cables are available up to 300 kV voltages.

DC LCC Systems

The technology can presently handle with high power levels, however LCC is larger and heavier than VSC and hence will be more difficult than VSC to implement in an offshore location. Application of LCC within multi-terminal system is also more problematic due to the need to reverse polarity when reversing power flow, and the fact that a commutation failure would shut down a multi-terminal scheme.

LCC[MW]	Onshore size[m]	Offshore size[m]	Weight[T]
600	200×120×22	Not used	?

A maximum 2GW LCC system was considered as available for power transfer in the future for the purpose of these studies. This can be obtained by a bipolar configuration using a 500 kV DC voltage with a mass impregnated (MI) cable. Extruded polymeric cables are not used for LCC conductors due to the high harmonic stresses. The system can have a 1 GW modularity in construction as well as in operation; as a bipolar system can actually work in monopolar configuration. An example of the cable and DC units are shown in figure 3.6.

Figure 3.6: Mass Impregnated cable in Bundle arrangement

The conductor can be built from copper or aluminium and the insulation from the layers of high density oil and resin impregnated papers. The insulation is surrounded by a lead sheath (to protect the insulation from seawater) which is then covered with extruded polyethylene. A final layer of polypropylene string and galvanized steel wire armour is applied. The cable can be installed at depths of up to 1650 metres.

Fixed capacitive compensation and tuned filters with associated switchgear are required on the AC bus of each converter and make the space requirements of LCC technology large. The former are required since the converter absorbs reactive power whilst the latter as the converter commonly draws no sinusoidal current and requires AC filtering to remove the harmonics to prevent them entering the AC network. Moreover its need of a strong AC grid to operate otherwise there is the possibility of commutation failures, makes the lC more complex to connect offshore winfarm as additional compensators such as STATCOM or rotating electrical machine are required to provide an AC voltage source compare to VSC.

HVDC VSC Systems

Voltage source converters (VSC) are bidirectional rectifiers/inverters used to convert between AC and DC for HVDC transmission. As already said, VSC is an alternative to LCC HVDC and utilizes newer technology offering more flexibility in terms of operation and the requirements of the AC grid it is connected to. VSCs can operate through 0MW without the need to swap pole voltages and can therefore use extruded cables. VSC HVDC is able to connect weak AC grids, allowing connections to electrical islands such as offshore wind-farm without the need for additional equipment such as STATCOM(Static Compensators) to provide a commutation voltage. HVDC VSC technology can be used to build DC multi-terminal networks with greater flexibility compared to LCC HVDC. The technology is usually installed in bipolar configuration with

each pole of equal voltage magnitude from the earth but opposite in polarity, e.g ±300kV, Bipolar systems can be designed to be switched into monopolar mode with an earth return (if allowable) or metallic return (if installed) by connecting two VSCs in series. This topology allows the HVDC link to operate at half rated power in the event of a pole failure.

For the purposes of this study, a 1 GW system is expected available and assumed, using a 300 kV DC rating with a 1667 Amps XLPE cable. At present, no monopolar configuration has been proposed and the system can therefore be only in an ON/OFF states. The limitation with the power capability is currently the rating of XLPE extruded cables. Higher voltages and power ratings could be achieved with HVDC VSC with mass impregnated cables or overhead lines: the former are typically more expansive.An example of DC cables are shown in figure 3.7.

Figure 3.7: Extruded Cable

Subsea XLPE cables are segments copper insulated by extruded XLPE layers. As there are no magnetic losses with DC cable, galvanized steel wire can be used for the armour. Galvanised steel wire has better tensile properties the copper or aluminium and as HVDC cables are lighter than HVAC cables for the same amount of transmitted power, there is less tensile force during laying , reducing the stress on the cable.

Table 3.4, shows the electrical parameters for both LCC and VSC cable technologies used in the studies.

DC cable	R	X	Tgd	C	Snom
Type	Ohm/km	(Ohm/km)	(p.u.)	(nF/km)	MW
XLPE 1800 mm2 Cu 320 kV	**0.0101**	na	na	na	1000
PPL 2000 mm2 Cu 500 kV	**0.009**	na	na	na	1000

Table 3.4: Electrical Parameters for DC cables

VSC tecnology is available as two, three or multilevel covnerters. Multilevel VSC is a recent development and has the advantage of requiring less AC filtering and has lower loss per converter.Losses for a multilevel converter are aproximately 1,3% of transmitted power per converter, while two level converter losses are approximately 1,6-1,9% per converter. Multilevel converters are more expensive though.

Indicative dimensions for 2-level VSC are as follows (5):

VSC[MW]	Onshore size[m]	Offshore size[m]	Weight[T]
1000	120×60×23	80×40×35	2000

Moreover the VSC HVDC is able to black start an offshore island network energising the HVDC link with the onshrioe converter and then ramping up the voltage at the AC terminals of the offshore converter.This reduces transient caused by the inrush of energising tranformers and cables.

In the table below are summurized the technology and thier usage in the two interconnection system, DC and AC:

	LCC HVDC	VSC HVDC	AC
XLPE cable		✓	✓
MI cable	✓	✓	

3.3.3. AC versus DC

There are technical and economical reasons for the selection of AC or DC technologies. However, when dealing with cable connections ,the area can overlap and a large 'grey zone' which is dependent on the power transmitted, the load factor of the connection, the technology used, the voltage level and the system configuration. In principle, some technical issues prevent the use of AC for long distances. This is due to the AC electrical parameters of the cable, which determine a large charging current and voltage rise in particular system loading conditions. A suitable reactive compensation strategy can be utilized but, even if employed provides a limit in the range of 100-150 km for 400 and 220 kV respectively. When exceeding these distances, DC connection is necessary. The technical advantages for a DC link are related to the transmission losses, as no skin effect and induced currents take place. However, high losses are also part of the AC/DC unit, so that only after a suitable length the DC system is economically preferable. An analysis of the breakeven point is carried out based on an example of 1 GW transfer, point to point. The results are shown in figure 3.8. No reliability criteria are taken into account.

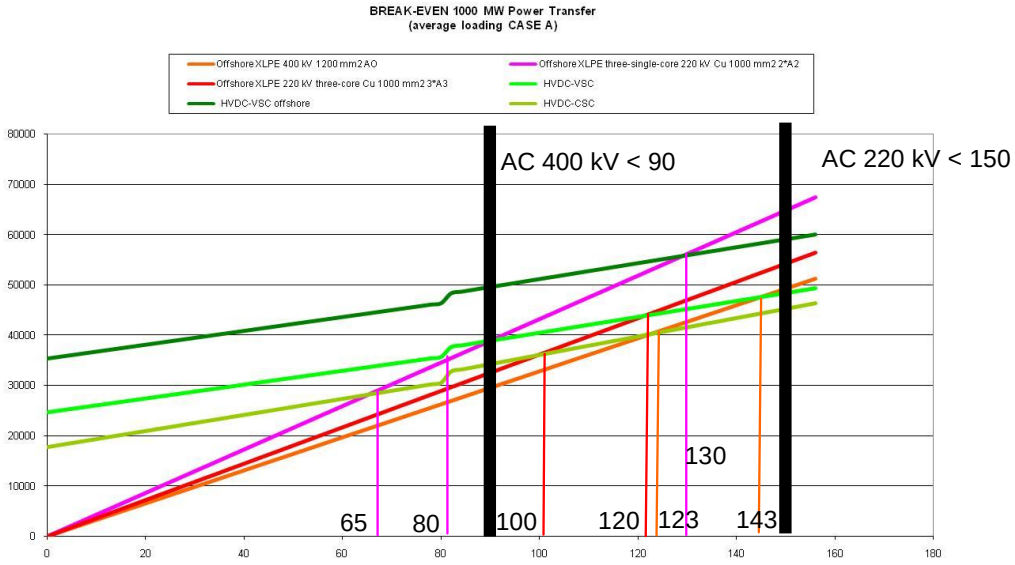

Figure 3.8: Cable break-even distances

The best AC cable solution is 400 kV XLPE. It benefits from a smaller number of cables to achieve the same capacity, which reduces cable laying. It should be noted, however that the feasible maximum single length is in the range of 90 km.No break-even point exists with HVDC technology within the length that is feasible with AC cable technology. The AC 220 kV can be extended further due to the lower charging current of the cable. The limiting distance is in the range of 150 km. It should be noted that both 220 kV technologies (single and 3 core) are more expensive than the 400 kV solution in the analysis, because of the number of circuits required to deliver the same power. The AC single core (magenta line), quickly becomes the most expensive, the break-even point is reached with LCC technology at 65 km, VSC onshore at 80 km and VSC offshore/onshore at 130 km. Alternatively, AC three-core cable has a breakeven point at 100, 120 and above 150 km for LCC, VSC and offshore VSC, respectively. For distances above 150 km, only DC technologies

are feasible with LCC more efficient for a point to point circuit. For distances below 65 km, AC technology is feasible with AC 400 kV more efficient for a point to point circuit. For length between 65 and 150 km, both technologies can be applied with limits on the 400 kV. VSC is always more expensive than conventional due to higher losses, however, it can be the only feasible solution for connection offshore or in an evolving scenario from a point-to-point to meshed DC system.

An interesting aspect of XLPE cable is its adaptability to be operated at either AC or DC. The two technologies are manufactured in a slightly different way and the insulation compound needs further treatment if it is used for DC. Therefore, in the longer term period, an infrastructure that is born AC because of short initial length and that becomes either not technically feasible or desirable to be operated as AC after some years, may be modified to DC operation by placing AC/DC conversion units into the circuit.

3.4. The reactive problem

The reactive problem has become more relevant and more important due to the increasing complexity in the operation and structure of the system, together with an expected larger amount of HVAC Cable, and has a significant influence on secure and economic operation of the systems itself. In Fig. 3.9 are shown the percentage of cables in the word transmission system.

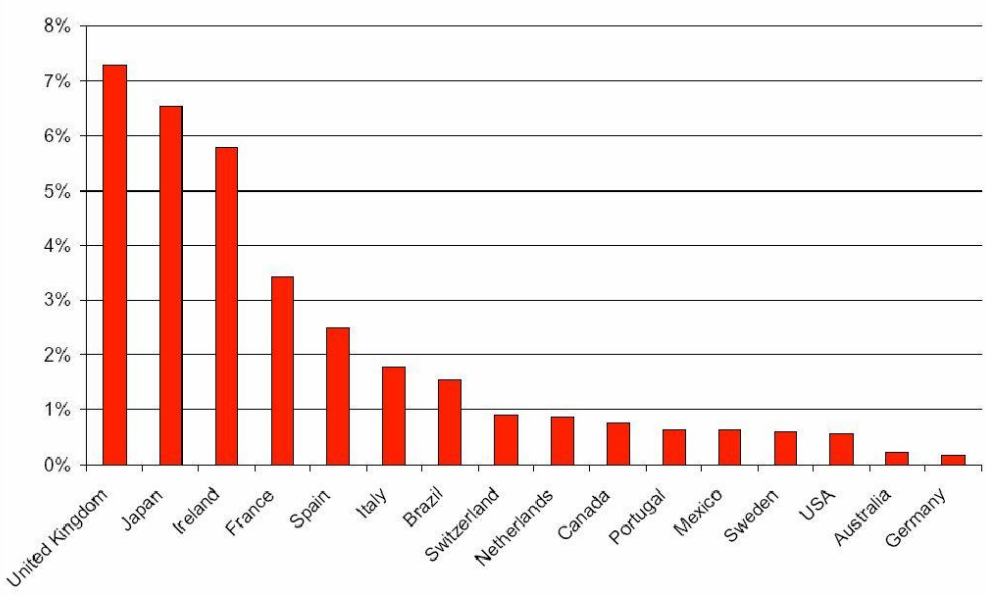

Figure 3.9: Statistics of AC underground cables in power networks [CIGRE]

One main priority for a system is to maintain adequate voltage magnitude so that, when the system nominal load increase, the actual power transferred to the load will increase. This ability is referred to as voltage stability and if it not guaranteed, a system voltage collapse that may lead to partial or full power interruption in the system may occur.

Along a transmission system, each component of the grid plays a role in the reactive power exchanges: cables, transformers equipped with on-load tap changers, wind turbines and converters. While some of them are uncontrollable devices from the reactive point of view, there are many reactive compensation devices used to provide technical solutions to voltage stability problems. Let's describe their main feature and limitations.

CABLES

Considering the cables spoken about in the previous paragraph, some studies carried on by Eirgrid have put in evidence for diverse technologies of cable the correspondent reactive generation. This investigation has clearly concerned the AC cables, which produces a considerable amount of reactive power with a huge impact on the flows along the grid, whilst the DC cable itself don't deal with this power form which is instead associated to the converter, i.e.is the interface between AC and DC areas.

For the base case in Irish only study, In Figure 2 the extension of BASECASE ESP scenario analyzed in the previous chapter is shown in terms of kilometers of circuit for different alternatives and a relevant estimation of the quantity of reactive power to be compensated is shown in Fig.2.

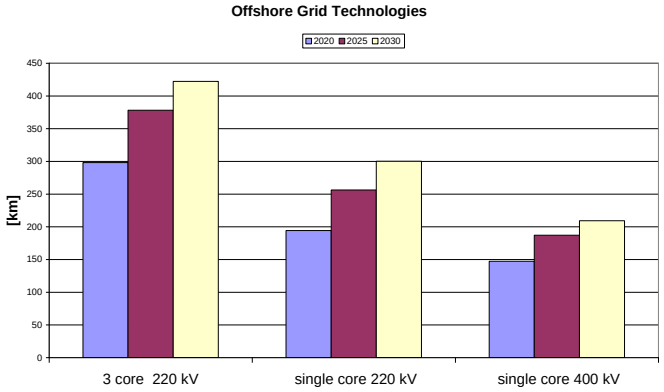

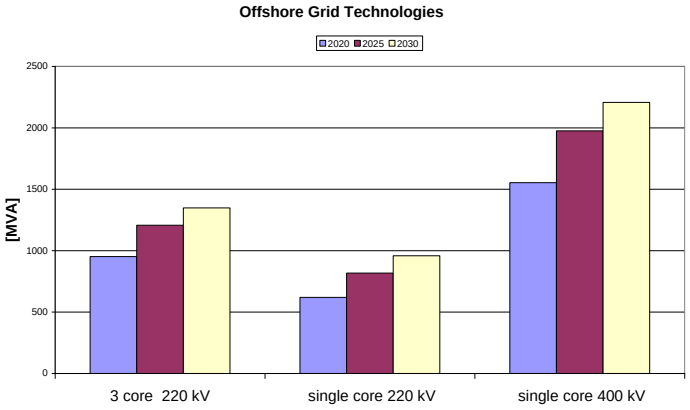

To point out is the dependency of the reactive power produced by cable by the square of the voltage. Therefore, not surprisingly, the major impact is due to use of a 400 kV offshore strategy, as oppose to a 220kV as the 220 kV single core has the least reactive impact.

For the scenario MID5, the results are heavier due to the more installed wind power.

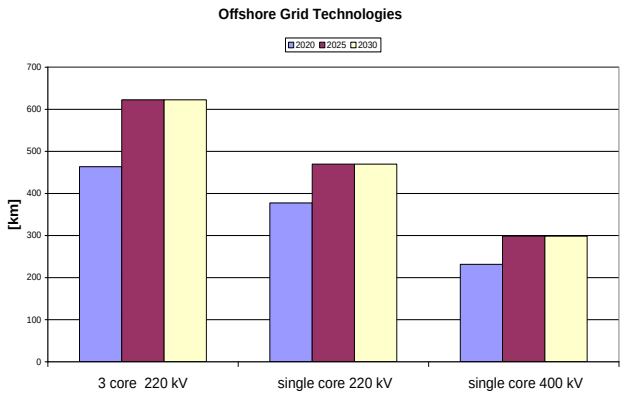

In

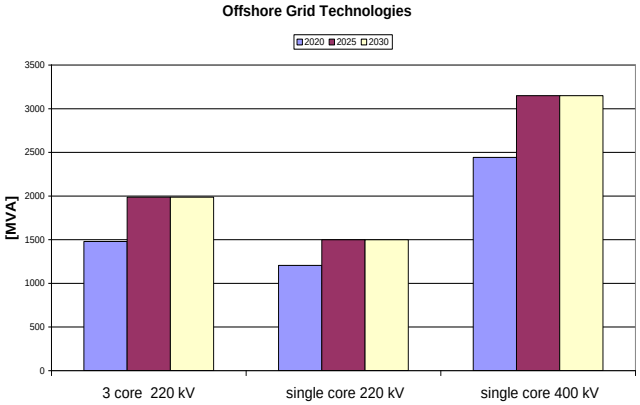

this scenario moving from 300 to 700 km determines the variation as a result of moving between each cable type from Table 8.4. The increase in the length is due to the increase of the installed wind power. In term of reactive impact single core 220 kV is slightly better than the three core alternative.

For the MID10, due to a more dispersed wind offshore generation expansion, the requirements in this ESP scenario for the variation in cable type is the widest of those analysed. In 2030 it is expected between 600 and 1000 km, see Figure 8.12.

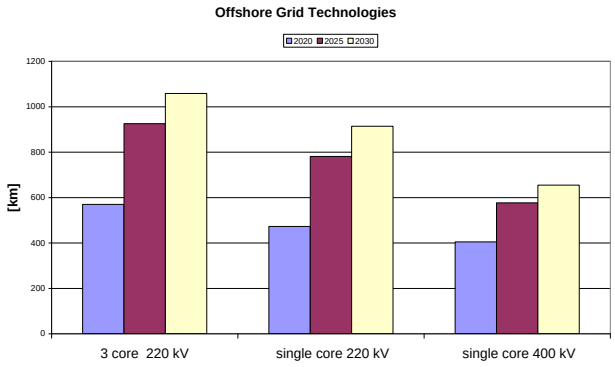

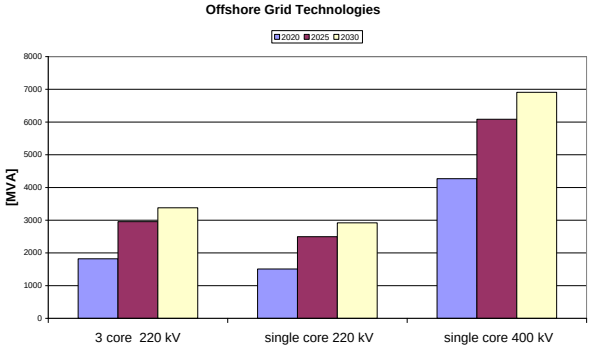

To provide absolute certainty, the reactive compensation issue for the amount of AC cable in these scenarios would require a more detailed and robust examination study in order to verify that the ESP's could be sustainably connected from only the All Island transmission network. From the results collected it is clear the dependence of reactive production from the length of the system.

There are some example of worldwide where large portion of the system is undergrounded; in Singapore, where a 650 km of 220 kV Cable and 111 km of 400 kV Cable have been realized as well as in TEPCO with 1700 km of 275 kV Cable and 80 km of 500 kV Cable.

The reactive compensation has economics benefits that may be relevant in a long term planning. These can be categorized as reduced power losses, exchanging reactive power flow to real power flow and increase transfer capability limit due to increased voltage stability,although the main function of var devices reactive power compensation is for voltage support to avoid voltage collapse. The reduction of power losses is explained considering that reactive power is principally a local issue and its injection reduces the reactive flow along the link, since the real power losses are connected to the square of the current, losses will be reduced if the current is reduced. This loss reduction represents reduced total generation and saving in cost. Besides, this leads to transferring cheaper real power while keeping the same transfer capability.

So, when the distances becomes relatively long, a DC alternative could be considered, compared in term of how economically viable it would be for this application, considering the high initial investment cost for the converters with the compensation that the AC cable would require. In the DC option there is no reactive power production by the cables, such as the AC cables, that themselves represent a VAr sources that have to be taken into account as supply reactive power into the grid and in an optimal view to reduce losses, long AC cables need, to be feasible. But, on the other side, the DC transmission requires converters, which are fed by reactive power that is up almost the 50-60% of active power transmitted. Not less important, they represent the major cost for a DC asset.

Shunt capacitor can be mechanically switched or fixed and are installed as banks at substations or near loads. Their main advantage is the much lower cost compared to whatever other var sources. Moreover their switching speed can be quite fast with current limiting reactors to minimize switching transients. Among the disadvantages there is that reactive power output drops with the voltage squared and that for transient voltage instability the switching may not be fast enough to prevent induction motor stalling. If these ones are large in size, they may be equipped by tap changers so they can be controlled in smallest steps. Hence, a precise control of voltage is not possible, but only in a discrete way. If voltage collapse results in a system, the stable parts of the system may experience damaging overvoltage immediately following separation. Beyond a certain level of compensation, a stable operating point is unattainable. Capacitor banks are modelled as discrete devices, configured with several steps to provide a limited amount of control variable. For the converters, switched shunt capacitors may be substituted in their function by AC harmonic filters located in a HVDC station, with the advantage to meet a double purpose: provide capacitive reactive power and filtering

unwanted harmonic from the converter busbar. So, where there is a requirement for additional reactive power support in excess of that provided by the AC harmonic filters, shunt capacitors are installed and it is more common to tune them at a known frequency , using a small series reactor: as tuning the capacitor to a known frequency avoids the risk of unpredicted resonances occurrence with the power system, which could lead to capacitor failure. Moreover if the reactive power generated by the harmonic filters required for filtering may exceed reactive power exchange limits, particularly at low DC, it is sometime necessary to include one or more shunt connected reactors to provide additional reactive power absorption. Therefore , shunt reactors are mainly used to keep the voltage down by absorbing reactive power in the case of light load and load rejection. They work for compensating the capacitive load of transmission lines. For offshore applications, the open rack outdoor capacitor banks are available up to 600Mvar and 765kV.

Terminal characteristic of shunt capacitor (6):

On the other side, shunt reactors are mainly used to keep the voltage down by absorbing reactive power in the case of light load and load rejection. They work for compensating the capacitive load of transmission lines and provide a means to regulated network voltage. Shunt reactors are utilised at the onshore interface point and possibly at the offshore substation platform.

Especially, due to the increasing need for fast response for power quality and voltage stability, the shunt dynamic var compensators FACTS (flexible AC transmission systems) such as Static var Compensators (SVC) and Static Synchronous Compensators (STATCOM) have become feasible alternatives to a fixed reactive source, and therefore have received intensive interests.

A static var compensation (SVC) is a power electronic device whose output is adjusted to exchange capacitive or inductive current so as to maintain or control, in a fast and precise way, specific power system variables, which typically is the terminal bus voltage. The only problem is a degradation in reactive capability as voltage drops. SVC are built froma combination of thyrisotr controlled reactors (TCR), thyristors switched reactor (TSR) and thyristor switched capacitors (TSC).

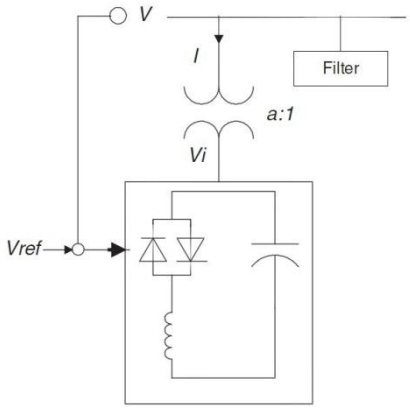

Figure 3.10: SVC

SVCs can be used with AC or LCC HVDC based offshore transmission networks but are not requires for VSC HVDC because it can inherently control Mvar output.

As with the SVC, the STATCOM provides dynamic reactive power to the AC system. However, whereas the SVC uses reactive passive component to provide the reactive power, the STATCOM generates a synthetic, sinusoidal voltage waveform at its terminal using a power electronic converter. So, it is a voltage-sources converter based device, which convert a DC input voltage into an AC output voltage in order to compensate the active and reactive needs of the system. The synthetic sine wave can be controlled in amplitude and phase with respect to the AC system voltage waveform. By adjusting the phase of the STACOM voltage to be above or below the AC system voltage waveform, reactive power can be generates or absorbed. As main positive characteristic, their maximum reactive power output is not affected by the voltage magnitude . Therefore, they exhibits constant current when the voltage is low under the limit. In addition, the advantage of a STATCOM over an SVC are the reduced land area requirement (as the passive component are eliminated), a faster response time and an ability to provide greater capacitive var output of an SVC falls in proportion to voltage squared, whereas that of a STATCOM only falls in proportion to voltage. As disadvantage there is the lack of a short-term overload capability of generators and synchronous condensers.

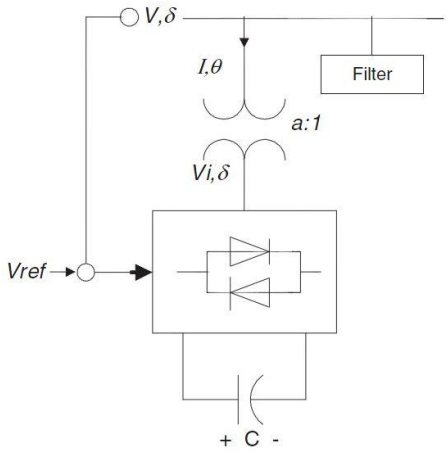

Figure 3.11: STATCOM

A comparison of the costs for shunt controller is given in table 3.5:

Shunt controller	Cost(€/kvar)
Shunt capacitor	8
SVC	40
STATCOM	55

Table 3.5: Cost comparison of shunt controllers

These are the tools will be modeled into the mathematical model as explained in chapter 5.

CHAPTER 4
SUMMARY OF REACTIVE POWER PLANNING (RPP) METHODS IN THE LITERATURE

4.1. A first glance

Since the importance to study the reactive issue for the reliability and security of the grid has emerged, var tools has been used into the network to guarantee a satisfactory system operation and adequate voltage levels as well as the reduction of the transmission losses, at a minimum cost. Traditionally the location for placing these were either simply estimated or based on the TSO's experience defined. An overcome of these assumptions is the reactive power planning RPP (or var planning) methodology, whose focal purpose is to provide the system with sufficient and optimal allocation of reactive power resources (RPS) to enable it to be operated economically and in secure conditions in both pre and post contingency states and to tick future location, types, sizes and times of the installation of RPS. Such problem, at a first glance, can be formulated as an OPF (Optimal Power Flow) as it involves the determination of the instantaneous "optimal" steady state of an electric power system. It is a large scale nonlinear optimisation problem (NLP), often not easy to solve. That is because the OPF is not a convex problem: the positive properties of the convex functions, that any local optimum is also globally optimal, cannot be used. Moreover the presence of switchable shunt devices when they are modelled as discrete control variables complicates the research of the solution further. Therefore the success in getting a result to the var investigation is a good combination of a smart mathematical formulation with an as well as fine solving tool to implement it considering that most general nonlinear programming techniques might converge to a local minimum instead of a unique global minimum as drawn in fig. 4.1. Also the initialisation decoupling may lead to different path of solutions.

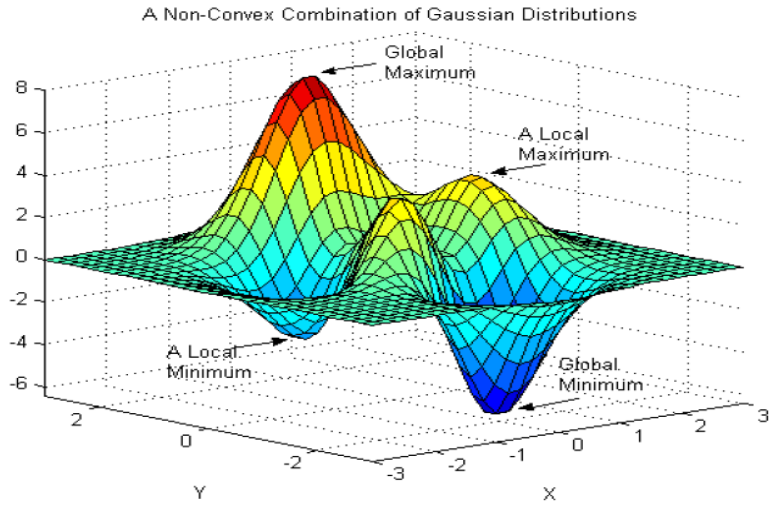

Figure 4.1: Non convex problem

4.2.Mathematical model: Objective functions

Generally, an optimization problem has, as mathematical model, an objective function (OF) to be minimized (or maximized) and some constrains to fulfil:

$$Min\ or\ Max\ \ f(u,x)$$

$$subject\ to$$

$$equality\ constrains\ \ g(u,x)=0$$

$$inequality\ constrains\ \ h(u,x)\geq 0$$

Where u is the set of controllable variables in the system and x is the set of dependent variables called state variables. There is no a single formulation of the problem and a single solution approach but they may vary considerably in their adaptability to the modeling and solution requirements of different engineering application. Considering the RPP, it is a large-scale nonlinear optimization problem because of the large number of variables and uncertain parameters in the model and the nonlinear nature of the OF and constrains. Unlike conventional power flow algorithms that do not automatically minimize any objective functions but only obtain a single feasible operating point, the aim for this OPF is to search the optimal control variables for a steady-state power system with a given objective function. Because of the complicated objective functions, constraints and solution algorithm RPP is identified as one of the most challenging problems in power system. All the feasible solutions identify a feasible region. An optimal solution can be selected from the feasible region to obtain a desired objective by adjusting the optimal setting for the controllable variables subject to the constraints. Some main assumption are typically considered while formulating the RPP in the literature (7):

- the whole system under analysis is balanced;
- the real and reactive power represent fundamental frequency power and any additional power at harmonic frequency are negligible;
- in the model the size of the var source is treated mainly as a continuous variable though it is in fact discrete.
- The reactive capability of a generator is portrayed by the conventional PQ-diagram but for the planning study it is sufficient to assume a fixed upper limit Q_{max} relevant to the generator MW output.

Making a review of the OF for RPP, it is possible to summarize different types depending on the optimization strategy chosen while fulfilling the requirements of the grid codes. Some may be cost-based which means to minimize the investment cost of the reactive supply facilities required, real power losses costs since they are quoted using the full feed-in tariff and fuel costs.

Other possible objectives refer to the secure operating condition of the system: for example, they may consist in minimizing the deviation from a given schedule of a control variable (i.e. voltage) or in maximizing voltage stability margin.

More useful it may be to study a multi-objective functions (MOF), built by a linear combination of *i* single OFs. The general definition of a MOF comes above and usually the weights α_i to sum the different OFs are decided by translating the power or the energies or , in general, the units of some OFs into euros.

$$Min\ or\ Max\ \sum_i \alpha_i \cdot f_i$$

Leaving the MOF concept, in the following we will discuss what kind of issues, taken one by one, may be OFs for an RPP analysis.

a. Continuous var cost

The simpler function to consider is the investment costs in reactive production equipment; it may be described in two different ways, leading to two different types of problems. The first formulation, resulting in a NLP problem, is to model var sources costs through a linear function with no fixed costs as:

$$f_1 = \sum_k C_{1k} \cdot W_{ck}$$

where:

W_{ck} is each newly installed var device

C_{1k} is the cost for each var device

Hence $W_{ck}$is a vector composed of all the var sources size and the costs C_{1k} are commonly expressed as €/(Mvarh).This means that the problem does not account for the var device sizing. This formulation would also bias a solution toward placement of several small reactive size sources instead of a small number of larger ones.

b. Discrete var cost

To avoid this consequence, a second formulation for the OF is:

$$f_2 = \sum_k (C_{0k} + C_{1k} \cdot W_{ck}) \cdot x_k$$

where:

C_{0k} is the fixed cost for each var device [€/ hour]

C_{1k} is the variable cost for each var device

x_k is a vector or binary variables

Therefore, the introduction of fixed costs, The considering the fixed cost C_0 complicates the problem from a NLP to a mixed integer non linear programming (MINLP) because of the presence of the binary variable x_k to indicate whether the var source will be actually installed or not at a bus k. This slight difference in the cost model, however, leads to huge differences in the optimization model and the corresponding mathematic technique to solve it.

c. var cost and real power losses

When the aim is to combine the search for the best investment cost keeping the losses as low as possible, a practical useful common objective may be considered: it is based on the var costs above described in f_2 together with a term C_2 to represents the cost of real power losses:

$$f_3 = f_2 + \sum_{j}^{N_c} C_2 \cdot (P_{loss})_j$$

where:

C_2 is the €/ MWh

P_{loss} are the losses valuated at the slack bus

N_c number of cases

This evaluation can be made not only for losses consumed in the base case but even in all contingency cases.

d. Minimization var cost and generator fuel costs

An alternative to the cost of real loss is to use the fuel cost for generation as direct measure of the operating cost. In fact, the minimization of the real power losses cannot guarantee the minimization of the total fuel cost. Actually the minimization of the total fuel cost includes the cost reduction due to the minimization of the real power loss. Therefore, an OF is so written considering, beyond the investment for the reactive sources, the cost of the individual generating units i:

$$f_4 = f_2 + \sum_{i} (a_0 + a_1 \cdot P_i + a_2 \cdot P^2{}_i)$$

where the cost function for the i-th generators is modeled by a quadratic function and $a_0, a_1[\frac{€}{\mathrm{MW}}], a_2[\frac{€}{\mathrm{MW}^2}]$ are the relevant cost coefficients, which are not always available in electric market.

e. Minimization deviation from a specified point

So far, only costs have been taken into account, but the goal of the RPP may deal with both economical and security aspects, considering that the main function of var device compensation is to provide voltage support to avoid instability or a large scale collapse. Therefore the objective may consider some technical merits such as either the *minimum deviation of the control variable*, such as voltage, from a given target value:

$$f_5 = \sum_{i} \frac{|V_i - V_{target}|}{V_{imax}}$$

or, *voltage collapse*, with the dual purpose of maintaining voltage profiles within specified limits, and increasing the security margin of anticipated operating conditions with respect to voltage collapse.

$$f_6 = \frac{\sum_i S_i{}^{critical} - \sum_i S_i{}^{normal}}{\sum_i S_i{}^{critical}}$$

where S_i^{normal} and $S_i^{critical}$ are respectively the MVA loads of load bus i at the normal operating state B and at the voltage collapse critical point (PoC) A as shown in fig. This analysis is carried on for power system that are more stressed and for which voltage is a poor indicator of proximity to system collapse condition.

figure

It is important to underline that if both security and cost are included in the same objective function to build a MOF, then the weights have to be defined accordingly.

4.3.Mathematical model: Constraints

The remaining part of the problem is made by the equality and inequality constraints which have describe the real limits into which the actual operating.

Normally, they include non linear AC power flow equations corresponding to both real and reactive power as equality constrains.

Moreover, the constraints should also consider transmission security (or contingency) and voltage stability. Some researches (7) use the topology of constraints as key for a model classification: an optimization model is called the OPF model if respects the PF in the normal state (N). When the analysis is spread over not only normal state , but also the contingency (N-1 state), this is referred to as Security constrained OPF (SCOPF). Since there is not the guaranty that voltage collapse margin still exists when contingencies actually occur, including some voltage stability constraints in the contingency state results in the so called SCOPF_VS model.

The different OF described in the previous section, may be combined with one of these constraint models to formulate the RPP problem except that voltage stability may be modeled as an objective function or as constraints. Adding constraints requires much more computational effort, in general. The challenge lies in how to efficiently incorporate the expected new stability margin into the optimization model of var location and sizing. The challenge of security constraints is mainly computational rather than in modeling, because each contingency case can be modeled in a way similar to the base case but it makes the problem more and more large.

In the following, the main formulation adopted for the constraints are presented.

The OPF is a static constrained non linear optimization problem and its development has closely followed advances in numerical optimization techniques and computational methods. Its formulation is :

$$\begin{aligned} Min \quad & f(u,x) \\ subject\ to \quad & g(u,x) = 0 \\ & h(u,x) \geq 0 \end{aligned}$$

The objective function $f(u,x)$ is scalar; the equality constraints $g(u,x)$ are the conventional power flow equations and sometimes they may include a few special equality constraints such as the limit of the number of potential var compensation devices. Inequality constraints $h(u,x)$ represent the physical limits on the

control variables u, and operating limits on the power system. Some possible items for the variable u and x are listed in the Table 4.1:

Control variable u
Generator active power output P_{gen}
Regulated bus voltage magnitude V
Variable transformer tap setting
Phase shifters
Switched shunt reactive devices
Load to shed in special conditions
State variable x
Voltage Magnitude at load buses
Voltage phase angle at every bus ϑ
Line flows

Tabel 4.1:Variables

The typical equality constraints are the power flow equation for both real and reactive power:

$$\begin{cases} P_{gi} - P_{li} - P(V,\vartheta) = 0 \\ Q_{gi} + Q_{ci} - Q_{li} - Q(V,\vartheta) = 0 \end{cases}, \qquad \forall\, bus\ i$$

The typical (minimum set) inequality constraints, for the N-secure state, are described in Table 4.2:

Control variable limits	Explanation
${P_{gi}}^{min} \le P_{gi} \le {P_{gi}}^{max}$	Real power generation limits for the i-th generator
${V_{gi}}^{min} \le V_{gi} \le {V_{gi}}^{max}$	PV bus voltage limits for the i-th generation bus
${T_l}^{min} \le T_l \le {T_l}^{max}$	Tap changer limits for the l-th tap-changer
${Q_{ci}}^{min} \le Q_{ci} \le {Q_{ci}}^{max}$	var source size limits for the i-th compensation device
State variable limits	
${Q_{gi}}^{min} \le Q_{gi} \le {Q_{gi}}^{max}$	Reactive power generation limits for the i-th generator
${V_i}^{min} \le V_i \le {V_i}^{max}$	PQ bus voltage limits for the i-th load bus
$\lvert LF_l \rvert \le {LF_l}^{max}$	Line flow limit in terms of apparent power

Tabella 4.2: Constaints

With the development of the SCOPF model, the goal of RPP is extended so as to guarantee feasible operation both under normal N-secure condition and after contingencies, such as outages of transmission branches, generation units or substation buses (N-1 conditions). Therefore the model integrates the security (contingency) constraints into the OPF formulation. The additional contribute are that the nonlinear equality and inequality constraints must be fulfilled under N and N-1 conditions. Therefore the SCOPF determines an optimal operating point such that, in case of any contingency in a given list, the post-contingency state will remain secure (within operating limits). The expanded formulation which include contingency constraints is :

$$Min \qquad f(u^0, x^0)$$

$$subject\ to \quad g^k\left(u^k, x^k\right) = 0, \text{ for } k = 0,1, \ldots . N_c$$

$$h^k\left(u^k, x^k\right) \ge 0 \text{ for } k = 0,1, \ldots . N_c$$

where the superscript "0" represents the pre-contingency case being optimized and the superscript "k" represents the post-contingency states for the N_c contingency cases.

The complexity of the SCOPF model increases significantly compared with the OPF since for each bus both the pre contingency and post contingency must be fulfill: this is equal to verified for each bus $(k+1)\cdot m$, where k are the number of contingencies and m are the total constraints.

Moreover, the SCOPF is aimed at scheduling the power system controls to achieve operation at a desired security level. The security levels treated that can be adopted are: level 1, "secure" and level 2 "correctively secure".

Under the security level 1 (preventive mode), which is more expensive than the level 2, all load should be supplied and no operating limits should be violated in case of a contingency; the power system survives to any of the relevant contingencies without relying on any post contingency corrective action.

Under the security level 2 (corrective mode), any violation caused by a contingency can be corrected by appropriate control without loss of load, within a pre-determined period of time. Since the SCOPF takes into account steady state contingencies, its solution is not assured to be transiently stable.

Due to the growing interest to include voltage collapse as constraints in RPP, since reactive power compensation can change voltage collapse margin that in turn will impact the generation dispatch, models that take into account this additional constraints in the contingency states are defined as SCOPF-VS. They exploit the voltage collapse analysis based on P-V and V-Q curves, to determine how far the system is from the critical point calculated as an optimization problem, considering a given pattern of load increase and generator. Including a security margin (SM) as the constraint has an important security advantage: beyond to guarantee that the voltages at all buses lie within a predefined range at normal condition, it ensures the operating point even after contingency is away from the critical point at least by a pre-defined "distance" measured in MVA, called S-margin or MVA-margin.

Fig 4.3 shows the PV curves before and after contingency and the reduced SM at post-contingecy:

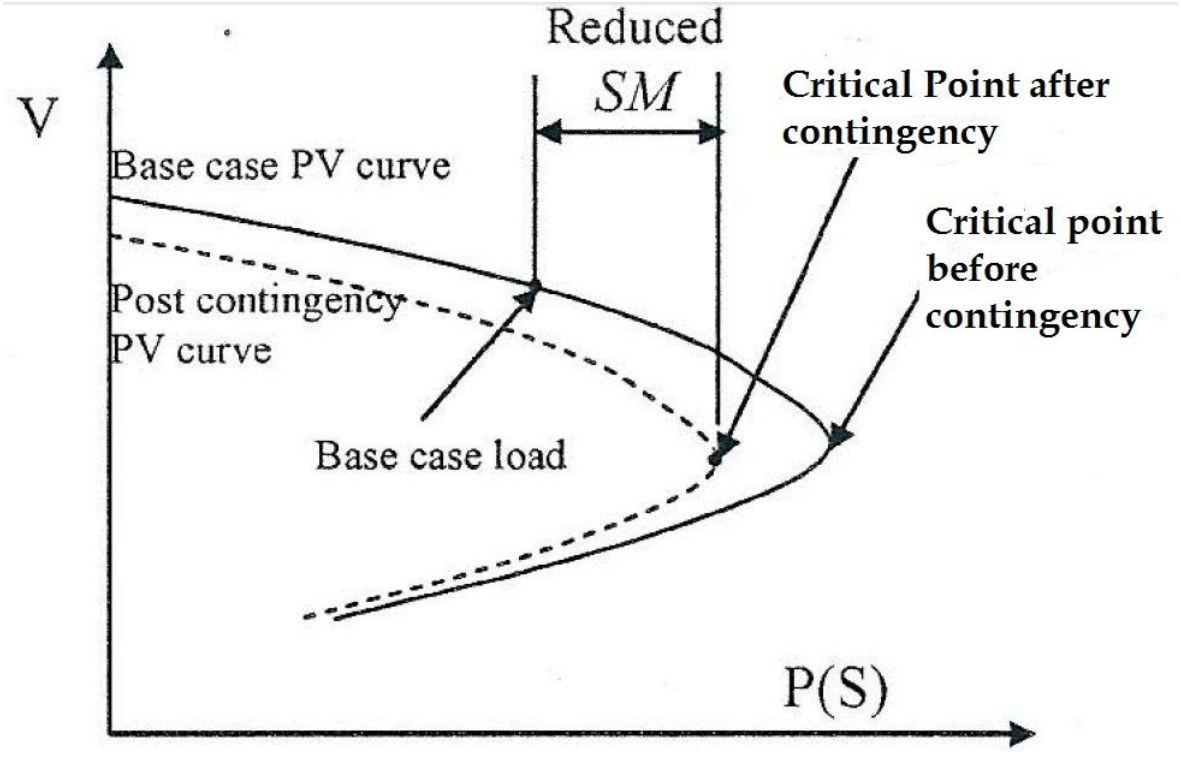

Fig 4.2: PV curve

The voltage collapse margin may be represented by a voltage security index to indicate the closeness to critical point from the present system load level and it may be used into a RPP problem to choose the weak buses in order to reduce the complexity by reducing the candidate locations.

The complexity of the SCOPF-VS lies in the requirement of having two sets of network variables and power flows constraints corresponding to the "normal operation point" and to the critical state for each contingency considered. As an alternative some papers (8) have explored the use of statistical linear/quadratic approximation of the path of critical point, as shown in fig.4.3:

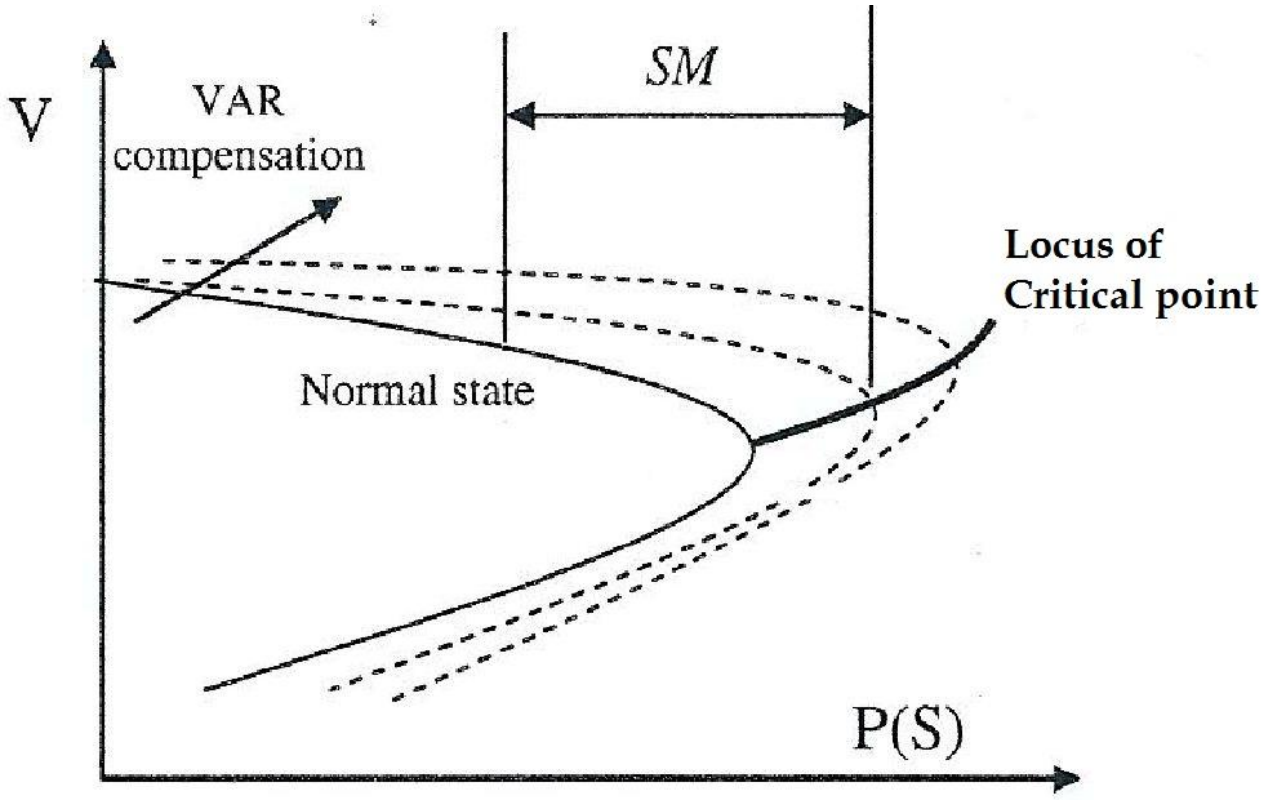

Figura 4.3:PV curve with quadratic approximation for the critical point

It should be noted that some alternative approaches in RPP use sensitivities analysis based on various indices to avoid the complicated optimization formulation, with a trade-off in accuracy. Actually the sensitivities analysis may also be used as a pre-screening to filter some less competitive solution and then they are combined with an optimization-based approach to find the best solution.

4.4.Mathematical model: Solving methods

The solution techniques for the OPF problem have evolved over many years and from the literature (9) nine categories of methods have been finally pointed out;, each of them has advantages as well as disadvantages in trying to solve the RPP. These can be divided into three main groups depending on whether they can find a global solution: conventional algorithms, intelligent searches and fuzzy set.

The first group emphasizes accurate and exact computation, but may fall down on achieving the global optimum, converging only to a local optimal solution; consequently, a new category of advanced optimization tools, the second, has emerged to cope with some of the traditional optimization algorithm shortcomings, being able to guarantee the global optimum, but they need more computing time. The last

application, fuzzy set, addresses uncertainties in objectives and constraints. These categories include methods as follows:

1. conventional algorithms

- Linear Programming (LP)
- Nonlinear Programming (NLP)
- Mixed-Integer Nonlinear Programming (MINLP)
- Decomposition Method
- Heuristic Methods (HM)

2. Intelligent searches : stochastic search algorithms advanced optimization

- Simulated Annealing (SA)
- Evolutionary algorithms (EAs)
- Tabu Search (TS)

3. Fuzzy set application

In the following a short description of the first two sets of the methods is provided.

Linear Programming (LP)

The LP approach has several advantages:

- the reliability of the optimization, especially regarding the convergence properties.
- Another is its ability to recognize problem infeasibility quickly.
- The ability in accommodating a large variety of power system operating limits, including the very important contingency constraints.

Nevertheless, its range of application in the OPF field has remained somewhat restricted because of the inaccurate evaluation of system losses due to the linear assumption and its following inability to find an accurate solution as opposed to the nonlinear power system model; moreover, it has a high possibility to be trapped in a locally optimal solution. This method has been adopted by ESP as already described in Chapter 2.

NON Linear Programming(NLP)

To solve a nonlinear programming problem, the first step is to chose a search direction in the iterative procedure, which is determined by the partial derivative of the equations, on a so called Gradient Base. Taking into account the first partial derivate, the method has referred to as Generalized Reduced Gradient (GRG) for OPF implementation. If the second-order partial derivatives (the Hessian) of the power flow equations and other constraint are computed, the method is the Newton's Approach based on successive quadratic programming (SQP). This method solves the Karush-Kuhn-Tucker(KKT) conditions for the original problem and it is better than the GRG method as far as convergence rate is concerned.
When these NLP implementations are applied to large power system, they show two major problems: the first is the slow convergence rate due to the zigzagging in the search direction even though a global convergence can be guaranteed independent of the starting point; the second one deals with different optimal

solutions that can result from different starting point, because the method can only find a local optimal solution.
As the result in moving towards other approaches, listed below, the running time becomes longer and the algorithm possibly less robust.

Mixed- Integer Nonlinear Programming(MINLP)

The general formulation for a MINLP is:

$$\begin{aligned} Min \quad & z = c_1 x + c_2 y \\ subject\ to \quad & Ax = b \\ & A_1 x + A_2 y \geq b \\ & x, y \geq 0\ , y\ integer \end{aligned}$$

Wherec_1, c_2, A_1, A_2, b are all parameters. Theoretically, the var planning problem can be formulated as a nonlinear mixed-integer programming optimization method with a binary variable representing whether new var control devices should be installed or not, while the size of reactive compensation devices is still treated as continuously differentiable. To solve that, some reference employ the branch and bound (B&B) technique which is a typical method for integer programming. A decomposition technique may be then employed to decompose the problem into a continuous and an integer problem. However, such a procedure makes the algorithm rather complex.

Decomposition Method

This method, can greatly improve the efficiency in solving the problem as it allows the application of separate methods for the solution of each subproblem reducing the dimensions of the problem. The gain regards a significant reduction of the number of iterations, of the required computational time and of the memory space.

Heuristic Method (HM)

Heuristic means a simplification or educated guess that reduces or limits the search for solution in dominia that are difficult and poorly understood. Often they don't guarantee even a feasible solution and so are used with no theoretical guarantee. Sometimes, they are combined with conventional optimization methods to solve the RPP problem.

Simulated Annealing (SA)

This is a stochastic algorithm aims at minimizing numerical function of a large number of variables. It allows random upward jumps at judicious rates to provide possible escapes from local energy wells and therefore it converges asymptotically to the global optimal solution with probability one. Commonly, it is combined with many other approaches such as Genetic Algorithms.

Evolutionary algorithm (EAs)

Considering that a natural evolution is a population-based optimization process, an EA is different from the other methods because it does not need to differentiate cost function and constraints and as SA, converge to the global optimum solution with probability one. This category includes evolutionary programming (EP), evolutionary strategy (ES) and genetic algorithm (GA). All of them are based on mechanics of natural selection such as mutation, recombination, reproduction, crossover, selection, etc.

Tabu Search (TS)

The TS is an iterative search algorithm , characterized by the use of a flexible memory. It is able to eliminate local minimum and to search areas beyond it.

The last group of solving methods tries to deal with a delicate issue: the uncertainty. The data and parameter used in RPP are usually derived from many sources with a wide variance in their accuracy. For example, although average load is typically applied in RPP, the actual load should follow some uncertain variation. In addition, the cost of generators and var compensators saving may be subject to uncertainty to some degree. Therefore, uncertainties due to insufficient information may generate an uncertain region of decisions. Consequently, the validity of the results from average values cannot represent the uncertainty level. Hence, to account for the uncertainties in information and goals related to multiple and usually complicate objectives in RPP, the use of fuzzy set theory may play a significant role in decision-making. The fuzzy set, can be applied not only to objective function, for instance to handle the uncertainty of different goals for MO optimization, but also to constraints. Maximizing these satisfaction parameters, which represent the degree of closeness to the optimum and the degree of enforcement of constraints, the result is the minimization of power losses and var costs while increasing the voltage security.

CHAPTER 5
DATA REPRESENTATION: MODELLING ELEMENTS (AC-DC LINK)

Modern high voltage transmission systems are not only made by lines and transformers but also by a growing number of power electronic devices with the aim of enhancing the power transfer controllability under secure operating conditions. Among them, FACTS (Flexible AC Transmission System) and HVDC (High Direct Current Transmission). This chapter describes the incorporation of this relevant power electronic technologies models in conventional AC power system analysis. First, a description of the how all the basic components (busbar, links, transformers) of the grid have been modeled for the study will be provided. The principal assumption for the following analysis is the use of per unit approach for all the parameter.

5.1. HVAC transmission

HVAC TRANSMISSION LINE:BUS

The buses bring the information of what has been connected to them. Typically, they are PQ, PV if they are connected a load and a generator respectively. Moreover slack bus is also required as reference for the voltage angles. Enlarging the system with a DC subsystem, new components, i.e. converters, are needed to build the interface between the two grid, AC and DC grid. Therefore in the model,each bus can be classified according to the scheme in fig 5.1:

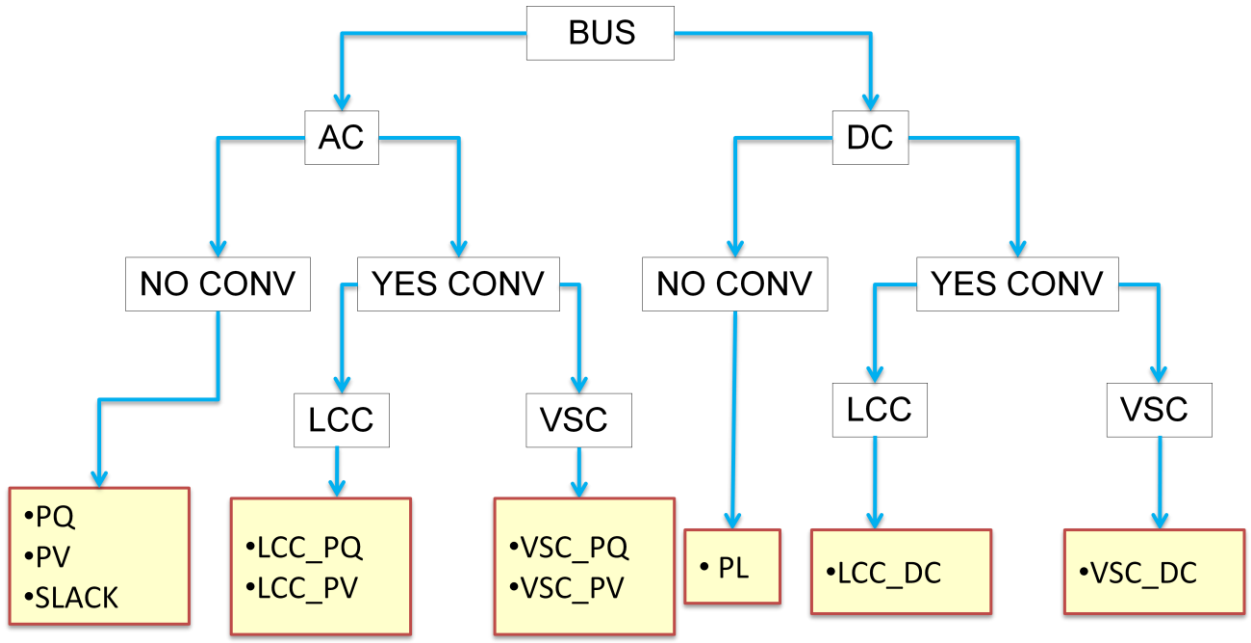

Figure 5.1: Bus type

This representation points out for each bus, AC or DC, its connection to a converter. It is possible therefore to have PQ,PV and SLACK type for buses not connected to any converter in the AC grid, whilst the dual in DC grid will be only active power load (PL). Whilst if a bus is linked to a converter, it will be additionally classified as LCC or VSC on the base of the type of converter and sequentially this bus will keep its label PQ or PV if it belongs to an AC grid, otherwise it will be only LCC_DC or VSC_DC. For the reference bus usually the magnitude of the bus voltage and the bus angle are the fixed. Obviously, there must be only one reference bus for each separated AC system. For our purpose, only the bus angle is kept equal to zero, whilst the magnitude of the voltage also for this kind of bus is allowed to vary within the limits, as well as for all the other kind of buses, in the sense that the voltage is a control variable for the optimization. We will consider a bus as a PV bus when at least one generator is assigned to the bus. The active power injected, which is the sum of the active power outputs of generators assigned to the bus, is specified as the nominal power and it is the starting point, as well as the bus voltage which corresponds to that provides by the machine. The starting point is the initial value which has assigned to the control variable at first when running the algorithm. Only for the PQ bus, both the real and reactive power are known and kept fixed over the whole running of the model. The variation of the load has been represented inside the different scenario assumed, neglecting any variation within the same scenario.

HVAC TRANSMISSION LINE:BRANCHES

Each AC links is represented by the Π model, which considers both longitudinal $Z_L$and transversal parameters Y as shown in Fig.5.2.

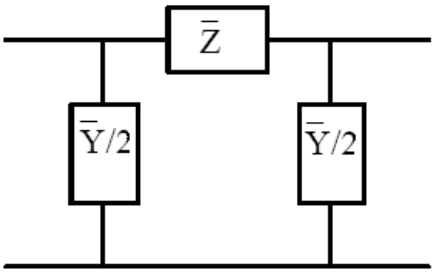

Figure 5.2: π representation line

The former taken into account the resistance R and the inductance X, whilst the latter combines the susceptance B (associated to the capacitance C of the link) and the conductance G, that can be neglected for our purpose. As result, a line is defined by a impedance Z_L and an admittance Y_L:

$$\overline{Z_L} = R + jX$$

$$\overline{Y_L} = jB$$

In Table 5.1, the direct sequence electrical parameters are shown for the types of transmission cables used in the study.

	R [Ω/km]	X [Ω/km]	C[nF/km]	S_{nom}[MVA]
AC BRANCH				
Overhead line 220 kV	0.055	0.42	8.7	518

Cable submarine Single core 220kV	0.046	0.07	198	460
Cable buried onshore 220 kV	0.025	0.152	240	600
DC BRANCH				
VSC cable 320kV	0.0101	0	0	500
LCC cable 500kV	0.009	0	0	1000

Table 5.1 Electrical parameters of Transmission Alternatives

For the VSC circuit, it is necessary a bipolar asset, without the possibility to use half circuit in case of any fault. For this reason (schema del VSC collegamento) the model need to take into account this aspect we have to consider two converter

For the LCC instead, monopolar unit are used and the resistance value has been multiplied for two sp that the total resistance of both the going and returning circuit has been considered.(schema del LCC collegamento)

Most of the existing onshore infrastructures are based on overhead lines and this is also the main technology for onshore reinforcements especially at high voltages. Onshore cables (buried cables) are only usually applied in densely populated areas and for submarine interface. To match the overhead line capacity a large cable core spacing of 700 mm, has been considered and adopted for the studies. Offshore cables are the only asset for an AC connection. In that case, electromagnetic phenomena have been thoroughly investigated and they have been taken into account into the value of their parameters. That means that the values by which the lines are described, already are increase to consider phenomena that may have influence.

Aside from the technical driven problems other development issues can arise which must also be solved. Three of them that impact on the critical length of a cable can be singled-out:

- steady state angle stability
- Charging Currents
- Voltage drops

For an AC cable, shunt and longitudinal losses have been considered as well as the losses associated in the compensation devices. An 80% compensation ratio has been assumed and the link is compensated split, with 50% of the required compensation at each end, as seen in Chapter 3. The maximum permissible voltage difference between the reference voltage and highest variation along the cable is assumed to be 5%, constraints that has been introduces into the equations.

The calculation of the admittance matrix to use in the power flow equation is explained in Appendix B.

5.2.HVDC transmission

Compared to the AC model, HVDC technology can provide the network flexibility to control the power flows through the DC links. The need to analyse this technology comes up as it has been introduced by selection with the ESP Optimisation procedure because of this ability in controlling power flows and due to the geographic distance of offshore installations. Besides, multiple HVDC units pose an issue related to coordination of their control, which may be smart and efficient. The increasing complexity and scale of the transmission network has driven the market interest in transferring power over long distances, and the need for power flow control as a consequence of the increasing penetration of variable generation sources has been a driver factor for the installations of DC circuits, not only as point to point connections but also in a more complex meshed, multi-terminal structure. These must somehow be integrated with the existing and/or future AC network. Therefore, it is of paramount importance to develop tools able to manage this mixed AC/DC nature which is part of the concept of the future ‘Smart’ Transmission systems.

A basic schematic diagram of a two-terminal HVDC link interconnecting buses (*r*) (rectifier) and (*i*) (Inverter) is illustrated in Fig. 5.3.To understand how HVDC works, we must understand the operation of the two single converter bridge on which HVDC is based.

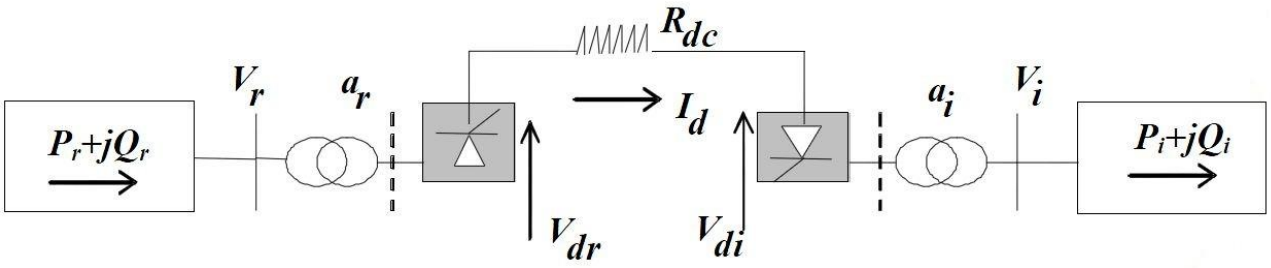

Figure 5.3: HVDC link

The main element for these links is the converter in its two different types: LCC and VSC. From the offshore collection point , the transmission link to shore can be,in principle, HVAC but also HVDC with thyristor-based line-commuted converters (LCC) or VSC-HVDC. The former technology has proven itself on onshore applications and could be cheaper than VSC_HVDC for power ratings of hundreds of MW, but it seems not particularly well suited for offshore application both for the large space that it would require and for the high susceptibility to AC network disturbances (resulting in converter commutation failures) which can temporarily shut-off the HVDC system. On the contrary, VSC-HVDC is recently becoming a reliable option for connecting wind farms to the HV grid due to its capability to control real and reactive power independently and to the controllers speed, stability and control accuracy.

LCC-HVDC

The simplest type of converter bridge suitable for 3-phase HVDC applications is the 6-pulse bridge, also known as the Graetz bridge. It is composed of unidirectional devices, such as diodes or thyristors. These last are more commonly used and beyond to permit the current flow in only one direction, they include a 'gate' terminal to turn on the valve, but not to turn it off. The control takes place by a firing angle α defined in Fig. 5.4

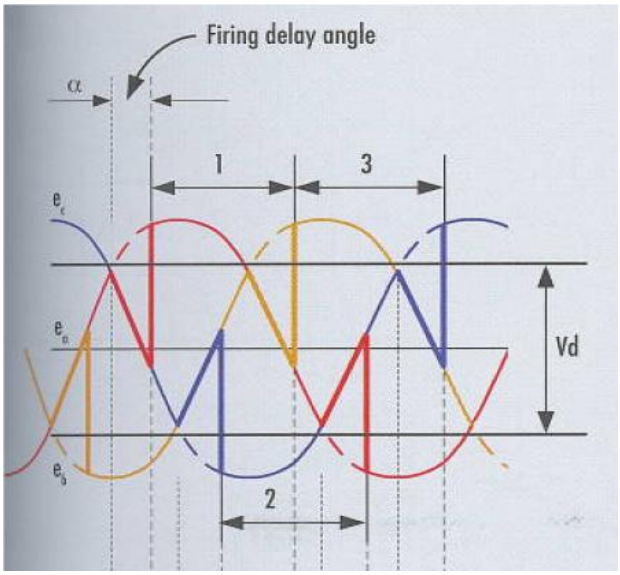

Figure 5.4: Ideal controlled 6-pulse bridge operation

It can been seen that, by introducing a delay in firing the thyristors, the area under the curve, representing the average DC voltage has reduced, compared to what it would have been without the delay. The numerical value of the DC voltage V_d is:

$$V_d = V_{d10} \cdot cos\alpha$$

where $V_{d10}$is the average voltage ideal, without delay in firing for the valves:

$$V_{d10} = \frac{3}{\pi} \cdot \sqrt{2} \cdot \sqrt{3} \cdot E_{rms} = \frac{3}{\pi} \cdot \sqrt{2} \cdot E_{ac} = k_1 \cdot E_{ac}$$

where $E_{ac}$is the line-to-line applied AC voltage. Moreover there is another aspect to consider for a good modeling of the converter. In the connection between the converter and the AC circuit, there is always some inductance, in order to limit the valve current during a fault: this phase inductance may be in the form of dedicated coupling reactors (typically air-cored, air-insulated reactors), but it is more commonly a result of the leakage reactance of the converter transformer. In addition, other minor inductances will contribute to the phase reactance, such as a series filters connected to the converter or the series impedance within a valve. The total inductance in each phase is referred to as the commuting impedence 'X_c'. In the next analysis, a further assumption is made: that the commuting impedance in each phase connected to the 6-pulse bridge are equal. During a commutation event, the valve that was conducting changes its current between zero and 1p.u. and a new valve starts to conduct the current. This phenomenon requires a time called overlap time; it is normally referred to with the symbol μ which is a function of the operating current and the transformer leakage reactance, as shown by:

$$\mu = cos^{-1}\left[\cos(\alpha) - \frac{2 \cdot X_c \cdot I_d}{\sqrt{2} \cdot E_{ac}}\right] - \alpha$$

where I_d is the DC current. It produces a further reduction for the voltage average value:

$$V_d = k_1 \cdot E_{ac} \cdot cos\alpha - \frac{3}{\pi} \cdot I_d \cdot X_c$$

This expression describes the actual operation mode for a rectifier.

By increasing the firing angle α beyond π/2, the DC terminal voltage will be negative. This is the inverter-mode operation

which let the real power flow from the DC side to the AC side by inverting the phase to phase voltage, while the DC current flow through the 6-pulse bridge cannot change direction. Since the firing angle for an inverter becomes large, normally it is more common to refer to the extinction angle γ, which represents the angle between the end of the overlap period and the angle corresponding to the moment the voltage, across the valve, becomes positive again. Its expression is:

$$\gamma = \pi - \mu - \alpha$$

It is important to note that since there is a symmetry for the wave shape of the rectifier and the inverter, it the equations for the rectifier operation can also be used for the inverter operation, simply by replacing the firing angle α with the extinction angle γ and noting the change in voltage polarity. Hence, for inverter operation, the equations become:

$$V_d = k_1 \cdot E_{ac} \cdot cos\gamma - \frac{3}{\pi} \cdot I_d \cdot X_c$$

In our model, which is based on power flows, the DC current has been substituted by the relative expression expressed by power:

$$I_d = \frac{P_{conv}}{Vd} \cdot sign(P_{conv})$$

Since the voltage magnitude has been considered, E_{ac} and V_d are always positive; to represent that the current is unidirectional and always positive, due to the physical features of the converter, we have to add $sign$ which is equal to 1 for the rectifier condition, whilst it is equal to -1 for the inverter operation.

Form the system point of view, LCC converters are a reactive power load as they operate with a delayed firing angle and therefore the real power, supplied or consumed, brings consequently reactive power absorption Q_{conv} which is calculated as

$$Q_{conv} = P_{conv} \cdot \tan(\phi) \cdot sign(P_{conv})$$

Since the tangent function is highly discontinuous and non linear, the equation for Q_{conv} are better replaced as follows where the $sign$ is required to have a Q_{conv} always as absorption:

$$Q_{conv} = \frac{a \cdot E_{ac} \cdot sin(\phi) \cdot P_{conv} \cdot sign(P_{conv})}{Vd}$$

The angle ϕ is the phase between the converter transformer line side AC voltage and the fundamental component of the converter phase current and a is the tap ratio having considered a transformer between the AC grid and the converter. Taking into account also the commutation aspect, the converter transformer impedance introduces an additional lag in the current, which is observed as the overlap angle μ.

Assuming an ideal converter (neglecting the losses) a commonly used method for the calculation of the angle ϕ is known as the Uhlmann approximation (10). This approximation assumes that the converter line winding currents are trapezoidal, that is, that the DC side series reactance is infinitive. This approximation provides a reasonable estimate of the reactive power absorbed at high current , close to 1p.u., but can become significantly inaccurate if the AC voltage is low or if the overlap is large. to provide a reasonable estimate of the reactive power absorbed at high DC current.

$$\cos(\phi) = \frac{\cos(\alpha) + \cos(\alpha + \mu)}{2}$$

In the model formulation, each converter terminal is therefore represented as below:

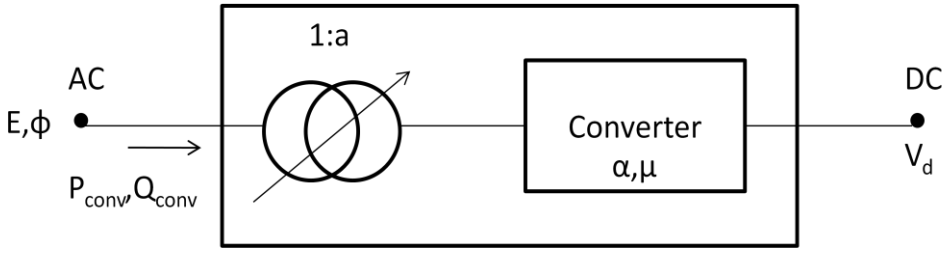

Figure 5.5: AC/DC system interface

by a five variable set $\bar{x}$ of variables, described by non-linear equations, which are then combined with the ac system equations and solved using either simultaneous iterative algorithms:

$$\bar{x} = [V_d, P_{conv}, a, cos\alpha, \cos(\alpha + \mu), \phi]^T$$

The selection of variables to constitute the vector $\bar{x}$ and formulation of the equations require several basic assumptions which are generally accepted in the analysis of steady state AC-DC converter operation. First, the AC voltages at the terminal buses are perfectly balanced and sinusoidal. Thus, a perfect AC filtering of all harmonic currents and voltages generated by the converters is assumed. Correspondingly, a perfect filtering on the DC side too is assumed and the DC current and voltage contain no sinusoidal components. Furthermore, the losses and magnetizing admittance of the two-winding converter transformers are ignored.

Under balanced conditions, similar converter bridges connected to the same AC-terminals busbar will operate identically, regardless of the transformer connection. To complete the description for each converter, beyond the equations which describes the working conditions, there are two other equations related the DC variables according to the connection in place at the DC terminal. The set of the relationship which describe

the steady state behavior of the converter connected to the AC bus trough a transformer with a tap ratio a are:

$$R(1) = V_d - k_1 \cdot a \cdot E_{ac} \cdot cos\alpha + \frac{3}{\pi} \cdot X_c \cdot \frac{P_{conv}}{V_d} \cdot sign(P_{conv})$$

$$R(2) = Q_{conv} - \frac{a \cdot E_{ac} \cdot sin\,(\phi) \cdot P_{conv} \cdot sign(P_{conv})}{Vd}$$

$$R(3) = \cos(\phi) - \frac{\cos(\alpha) + \cos\,(\alpha + \mu)}{2}$$

$$R(4) = f(V_d, I_d)$$

$$R(5) = cosau - \cos\,(\alpha) + \sqrt{2} \cdot X_c \cdot \frac{P_{conv}}{V_d \cdot E_{ac}}$$

As for a converter $X_c is$ constant. E_{ac} is the calculation result of AC system. In order to reduce nonlinearity of the equations, $\cos(\alpha)$is selected as variable rather than α.

VSC-HVDC

This converter is composed by a different kind of valves, the IGTB, which are able to be switch on and off through a command. To highlight the different behaviour from the LCC, the bi-directional reactive power flow through it has been introduced, instead of a only absorption by the LCC. The reactive power is only connected to the active power by the capability limits of the converter, as they are described furthermore. The mathematical relation which describe the relationship between the AC and DC voltage at the ends for each VSC is:

$$V_d = m * \sqrt{2} * E_{ac}$$

where m is the modulation index: it represents the command to give to the valves by comparison between a carrying waveform and a modulate waveform.

Although the model has been described neglecting the losses, they are relevant to distinguish LCC and VSC technology: actually they are consistent for high rate power, in particular at present for the VSC type and therefore greatly influence the solution. Furthermore, it has to be underlined that converter losses may be divided into two parts: voltage dependant and current dependant losses (5) as represented by the fig 5.6:

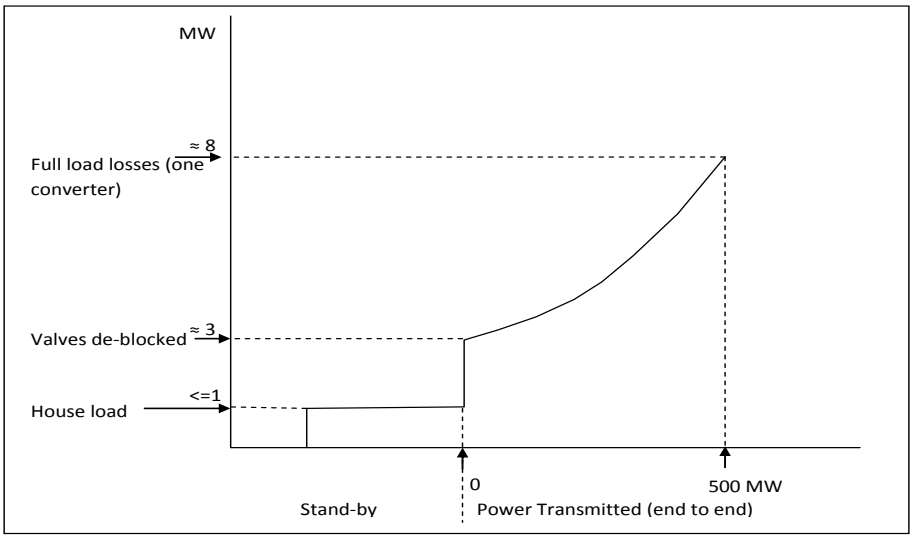

Figure5.6 : Converter Losses in VSC

Looking at the graph, it can be seen these two contributions and the value in MW that this losses may assume: at very low power working losses are around 3 MW and under full working conditions they can reach on a quadratic curve, value around the 8MW.

Referring to the Table 2, it can be noted that conventional LCC Converters are much more efficient that the VSC types. However, recent advancements in the technology by manufacturers are leading their future predictions for VSC technology to become close to 1% total in the near future. For our analysis, the converters losses have been modelled referring to this table:

	VSC	LCC
Total	1.60%	0.70%
No-Load+Deblock	0.60%	0.20%
Current Dependant	1.00%	0.50%

Table 5.3: Assumptions for Converters Losses Calculation

Therefore to include the losses inside the model a modification has been introduced at the DC side: a fictitious branch has been added with a resistance R_{loss} that represents the current dependant losses; the no load losses have been represented by a load absorbing $P_{fix,}$ located at the DC bus connected to the converter. The values for the resistance and for the load have been calculated respectively for the LCC and VSC from the table 5.2. Therefore the final model that describes each converter is show in fig. 5.7, where the ideal converter has been highlined by a dotted line, while the real one by a continuous line:

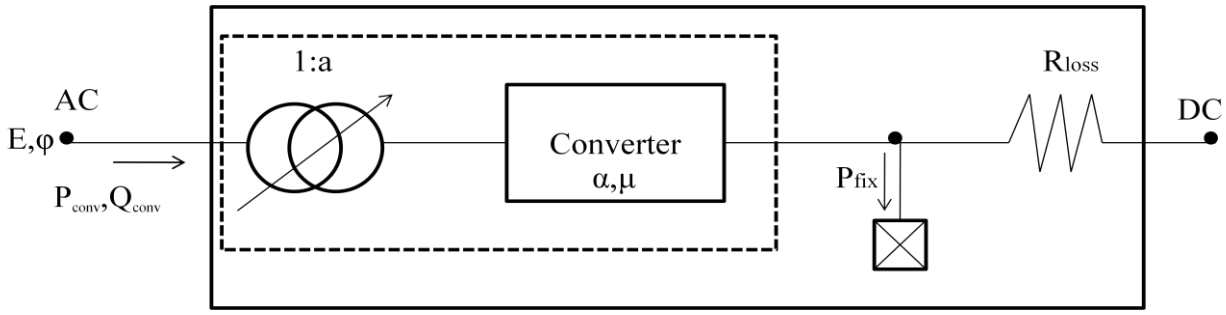

Figure 5.7: Model for the losses of the converter

To complete the representation for both converters, the capability limits have been considered. Real and reactive power capability is usually illustrated in an MVA-plane. From a power system stability point of view there are mainly two factors that limit the active and reactive power output from an HVDC converter. The first one is the maximum current passing the valves, which gives directly the rated MVA capacity, and the second one is the maximum DC-voltage. Depending on cable design there can also be a third limiting factor present and that is the maximum current in the DC-cable. These limits are shown in figure 5.8.

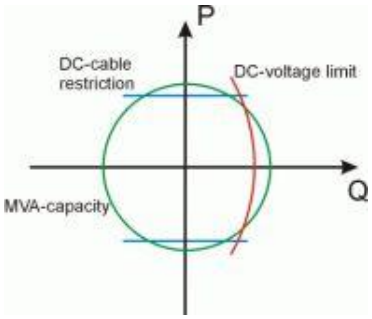

Figure 5.8: Capability curves

For LCC technology only the region corresponding to the negative reactive (left region) power has to be considered. Instead for VSC the available operating zone is both for positive and negative reactive power value. Focusing only on the VSC technology, we can see that if voltage decreases the MVA capacity will shrink proportionally to the voltage drop. Moreover, since this HVDC is a voltage source converter this means that we cannot raise the AC voltage above a certain level. The level is given by the maximum DC-voltage we allow on the DC apparatus (cable, capacitors etc.). Looking at this limit in the power plane shown in Fig.5.4, we see that the maximum DC voltage defines a maximum reactive power arc in the power plane. If the AC voltage decreases the difference between the maximum DC voltage and the AC voltage will increase. It is then possible to inject more reactive power, i.e., the red arc will move to the right in the figure. This movement is opposite to the shrinking green MVA circle. Another restriction can be the capacity of the DC cable buried in the ground. It can be observed the fact that for low AC voltages the MVA limit is dominating. For high AC voltages the DC-voltage limit is quite restrictive but in that case the injection of reactive power is not likely to occur. The absorbing reactive capacity given by the MVA circle is hence much more important for high AC-voltage. In brief, the MVA-capacity limit is in many situations the most restricting one.

The figure below shows how the limits vary with voltage.

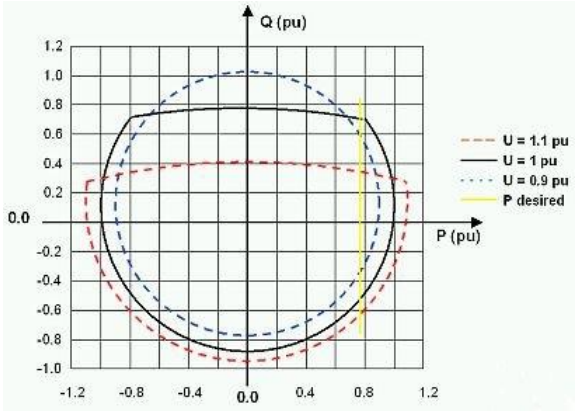

Figure 5.9 Capability curves depending on voltage magnitude

However these limits are not significant because, as the voltage increases, the converter are not required to increase in turn its reactive power production, and so the reduction of the operating area are in the region of the positive reactive power is not influent.

For all these reason the constraint for the capability limits for both LCC and VSC technology are expressed as:

$$P_{conv}{}^2 + Q_{conv}{}^2 \leq A_{conv}{}^2$$

DC CABLE

DC technology that have been considered in the studies are better described in the following. As already stated, the electrical parameters of transmission equipment affect their use in transmission systems and the operation condition in general. Their values are collected in table 5.3.

DC cables	R	X	Tgd	C	Snom
Type	Ohm/km	(Ohm/km)	(p.u.)	(nF/km)	MW
XLPE 1800 mm2 Cu 320 kV	**0.0101**	na	na	na	1000
PPL 2000 mm2 Cu 500 kV	**0.009**	na	na	na	1000

Table 5.3: DC cable parameters

It should be noted at present that to build a 1GW DC cable circuit requires a dual cable circuit bundled. Therefore the DC Resistance is lower than the equivalent AC resistance, due to the number of cables, the lack of skin effect and the induced current in the sheath. These advantages however are partially reduced by the high losses in the DC converter units, in particular for VSC type.

At present XLPE technology, which has been applied since the 1990s, is adopted in Ireland, in comparison to oil filled cables mainly because of its lower maintenance, less environmental impact, and costs. This technology is available up to 500 kV.

HVDC CONFIGURATION

HVDC schemes can be divided into two basic types:

- back to back schemes (Fig 5.10), where both converter stations are at the same location
- transmission schemes (sometimes also known as point-to-point schemes), where the two converter stations are at different locations and connected by DC lines and /or cables.

The back to back converter has no transmission line and both converters are located at the same site. it is normally used to create an asynchronous interconnection between two AC networks, which could have the same or different frequencies.

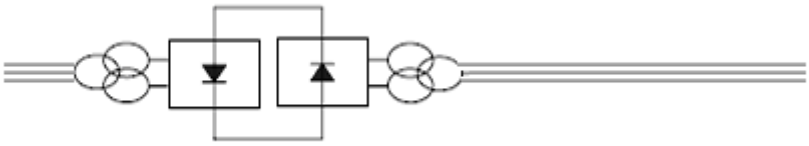

Figure 5.10: Back to Back Transmission

Transmission schemes are commonly used for bulk energy transmission over long distanced, or for submarine cable connection. The two converter stations are connected together via DC overhead line, DC cables or a combination of the two. The cooling system, auxiliary system and control system are separate for the two converter stations. there are two main common configurations: the monopole and the bipole.

The monopolar HVDC scheme is the simplest arrangement, where each end of the scheme has just one converter. it normally has one HV conductor and a return conductor. The return conductor could be either a dedicated metallic conductor (metallic return), or an earth and /or sea conductor (ground return). The latter arrangement requires an electrode line and a ground or sea electrode built for continuous operation. On the other side, the former arrangement, shown in Fig 5.11, usually consists of one high voltage and one low voltage conductor, but could consist of two conductor at positive and negative half voltage.

Figure 5.11: Monopole with Metallic Return

This configuration is used as the first stage of a bipolar scheme, avoiding ground currents when construction of electrode lines and ground electrodes is environmentally unacceptable It is also used when the necessary length of electrode line , or the value of the earth resistivity, would result in an uneconomical solution.

The monopolar configuration will be adopted for our analysis for the LCC technology.

The bipolar configuration contains two independent poles, each consisting of an independent converter (normally 12-pulse). there are two possible schemes: with or without earth return.

In the first asset, Fig. 5.12, there are two conductors , one with positive and the other with negative polarity with respect to ground for power flow in one (or both) directions.

Figure 5.12: Bipole with Earth Return

The bipole DC configuration with a working earth return has a 50% redundancy rate, meaning that with one pole out of service, the remaining pole operates in monopole mode and can still transmits 50% of the link power. The bipolar configuration comes with an extra expense.

The other configuration, without earth return is shown in Fig. 5.13. In this case HVDC the connection gets lost as one converter is out of service. This is the arrangement which has been chosen for the VSC techology, where the two converters at each pole, have been modelled as one unique converter with a double rated voltage and power.

Figure 5.13: Bipole with Earth Return

5.3.VAR devices

SHUNT, SVC AND STATCOM ELEMENTS

Shunt reactors and capacitors are used in power system for reactive power control. The data for these elements are usually given in terms of their rated MVA and rated kV. The equivalent phase admittance in p.u. is calculated from these data. This are the focal elements for the grid. Since they have a size, they need e discrete variable to be really modeled. In the study, it is considered the size as given and also the cost associated to their installation. SVC and STATCOM provide a dynamic control of the reactive power so they have been identified with a continuous variable.

It is important to know for both of the types sources that, while the converter transformer is fitted with a tap changer to compensate for variations in AC system voltage, other reactive compensation equipment connected to the busbur, such as var devised, may not be compensated. Therefore, the reactive power these devices generate will vary with AC system conditions and it will be taken into account as,

$$Qshunt = Qshunt_0 \cdot \frac{Vac^2}{{Vac_0}^2}$$

where:

$Qshunt$ = the actual reactive power supplied by the var sources

$Qshunt_0$ = the reactive power supplied by the var sources at 1.0 p.u.

Vac^2=the actual busbar voltage

${Vac_0}^2$=the 1.0 p.u. value of AC system voltage

Other factors will affect the actual reactive power generated by the var sources such as component manufacturing, tolerance and ambient temperature. These variations have been neglected in our model when calculating the net reactive power exchange with the AC system.

5.4.Generator and load

The load is represented as a fixed absorption of active P_d and reactive power Q_d, as depicted in Fig. 5.14:

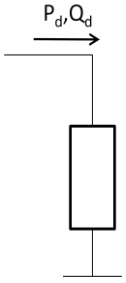

Figure 5.14: Load

The power factor $cos(\varphi)$ has been obtained considering that:

$$tg(\varphi) = \frac{Q_d}{P_d} = 0.5 \rightarrow \cos\big(arctg(\varphi)\big) = 0.894$$

To allow the grid to be flexible, the model has provided the possibility for load shedding , which is modeled as a fictitious generator that can supply both active (LSHP) and reactive (LSHQ) power if the grid is not able to do it as depicted in Fig. 5.15.

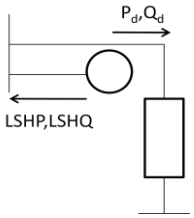

Figure 5.15: load shedding

Instead generator in the model are by managing the demand-supply balance through the dispatch of power stations in economic merit in order to increase or decrease their megawatt output.

The model provides a representation for generation distinguishing it into two types: conventional and offshore. Conventional generators are able to vary their active power generation in a fixed range ± 10% of the nominal value of the power which has been given as data input. Instead for the offshore production has been considered a smaller range , ± 1% , as it should be fixed in each scenario for which the variability of the wind has already been evaluated. A fictitious load curtailment has been introduced with a high price at the offshore bus in view of overloading for the link. And at the same way, an unlinked for each conventional generator has been introduced.

The reactive power is free to change in a range delimited by the capability curved (11) as shown in fig.5.16.

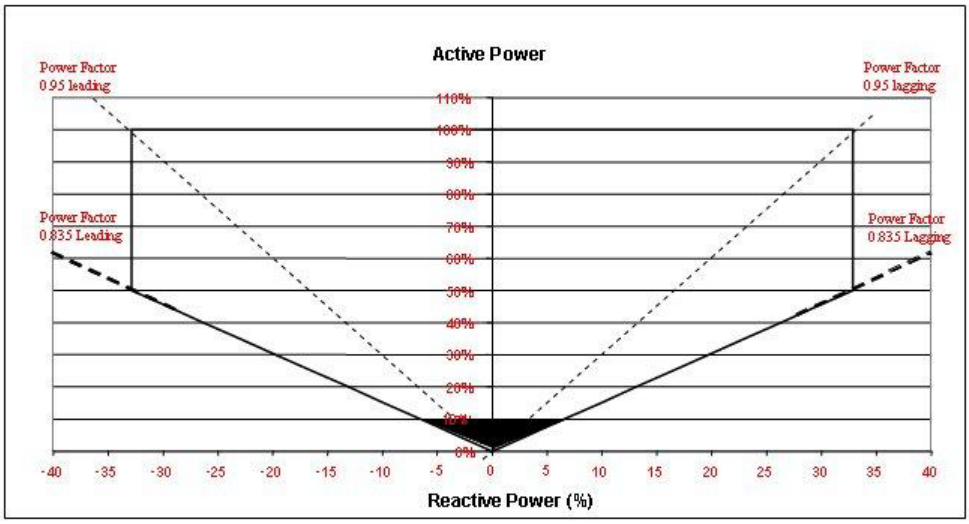

Figure 5.16: capability curve

Above, the mist lines region of the graphic is wider than the real part chosen for each generator in our study: for each one, a power factor limit of 0.95 has been chosen, considering that its real power is within a range around the 100%, established as the reference power.

CHAPTER 6
MATHEMATICAL MODEL AND SOLVER

Since the previous approach that has been elaborated in order to look at new possible economic and secure topology of the grid exploited a DC Power Flow, by which every difference between AC and DC link gets lost. This choice has soon looked like not enough for a next analysis whose focal point is to investigate a VAR compensation over a period of one year: this requires a methodology that keeps the information on the diverse behavior of AC and DC link on the reactive issue and therefore an AC Power Flow. This investigation aims both at satisfying security criteria on the voltage levels and has its goal in advantageous investment in various possible working conditions, either during peak hours, when high loads determine the lowest voltage levels, or during slack hours when the Ferranti effect can occur, due to long links, that arises the voltage at undesired high level. Hence, these two extreme situations lead to deal with the importance of installing respectively shunt capacitor and shunt reactors banks. In addition, there is the need to cope with an electric network made for most by cables, due to the connection of offshore plants; this increases more straightforward the importance to consider this issue, which still remains a very much actual question, although has already partially been analyzed in the last years, as reported in the chapter 4. The VAR study has focused on one year, spelt in more scenarios for assessing the variability of the generation and demand values. The interesting challenge for the model is in working for an embedded grid AC/HVDC defining its topology and the main settings. The mathematical formulation of the model has then implemented in GAMS and solved by LIDOGLOBAL solver.

6.1.Assumptions

Due to the large scope of the model, some simplifying assumptions had to be made. RPP is typically identified as an optimization problem in power system, known as OPF. The difference from a conventional Power Flow algorithm, which only obtains a single feasible solution, is the explicit declaration of trying to minimize or maximize any objective functions chosen as the best goal to reach. Hence, a first assumption is considered starting from the power flow : since it is purely a fundamental frequency steady state study, it doesn't require waveforms information, so the active and reactive power represent fundamental frequency power and any additional power at harmonic frequency is negligible; this condition implies that all variables and parameters remain constant for the considered period. Hence, AC voltages at the terminal buses are considered as perfectly symmetrical and sinusoidal. About the location of var sources, the study will take into account in the training off the worst likely case, where at least the possible locations for var sources will be as many candidate busses as those of the whole system. This initial assumption makes the problem simpler, since no binary variable are necessary. Moreover, it has been supposed that the capacitors at HV level can be switched off whenever it is suitable. About the size, both a continuous model and discrete model have been developed to provide information about the need to install the reactive devices by the former, and a more realistic point for further investment plans by the latter.

The reactive power is relevant due to the presence both HVDC cables, whose converters to join them to the grid require reactive power up to 50% of the whole amount produced, and AC cables with higher production of reactive power which is compensated till a maximum 80% of the whole reactive value. Each generator is assumed able to provide the required real power, within fixed constraints. The considered period is one year

which has been represented by a number of scenarios with different demand levels and generation outputs for both renewable energy sources and thermal power plants. For these scenarios, different wind levels have been considered. It is clear that the more the scenarios, the more the analysis is realistic.

6.2.Problem formulation

To represent an AC/HVDC mixed grid, the basic AC power flow equations have to be integrated with the relationships describing the HVDC behavior. It has been assumed for our explanation that the bold notation symbolizes a vector of elements. Let us consider a bus where no converters are connected. For all of those buses, two power mismatches (real $\Delta \boldsymbol{P}$ and reactive $\Delta \boldsymbol{Q}$) have to be considered :

$$\Delta \boldsymbol{P}(\boldsymbol{E}, \boldsymbol{\theta})$$

$$\Delta \boldsymbol{Q}(\boldsymbol{E}, \boldsymbol{\theta})$$

depending on $\boldsymbol{E}$ and $\boldsymbol{\theta}$ that are the vectors of respectively the voltage magnitudes and the phase angles. Instead, for a bus which is an AC terminal of an AC/DC connection, the balance gets modified into

$$\Delta \boldsymbol{P}_{term}(\boldsymbol{E}, \boldsymbol{\theta}, \boldsymbol{x})$$

$$\Delta \boldsymbol{Q}_{term}(\boldsymbol{E}, \boldsymbol{\theta}, \boldsymbol{x})$$

where the vector $\boldsymbol{x}$ has been introduced in chapter 5. There is a set of equations to identify the active power balance for DC busses:

$$\Delta \boldsymbol{P}_{DC}(\boldsymbol{E}_{DC})$$

where $\boldsymbol{E}_{DC}$ is the correspondent vector of the voltage magnitudes. All of these relationship will be explicated ahead and the resulting model of a generic AC-DC power flow problem may, therefore, be summarised as the solution of the following equations (12):

$$\begin{bmatrix} \Delta \boldsymbol{P}(\boldsymbol{E}, \boldsymbol{\theta}) \\ \Delta \boldsymbol{P}_{term}(\boldsymbol{E}, \boldsymbol{\theta}, \boldsymbol{x}) \\ \Delta \boldsymbol{Q}(\boldsymbol{E}, \boldsymbol{\theta}) \\ \Delta \boldsymbol{Q}_{term}(\boldsymbol{E}, \boldsymbol{\theta}, \boldsymbol{x}) \\ \boldsymbol{R}(\boldsymbol{V}_{ac}, \boldsymbol{x}) \\ \Delta \boldsymbol{P}_{DC}(\boldsymbol{E}_{DC}) \end{bmatrix} = 0$$

where $\boldsymbol{R}(\boldsymbol{V}_{ac}, \boldsymbol{x})$ is the set of equations for the converters.

OBJECTIVE FUNCTION

The goal of the optimisation problem considered is to satisfy all of the defined constraints while minimising the objective function OF:

$$\textit{Min}\ \mathbf{OF}$$

In our case, OF is a multi objective composed of six cost contributions which are of great concern to system planners where the scalar objective function has been defined as:

$$\mathbf{OF} = w_{ope}(Oper\_cost) + w_{Qs}(Inves\_cost) + w_{EXTRA}(Extra\_cost) + w_{LS}(Cost\_LSH) + w_{OFF}(Cost\_curt) + w_{GS}(Cost\_GSH)$$

The first one addresses loss reduction (operational efficiency). The second and third one are related to var and EXTRA sources expenditures, such as purchase, instalment and maintenance (minimum investment). The fourth objective is related to load shedding. The fifth and the sixth are about the curtailment for both the offshore and conventional generators. The aim is to minimize these different objective functions singularly or all together such as in a multi-objective optimal var planning problem as defined in Chapter 3. This can be achieved introducing weighting factors as w_{Qs}, $w_{extra}, w_{LS}, w_{ope}, w_{OFF}, w_{GS}$, set 1 or 0 to establish practically which function must be taken into account in the objective function time by time.

Investment Costs

The installation and purchase of new reactive power sources has three components: the purchase of capacitors, their installation costs and the additional protection devices costs. In our case, a unique value C_{1k} [€/kvar] that includes these three components will be considered for the continuous var sources and its value is 8[€/kvar]. Therefore costs for the installation in k€, are defined as:

$$Inves\_cost = \frac{1}{1000} \cdot \sum_{bus} \{C_{1k} \cdot \alpha \cdot (Qinj\_max_k - Qinj\_min_k) \cdot baseMVA\}$$

This is the unique cost that doesn't have a dependency from each scenario as it represents the resulting cost associated to the final size of both capacity, $Qinj\_max_k$, and reactors, $Qinj\_min_k$, that the program offers as the best solution to cover any condition during the whole year. To take into account that the total investment is spread over more the one year,, the coefficient α has been introduced as discount rate considering an interest rate of 5,63% and an investment lifetime of 43 years and it has been calculated as:

$$\alpha = \frac{1}{(1 + 0.0563)^{43}} = 0.09487$$

If necessary, the system may pay for extra var equipment to meet the reactive power requirements.

$$Extra\_cost = \frac{1}{1000} \cdot \sum_{bus} \{CEX \cdot \alpha \cdot (EXTRA\_max_k - EXTRA\_min_k) \cdot baseMVA\}$$

Where CEX [€/kvar] , which is the penalty cost for extra reactive sources, is set to 800[€/kvar].

Penalty for re-dispatching or Operating Costs

Generator has left free to vary its production $P\_gen_{k,NS}$ inside a fixed range, imposed by inequality constraints, in order to evaluate energy losses over the whole year valuating the delta values from the starting point $Prif_{k,NS}$ by the cost coefficients $C1_{gen,NS}$ e $C2_{gen,NS}$ for each generators according to a merit order of different generation technologies: while renewable wind and hydro generation is implemented with zero marginal generation cost, conventional generation plants face costs for fuel and CO_2 allowances.

$$Oper\_cost = \sum_{NS} \left\{ PS_{NS} \cdot \left[\sum_{gen} \left(\left(\frac{C1_{gen,NS}}{1000} + \frac{C2_{gen,NS} \cdot Prif_{k,NS}}{1000000} \right) \cdot \left(P\_gen_{k,NS} - Prif_{k,NS} \right) \cdot baseMVA \right) \right] \right\}$$

Where PS_{NS} is the number of hours related to each scenario.

Penalty for load shedding

$$Cost\_LSH = \frac{1}{1000} \cdot \sum_{NS} \left\{ CLS \cdot PS_{NS} \cdot \left[\sum_{k} LSPA_{k,NS} \cdot baseMVA + \sum_{k\_dc} LSPD_{k\_dc,NS} \cdot baseMVA \right] \right\}$$

Where CLS is the penalty cost for load shedding.

Penalty for generation shedding

$$Cost\_GSH = \frac{1}{1000} \cdot \sum_{NS} \left\{ CGS \cdot PS_{NS} \cdot \left[\sum_{load\_bus} GSP_{k,NS} \cdot baseMVA \right] \right\}$$

Where CGS is the penalty cost for generator shedding.

Penalty for offshore curtailment

$$Cost\_curt = \frac{1}{1000} \cdot \sum_{NS} \left\{ COFF \cdot PS_{NS} \cdot \left[\sum_{k} Pcurt_{k,NS} \cdot baseMVA \right] \right\}$$

Where COFF is the penalty cost for offshore curtailment. This penalty factor related to the wind energy not delivered reflects the market price, and notably the price paid for the wind under refit regardless of network constraints. Refit tariff is set up in Ireland and Britain at:

- 60 Euro/MWh onshore
- 140 Euro/MWh offshore
- 220 Euro/MWh for waves
- 150 Euro/MWh for GB Offshore

Raising the penalty factor, the effect is to encourage the grid to enhance the matching generation and load in order to avoid curtailments for any transfer of power, and the reverse if the penalty is lowered. For instance, with 10000 Euro/MWh, virtually any solution will be preferable to curtailment and with 0 Euro/MWh the reverse. Therefore using both 10000 and 0 Euro/MWh should the range of variation of the solution about the reactive support.

EQUALITY AND INEQUALITY CONSTRAINTS

In the following description, we will assume the subscript k as general bus in the grid and *NS* to indicate the considered scenario.
Concerning equality constraints to the AC part of the grid, the basic set of equality constraints is made of equations of both real $(P_{k,NS})$ and reactive $(Q_{k,NS})$ power injections at each AC bus, where the parameter

conductance G_{km} and susceptance B_{km} are the elements of the admittance matrix $[Y]$, as described in Appendix B:

$$P_{k,NS} = G_{kk} \cdot {E_{k,NS}}^2 + E_{k,NS} \cdot \sum_{m \in \Omega} \left\{ E_{m,NS} \cdot (G_{km} \cdot cos(\theta_{k,NS} - \theta_{m,NS}) + B_{km} \cdot \sin(\theta_{k,NS} - \theta_{m,NS})) \right\} , (k \in N_B)$$

$$Q_{k,NS} = -B_{kk} \cdot {E_{k,NS}}^2 + E_{k,NS} \cdot \sum_{m \in \Omega} \left\{ E_{m,NS} \cdot (G_{km} \cdot sin(\theta_{k,NS} - \theta_{m,NS}) - B_{km} \cdot \cos(\theta_{k,NS} - \theta_{m,NS})) \right\}, (k \in N_B)$$

Where N_B is the set of AC bus, considering also the slack bus; Ω is composed of m, AC buses linked to the bus k except k itself, since its contribute is taken into account separately by G_{kk} and B_{kk}. Consequently, for each AC bus, four variables have been introduced: besides $P_{k,NS}$ and $Q_{k,NS}$ power, there are bus voltage magnitude $E_{k,NS}$ and the angle $\theta_{k,NS}$.
Having these variables, the following step is to calculate net active and reactive balances at each bus considering their type, according to what has been already explained in chapter 5: PQ, PV, slack, LCC_PQ, LCC_PV, VSC_PQ,VSC_PV.
The equations which relate to the AC system variables are derived from the specified AC system operating conditions. The only modification, required to the usual real and reactive power mismatches, occurs for those equations which relate to the converter that acts as interface between the two areas of which the grid has been represented: AC and DC.
In this case for each converter two more powers will be considered: the real power and the reactive power that pass through the circuit component.

Each PQ bus has normally a net active power injection equal to the the absorption due to the presence of the fixed load, $Pd_{k,NS}$. Moreover, the possibility for load shedding ($LSPA_{k,NS}$), since its technical and economical importance, has been traduce into a mathematical constraint as explained in Chapter 5, modelling it as a fictitious generator which can turn on if for any other problem the load would not have supplied. The resulting balance equation is:

$$LSPA_{k,NS} - Pd_{k,NS} = P_{k,NS} \ , \qquad (k \in N_L)$$

Where N_L is the PQ bus set. The variable $LSPA_{k,NS}$ is constrained as follows:

$$0 \leq LSPA_{k,NS} \leq Pd_{k,NS}, (k \in N_L)$$

Connected to real load shedding there will be a reactive load shedding which will shows up at the reactive equation. Since the impossibility to feed the load is a damage for the grid, its effect will be highly priced in the objective function by 5000 €/MWh.

Generation at a bus is given by the positive variable $P_{gen_{k,NS}}$, which represents all the generation typologies. Another variable required for the model, which has been introduced also in the Expansion Strategy Plan analysis (Chapter 2), is $Pcurt_{t,NS}$, offshore power curtailment which has been represented as a possible real power absorption for only offshore generators.

$$P\_gen_{k,NS} - Pcurt_{t,NS} - Pd_{k,NS} + LSPA_{k,NS} = P_{k,NS} \ , \qquad (k \in N_{OG})$$

with

$$0 \leq Pcurt_{t,NS} \leq Prif_{k,NS}$$

where N_{OG} is the PV bus set where there is an offshore generator. In this analysis the offshore generators are considered ad PV bus, where it is possible to achieve a voltage control thanks to the technologies adopted by Eirgrid.

A shedding also for conventional generators $GLS_{k,NS}$ takes a place inside the balance equation at PV bus :

$$P\_gen_{k,NS} - GLS_{k,NS} - Pd_{k,NS} + LSPA_{k,NS} = P_{k,NS}\,, \qquad (k \in N_{CG})$$

with

$$0 \leq GLS_{k,NS} \leq Prif_{k,NS}$$

Where N_{CG} is the PV bus set collecting conventional generating units.

Reactive power balance requires contribute $Qinj_{k,NS}$ given by the reactive sources. This has been defined as a continuous variable with a min-max constraint. If the bus is PQ, $Qd_{k,NS}$ is the absorption due the installed load; again, the possibility of a load shedding is taken into account by means of a constant power factor φ,

$$Qgen_{k,NS} - Qd_{k,NS} + \left(LSPA_{k,NS} \cdot tg\varphi_{k,NS}\right) + Qinj_{k,NS} + Extra_{k,NS} = Q_{k,NS}\,, (k \in N_L)$$

Since this equation is for PQ bus, $Qgen_{k,NS}$ is the fixed generated reactive power while $Qd_{k,NS}$ is the demand. To help the solution to converge, $Extra_{k,NS}$ have been set to be used on a high price condition, 500 €/kvar , assuming that the program has already chosen how to distribute the more convenient $Qinj_{k,NS}$. Instead, both PV bus and slack bus *k* have to obey to the following equality :

$$Q\_gen_{k,NS} - Qd_{k,NS} + \left(LSPA_{k,NS} \cdot tg\varphi_{k,NS}\right) + Qinj_{k,NS} + Extra_{k,NS} = Q_{k,NS}, (k \in N_G)$$

The previous relationships are related only to those buses without a DC connection. To include the latter circuit element, the new variables,$Pt_{conv,NS}$ and $Qt_{conv,NS}$ have been defined as the withdraw for each converter and the difference between LCC and VSC has been taken into account in this way: $Pt_{conv,NS}$, which represents the real flow through the device can be positive and negative for both the topologies; instead, $Qt_{conv,NS}$, which is the reactive power flow, can assume only positive value for the LCC technology, whilst it can be both positive and negative for VSC. The subscript "conv" indicates parameters referred to the converter itself. At the end of each AC bus belonging to the set $N_c$of the converter buses, the following active and reactive balances have to be fulfilled:

$$P\_gen_{k,NS} - S_{k,NS} - Pd_{k,NS} + LSPA_{k,NS} - Pt_{conv,NS} = P_{k,NS}, (k \in N_c)$$

In the case that a conventional generator is linked to the converter unit, the auxiliary variable $S_{k,NS}$ indicates $GLS_{k,NS}$; otherwise, if there is an offshore unit $S_{k,NS}$ is for $Pcurt_{k,NS}$.

The reactive balance is different for PQ busses:

$$Qgen_{k,NS} - Qd_{k,NS} + \left(LSPA_{k,NS} \cdot tg\varphi_{k,NS}\right) - Qt_{conv,NS} + Qinj_{k,NS} + Extra_{k,NS} = Q_{k,NS}, (k \in N_c)$$

and PV busses:

$$Q\_gen_{k,NS} - Qd_{k,NS} + \left(LSPA_{k,NS} \cdot tg\varphi_{k,NS}\right) - Qt_{conv,NS} + Extra_{k,NS} + Qinj_{k,NS} = Q_{k,NS}, (k \in N_c)$$

Let us now to consider the equations for AC/DC connection elements. Coming from the model used for converters and described in Chapter 5, the relationship between the AC and DC quantities for the LCC-HVDC converters is:

$$Vd_{k\_dc.NS} = K \cdot E_{k,NS} \cdot a_{conv,NS} \cdot \cos(\alpha)_{conv,NS} - \frac{3 \cdot XC_{conv} \cdot Pt_{conv,NS} \cdot sign(Pt_{conv,NS})}{\pi \cdot Vd_{k\_dc,NS}},$$
$$(k \in N_c, k\_dc \in N_{cd})$$

Where N_{cd} is the set of DC buses, end busses for the LCC converter. The reactive power absorbed by the LCC-HVDC terminal is:

$$Qt_{conv,NS} = \frac{a_{conv,NS} \cdot E_{k,NS} \cdot Pt_{conv,NS} \cdot sign(Pt_{conv,NS}) \cdot sin(\phi_{conv,NS})}{Vd_{k\_dc,NS}}, (k \in N_c, k\_dc \in N_{cd})$$

Furthermore, the following overlapping angle and firing angle relationships have been assumed :

$$cosau_{conv,NS} = \cos(\alpha)_{conv,NS} - \sqrt{2} \cdot XC_{conv} \cdot \frac{sign(Pt_{conv,NS}) \cdot Pt_{conv,NS}}{Vd_{k\_dc,NS} \cdot E_{k,NS}}, \qquad (k \in N_c, k\_dc \in N_{cd})$$

$$\cos(\phi_{conv,NS}) = \frac{\cos(\alpha)_{conv,NS} + cosau_{conv,NS}}{2}, (k \in N_c, k\_dc \in N_{cd})$$

For the VSC_HVDC is important to observe that the coefficient $m_{conv,NS}$ expresses how the average value of the dc voltage $Vd_{k\_dc,NS}$ and $E_{k,NS}$ may reciprocally vary:

$$Vd_{k\_dc,NS} = m_{conv,NS} * \sqrt{2} * E_{k,NS},, (k \in N_c, k\_dc \in N_{cd})$$

As a last constraint for both converters, there is the inequality by which the two power flows are linked to the rated values of the converter itself.

$$Pt^2{}_{conv,NS} + Qt^2{}_{conv,NS} \leq A^2{}_{conv,NS}$$

The last part of the model is focused on the representation of a general DC grid. In a steady state analysis, the overall flow pattern is dictated by the line resistances and the DC voltage magnitude differences between the DC busses. The resulting steady state model for a DC grid, is implemented using a pure resistance network. The current injected at a DC node *k_dc* can be written as the current flowing to the other *N* – 1 nodes in the network, linked by the lines ckt :

$$P\_DC_{k\_dc,NS} = Vd_{k\_dc,NS} \cdot Vd_{k\_dc,NS} \cdot G_{k\_dc,k\_dc} + Vd_{k\_dc,NS} \cdot \sum_{t,ckt} Vd_{t\_dc,NS} \cdot G_{k\_dc,t\_dc,ckt}, (k\_dc$$
$$\in N_{DC}, t\_dc \in \chi)$$

Where $N_{DC}$is the whole DC bus set and χ is the DC bus t_dc set except the bus k_dc.

Moreover, the sum of every element is connected to the DC bus must to be equal to the net injection coming from the DC PF. This has to be for converter buses:

$$-Pd\_dc_{k\_dc,NS} + LSPD_{k\_dc,NS} + Pt_{conv,NS} - Pfix\_loss_{k\_dc,NS} = P\_DC_{k\_dc,NS}, (k\_dc \in N_{cd})$$

Where $Pd\_dc_{k\_dc,NS}$ is the load for a DC bus and $LSPD_{k\_dc,NS}$ is the relative available load shedding for it. As described in Chapter 5, each converter has been modelled taking into account also its losses: those which are constant are indicate by $Pfix\_loss_{k\_dc,NS}$.

For DC buses without converter:

$$-Pd\_dc_{k\_dc,NS} + LSPD_{k\_dc,NS} = P\_DC_{k\_dc,NS}, (k\_dc \in N_{DC})$$

According to this formulation, if in the final result from the nonlinear search algorithm the reactive power in related bus is zero, it means that there is no need of capacitor bank or reactor bank in that bus. Trough this formulation, where the reactive variable has been modelled as continuous, the binary variable has been avoided, however, introducing the "sign" operator into the equation describing the converter 72ehaviour, the model results as a DNLP problem (Discrete Non linear Programming).

To define the domain, several inequality constraints that represent the system operational and security limits have been set up. The set of constraints includes the limits of all variables i.e. all variables and function limits, such as upper and lower outputs of transmission lines, generation outputs, stability and security limits.

The real power outputs for conventional generators are free to vary into a tight range, chosen as:

$$0.95 \cdot Prif_{k,NS} \leq P\_gen_{k,NS} \leq 1.05 \cdot Prif_{k,NS}, (k \in N_G)$$

where $Prif_{k,NS}$ the starting value for the real power for each generating unit. The choice of these limit values is due the fact that $Prif_{k,NS}$ is itself the result of a previous economical optimisation. Concerning the real power outputs for offshore generators, they have a tighter constraint since it has been considered that for each scenario the offshore output has already been defined by the availability of the wind which has been assumed constant in each scenario. A small range has been chosen for the successful of the mathematical computation:

$$0.99 \cdot Prif_{k,NS} \leq P\_gen_{k,NS} \leq 1.01 \cdot Prif_{k,NS}, (k \in N_O)$$

From the previous model (Chapter 2) based on the DC Power Flow, for which the losses are neglected, $Prif_{k,NS}$ is the resulting generation output and satisfies the following relationship for each scenario NS:

$$\sum_k Prif_{k,NS} = \sum_k Pd_{k,NS}, (k \in N_B)$$

After our optimisation, it will result:

$$\sum_k P\_gen_{k,NS} = \sum_k Pd_{k,NS} + LOSS_{NS}, (k \in N_B)$$

The reactive power each generator can produce is within the following range:

$$Qgen^{min}{}_{k,NS} \leq Qgen_{k,NS} \leq Qgen^{max}{}_{k,NS}, (k \in N_G)$$

where the extreme values of $Qgen$ are related to the capability limits considering a maximum power factor of 0.95.
The way to consider the var sources as continuous into the different scenarios leads to constrain them between two extreme value which are not connected to the single scenario, but keep the information of the maximum $Qinj\_max_k$ and minimum $Qinj\_min_k$ amount that has to be installed potentially in all AC bus to solve the problem along the whole year:

$$Qinj\_min_k \leq Qinj_{k,NS} \leq Qinj\_max_k, (k \in N_B)$$

The same for the extra amount of reactive power:

$$Extra\_min_k \leq Extra_{k,NS} \leq Extra\_max_k, (k \in N_B)$$

The information about the maximum and minimum var installed is important because it is included in the objective function as the relevant final investment cost as described by . A limit is imposed on the size of both $Qinj\_min_k$ and $Qinj\_max_k$, chosen arbitrary:

$$-15 \leq Qinj\_min_k \leq 0$$

$$0 \leq Qinj\_max_k \leq 15$$

whereas the constraints for the extra:

$$-15 \leq Extra\_min_k \leq 0$$

$$0 \leq Extra\_max_k \leq 15$$

When the branch of the circuit is a cable, a compensation up the 80% of the whole reactive power produced by cable has been accounted for , always making the program free to chose if use it or not, in half quantity at the two end buses, from and to bus belonging to the set N_{CA}:

$$-Qcomp_{k,NS} \leq Qinj_{k,NS}, (k \in N_{CA})$$

where the limit value is:

$$Qcomp_{k,NS} = \sum_{cable} \left(\frac{0.8}{2} \cdot b_{cable} \cdot {V_{max}}^2 \right)$$

To keep the model able to face every situation, the availability to install a further shunt, called $Extra_k$ is guaranteed at a high price, whose contribute compare in the OF as $\_cost$. This extra source is to understand if the grid needs a further var support, besides that it has already been located.

Since it is important that the power system operates in the steady state, with a voltage at the AC system busbar within their normal operating limits , the voltage magnitudes at each AC and DC bus in the network have been imposed to stay into a fixed range of:

$$0.95 \leq E_{k,NS} \leq 1.05, \quad (k \in N_B)$$

$$0.07 \leq Vd_{k\_dc,NS} \leq 1.05 \, , (k\_dc \in N_{DC})$$

While the maximum value for the DC voltage is commonly used, the minimum one comes from the experience by Eirgrid by Ewic Project (East West Interconnection project).

To complete the set of the constrains there are line flow thermal limits on both AC and DC branches, respectively collected into the set N_l and N_{l_dc}:

$$\left|LF\_AC_{l,NS}\right| \leq LF\_AC^{max}{}_{l,NS}, (l \in N_l)$$

$$\left|LF\_DC_{l\_dc,NS}\right| \leq LF\_DC^{max}{}_{l\_dc,NS}, (l\_dc \in N_{l\_dc})$$

In the table 6.1, a summary of all the variables is shown:

Description	Variable name	Lower	Upper	Starting point
BUS				
Magnitude Voltage at AC bus	$E_{k,NS}$	0.95	1.05	1
Magnitude Voltage at DC bus	$Vd_{k\_dc,NS}$	0.01	1.05	1
Angle of bus voltage	$\theta_{k,NS}$	-	-	0
Active power injection	$P_{k,NS}$	-	-	$P_{k,NS}{}^{0}$
Reactive power injection	$Q_{k,NS}$	-	-	$Q_{k,NS}{}^{0}$
REACTIVE SOURCES				
Maximum installed Reactive power	$Qinj\_max_k$	0	15	0
Minimum installed Reactive power	$Qinj\_min_k$	-15	0	0
Extra shunt capacitance	$Extra\_C_k$	0	15	0
Extra shunt reactance	$Extra\_R_k$	-15	0	0
GENERATORS				
Active power for conventional generating unit	$P\_gen_{k,NS}$	$0.95 \cdot Prif_{k,NS}$	$1.05 \cdot Prif_{k,NS}$	$Prif_{k,NS}$
Active power for offshore generating unit	$P\_gen_{k,NS}$	$0.999 \cdot Prif_{k,NS}$	$1.001 \cdot Prif_{k,NS}$	$Prif_{k,NS}$
Reactive power for generating unit	$Qgen_{k,NS}$	$Qgen^{min}{}_{k,NS}$	$Qgen^{max}{}_{k,NS}$	0
Power curtailment for offshore	$Pcurt_{k,NS}$	0	$Prif_{k,NS}$	0
Power generator shedding	$GLS_{k,NS}$	0	$Prif_{k,NS}$	0
LOADS				
Load shedding at AC bus	$LSPA_{k,NS}$	0	$Pd_{k,NS}$	0
Load shedding at DC bus	$LSPD_{k,NS}$	0	$Pd\_dc_{k,NS}$	0
CONVERTERS				
Converter active power demanded	$Pt_{conv,NS}$	-	-	0
Converter reactive power demanded	$Qt_{conv,NS}$	-	-	0
Firing delay angle	$\cos(\alpha)_{conv,NS}$	0	1	0
Transformer off-nominal tap ratio	$a_{conv,NS}$	0.8	1.2	0
	$\phi_{conv,NS}$	0	π	0
Firing delay angle and overlapping	$\cos au_{conv,NS}$	0	1	0
	$m_{conv,NS}$	0	2	0

Table 6.1: variables collection and their constaints

6.3.Model variation

In order to help the convergence, a mathematical trick has been adopted introducing the variables $\Delta up_{k,NS}$ and $\Delta lo_{k,NS}$ to make the load not fixed any more. Therefore, whenever there is a load, its demanded power $Pd_{k,NS}$ is modified into $Pd_{k,NS}(1 + \Delta up_{k,NS} - \Delta lo_{k,NS})$:

$$LSPA_{k,NS} - Pd_{k,NS}(1 + \Delta up_{k,NS} - \Delta lo_{k,NS}) = P_{k,NS}\ , \qquad (k \in N_L)$$

Moreover, a further specification has been modelled in order to introduce as much generality as possible to face a real grid transmission: due to the possibility to have more than one generators at one bus or different types (offshore or conventional), the variable $\boldsymbol{P\_gen_{k,NS}}$ is no longer sufficient alone, but it has been substituted by $\boldsymbol{Ptot\_gen_{k,NS}}$,according to the following expression:

$$Ptot\_gen_{\mathbf{k,NS}} = \sum_{a} \left(\mathbf{P\_gen}_{a,\mathbf{k,NS}} - GLS_{a,k,NS}\right) + \sum_{b} \left(\mathbf{P\_gen}_{b,k,\mathbf{NS}} - Pcurt_{b,k,NS}\right), \qquad (a \in C, b \in O, k \in N_G)$$

Where C is the set of all the conventional generators , O is the set of all the offshore generators. which are linked to the buses k belonging to N_G, set of the busses where there is at least one generator unit. The same conclusion can be drawn for those busses with more than one load.

Finally, the need to analyse exports and imports through those connections among different countries has led to introduce a new variable, $Export_{k,NS}$ to model the changed MW . Therefore, there will be a new set of busses, N_E , collecting all those busses where the export or the import is taken into account. The real power balance will result as:

$$Ptot\_gen_{\mathbf{k,NS}} - Pd_{k,NS} + LSPA_{k,NS} - Export_{k,NS} = P_{k,NS}, \qquad (k \in N_E)$$

These new flows have relevant economic influence and therefore have to be considered into the objective function as further cost items, $Cost\_Export$, defined as:

$$Cost\_Export = -\left\{\frac{1}{1000} \cdot \sum_{NS}\left\{Cexpo \cdot PS_{NS} \cdot \left[\sum_{k}\left\{Cexpo \cdot Export_{k,NS}) \cdot baseMVA\right\}\right]\right\}\right\}$$

where $Cexpo$ is 53,8 [€/MWh] comes from market estimation. The minus symbolises a gain if we have an export, otherwise with an import (negative value for the variable $Export_{k,NS}$) we will have a further cost.

6.4.Solution

The way to solve the system is an unified solution of the AC and DC equations that gives recognition to the interdependence of AC and DC system equations and simultaneously solves the complete system. This method is faster than one sequential cases, which has diverse steps, and provides fast and reliable convergences in several cases. The number of iterations did not exceed the number required for the AC system alone. Since our problem has resulted to be a DNLP type, after a thorough investigation LINDOGLOBAL of Lindo System (USA) has been found as the most reliable and comprehensive for this purpose.
In Appendix A there is a description of this solver, together with some of the most interesting solver to solve problem like these. The resolution step are shown in the flow chart of the algorithm following:

CHAPTER 7
TEST GRID: SIMULATION RESULTS

7.3. Test grid topology

The mathematical algorithm has been run to solve the RPP problem, considering the possibility to put a var sources (either capacitive or inductive) at each bus, in order to provide a safe working point for the grid. Therefore, this approach is helpful to identify busses vulnerable to voltage collapse and locations where injections of reactive power benefit the system most. The first analysis has been conducted on the test grid as represented in Fig 7.1. The pink lines represent the DC grid and the blue lines are for the AC connections. The grid is mainly made of overhead lines though there are cables, both HVDC and AC technologies, which have been indicated by dotted lines. The interface between the AC and DC system is represented by converters: the yellow squares are the VSC technology and the pink ones are the LCCs.

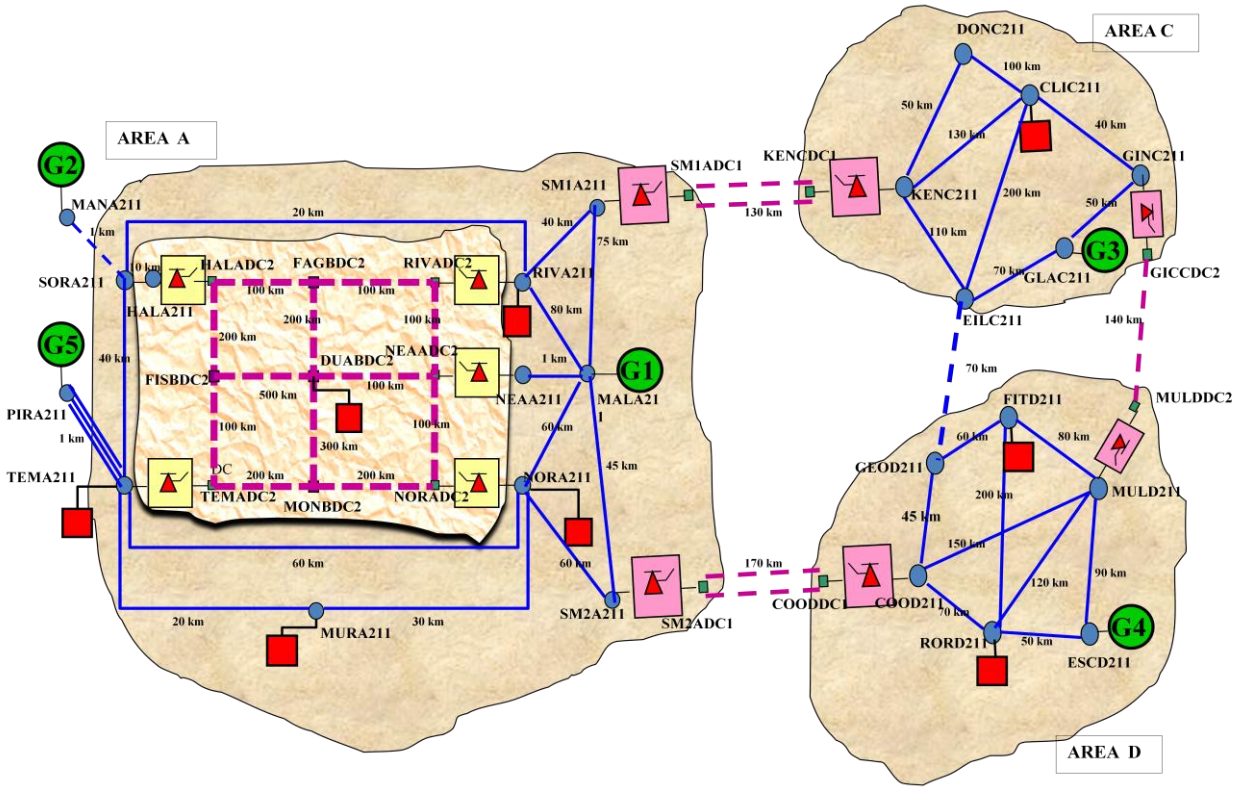

Fig. 7.1: Test Grid

This test system, in which three areas (A, C, D) have been pointed out, consists of five generating units, represented by green circles interconnected by a transmission network to serve a total load, whose each unit has been painted as red squares. The number of the units for each circuit element is collected in the Table 7.1:

Number of AC buses	**24**
Number of DC buses	**26**
Number of AC branches	**33**
Number of DC branches	**28**
Number of Generators	**5**
Number of Loads	**8**
Number of converters	**11**

Table 7.1: Dimension of the problem

The optimisation analysis is functional if conducted over a long period: therefore we will consider for the simulation one year, spelt in five scenarios to better follow the various demand over such a period. Each scenario is characterised by a particular condition of demand, which is collected separated in total and for each area (A, D, C), is described in Table 7.2:

	DEMAND [MW]			
SCENARIO	Pd_A	Pd_D	Pd_C	**Pd_tot**
1	620	160	160	**940**
2	600	112	80	**792**
3	1150	300	300	**1750**
4	780	100	100	**980**
5	1000	150	150	**1300**

Table 7.2: Demand for BASE CASE

It can be noticed how the scenarios are various as they work with different level of power. Scenario 1 and 2 can be assimilated to the summer valley; scenario 4 and 5 look like the summer peak; the scenario 3 can recall the winter peak, marked by the highest demand. Concerning the generation, the power of each generator unit has been chosen as starting value, coming from a previous dispatching conducted on economic base to satisfy fully the load demand neglecting the losses. Therefore the resulting generation for the BASE CASE matches perfectly the load and it is reported in Table 7.3:

	GENERATION [MW]			
SCENARIO	Pg_A	Pg_D	Pg_C	**Pg_tot**
1	630	160	150	**940**
2	610	162	20	**792**
3	1349	301	100	**1750**
4	790	175	15	**980**
5	1010	250	40	**1300**

Table 7.3: Generation for BASE CASE

For each scenario the total generation is equal to the total demand and a good balanced situation is clear for the scenario 1, see Fig.7.2, and 2.

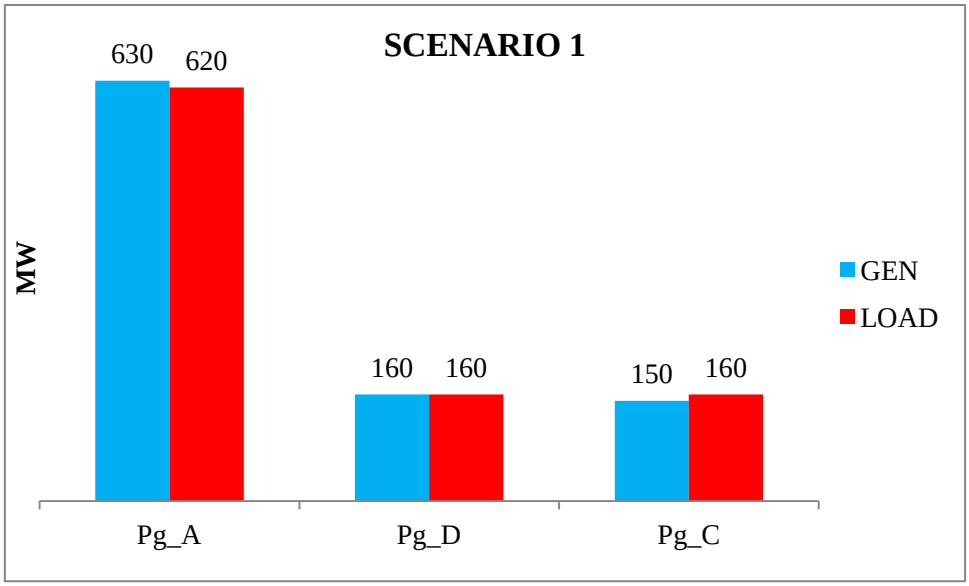

Fig. 7.2: Balances in each area SCENARIO 1

Nevertheless it can happen that into the different areas there are some evident unbalances, such as for the area C of the scenario 5 where the demand is 150 MW and the generation is only 40 MW. Indeed, an example of extra generation is for the area D of the same scenario, where the generation is 100 MW over the demand, as shown in Fig. 7.3.

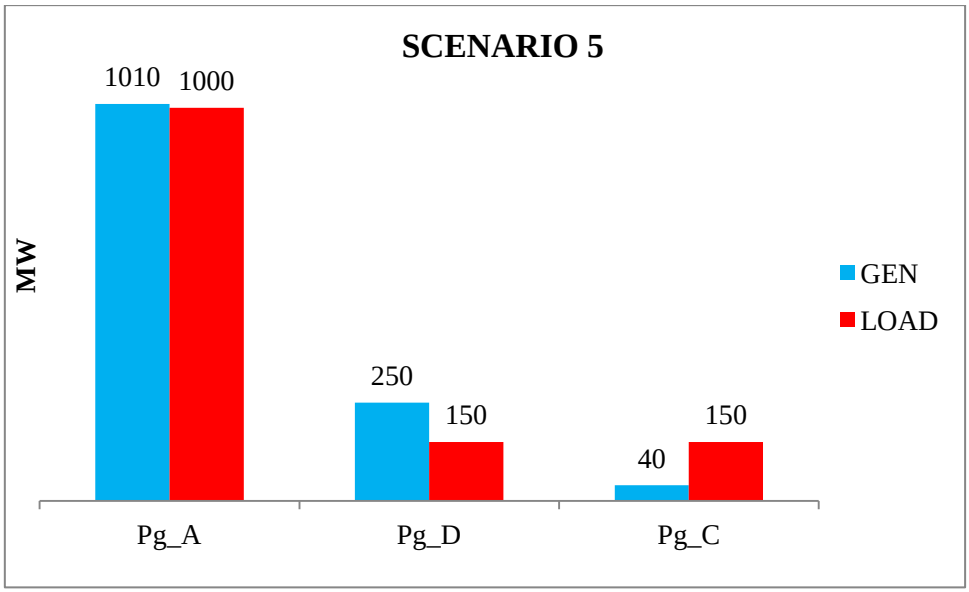

Fig. 7.3: Balances in each area SCENARIO 5

For our purposes, a sequential approach will be carried out while studying the problem. At first, we will focus on the analysis considering each single scenario, covering all the 8760 hours, where the correspondent demand and generation setting (BASE CASE) has been supposed to be unvaried along the whole year, in order to optimise the var installation along such a period. Afterwards, the problem will be run taking into account the combination of the five scenarios.

7.3. Sensitivities

In the test grid we have very long interconnections, hundreds of kilometers and this, together with the presence of cable, makes complicate the issue about the losses and an optimal reactive allocation. The first analysis will be focused on the BASECASE, where the grid is as depicted in Fig 7.1 and the load/generation is reported in table 7.3 and 7.4 for the different scenarios. Then, to test the validity of the model and to get deeply into some particular aspect of the system, the following different sensitivity studies will be considered:

- *Transmission technology sensitivities*
  - AC
  - AC + DC
- *Power wheeling capabilities*

While studying *Transmission technology sensitivities*, the topology of the test grid has been assumed equal for all the running, whereas the circuit technology has been varied, taking into account four different combinations:

1. *BASECASE*
2. *CABLE A*
3. *CABLE D*
4. *CABLE C&D*

In the first one, all the circuits are overhead lines except two submarine AC cables and all the cables composing the DC grid (dotted lines). The other three cases have been modified by a substitution of the AC overhead lines with onshore cable in, respectively, area A, D and D together with C. the case AC+DC is the investigation of the behaviour of the grid by replacement of the LCC by VSC, which will be the only connection typology between AC and DC grid.

The *Power wheeling capabilities* consists to stress the system to value its response by increasing the bulk of power flow from the area A towards the area C . It has been modified the BASE case, obtaining the wheeling cases, which consider a higher load located in the area C, exactly at bus CLIC211. This study allows to stress the grid with a power flow from west to east in order to analyze the reliability of the grid and the different need of reactive sources. In particular we will consider a wheeling from 0 MW to 1000MW, according to the table 7.4 for the demand and table 7.5 for the generation. The variation for the demand and generation concerns only the third scenario where the load has increased in the area C. Therefore the wheeling case will be analyzed only with regard to scenario 3.

SCENARIO 3	0 Wh	100 Wh	200Wh	300Wh	500Wh	700Wh	800Wh	900Wh	1000Wh
Pd_C	300	400	500	600	800	1000	1100	1200	1300

Table 7.4: Wheeling for the demand

SCENARIO 3	0 Wh	100 Wh	200Wh	300Wh	500Wh	700Wh	800Wh	900Wh	1000Wh
Pg_A	1349	1449	1549	1649	1849	2049	2149	2249	2349

Table 7.5: Wheeling for the generation

7.3. Single load/generation scenario

In all the figures which are going to come, the black arrows indicated the real power flow, while the red arrows are for reactive flows. In the green rectangles there are the generation output for the corresponding area, while in the red rectangles those for the demand.

BASE CASE

Let us to start considering the BASE CASE which has been assumed as reference case for all the following other cases. The base case has a grid composed mainly by overhead lines and with load/generation set as reported in table 7.3 and 7.4. Comparing the resulting objective function of each of the five scenarios in Fig. 7.4, it comes out how the total costs would seem strongly linked to the different levels of power for each scenario. Therefore the scenario 3 has the highest costs since its highest powers.

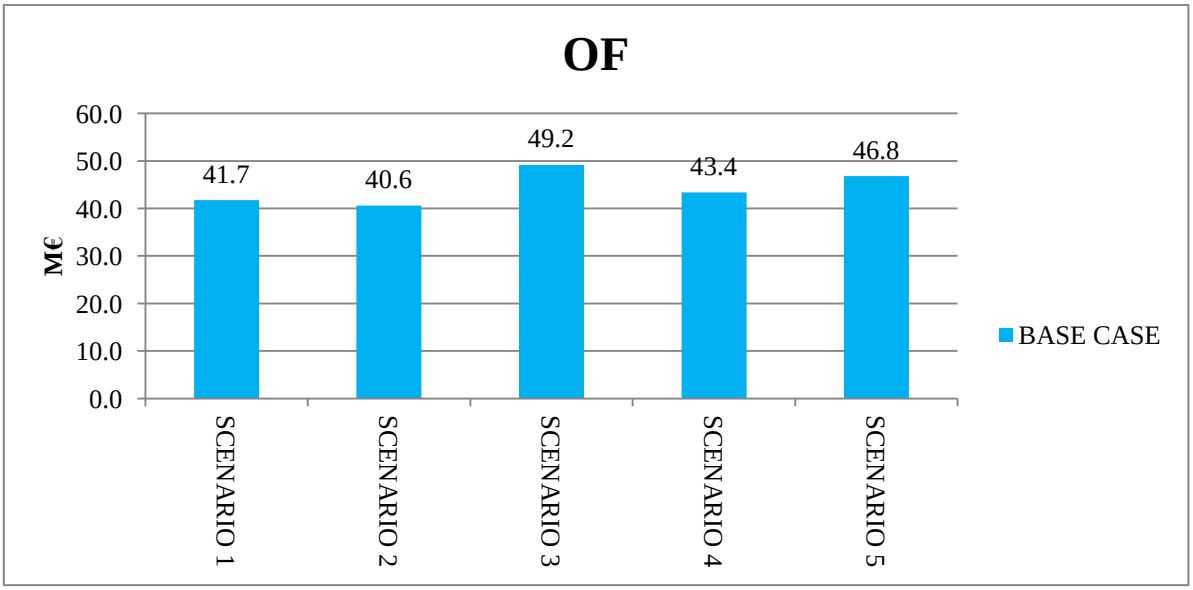

Fig. 7.4: Objective function BASECASE

Moreover it can be noticed close results for the scenario 1,2 and 4, which have a quite similar balanced load/generation condition, whilst the scenarios 3 and 5 are diverse. For that reason, we will focus our

attention only on the first scenario, together with the 3 and 5 to have a whole view of what are the possible working condition for the grid.

It is important to isolated the two costs affecting the OF: the losses costs and the var investment costs. The losses costs are represented by the redispatching costs which are clearly the main cost forthe OF, as it can been seen in Fig.7.5.

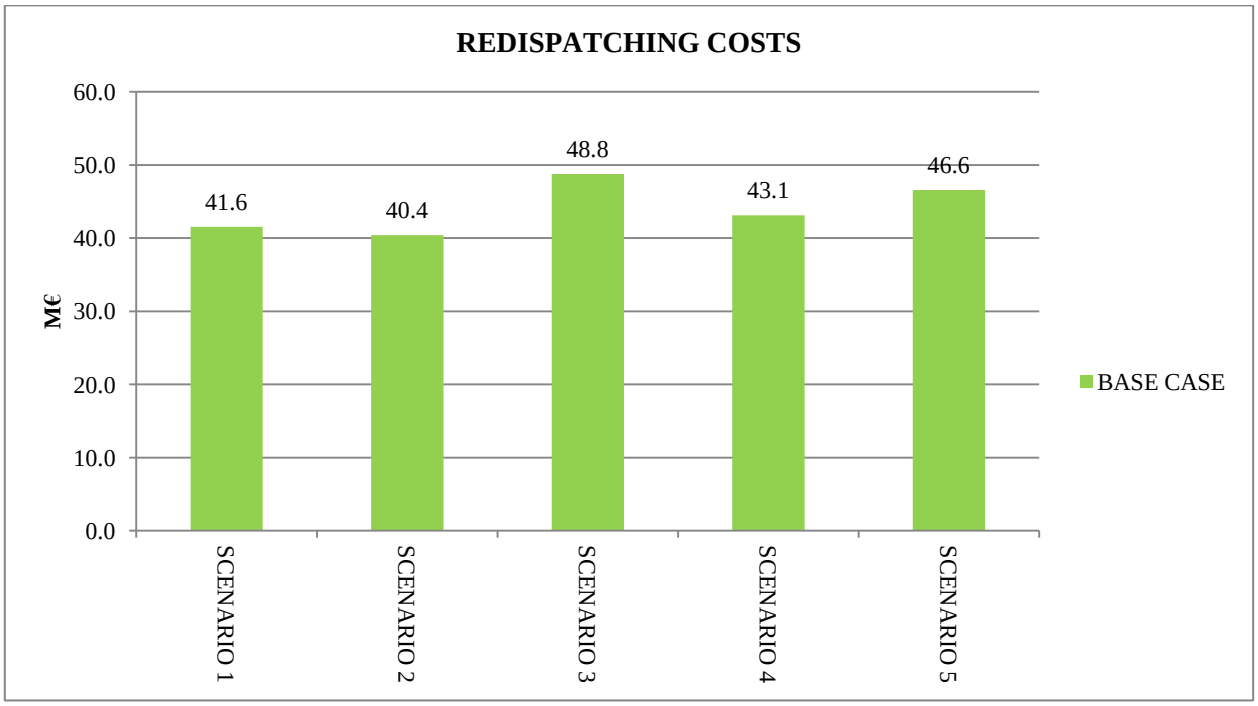

Fig. 7.5: Redispatching costs

The real value of the losses for each scenario increases with the power considered, so we find the highest value for the scenario 3. To have a perception of the goodness of the grid, the losses have been calculated as percentage of the ratio between the total losses and the total load (Fig. 7.6.) . It results that although the scenario 3 has many losses, it has a good management of the grid, being able to deliver the most of the generation to its loads.

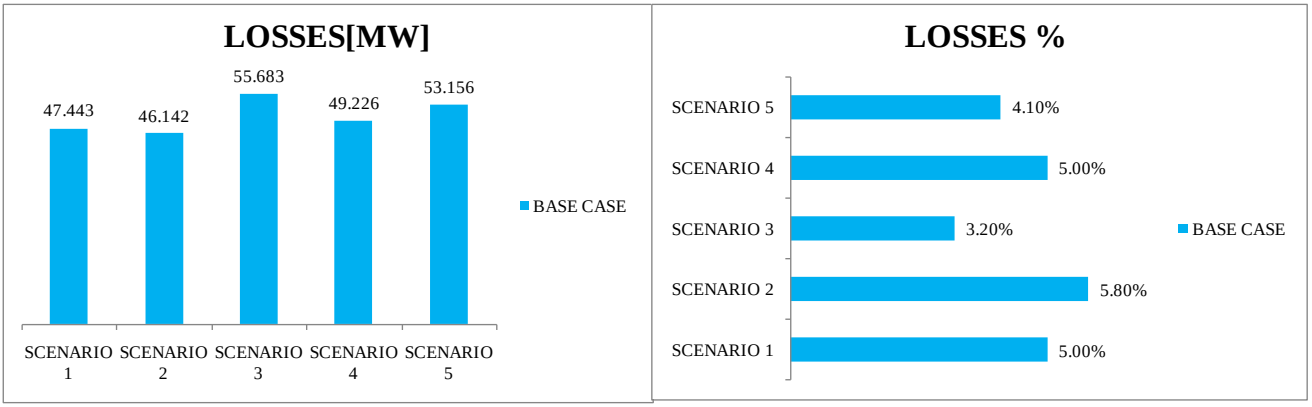

Fig. 7.6: Losses for BASECASE

The remaining part of the OF is composed by the investment costs for the reactive allocation, shown in Fig. 7.7.

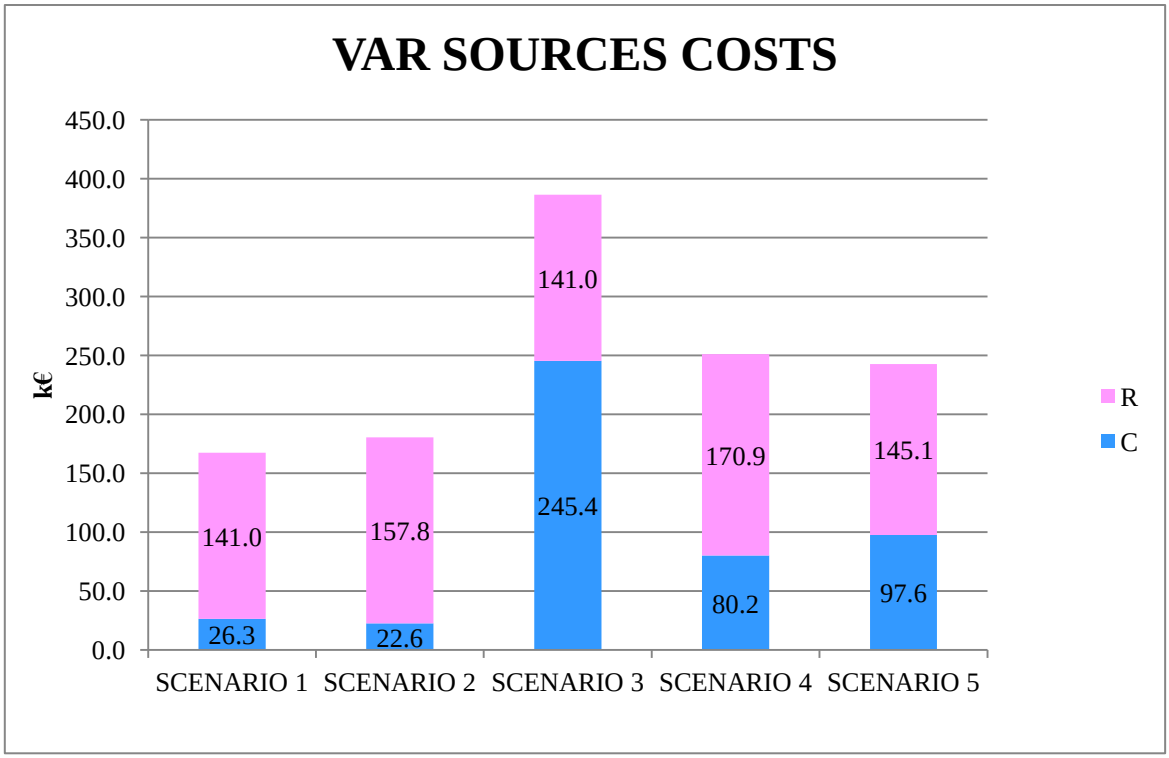

Fig. 7.7: Investment costs of capacitors (C) and reactors (R) for BASECASE

It can be stated that the costs related to the capacitive sources are more changeable than those for reactors along the various scenarios. Thus, with different load/generation conditions, the grid is more stressed by different requests of capacitive reactive power.

The results representation will be conducted by the real power point of view and by the reactive point of view and they have been drawn making a few assumption.

In all the graphs for the real power flows, there is a comparison load/generation for each area: PGEN is the optimized generation (dark green) compared to PGEN0 (bright green), which is the starting generation point. The local load is the red bar. and LOAD to deal with the losses and the need to feed at least the local load. Moreover, the real power through the major connections among the areas are set by black arrows. The indication for each converter of the power passing through, is given by the black graphs referred to all of them: as assumption, the negative values mean absorbed real power from the AC end (rectifier operation) whilst the positive value indicates a production of real power to the AC bus (inverter operation).

In all the graphs for the reactive power flows, there is a comparison of the total size (Mvar) of capacitors/reactors for each area, labeled respectively C and R. The local installation at each bus is given by the relative symbols and three different sizes have been assumed as in Fig 7.8 : the smallest indicate the size from 0 Mvar to 50 Mvar, the medium size is for the range 50-100 Mvar, while the big size represents var sources equal or bigger than 100 Mvar.

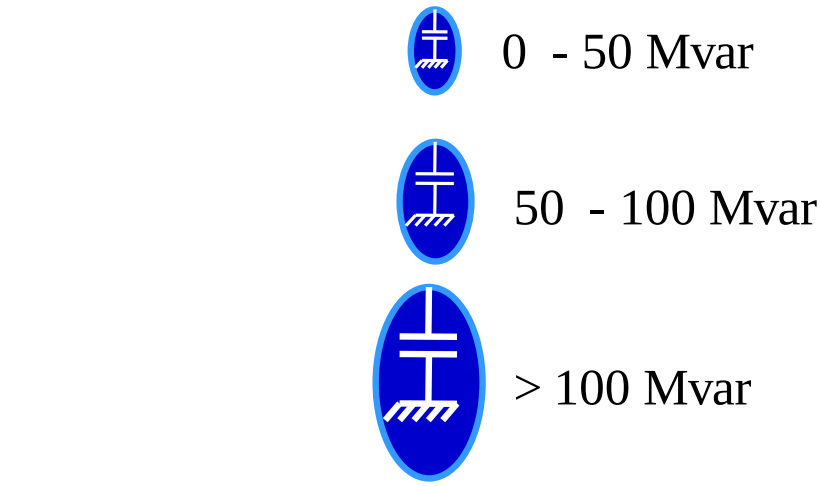

Fig. 7.8: Sizes for var sources

Finally, the indication for each converter of its reactive power is given by the red graphs referred to all of them: as assumption, the negative values mean absorbed reactive power from the AC end, whilst the positive value indicates a production of real power to the AC bus.

SCENARIO 1

The real power flow concerned the scenario 1 is represented in Fig. 7.9.

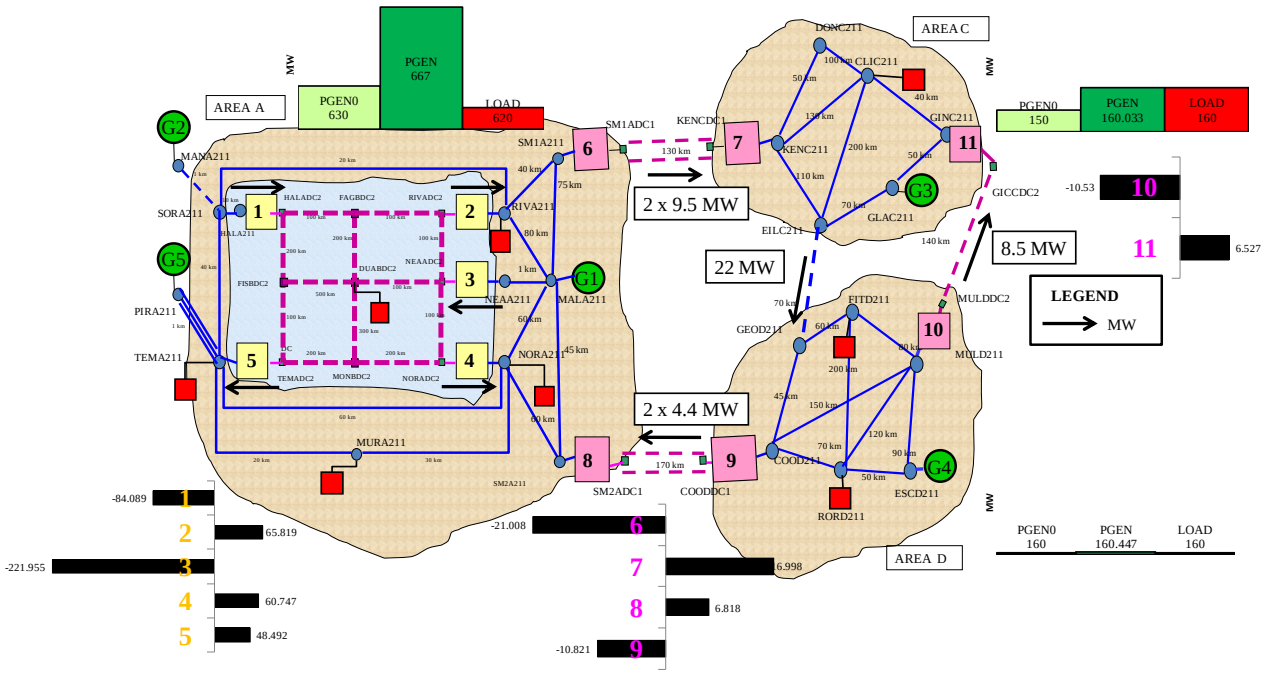

Figure 7.9: REAL POWER FLOW for BASECASE of scenario 1

It is interesting how the load in CLIC211 is fed mostly by the line GINC211-CLIC211 since it is the shortest path from G3. In this BASE CASE the losses, in Fig. 7.10, are given mainly by the converter losses, 6MW for the VSC technology and 2 MW for the LCCs, since the flow through the lines are low.

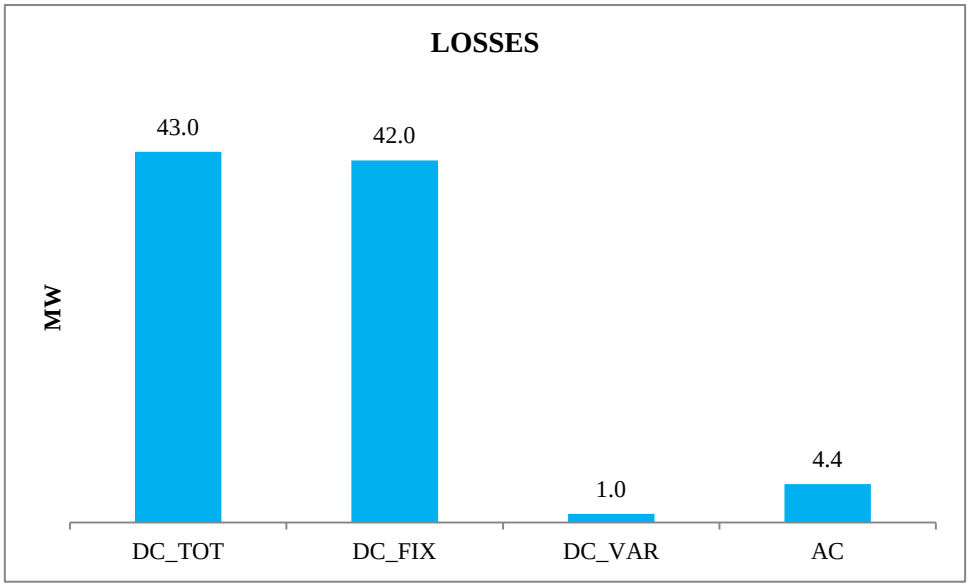

Figure 7.10: LOSSES for BASECASE of scenario 1

Concerning the reactive, the optimal installation is given by the Fig. 7.11:

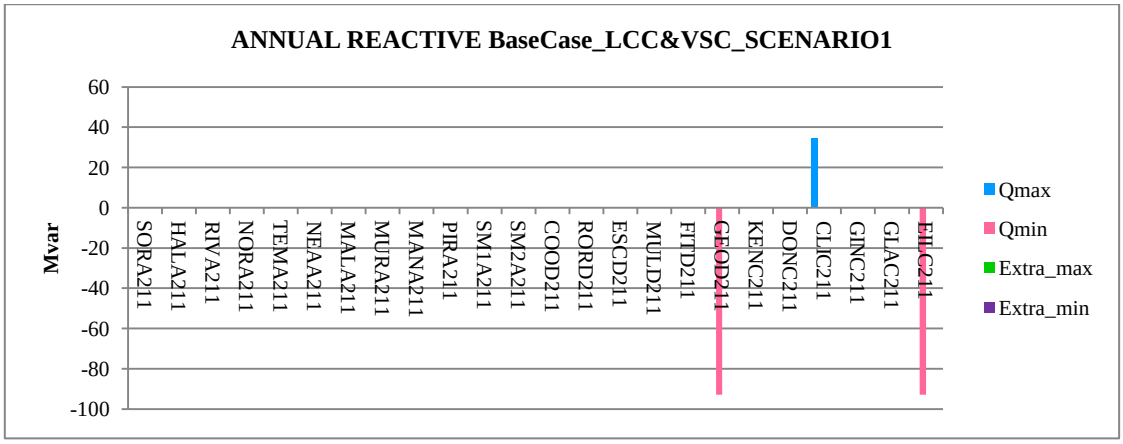

Figure 7.11: Annual reactive allocation for BaseCase LCC&VSC SCENARIO 1

The main necessitate of the grid is to compensate the reactive produced by the cable GEAID211- EILC211. The need to install a capacitor at the bus CLIC211 is not only to have a high voltage profile, 1.029 p.u., but to be improve the reactive flow towards the converter 7 and 11, which are LCCs and always absorb reactive power as shown by the correspondent red diagram. Moreover it can been seen that the generation G1 produces reactive which keep the voltage at that bus at the maximum value, 1.05 p.u. All these information are collected in Fig. 7.12:

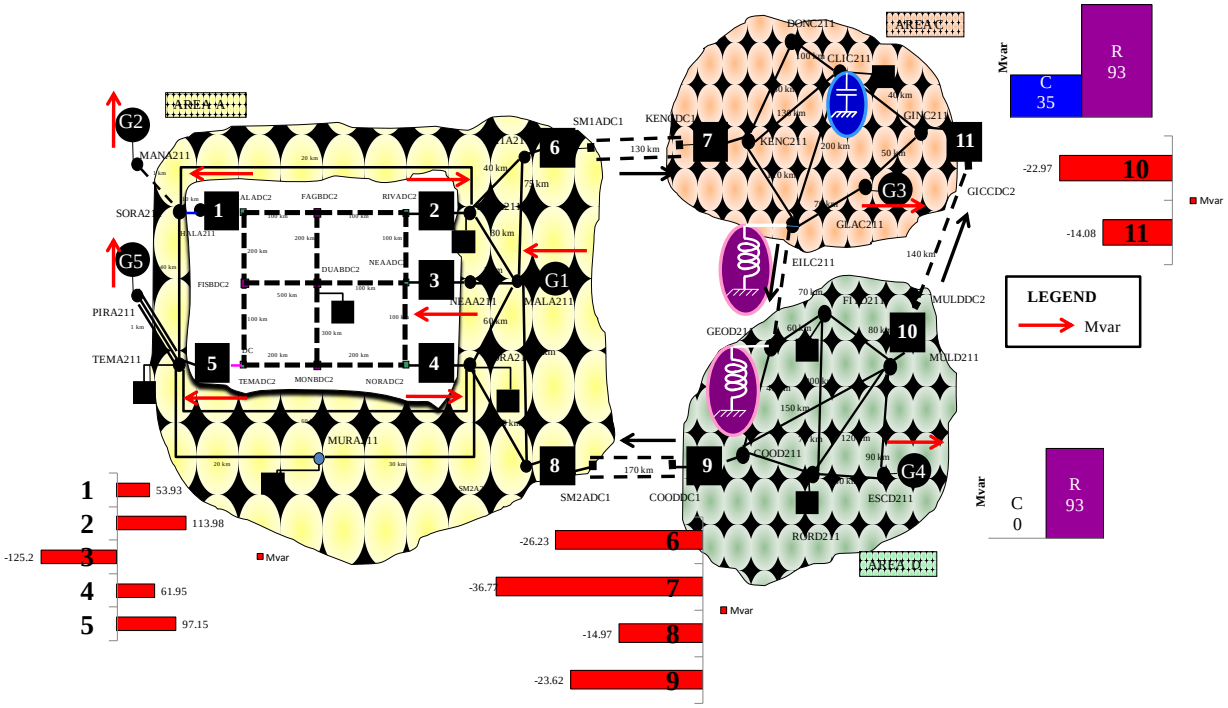

Figure 7.12 : REACTIVE POWER FLOW for BASECASE of scenario 1

It can be noticed how the reactive installed at the end of the cable GEOD211 an EILC211 are equal since it has been assumed that the compensation of the cable is allowed up to the 80% of the total reactive power produced by the cable spelt at the end of the cable itself, for the reason explained in Chapter 6. Moreover, in the area A, the VSCs are working to supply the reactive required by the loads

Speaking about the different technology, it can be noted that stressing the grid with a higher active flow, the LCC to be able to bring this power, have to absorb high reactive power; this lead to decrease the voltage magnitude at the connecting bus.The results collected above are a useful tool to understand how this device is important if smartly commanded in an overall way.

Let us to have a focus on the converter behaviour. We have modelled the converter as explained in Chapter 5 and as example let's consider the converter LCC 6 and 7 taken from the figure 7.12:

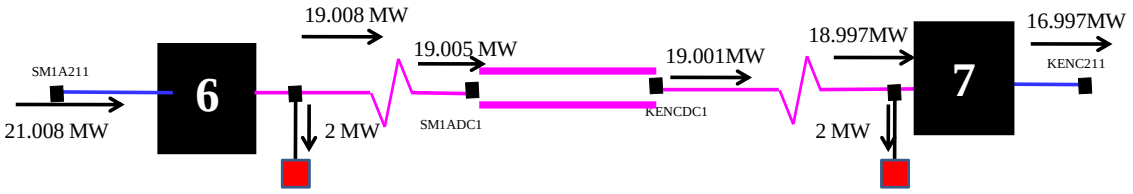

Figure 7.13 : Zoom on the couple of converter 6-7 for BASECASE of scenario 1

One important consideration is that to improve the power delivered by the converter, the model select as best option α equal to zero which is realizable for the rectifier, whilst γ equal 0 for the inverter is not practically reliable, since the range of value to guarantee the extinction of the commutation is over 15 degree. This can be notice in the scenario 3, where the high power flow from the west side towards the east side make the system to adopt its best solution. This is a limitation for the model, since has not been fixed limits for the extinction angle. For the other scenarios, instead, the γ angle assumes value different from 0. Moreover

there is another limit for the model for little flow there is an awkward behaviour: the fixed losses for the converter, deblocking losses, are feed by both the side of the branch to be able to generate the voltage with the right technology. Therefore there are these flows that have end in the fictitus load.

Moreover, for the LCC, the values of the parameter by which it has been described are collected in the Tab. 7.6, where the angle α is the command to turn on the valves of the converter. μ is quite low due to the small value of the current.

		γ [degree]	α [degree]	μ [degree]
6	RAD	-	50.788	0.896
8	INV	65.4	114.352	0.248
9	RAD	-	65.216	0.396
10	RAD	-	65.204	0.386
7	INV	64.919	114.453	0.629
11	INV	65.024	114.734	0.242

Table 7.6: Parameters for LCC converter for scenario 1

These parameters for each LCC are the control to have that real power flow in the grid for a smart management of it, together with the control to the generators.

SCENARIO 3

The third scenario offers a situation of unbalance for the area C, since to avoid a load shedding the grid has to find a solution to feed the load exporting at least 200 MW of power from the close areas.

Since the scenario 2 is similar, we will pass to the scenario 3, shown in Fig. 7.14.

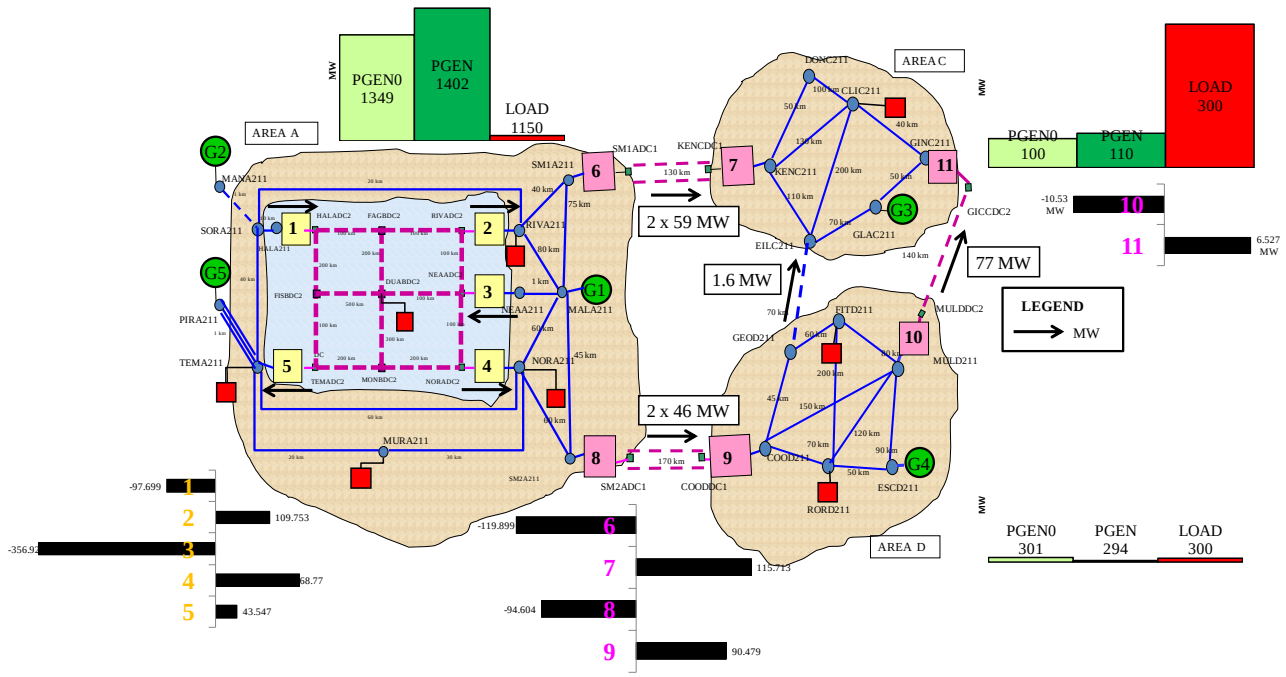

Figure 7.7: REAL POWER FLOW for BASECASE of scenario 3

Here, it can been seen how the flows are increased and are all directed towards the area C where the only generation G3 is not able to feed the load.

We can seen how the extinction angle γ is at last 15 degree, limit chosen to guarantee a secure commutation. Moreover the angle of commutation has higher value than the previous case, since the current is increased.

		γ	α	μ
6	RAD	-	14.546	8.324
8	RAD	-	16.169	6.349
9	INV	18.648	155.839	5.513
10	RAD	-	16.503	5.383
7	INV	15	157.044	7.956
11	INV	16.409	158.413	5.178

Table 7.7: Parameters for LCC converter for scenario 3

The LCC converter are working with higher real power and that leads to absorb higher reactive power. Therefore the installation of reactive sources is obviously more intense, above all those busses where there is the converter LCC as shown in Fig 7.15:

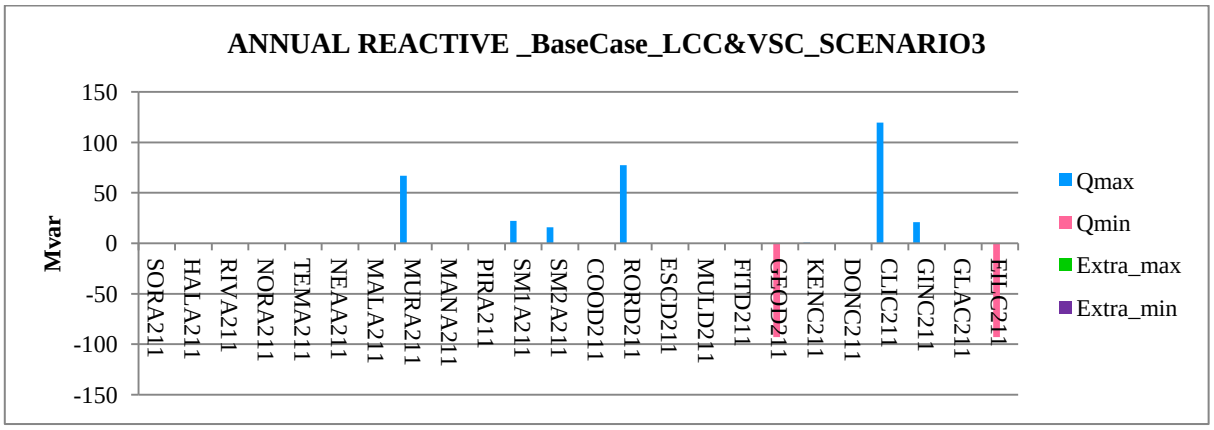

Figure 7.8: Annual reactive allocation for BaseCase LCC&VSC SCENARIO 3

The reactive representation in Fig. 7.15 is more clear about the collocation and the sizes of the var source.

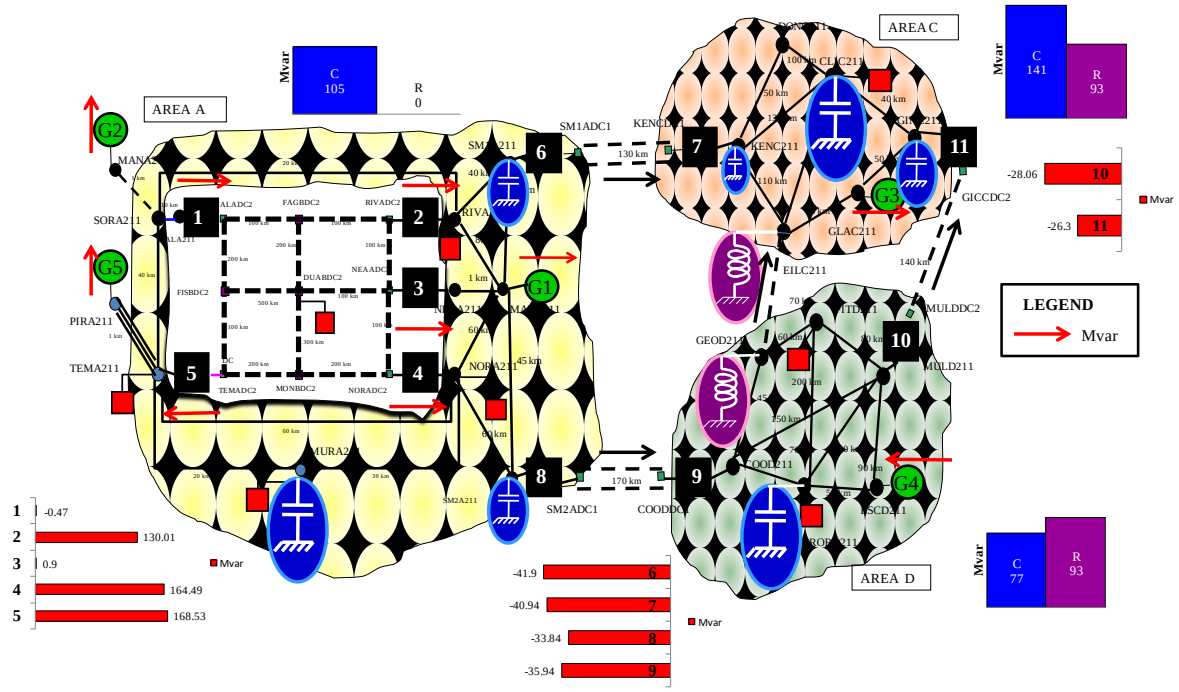

Figure 7.9: REACTIVE POWER FLOW for BASECASE of scenario 3

Comparing with the scenario 1, in this case the reactive installation remains the same, while varying the capacitive compensation due to the increase of the flow. The voltage profile is kept above the 1 p.u. in all the busses.

SCENARIO 5

We are going to examine the last scenario for the basecase:

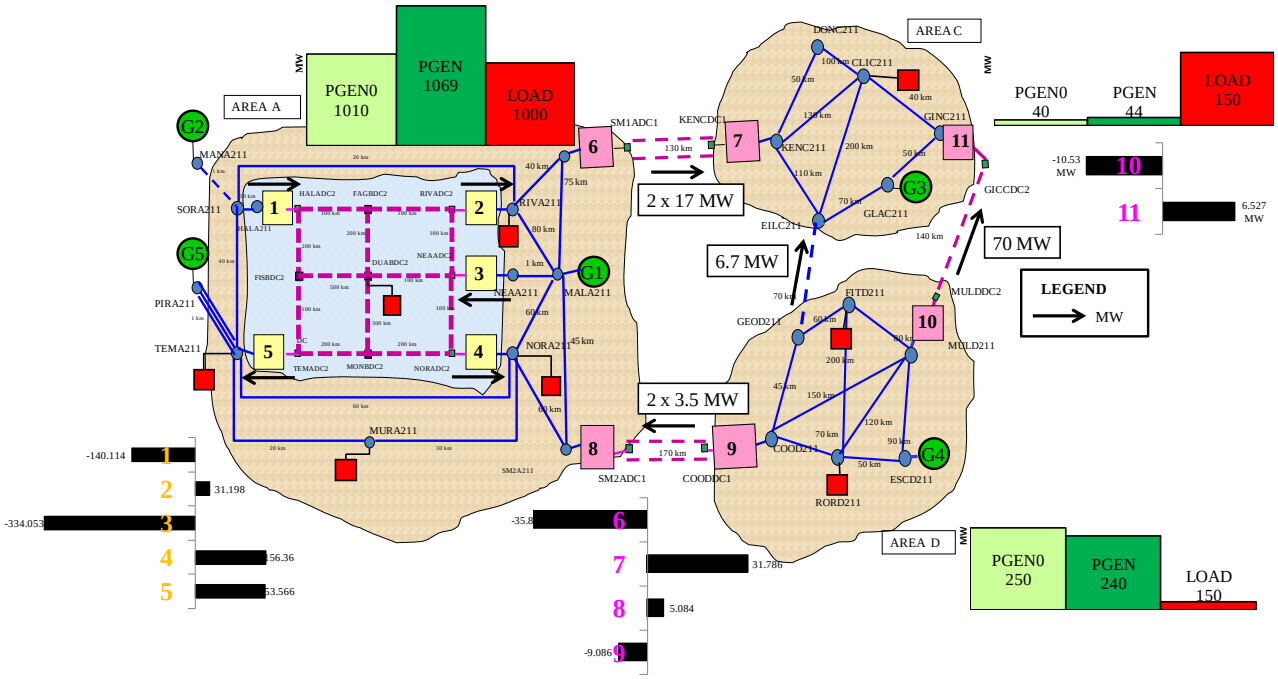

Figure 7.10: POWER FLOW for BASECASE of scenario 5

In this case, since the area D has an extra in generation, it is possible to export from this area toward the area C where there is a lack in generation to face the load.

The LCC converter are working with a precise set of parameters reported in table 7.3

		γ	α	μ
6	RAD	-	50.33	1.532
8	INV	65.422	114.392	0.185
9	RAD	-	65.276	0.332
10	RAD	-	25.779	3.697
7	INV	50.117	128.506	1.377
11	INV	25.262	151.153	3.585

Table 7.8: Parameters for LCC converter for scenario 5

Concerning the reactive, it has been decrease and put locally close to the two biggest load while reduce the losses.

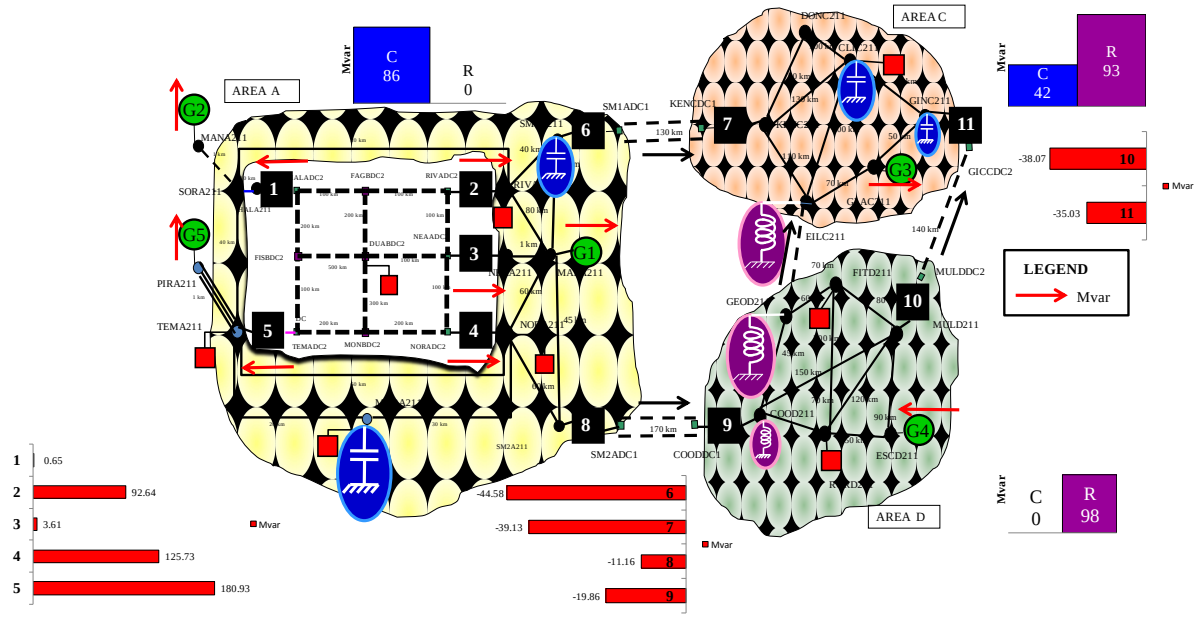

Figure 7.18: REACTIVE POWER FLOW for BASECASE of scenario 5

The right size are shown in Fig. 7.19:

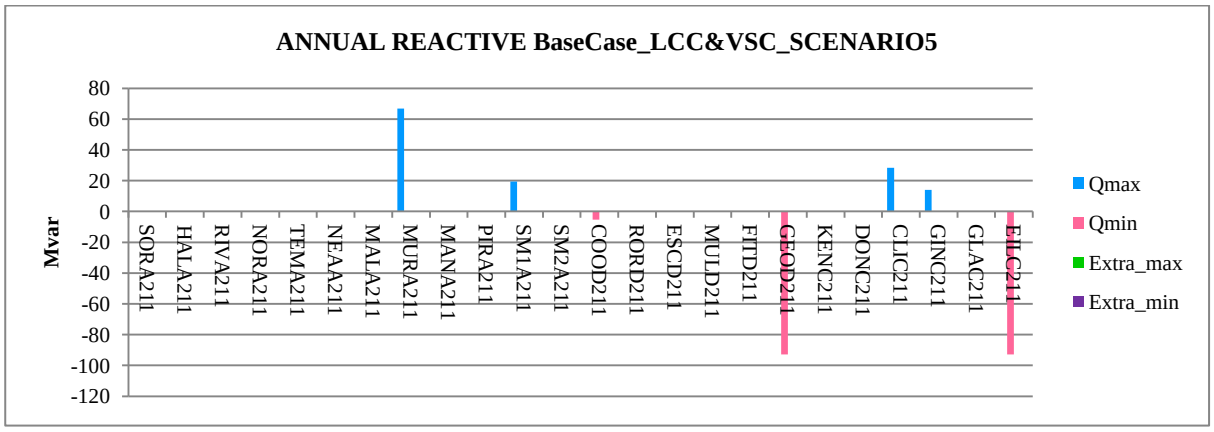

Figure 7.19: Annual reactive allocation for BaseCase LCC&VSC SCENARIO 5

Once the base case has been studied in all its scenarios, it is possible to consider that as starting point for further analysis, according a scheme as in Fig. 7.20.

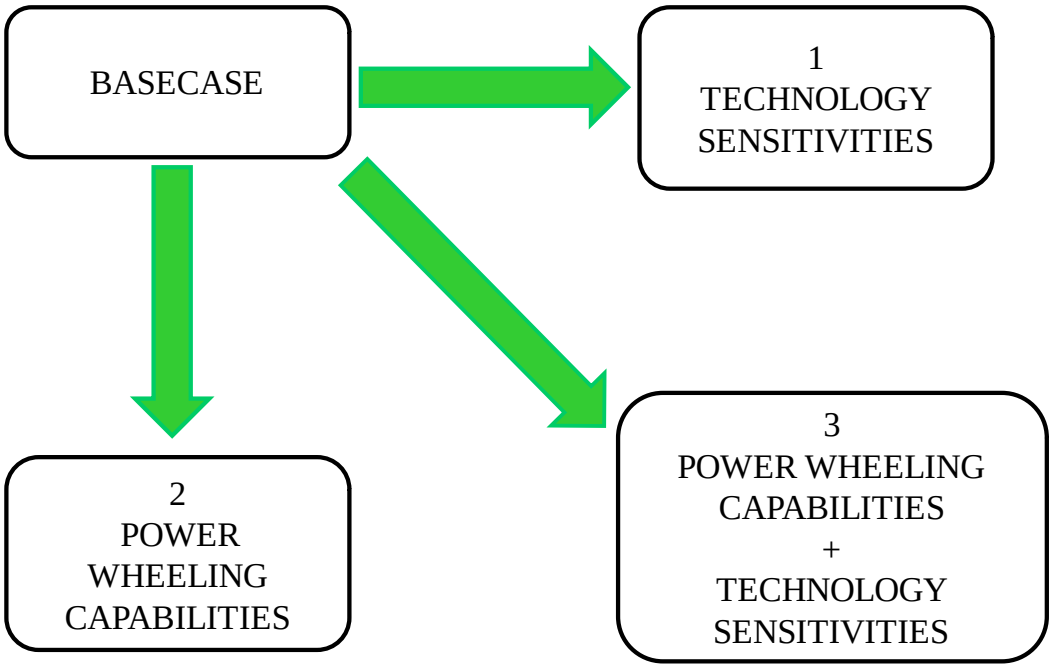

Figure 7.20 SCHEME of the sensitivities

Form the BASECASE we can carry on our analysis along a duplex path considering at first the AC technology sensitivity, after a power wheeling and finally these two aspects all together. Like for the BASECASE, the scenario 1, 3 and 5 will be analyzed more deeply changing the technology of the grid. Starting comparing the objective function is it clear how the change in area A have similar effect for the total costs over all the different scenarios, even something less. On the other side, the substitution on area D and C&D by cables, give different results for the two: CABLE D have a OF which decrease, which the CABEL C&D has a swinging trend.

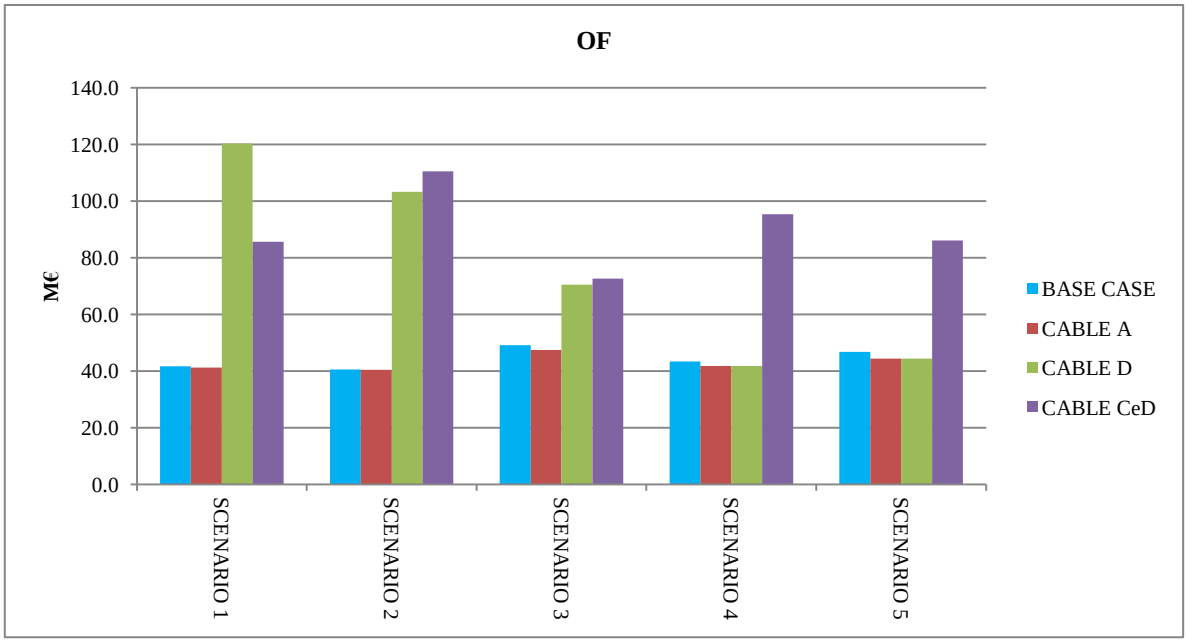

Figure 7.21: Objective function comparison for all the technologies cases

It is important to consider the two items making the OF:

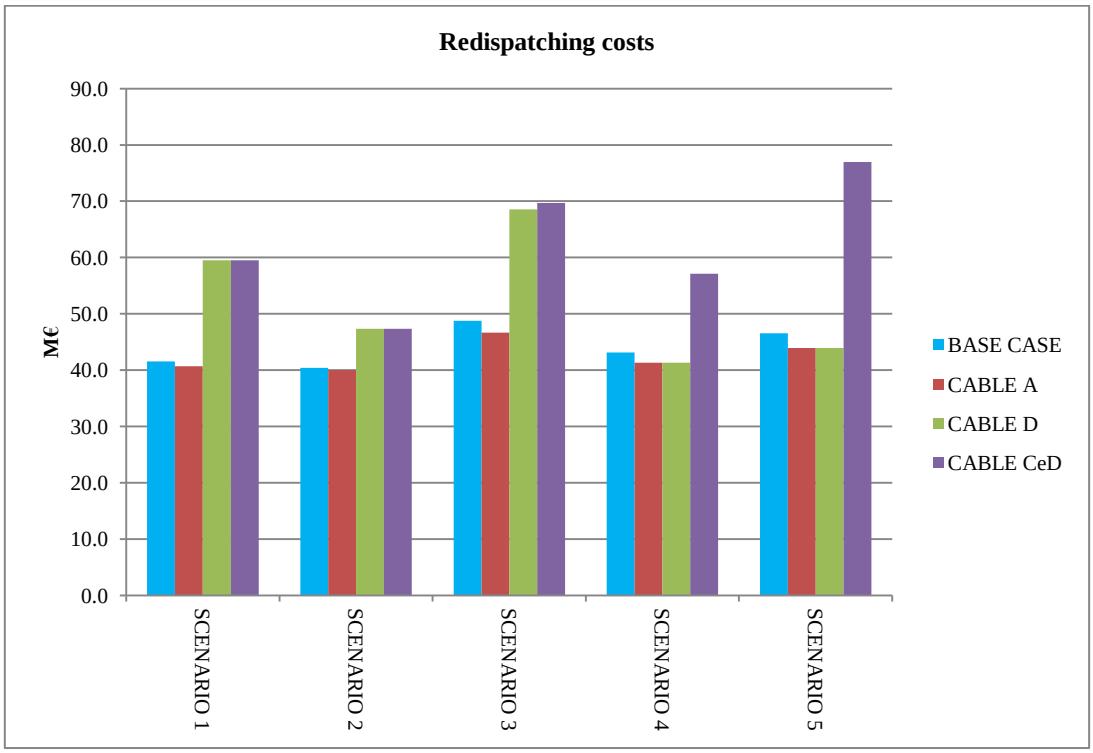

Figure 7.22 : Redispatching costs for all the technologies cases

The redispatching costs , in Fig. 7.22, are directly proportional to the losses: we can notice how the cases are similar two by two for the losses and that for the BASECASE and CABLE A this diagram have the same shape of the OF, whilst it is not true for the other two. Therefore it is useful to introduce the other costs associated with the var installation in Fig. 7.23.

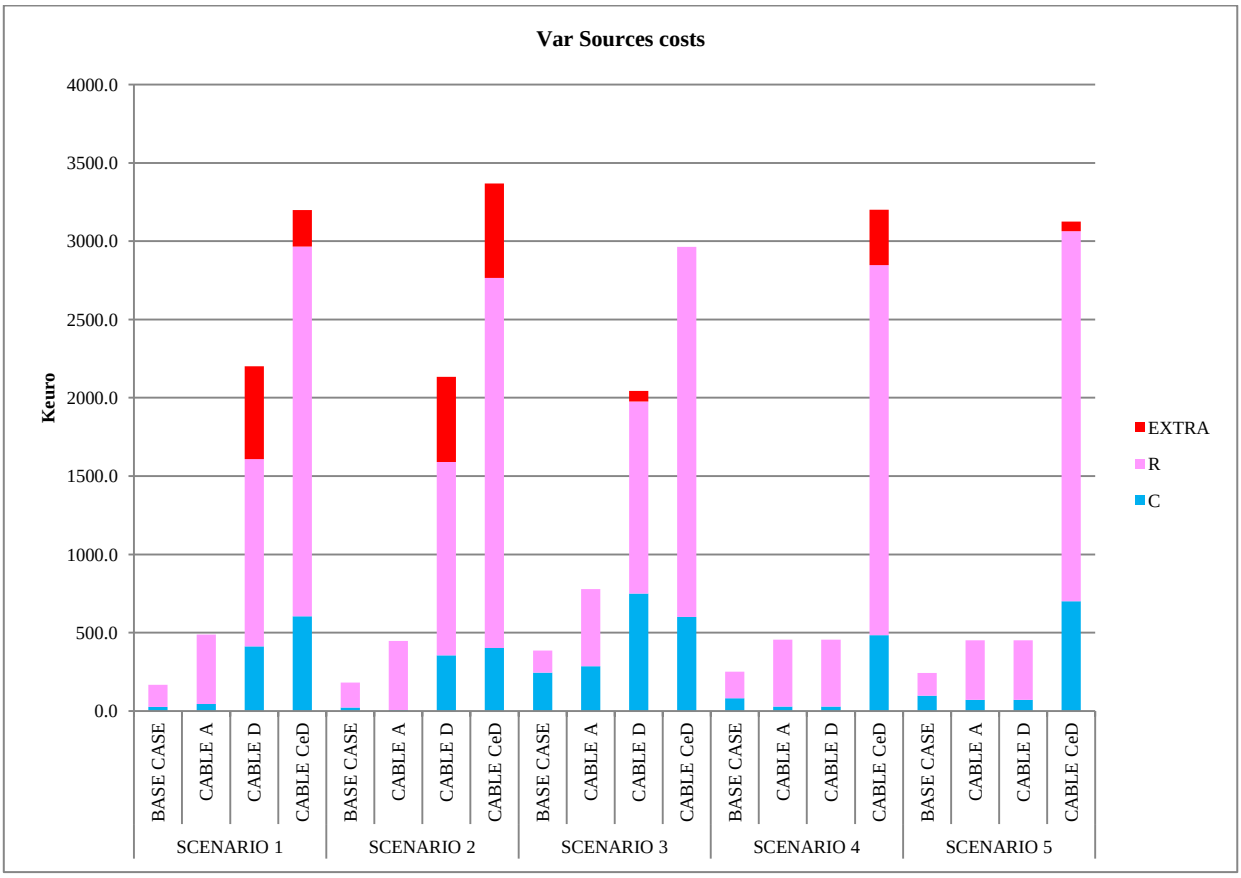

Figure 7.23: Var costs for all the technologies cases

It is clear how the presence o f cables modify widely the installation costs in a different way first of all for the cable D. We can notice how the cases similar two by two for the losses and that for the BASECASE and cable A this costs is quite equal over the different scenarios. That's because, even if there are a lots of cable in area A, the VSC technology can act as a reactor, limiting the var costs installation. Let's try to better understand these different behavior having a look to the results for the other scenarios.

CABLE A

Putting in area A only AC cables, it is changed the reactive condition of the grid, since the cables produce a large amount of reactive, as it was a big capacitance. Compared to the basecase, we will notice a similar capacitors installed, while there is a higher amount of reactors. These choise allow the grid to reduce its losses which are more expansive than var sources and therefore the total costs for the CABLE result lower than BASECASE, though very similar. The interest will be in studying how the VSC technology can be a good device to make the system working with lower losses and the indispensable var installation.

SCENARIO 1

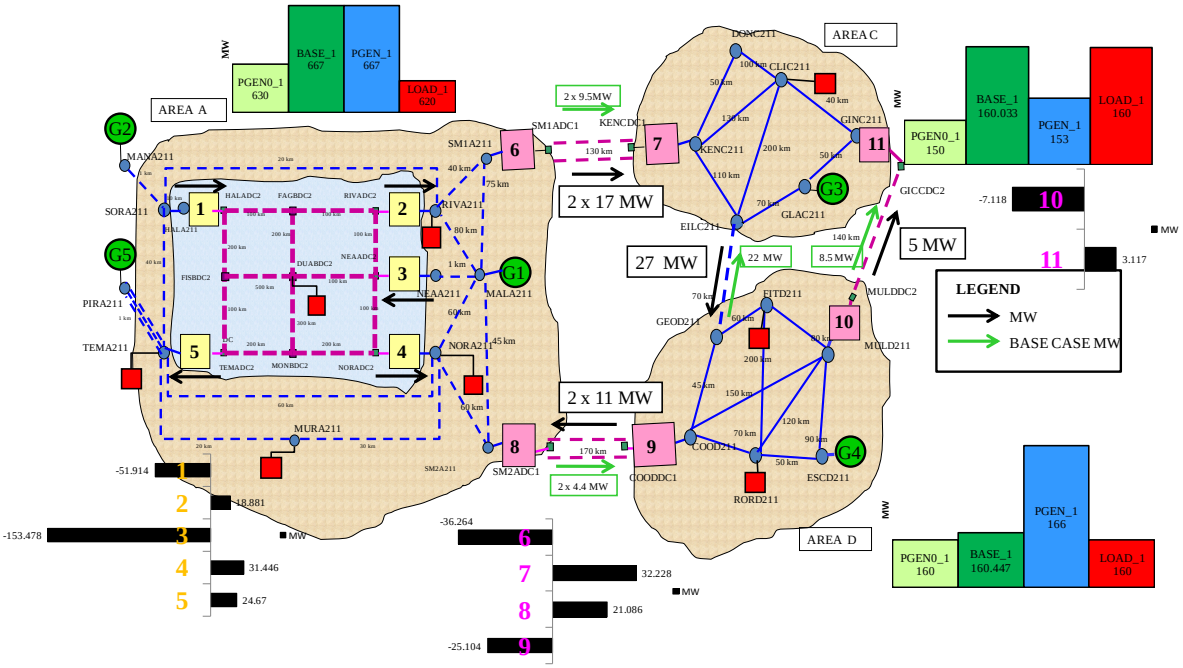

Figure 7.24: POWER FLOW for CABLE A of scenarios 1 compared with BASECASE

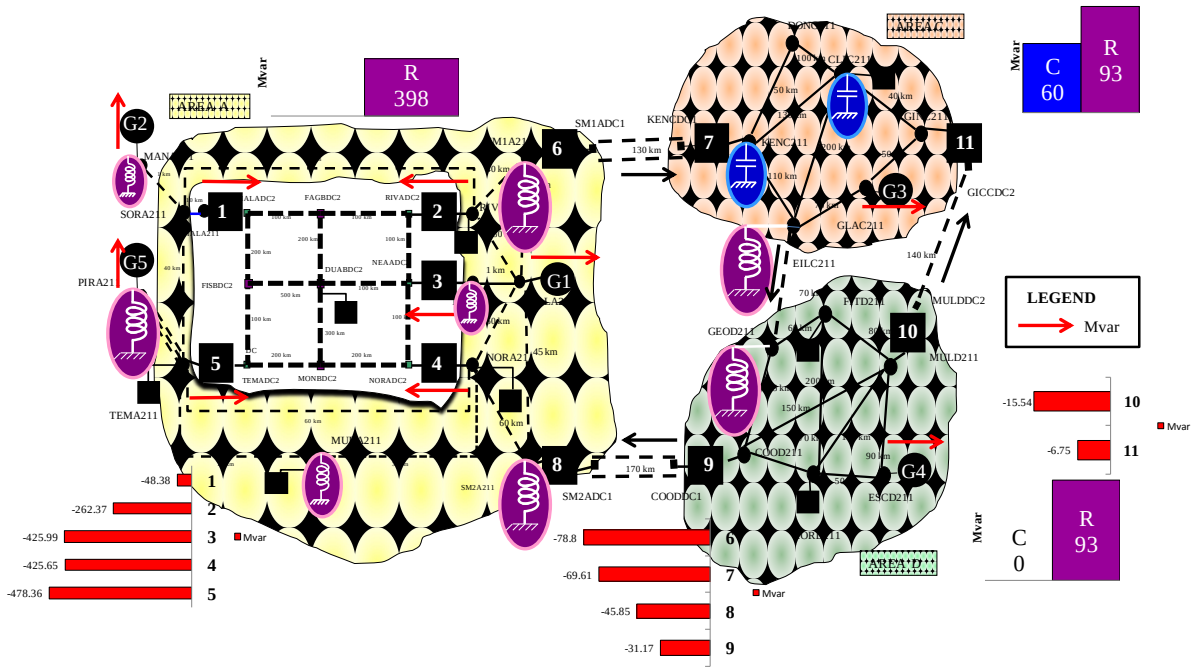

Figure 7.25 : REACTIVE POWER FLOW CABLE A of scenarios 1

SCENARIO 3

The value of the flow have been increased and

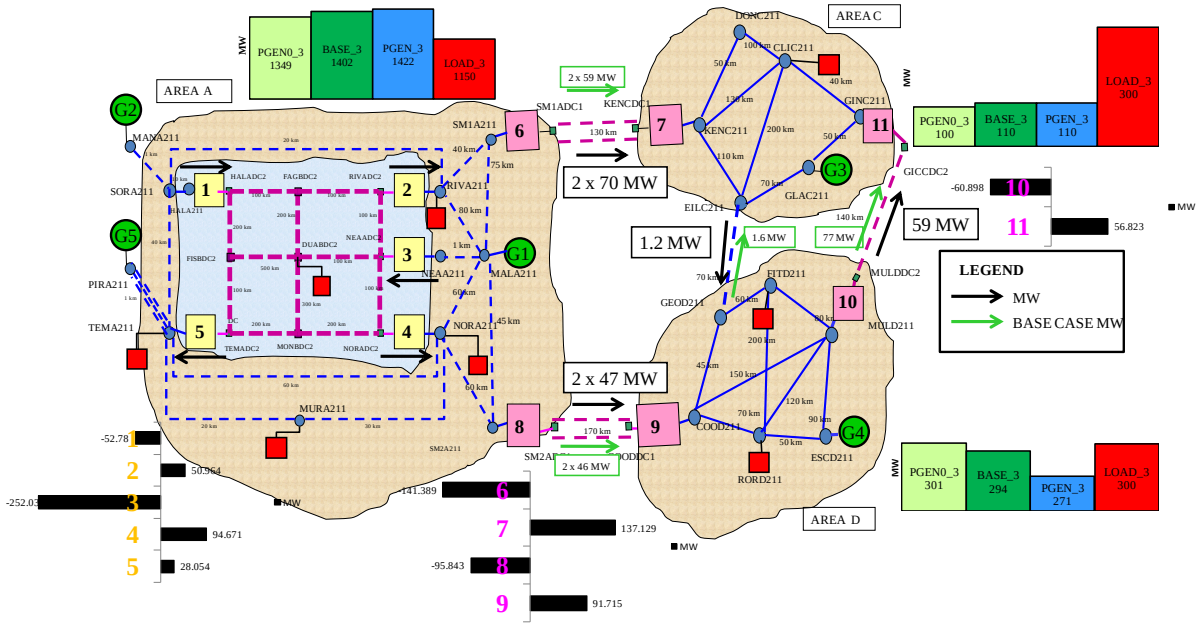

Figure 7.26: POWER FLOW for CABLE A of scenarios 3 compared with BASECASE

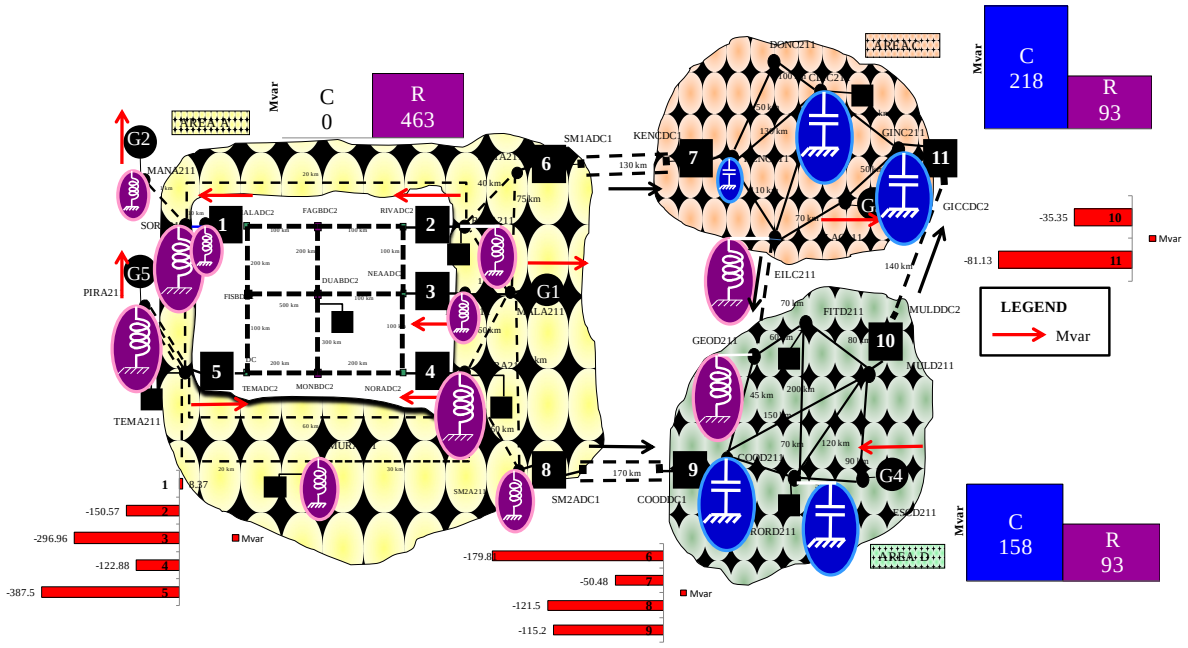

Figure 7.27: REACTIVE POWER FLOW CABLE A of scenarios 3 compared with BASECASE

SCENARIO 5

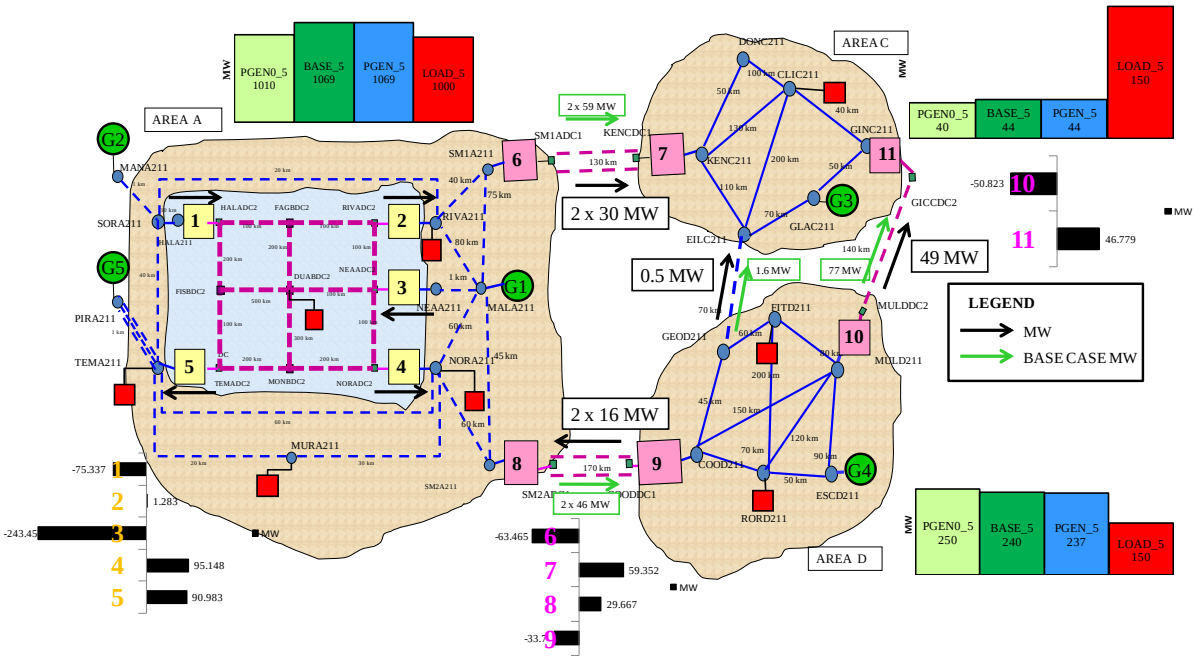

Figure 7.28: POWER FLOW for CABLE A of scenarios 5 compared with BASECASE

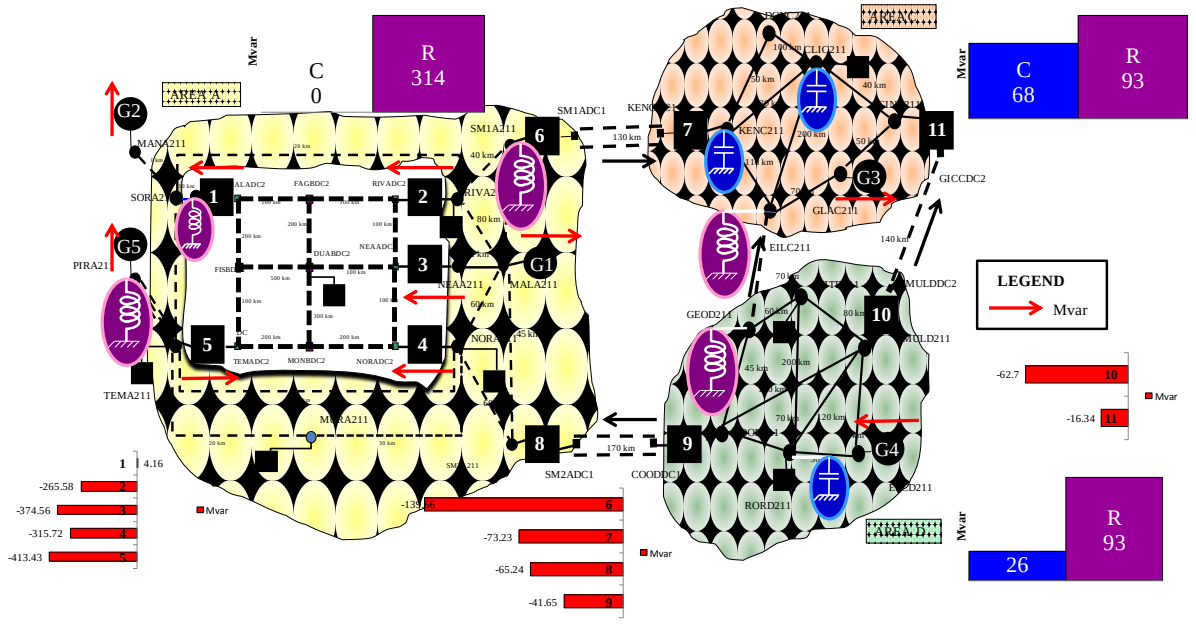

Figure 7.29: REACTIVE POWER FLOW CABLE A of scenarios 5 compared with BASECASE

There is the need to put reactor because of the lots of cable, although the VSC converters are all absorbing, as we can see by the red graph. The small size for the var sources is due to the fact that the generators are able to absorbe the reactive by themselves. It can been point out that substituting the cables in the area A, the grid requires some reactors but not of high size because this reactive power is used to supply the load and also can be manage by the VSC converter.

CABLE D

This case has much more losses.

SCENARIO 1

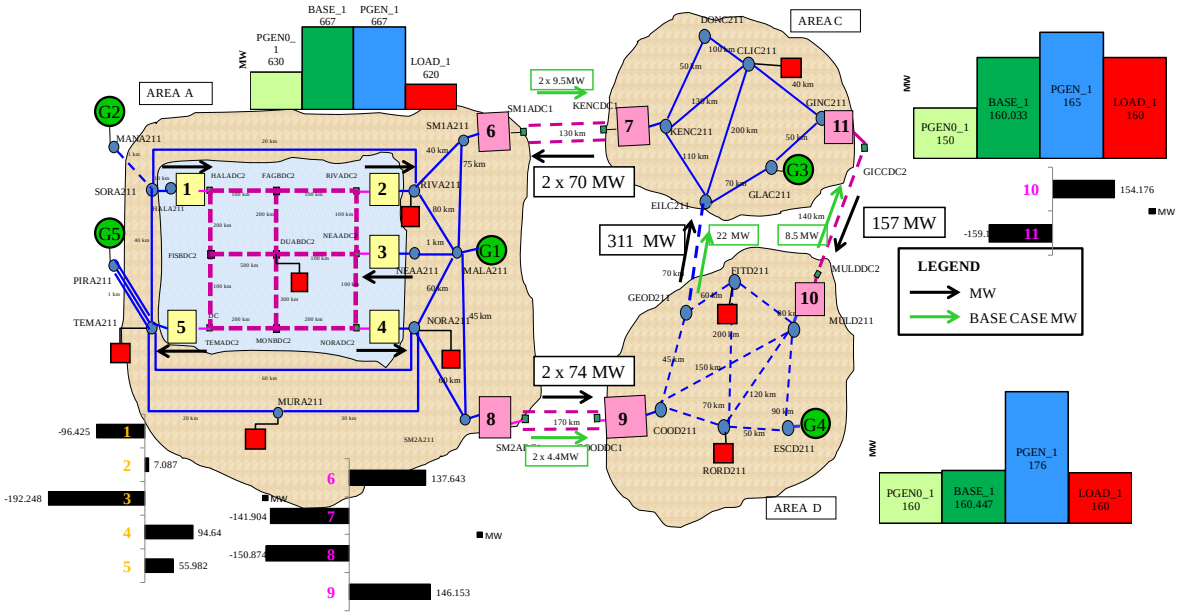

Figure 7.30: POWER FLOW for CABLE D of scenarios 1 compared with BASECASE

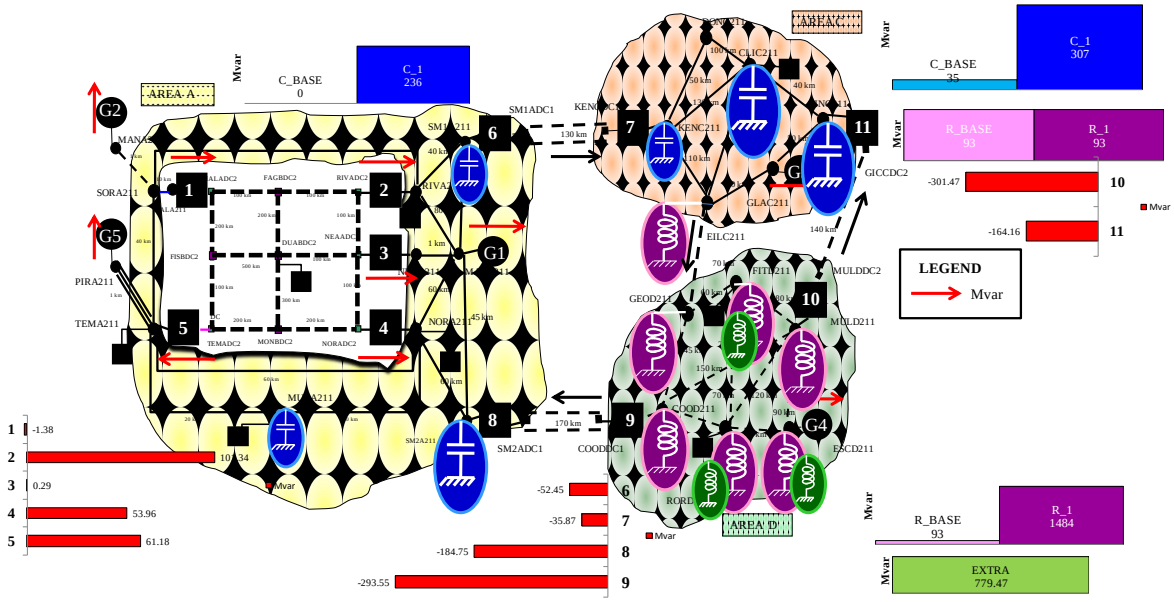

Figure 7.31: REACTIVE POWER FLOW CABLE D of scenarios 1 compared with BASECASE

SCENARIO 3

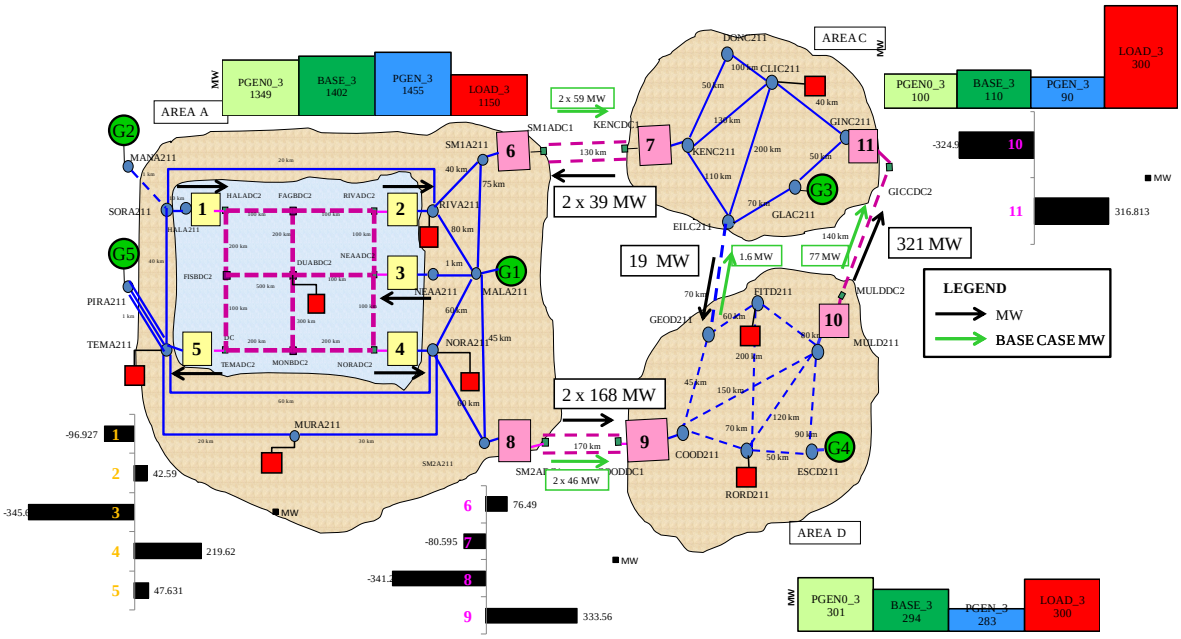

Figure 7.32: POWER FLOW for CABLE D of scenarios 3 compared with BASECASE

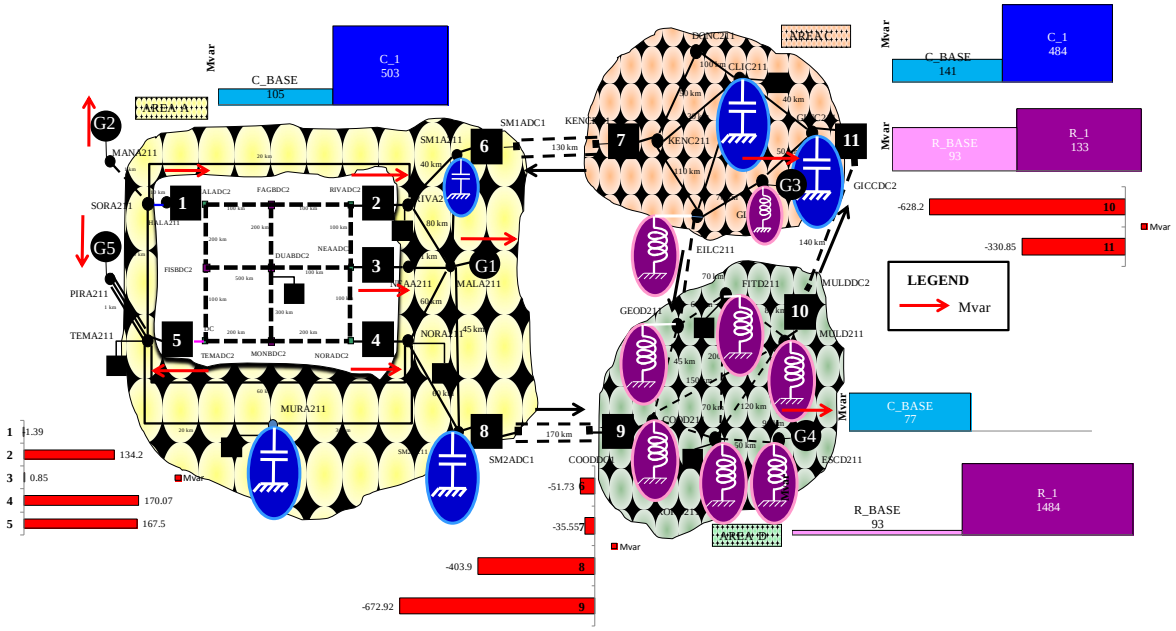

Figure 7.33: REACTIVE POWER FLOW CABLE D of scenarios 3 compared with BASECASE

SCENARIO 5

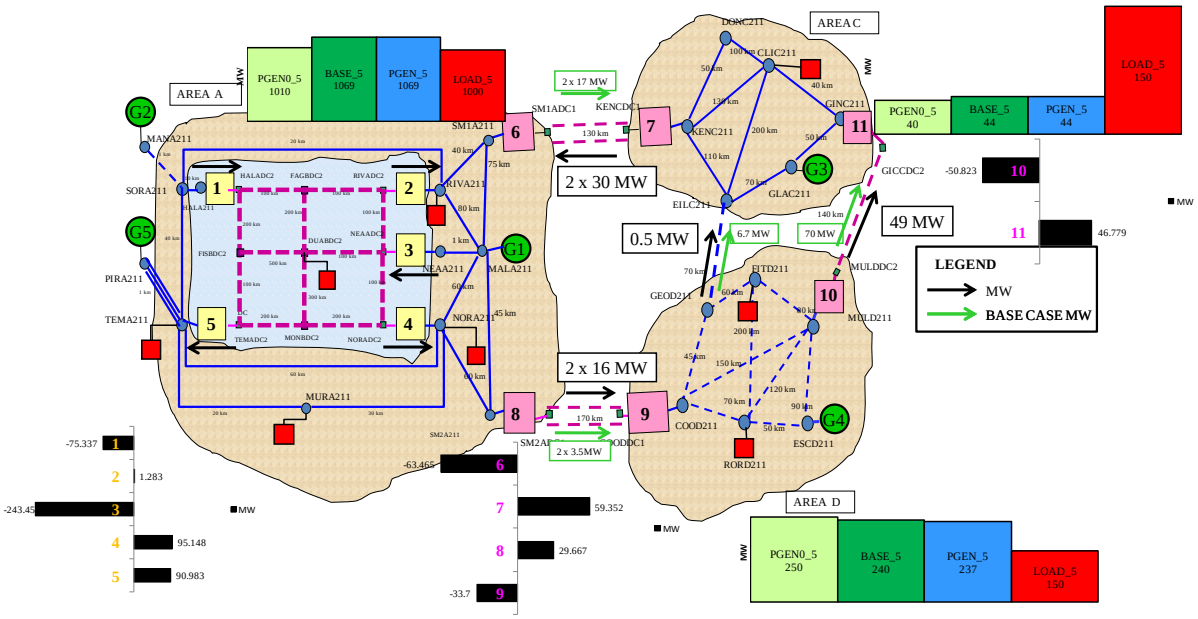

Figure 7.34: POWER FLOW for CABLE D of scenarios 5 compared with BASECASE

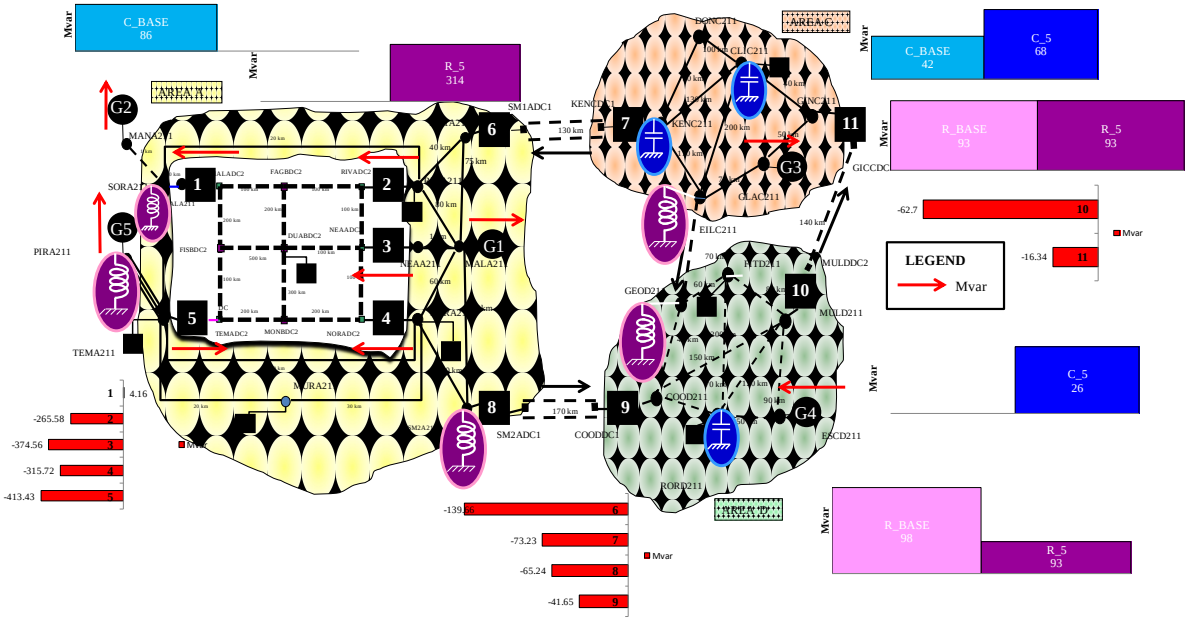

Figure 7.35 : REACTIVE POWER FLOW CABLE D of scenarios 5 compared with BASECASE

CABLE C&D

SCENARIO 1

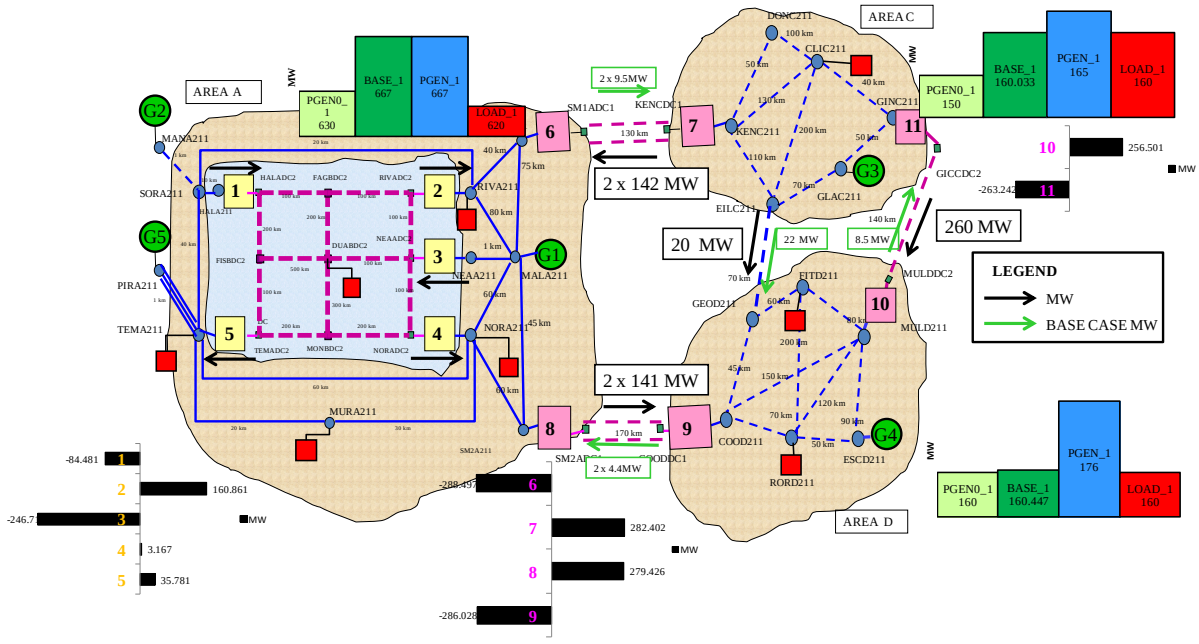

Figure 7.36: POWER FLOW for CABLE D of scenarios 1 compared with BASECASE

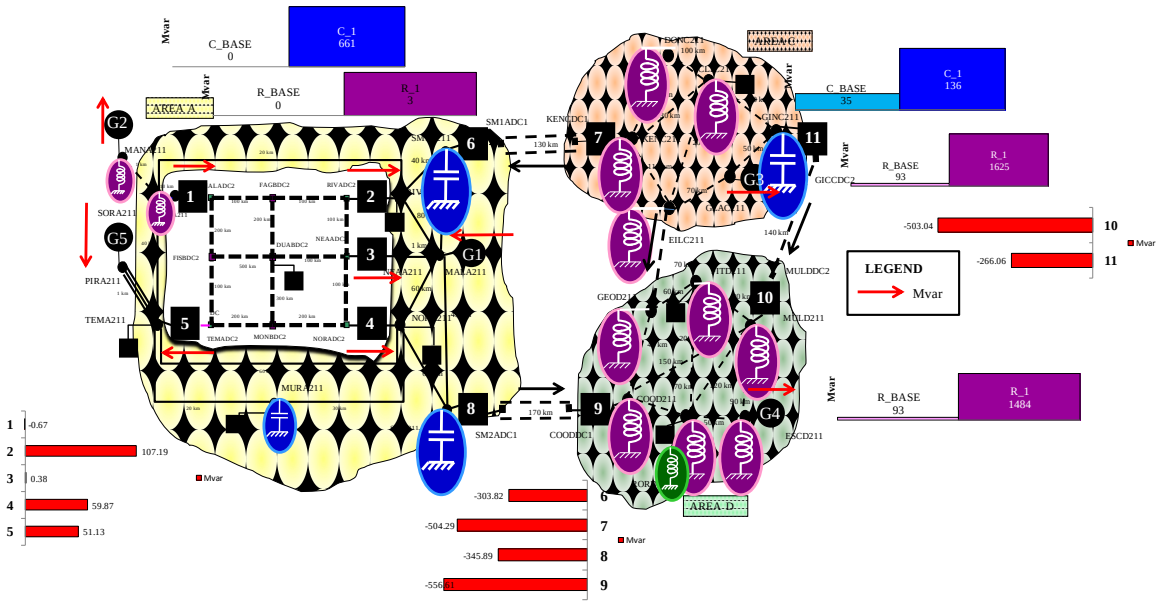

Figure 7.37: REACTIVE POWER FLOW CABLE D of scenarios 1 compared with BASECASE

SCENARIO 3

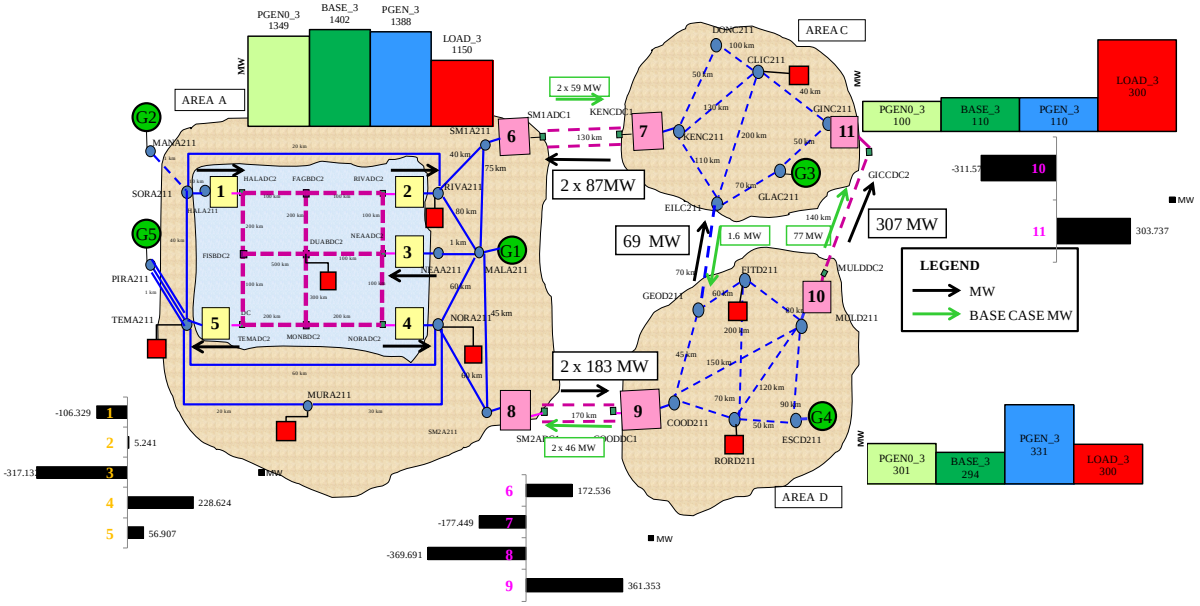

Figure 7.38: POWER FLOW for CABLE D of scenarios 3 compared with BASECASE

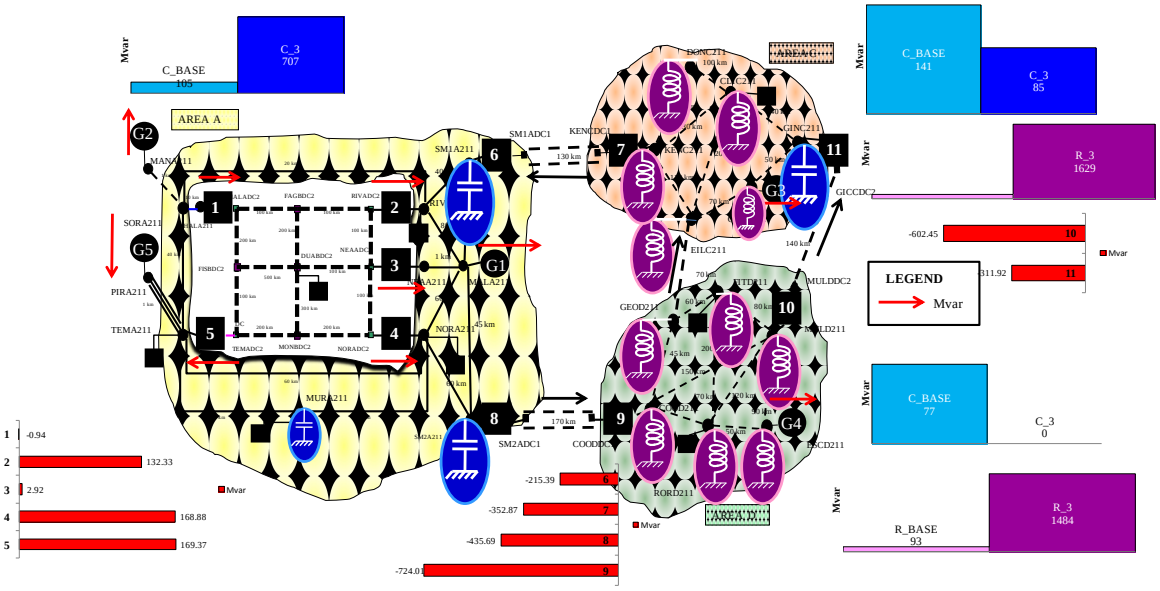

Figure 7.39: REACTIVE POWER FLOW CABLE D of scenarios 3 compared with BASECASE

SCENARIO 5

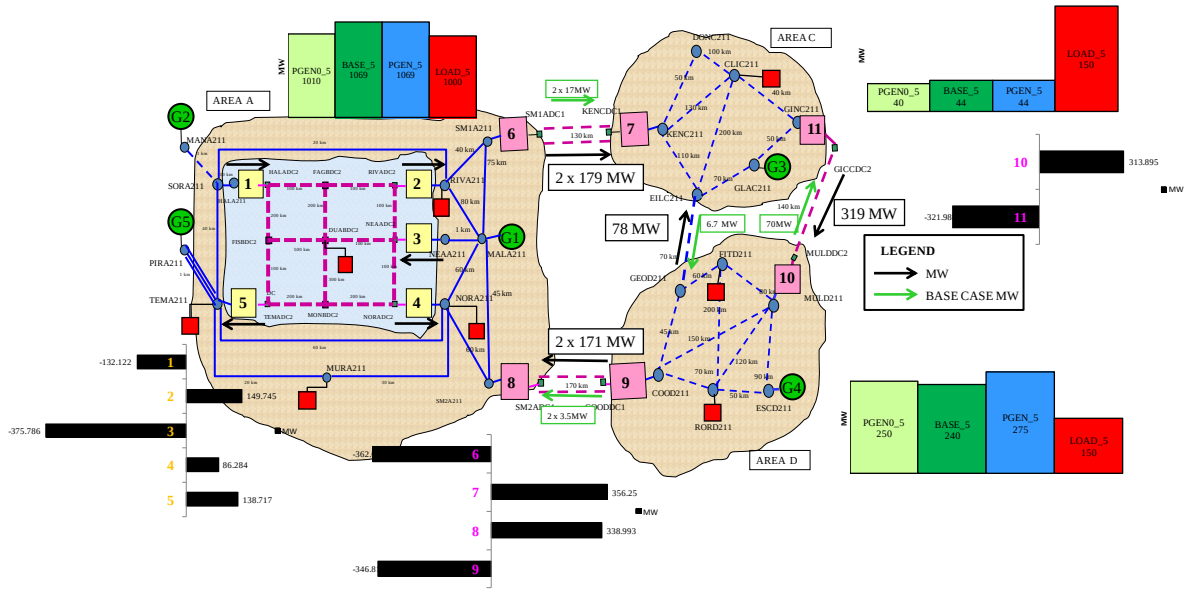

Figure 7.40: POWER FLOW for CABLE D of scenarios 5 compared with BASECASE

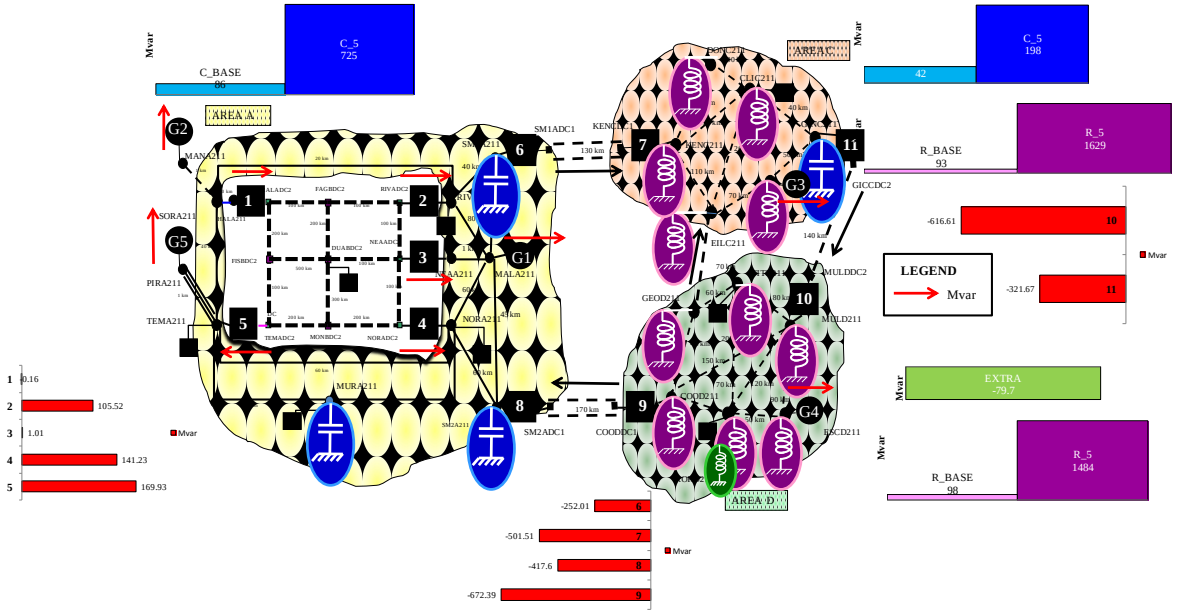

Figure 7.41: REACTIVE POWER FLOW CABLE D of scenarios 5 compared with BASECASE

As further analysis we have tried to substituted all the LCC technology with the VSC considering the scenario 3.

The BASE CASE and CABLE A are marked by an increase of the objective function since the VSC gives as result higher costs which are composed only by the losses and no var installation. The increase for the losses is because there are the double of the VSC and consequently the relative no load losses are doubled too.

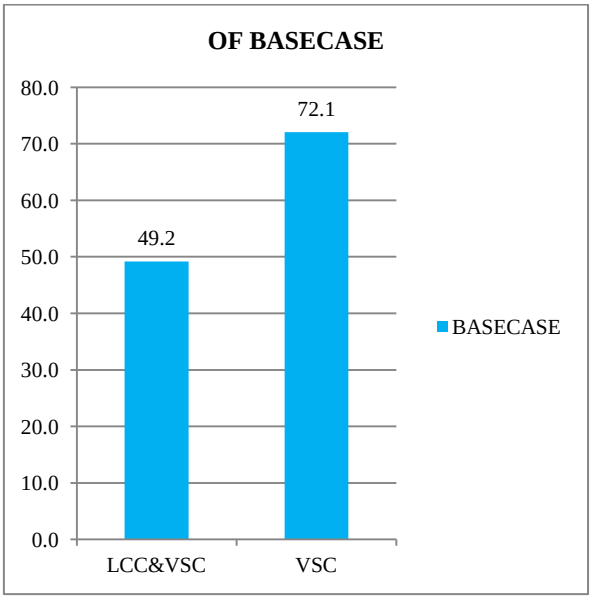

Figure 7.41: OF of scenarios 3 BASECASE: VSC and LCC&VSC

On the other side, the solution of the program is to use smartly the prerogative of the VSC to produce or absorb reactive. This allows to avoid the reactive installation which had been considered in the case with VSC together with LCC.

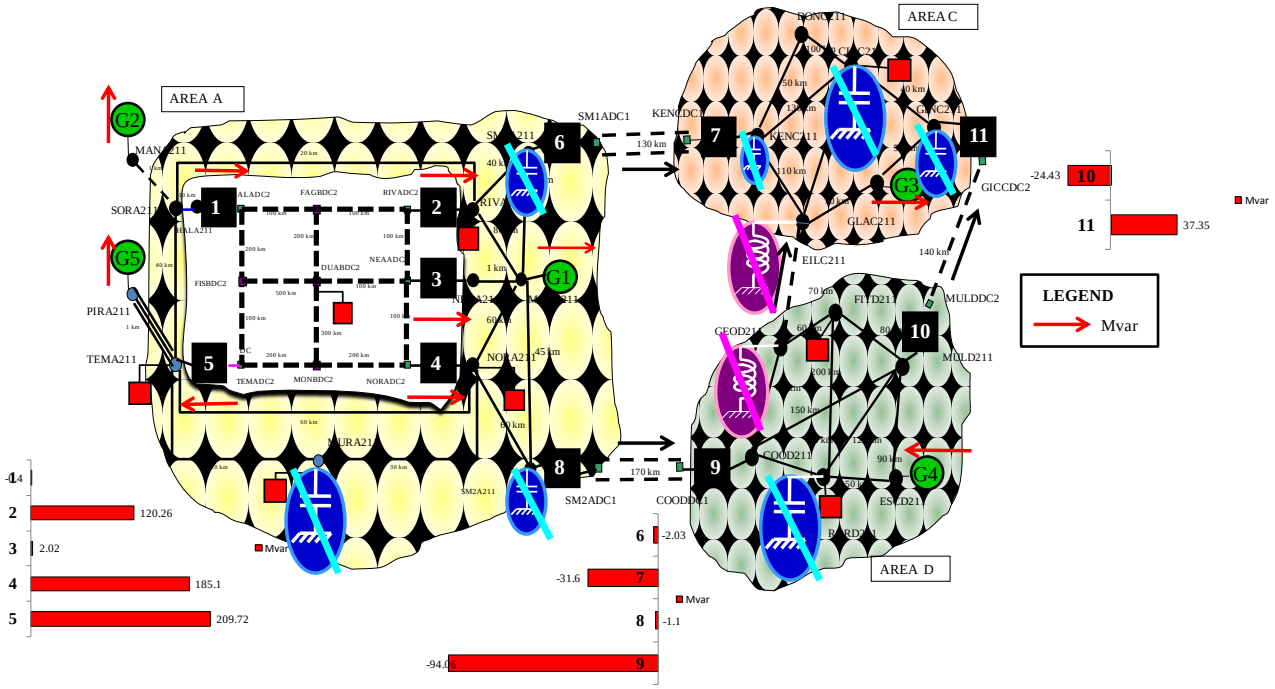

Figure 7.42: REACTIVE POWER FLOW BASECASE VSC of scenarios 3

It can be seen how where before there were two reactors, now the converter 7 and 9 are absorbing a great reactive. While in area A, where before there were capacitive installation, now the converter 6 and 8 have reduced their absorption so that even the load in MURA211 can be fed without a local compensation. Finally, the converter 11 is putting out reactive for that part of the grid which needed.

For the cable A the OF is:

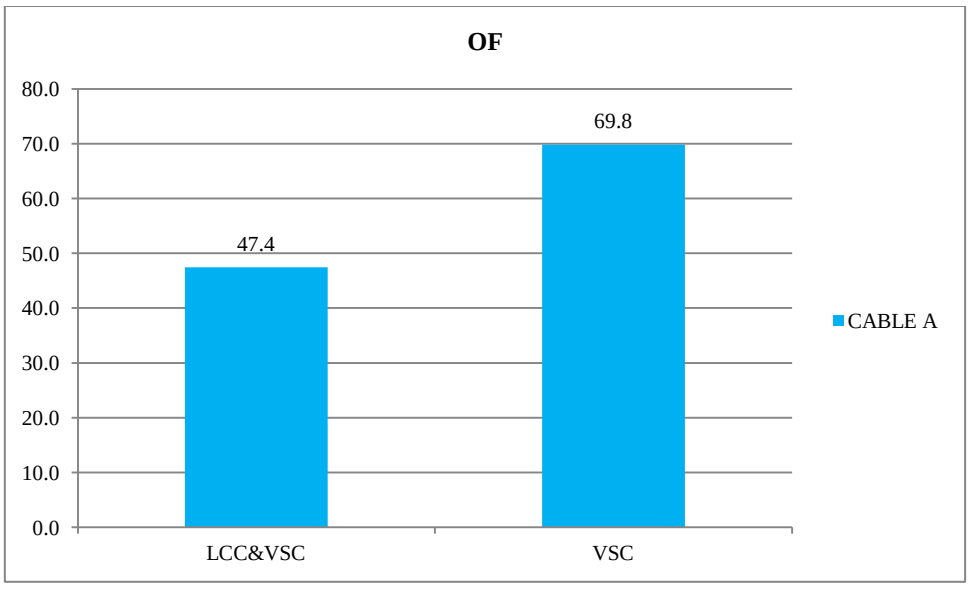

Figure 7.43: OF of scenarios 3 BASECASE: VSC and LCC&VSC

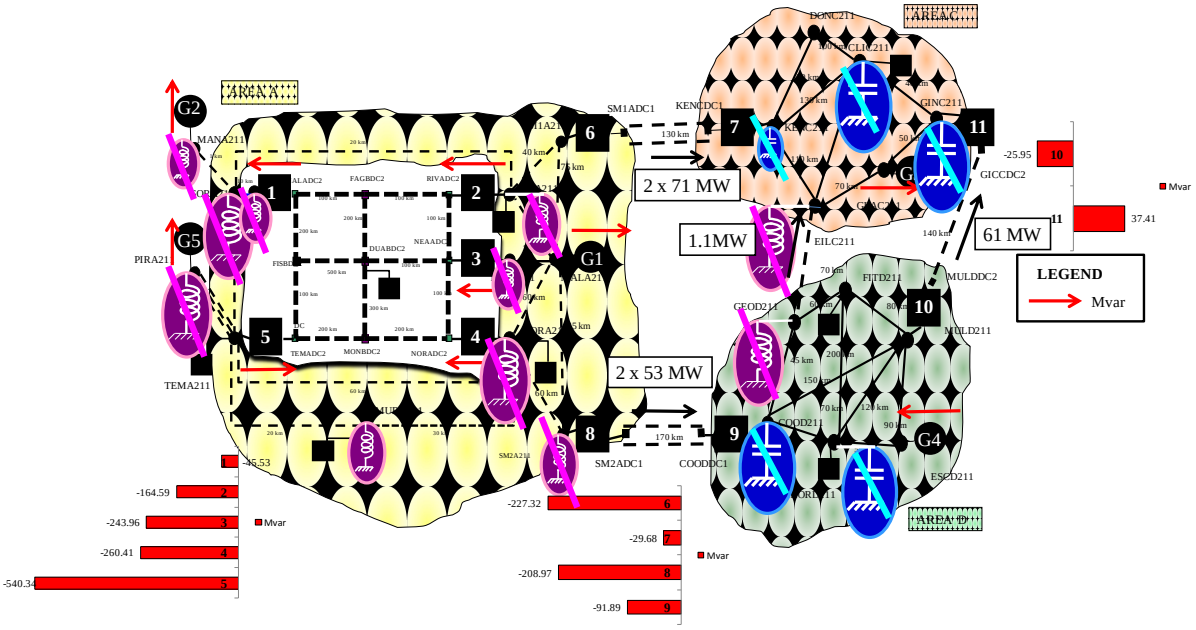

Figure 7.44: REACTIVE POWER FLOW CABLE A VSC of scenarios 3

Same consideration compensation. Finally, the converter 11 is putting out reactive for that part of the grid which needed.

WHEELING CASES

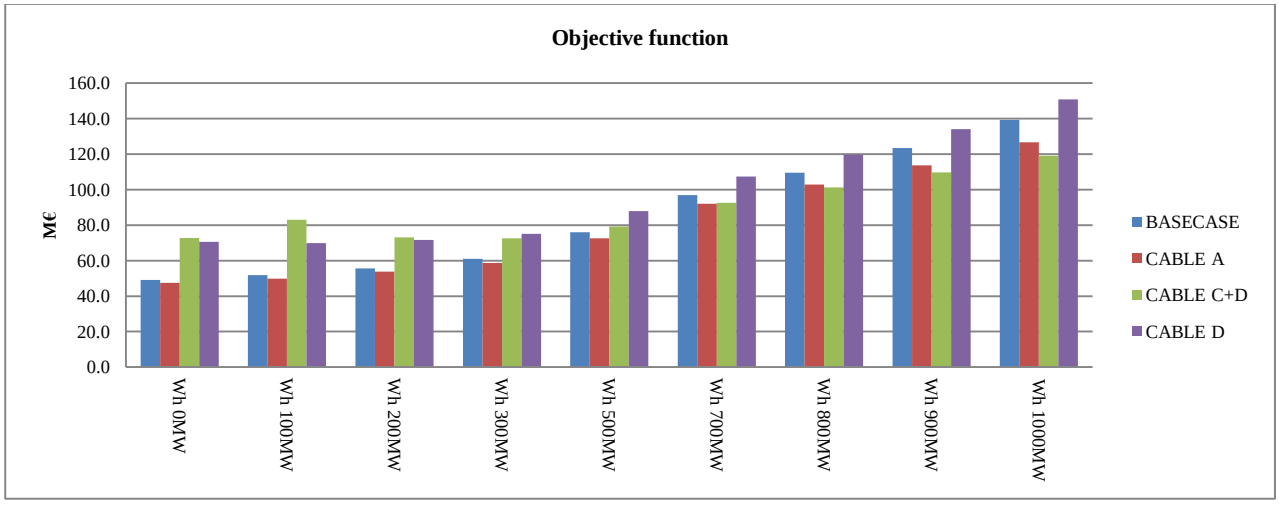

Figure 7.45: Objective function comparing all the wheeling cases

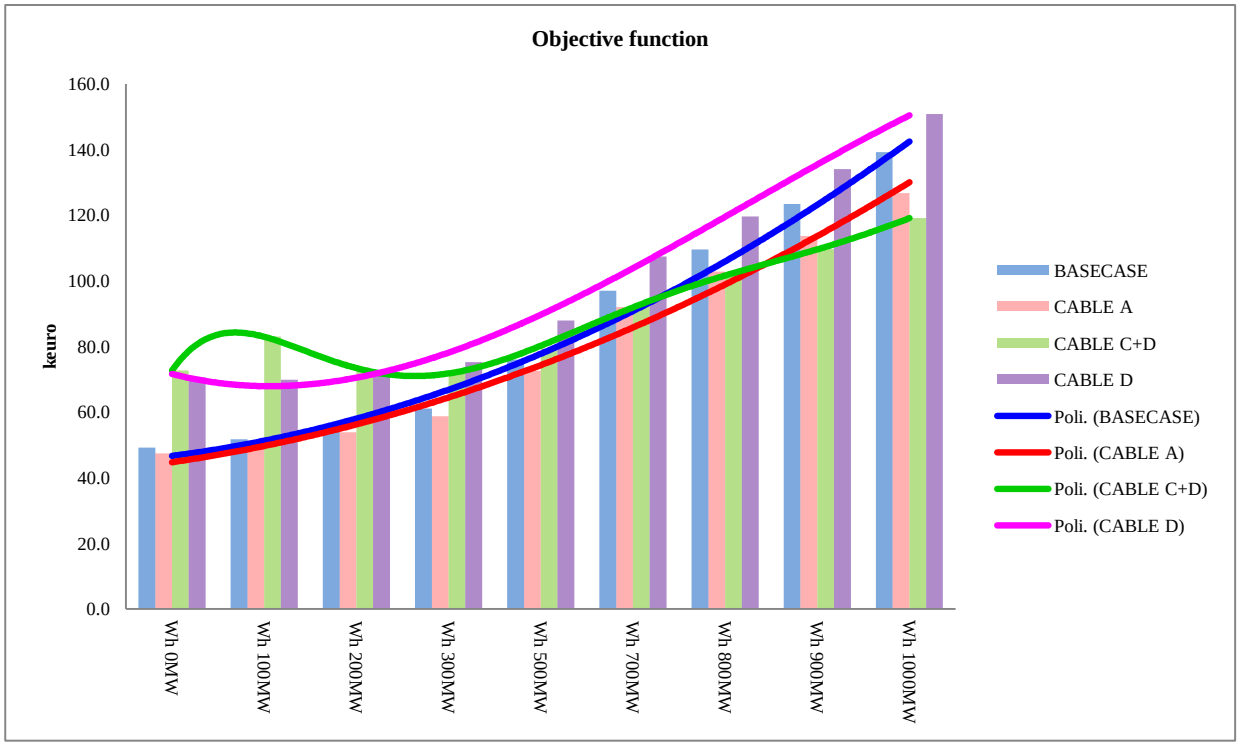

Figure 7.46: Trend of the objective function

From all the result, the optimization problem guarantees the respect of the constraints which have been stated in Chapter 6. Having a look to the Fig. 7.5, the general trend for the basecase and cable A is a gradual increase of the objective function with the higher real power flow. Instead, where the cables are located in area D or C&D, there is a general higher value at low power flow, while wit more consistent flows there is a synergy between the grid full of cables, which acts like a big capacitor and the converter that are working requiring much more reactive power since their need to have higher real power passing through. Considering the two cost items, as shown in Fig. 7.5 and 7.5, it is associated both the increase of the losses and higher amount of reactive, which has the more consistent weight.

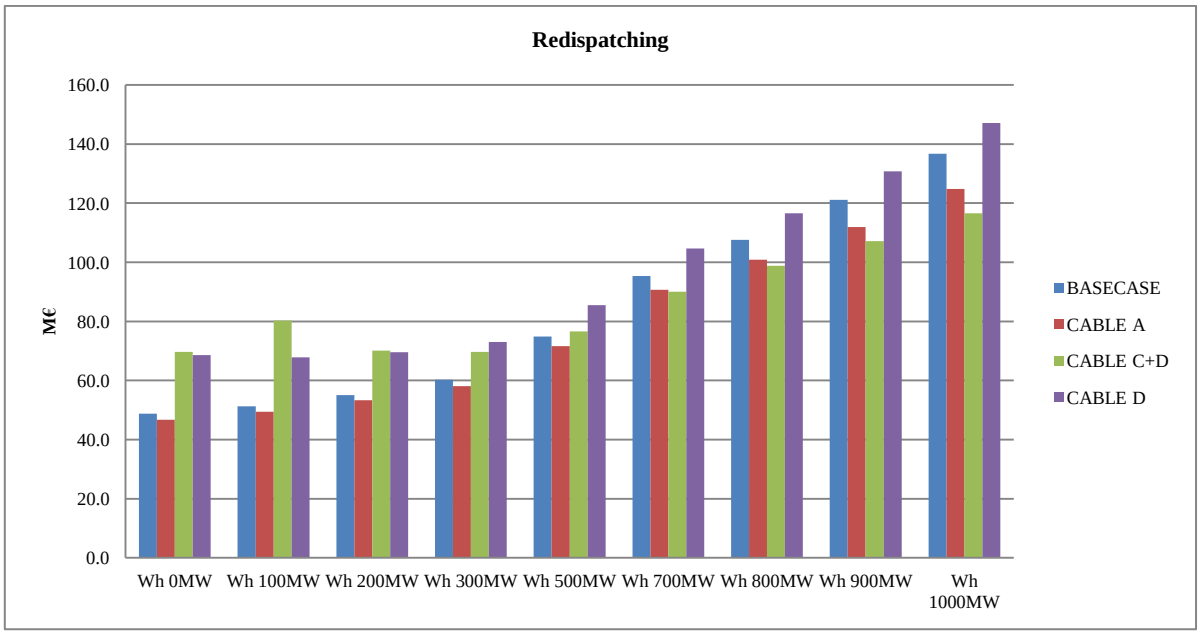

Figure 7.47: Redispatching costs for all the wheeling cases

From the redispatching cost, which are in our case equal for all the generators, it is soon evident the correlated losses grow due to the higher value of the power flow.

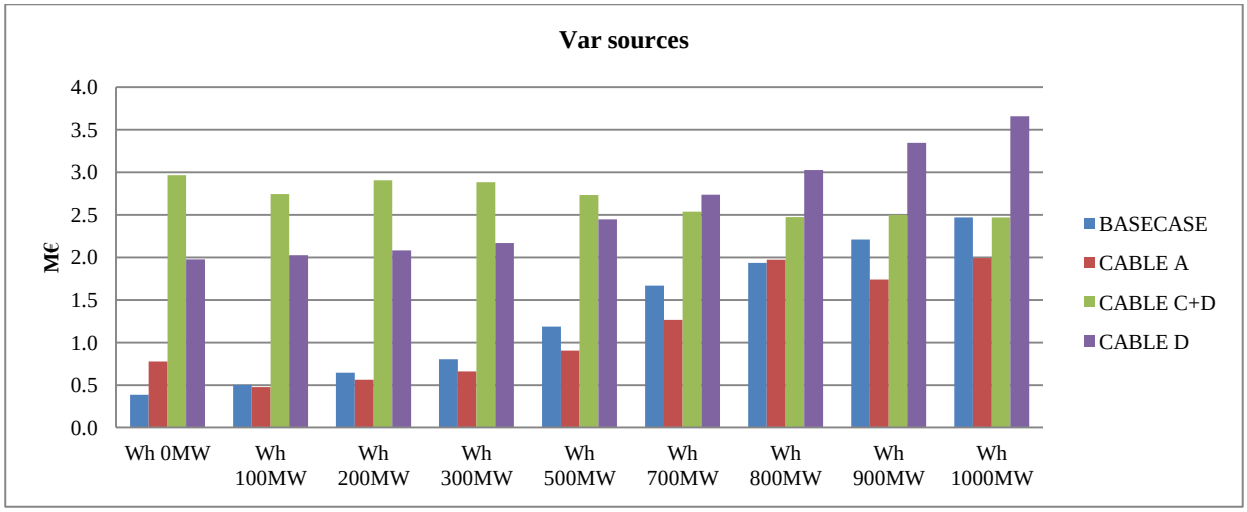

Figure 7.48: REACTIVE POWER FLOW CABLE A VSC of scenarios 3

Concerning the installation var costs, the increase in basecase and in cable A is due to the installation of capacitors banks only at those busses to sustain the voltage level from collapse, staying inside the given constraint, which is 0.95 p.u. However the AC system busbar voltages are determined largely by the reactive power flow within the AC system. The voltage across the system change, depending on the reactive power loads on the busbars and the length of the transmission lines interconnecting the busbar: increasing a new reactive power load at a particular busbar, the additional reactive power loading on that busbar will change the voltage at the other busbar. By switching the switchable reactive power banks on other busbar the voltages may again be brought back into their steady-state range.

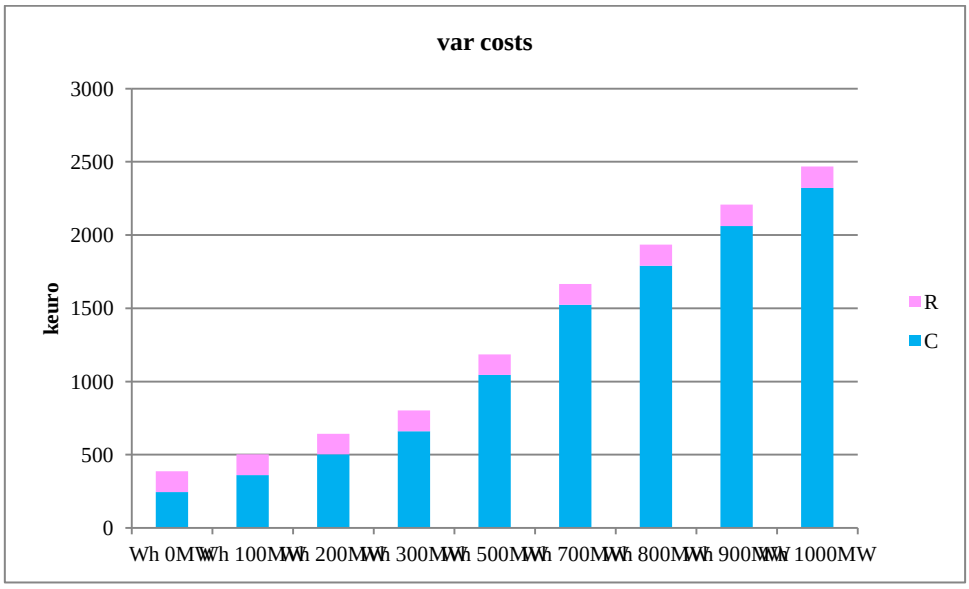

Figure 7.49: Var costs for BASECASE

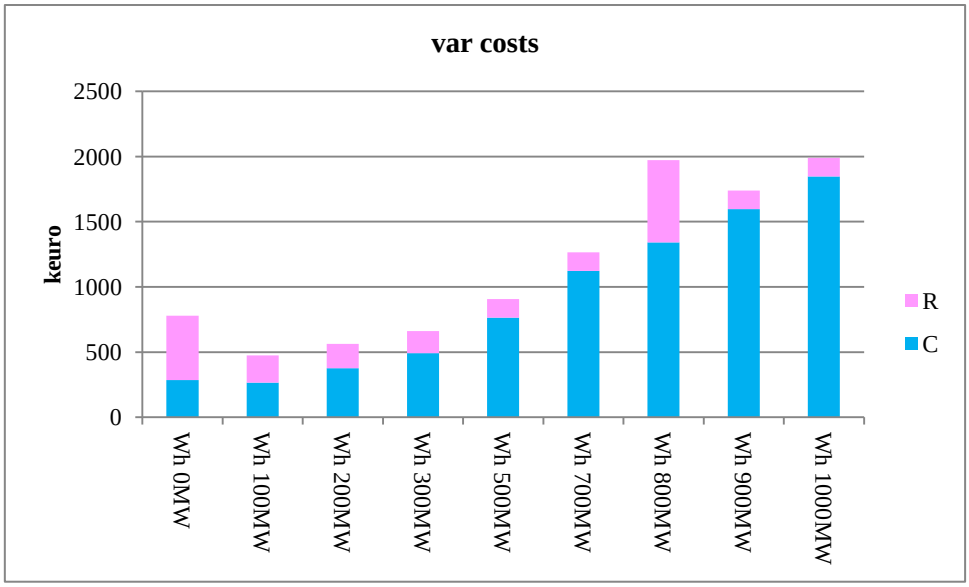

Figure 7.50: Var costs for CABLE A

Different behaviour for the other two cases where the grid can be seen as acting like a big condensator on the right. At first, when the lines are weakly loaded, the reactive power is not so well absorbed and the costs are high for the installation of inductive reactive which consequently decrease the voltage profile, increasing the load. In particular, for CABLE C&D at low wheeling (0 and 100) the losses are higher because of the capacitance effect of the right part of the grid. At higher flow, there is a reduction which can be explained by a good synergies between the cabled grid and the need of the converter to transmit a higher amount of power together with a good decision in the path of the power to feed the load in CLIC211. Increasing furthermore the wheeling it is more evident the increase of the losses due to the huge amount of transiting power, while the reactive costs are affected no longer. In CABLE D the trend of the reactive costs is much more characterized by the higher value and the losses as well.

To support these consideration, we will pay attention on the last two cases, CABLE D and CABLE C&D, considering the grid representation in case of 100 MW, 200MW, 700MW and 1000 MW wheeling.

CABLE D

The cables in the area D are for a total of 865 kilometres with a total reactive production at rate voltage of about 3000 Mvar. In Fig. 7.51, there are the costs for the reactive investment: the costs for the reactors are quite equal for all the cases, while the capacitors installation increase with the bulk of power.

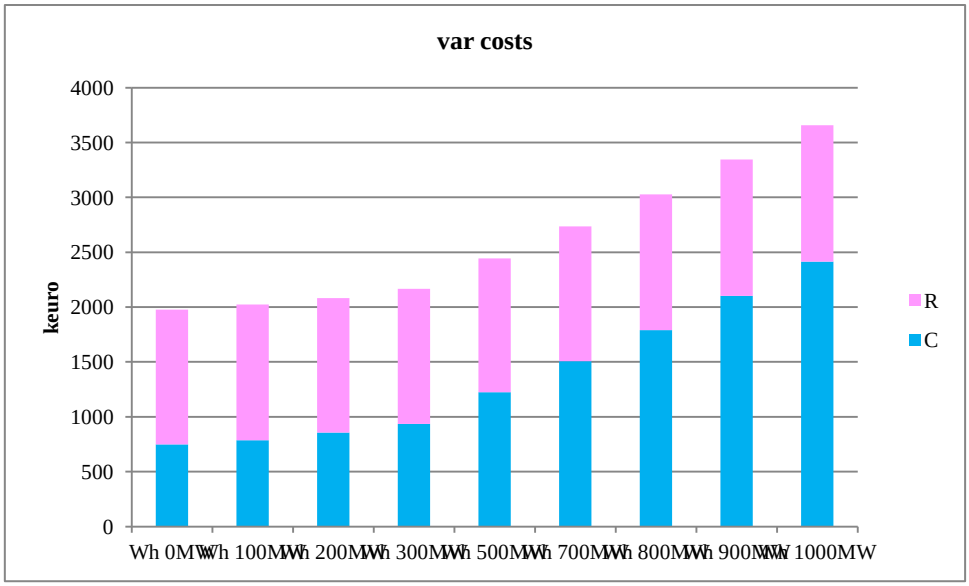

Figure 7.51: Var costs for CABLE D

In the case in Fig. 7.52, we can see how the flows are changing with the wheeling and the goal is to feed the area C where there is the changing load.

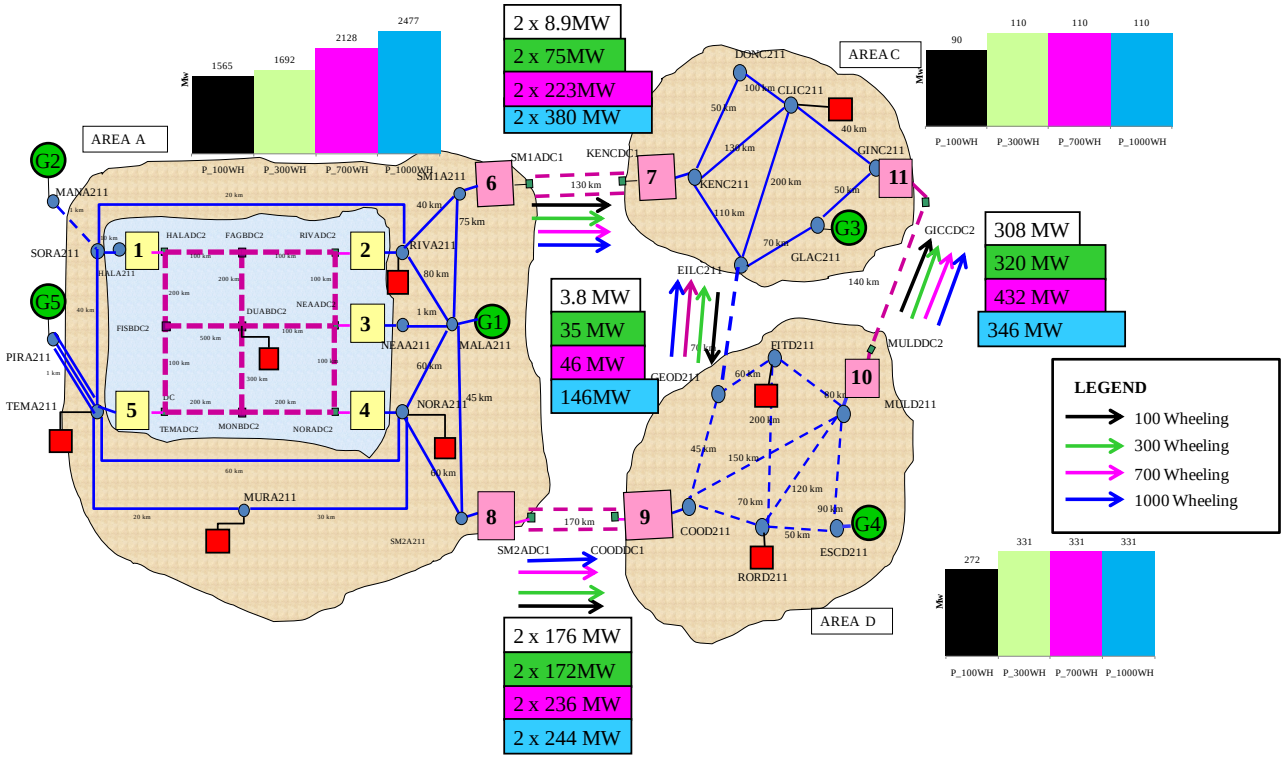

Figure 7.52: 100-300-700-1000MW Wheeling

To support this kind of flows, the grid need a good manage of reactive to avoid voltage collapse and to contain the losses.

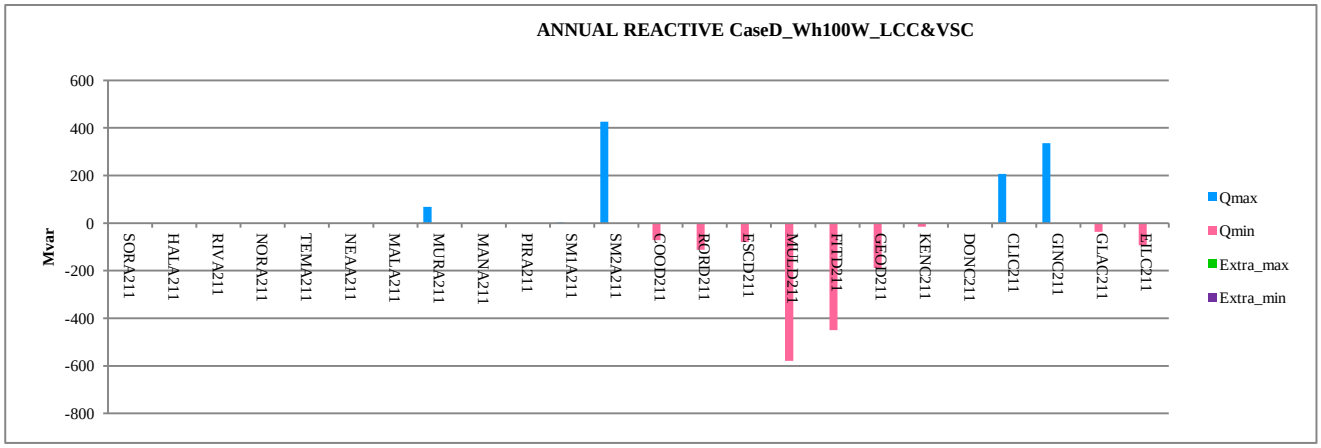

Figure 7.53: 100MW Wheeling Annual installation CABLE D

It is clear that is it better to allow the high real power flow along the DC connection since it let the converter be able to absorb more reactive. The main purpose is to feed the DC link between the area C and area D to supply the demand in C which at first is not satisfied.

Increasing the flow, the DC connection below is passed by a double amount of real power, making weak the other connection above.

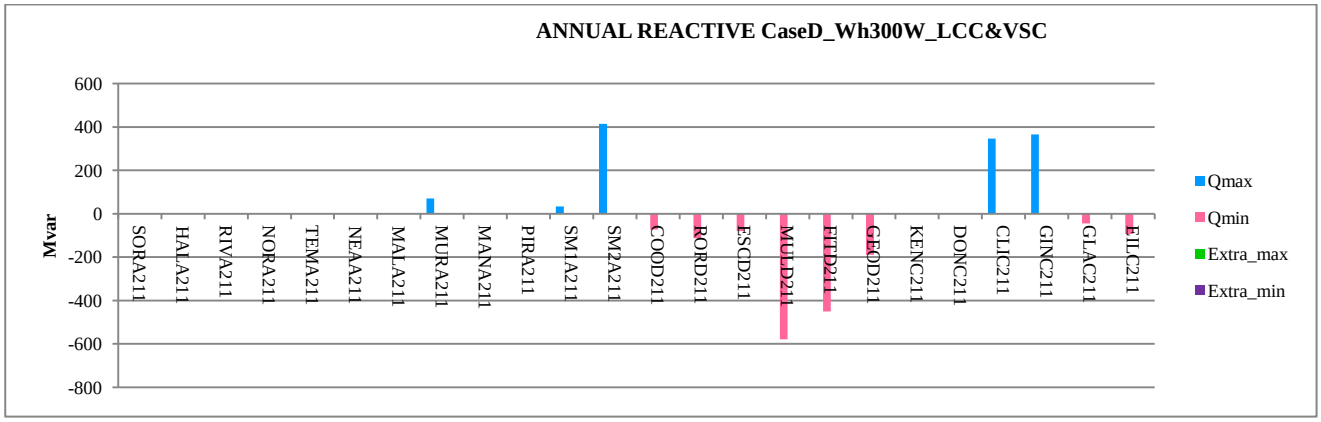

Figure 7.53: 300MW Annual installation CABLE D

As can been seen from the reactive costs, the light increase is due to the further requirement of reactive by the load in CLIC211 .

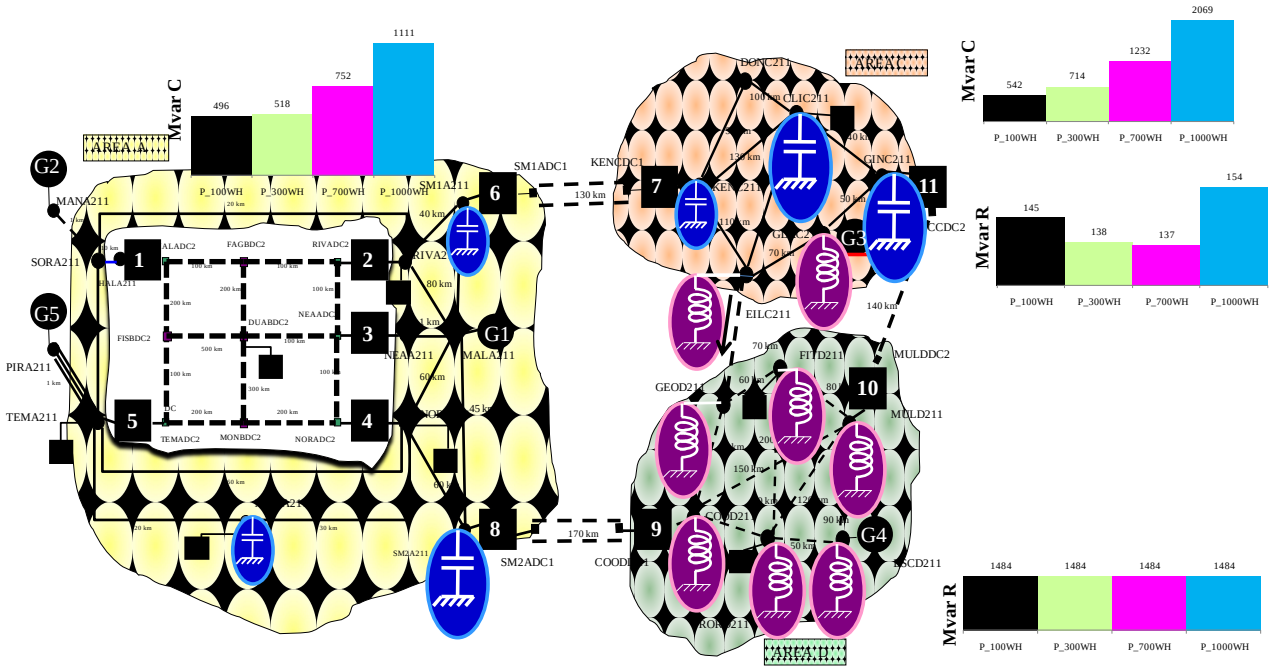

Figure 7.54: REACTIVE 100-300-700-1000MW Wheeling

The increase of the losses is explained by the increase of the AC flow.

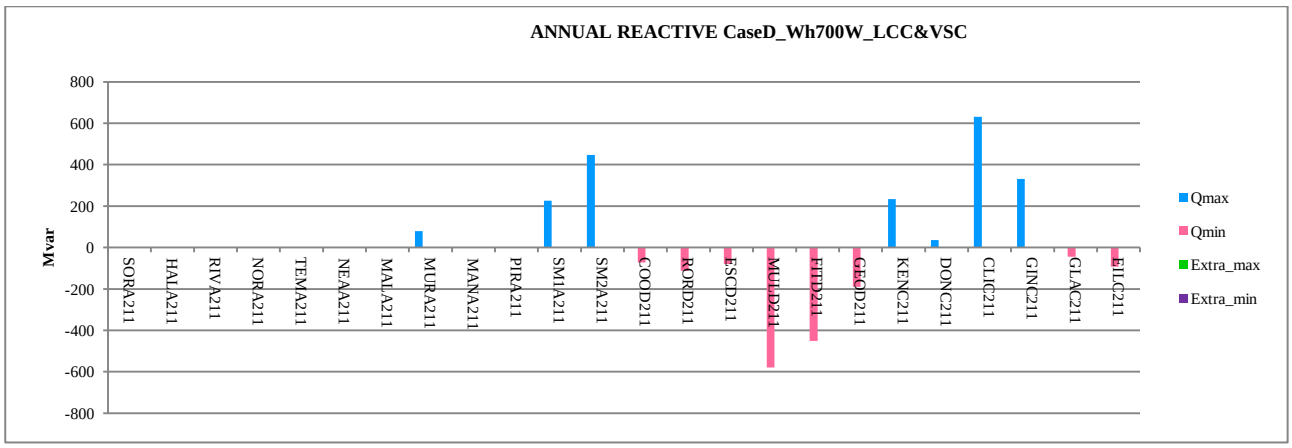

Figure 7.55: 700MW Annual installation CABLE D

The program select a very huge amount in at the load bus since the load requires 500 Mvar. The other capacitive units are used to lift up the voltage which at least must be 0.95p.u. Only in DONC211 the voltage is 0.958 p.u, a bit over its minimum limit and this is because of the double need of keeping the voltage inside the limit and at the same time providing the reactive power to the converter KEN from the closest bus since at the other bus other capacitors had already been put giving the minimum profile level.

The installation of capacitors aims at making the voltage profile reliable. All of those busses at which a capacitor has been installed, are the weakest busses for the grid, except DONC211 . Therefore a first conclusion about the voltage profile is that with the wheeling the voltage of a higher number of busses are going to collapse since the much reactive requirement by the converters SM1 and SM2. Another weak bus is MULD211 since the absorption by the converter and the further reactors to compensate the huge reactive coming from the cables.

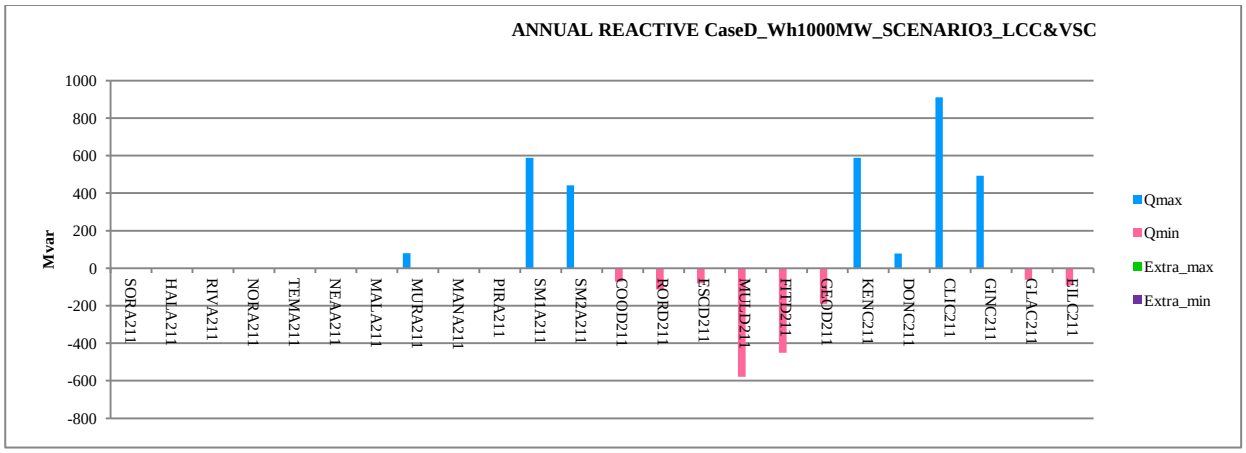

Figure 7.57: 1000MW Annual installation CABLE D

Let us compare the response of the grid is al of the LCCs are substituted by VSCs. The result in objective function is represented in Fig. 7.58

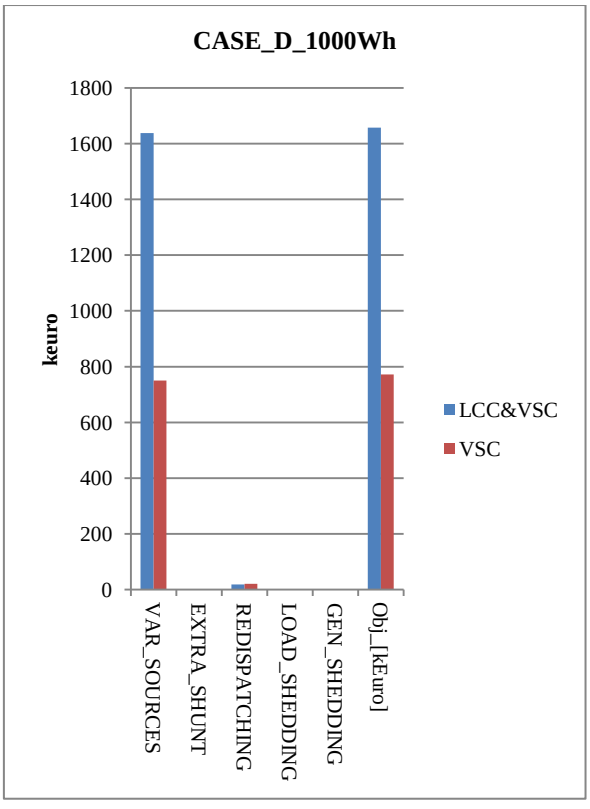

Figure 7.58: Comparison between costs for LCC&VSC technology and only VSC technology

It can be noticed how the losses are higher for the VSC case as better shown in Fig.7.59:

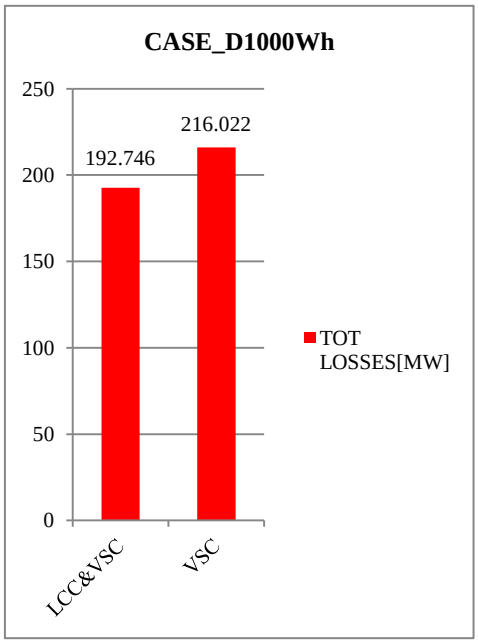

Figure 7.59: LOSSES

This results is due to the higher fixed losses for each VSC converter. Nevertheless, the bidirectional reactive power flow for the VSC units, allows a smarter and cheaper installation of reactive sources. In fact all of the busses where before had been put a capacitor, now don't need one because of the possibility of each VSC to inject reactive power in it, keeping the voltage at value up the 1 p.u.. Besides, there is a modification of the real power flow for the whole system which allows to feed the load in CLIC211 straightforward from the closest DC connection.

The size of the reactive sources are plotted in the Fig. 7.60:

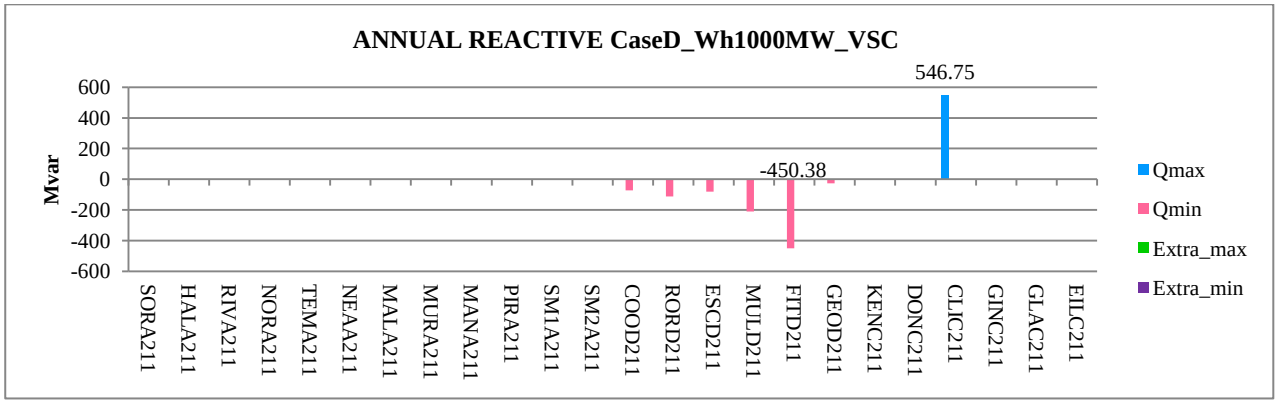

Figure 7.60: 1000MW Annual installation CABLE D with only VSC

CABLE C&D

The cables in the area C&D are for a total of 1615 kilometres with a total reactive production that can be estimated of about 5000-6000 Mvar, considering a production of 7Mvar/km. . This reactive production production by cables is not totally absorbed by the converters and the generators: therefore there is the need to install reactors. It can soon be point out that the VSC in area A provide reactive to AC grid to have high voltage profile, except the converter HAL, which absorb the reactive produced by the close cable MANA211-SORA211.

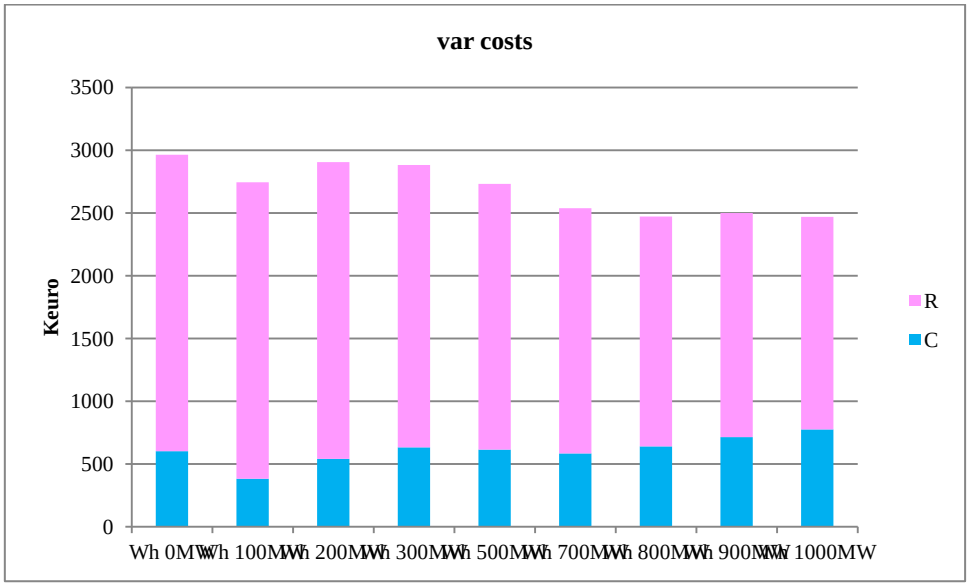

Figure 7.61: Var costs for CABLE C&D

It is clear the investment of reactor tends to decrease, while the capacitance are important to support the higher bulk of power. With mild powers, the grid needs a lot of reactor to absorb the excess and reduce the losses. The converters LCC are absorbing huge amount of reactive power.

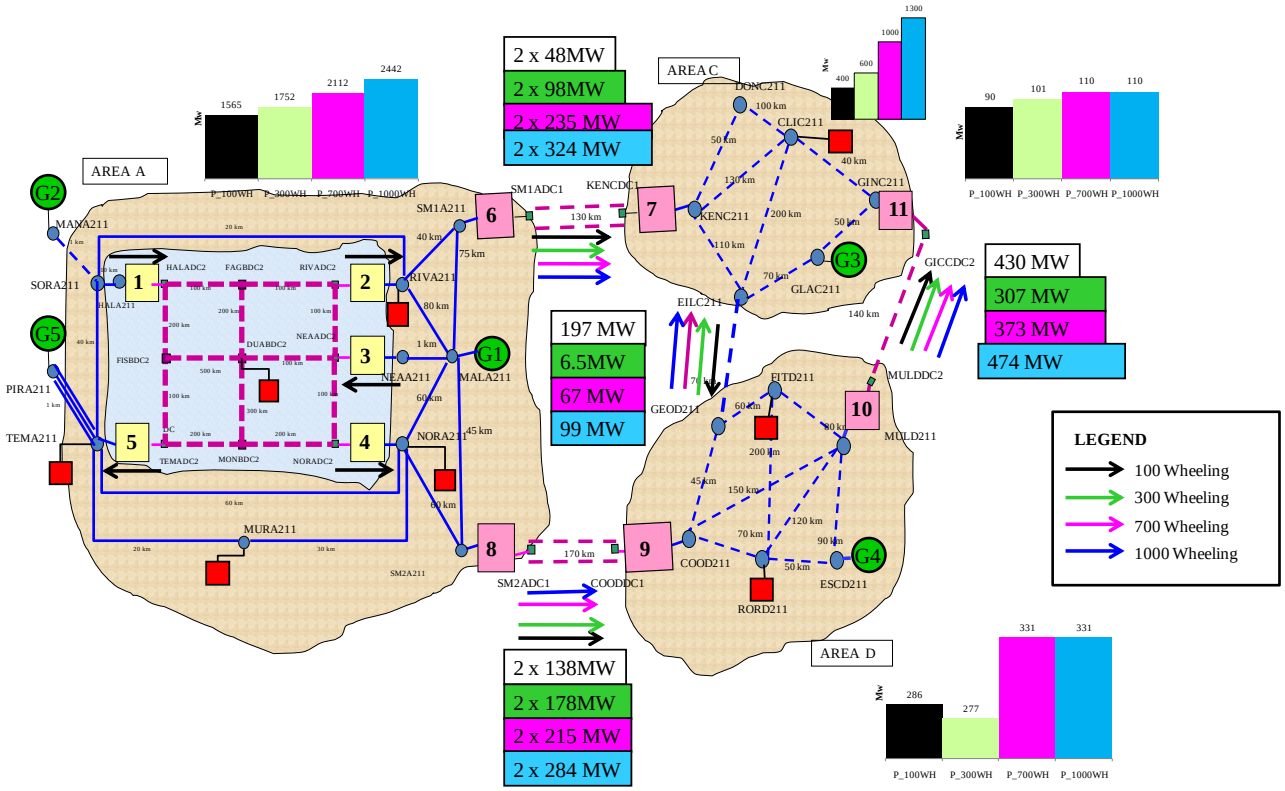

Figure 7.62: 100-300-700-1000 MW Wheeling CABLE C&D

The increase of the losses is explained by the increase of the AC flow.

Different is the behaviour from the reactive point of view: while the capacitors are located at strategic busses such as the load in MURA211, which is pretty far from any units producing reactive and at the busses where there are the tow LCCC converters, 6 and 8. In particular the figures 7.6, 7.64, 7.66, 7.67 show the precise size of reactive for the different wheeling cases.

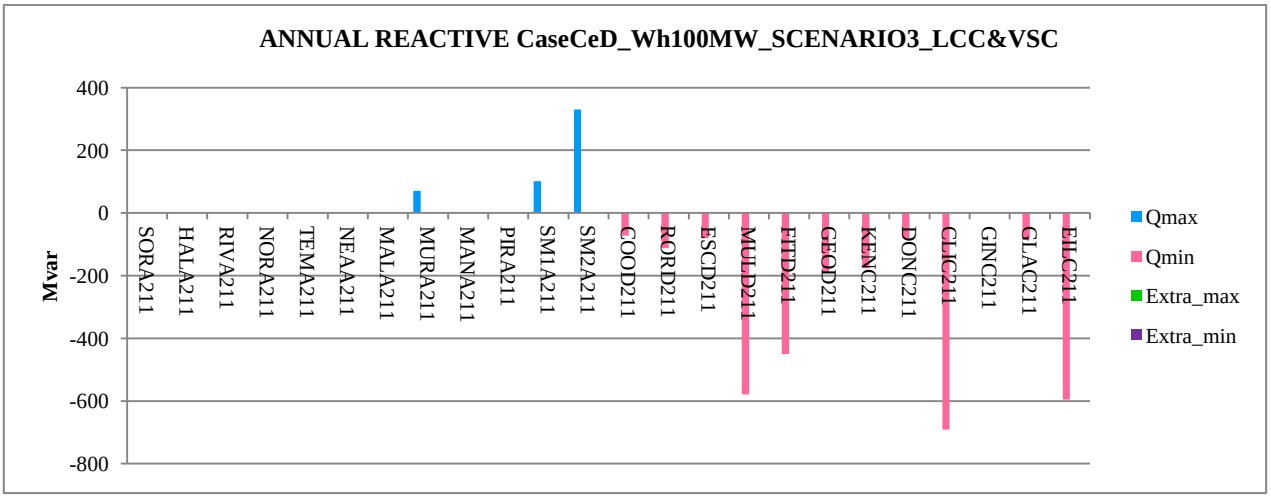

Figure 7.63: 100MW Wheeling CABLE C&D

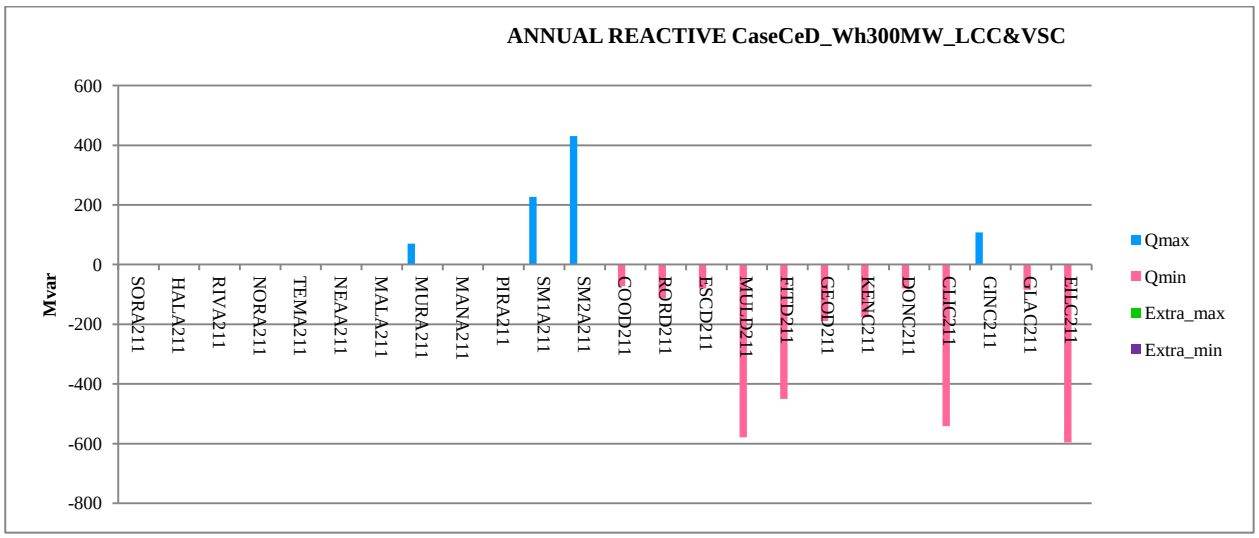

Figure 7.64: 300MW Wheeling CABLE C&D

Changing the power from the case 300 to the 700, it emergers how the reactors installed at bus CLIC211 has been decreased up to disappear for the last case of 1000 Wheeling.

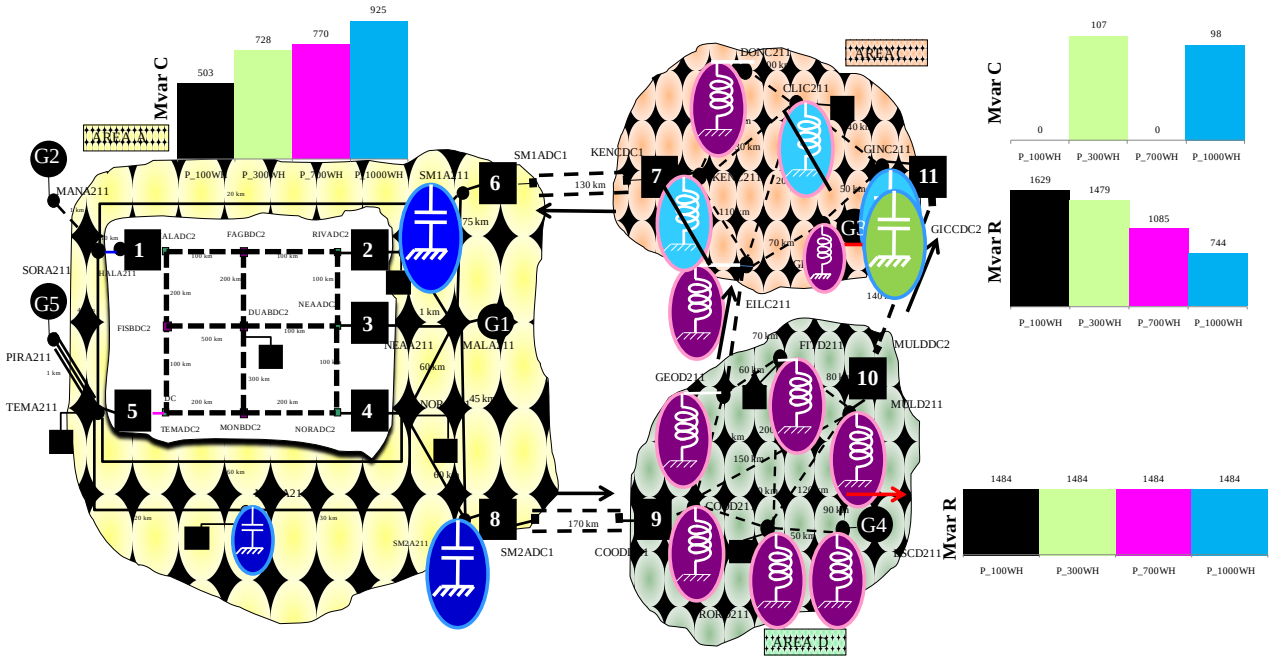

Figure 7.65: 100-300-700-1000 MW Wheeling CABLE C&D

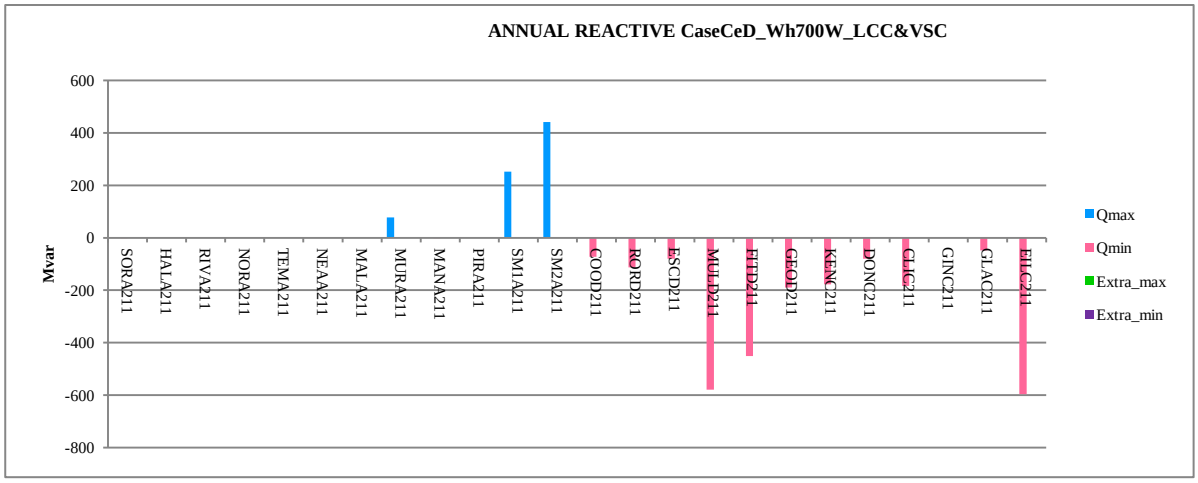

Figure 7.66: 700MW Wheeling CABLE C&D

The installation of capacitors aims at making the voltage profile reliable. All of those busses at which a capacitor has been installed, are the weakest busses for the grid, except DONC211. Therefore a first conclusion about the voltage profile is that with the wheeling the voltage of a higher number of busses are going to collapse since the much reactive requirement by the converters SM1 and SM2. The weakest bus under the voltage profile is MULD211 since the absorption by the converter and the further reactors to compensate the huge reactive coming from the cables.

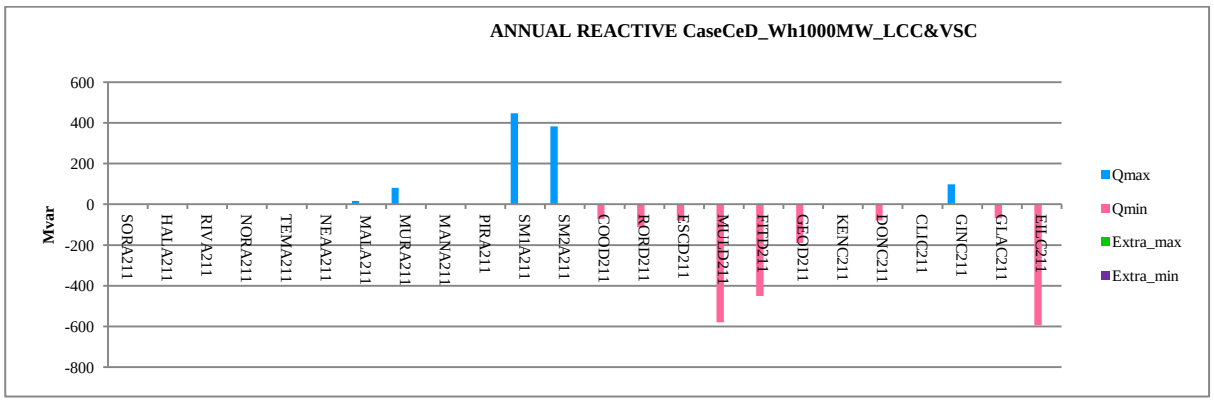

Figure 7.67: 1000MW Wheeling CABLE C&D

7.3.Multiple load/generation scenarios

The number of hours for each scenario, which represent a particular load condition, are shown in Fig. 7.68:

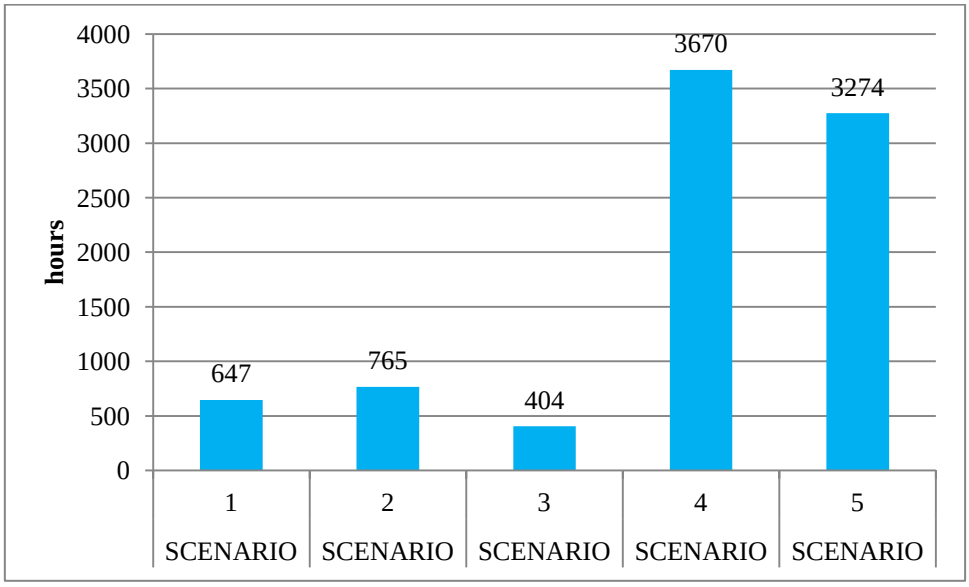

Fig. 7.68:Hours for each scenario

Therefore, the weight for each scenario can be better seen in percentage in Fig. 7.69:

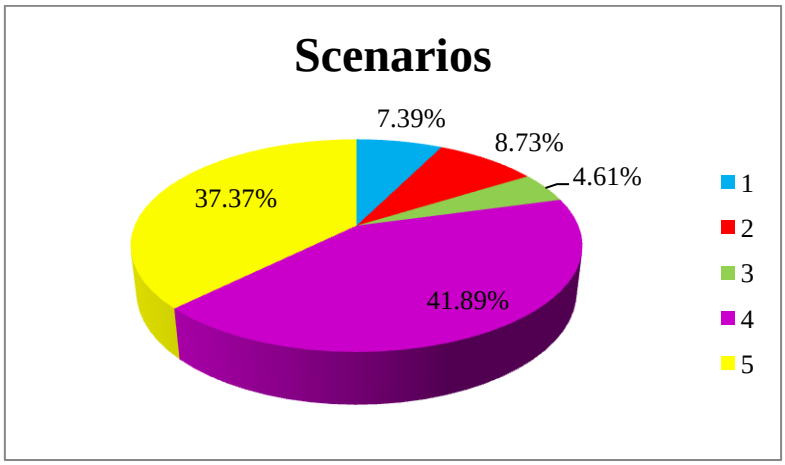

Fig. 7.69: Percentage of each scenario

We will consider the multiple scenario only for the base case since it will be possible to have a comparison between the different scenarios taken singularly and those considered all together.

The objective function is composed of the following items:

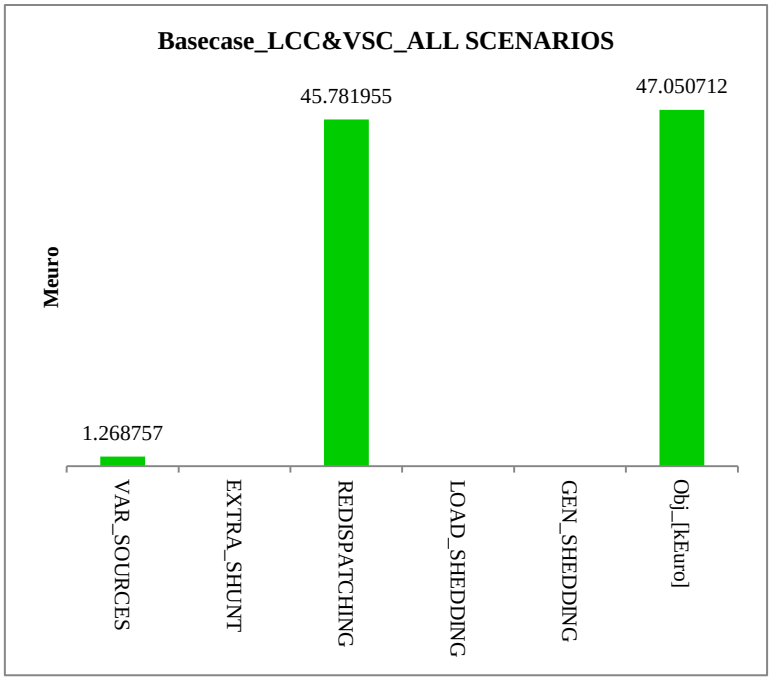

Fig. 7.70:COSTS for BASECASE mutliscenario

The var costs are so composed of:

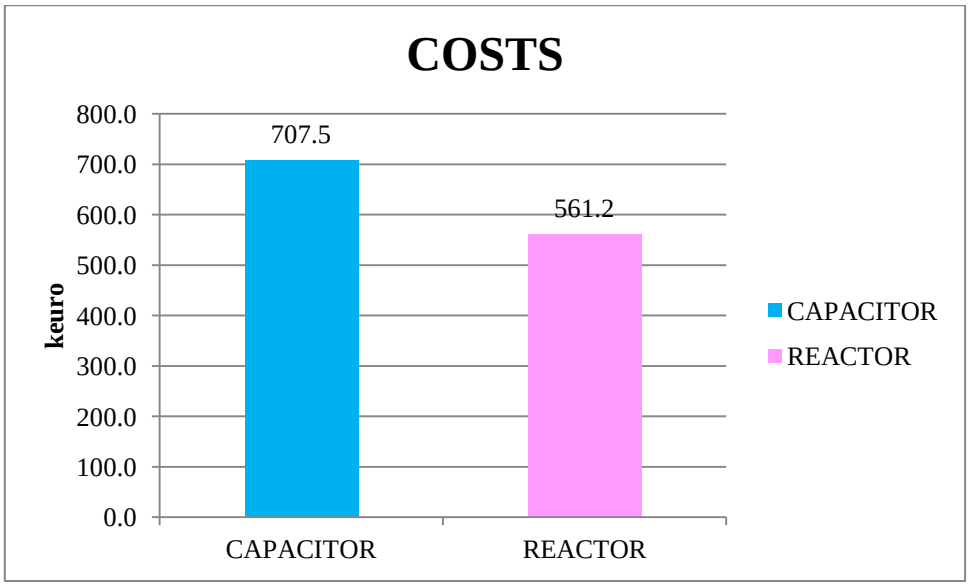

Fig. 7.71: VAR cost

Along one year, the main cost is due to the installation of capacitive reactive. The real losses are connected to the real power flows, which are much higher fir the scenario 3 as shown in Fig. 7.72.

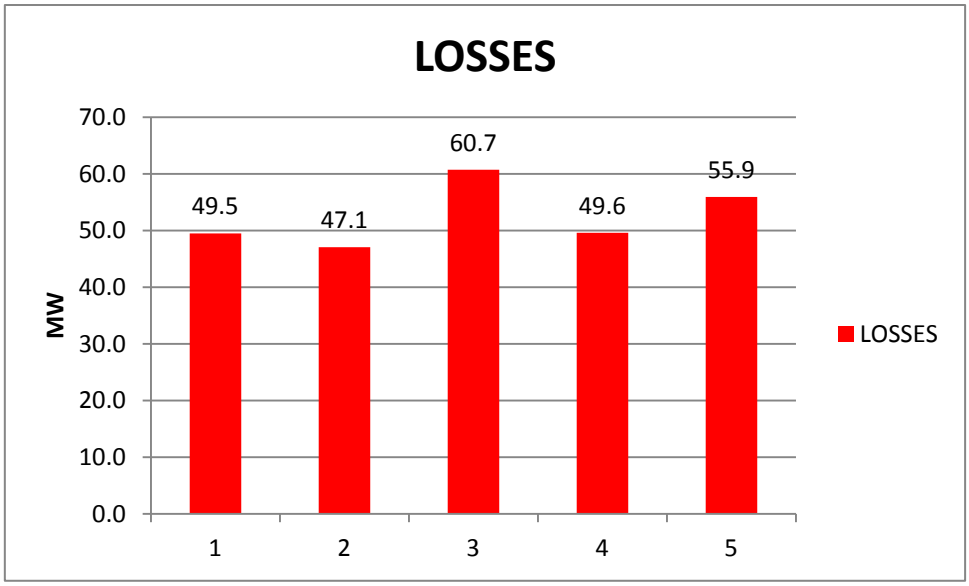

Fig. 7.72: Losses for each scenario

Since in each scenario there is also a different demand, it s significant to refer to it the losses, whose percentage is reported in Fig. 7.73:

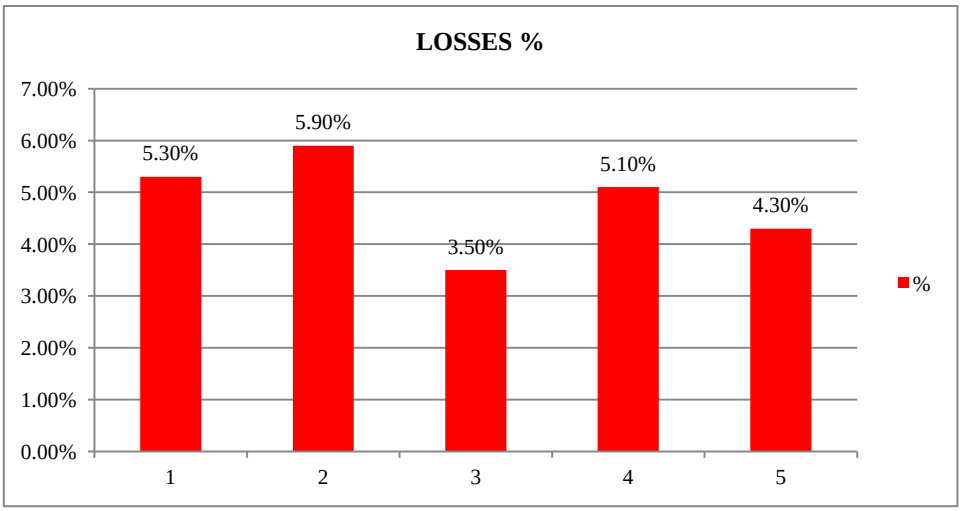

Fig. 7.73: Losses

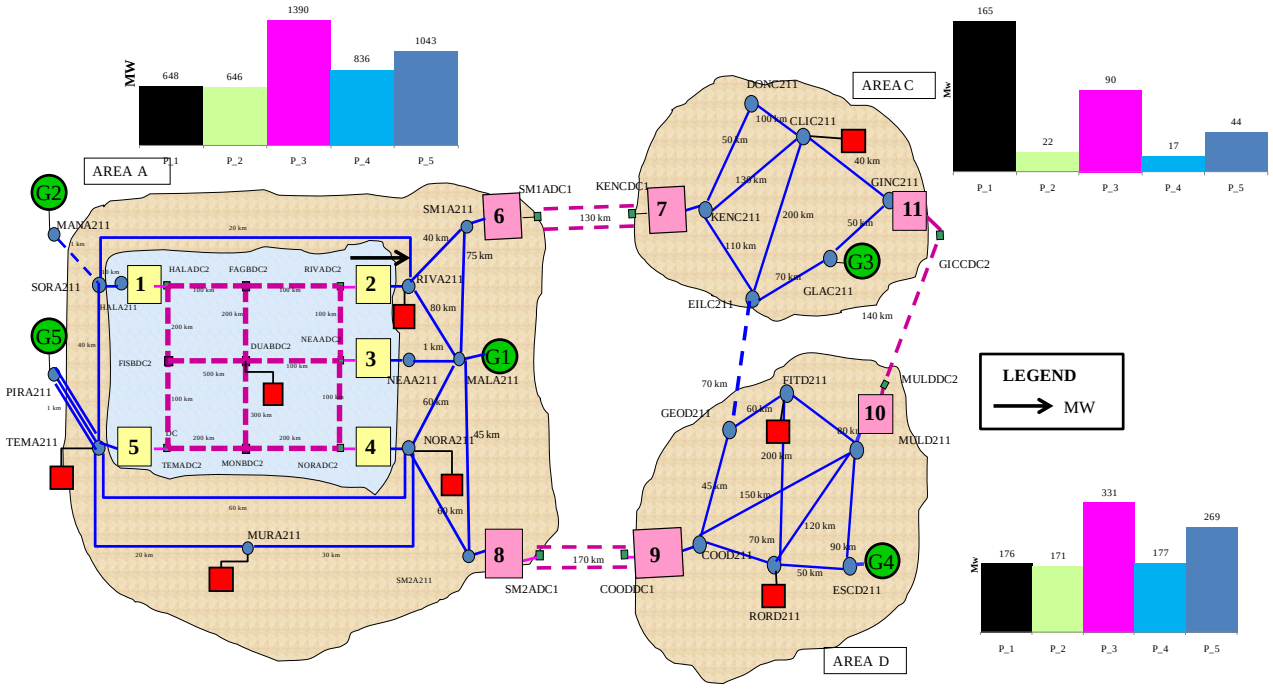

Fig. 7.74: Multiscenario basecase

The installation of the reactive is selected for better deal with the different scenarios along the year. In Fig. 7.75 is drawn the maximum installation at each bus, that doesn't mean that it is always the real usage.

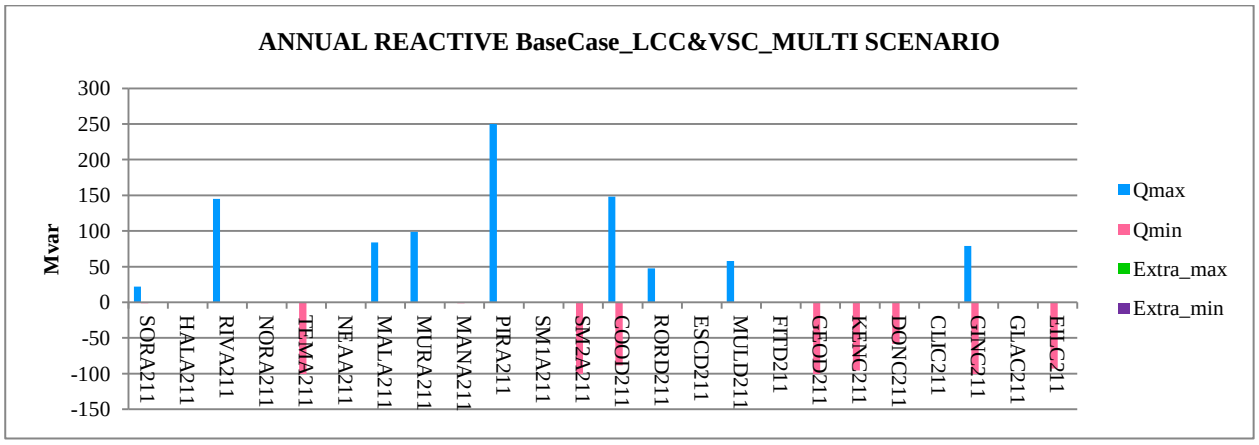

Fig. 7.75: Losses

Let's see how which is the real usage in these five scenarios considering all of them from the Fig. 7.76 to 7.80: we have drawn the reactive location in the grid for each scenario and there is also the relative graph considering the precise size of the reactive installed at each bus.

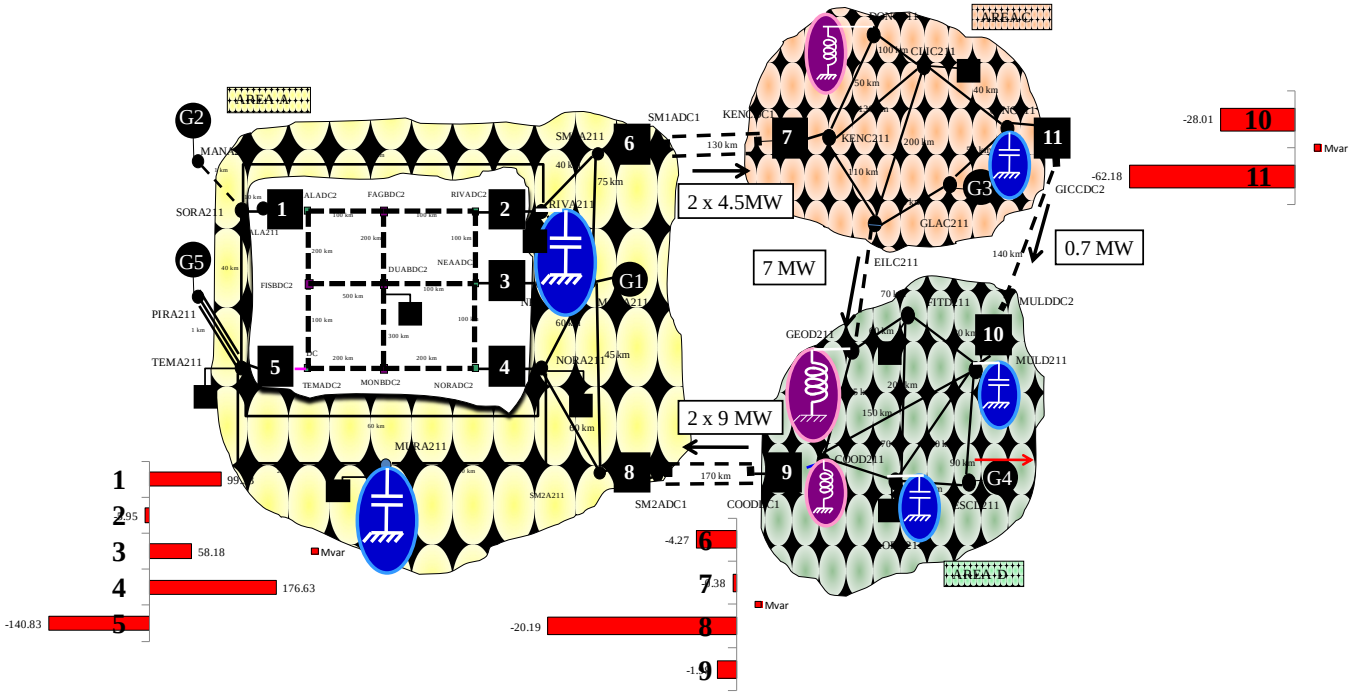

Fig. 7.76: Var use for SCENARIO 1

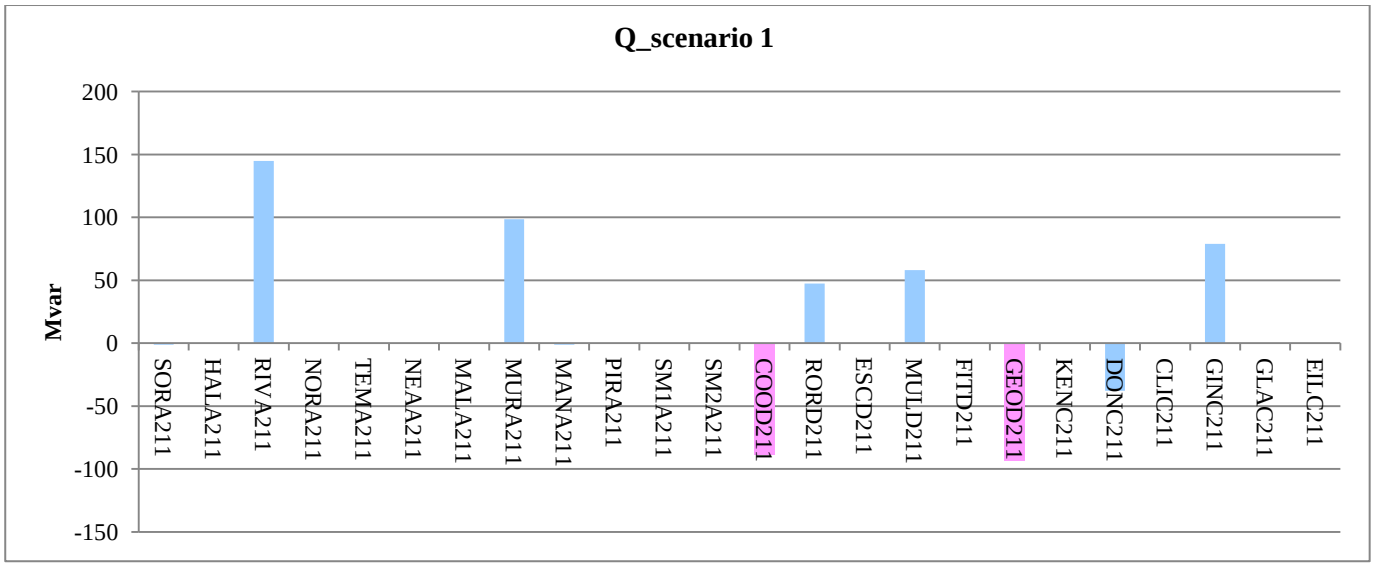

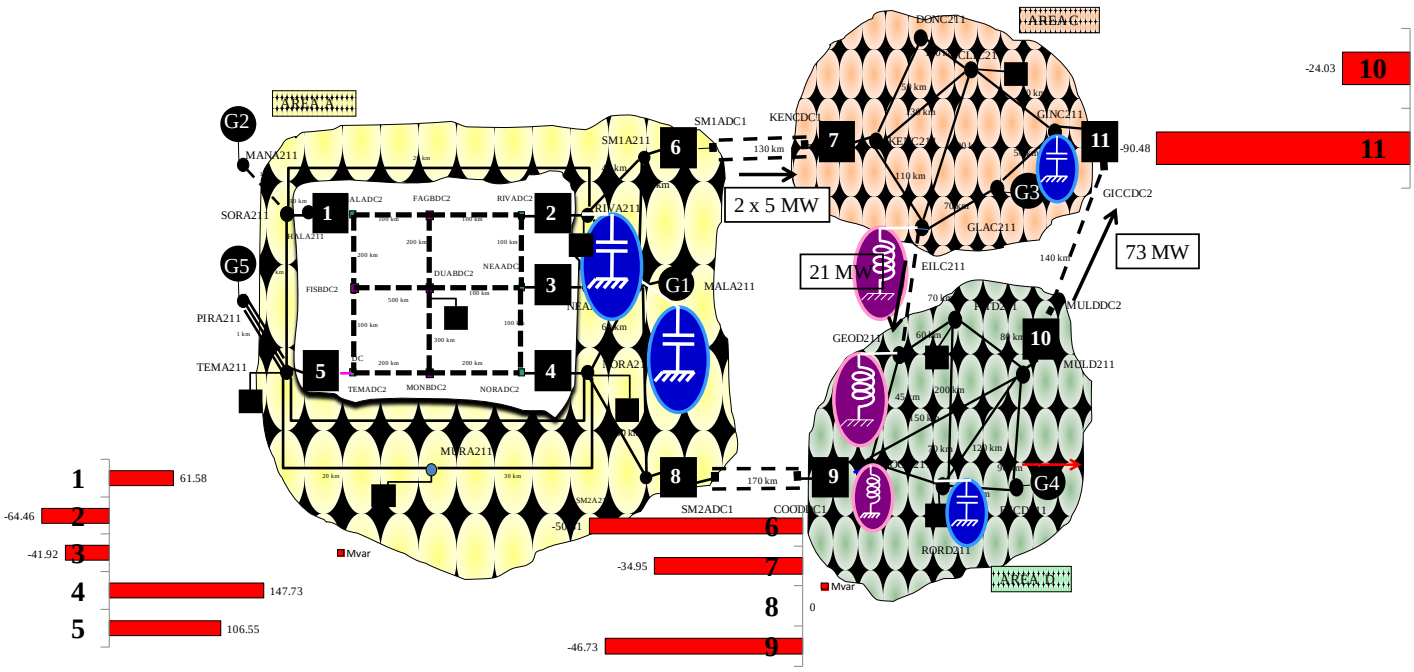

Fig. 7. 77: Var use for SCENARIO 2

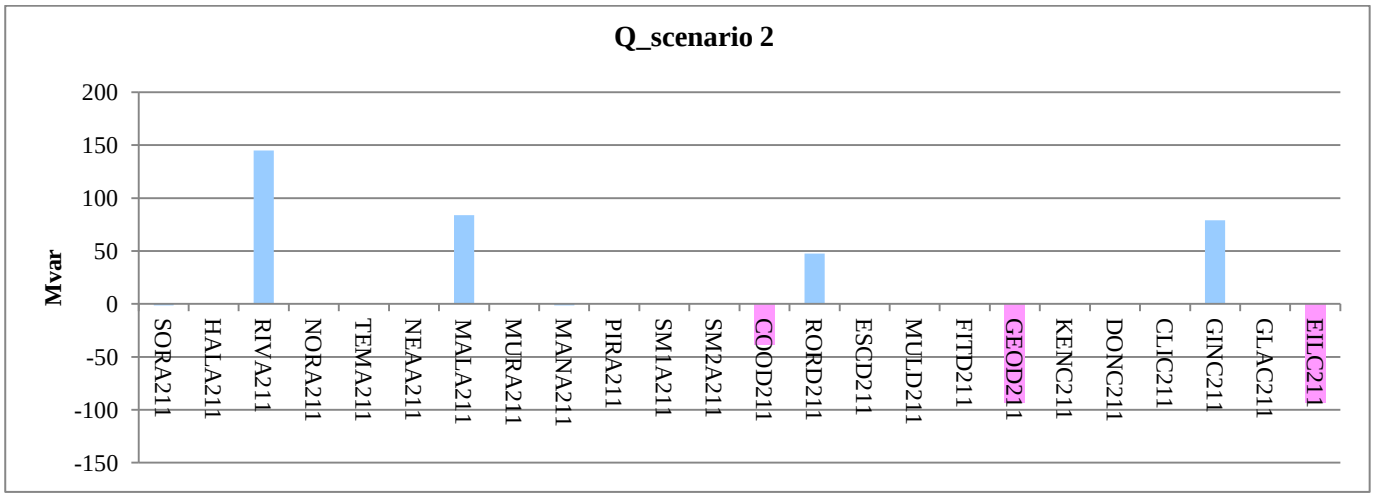

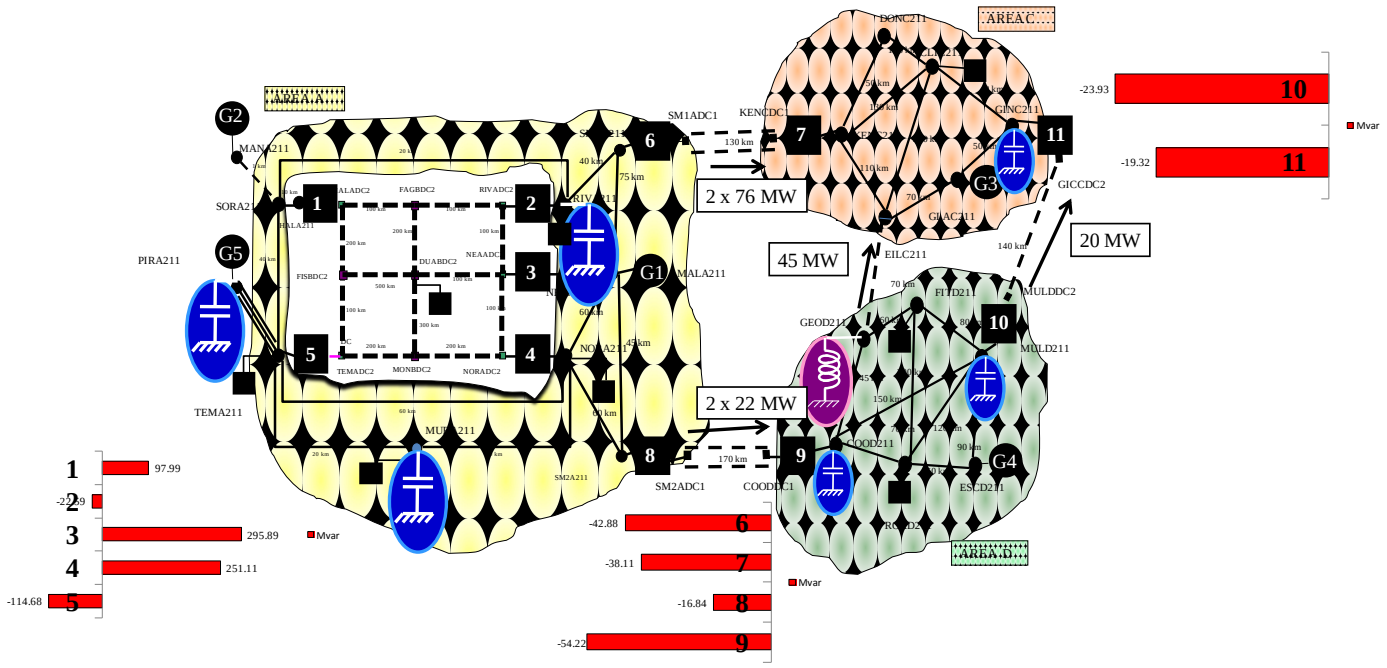

Fig. 7.78: Var use for SCENARIO 3

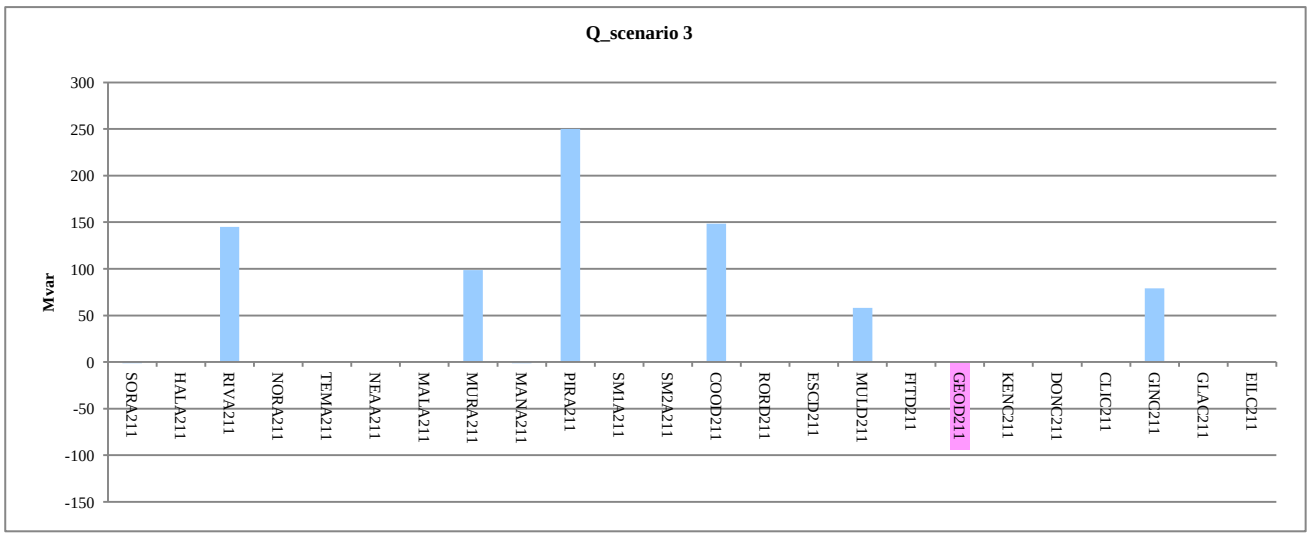

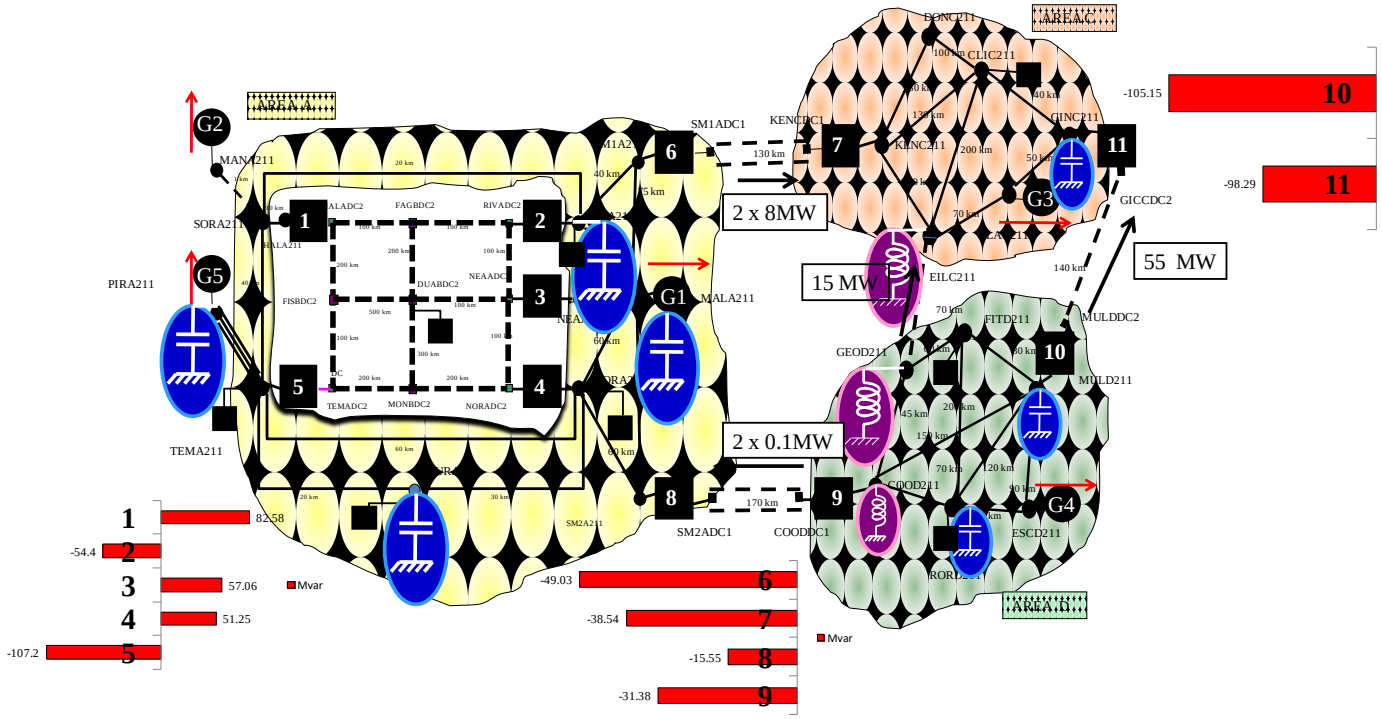

Fig. 7.79: Var use for SCENARIO 4

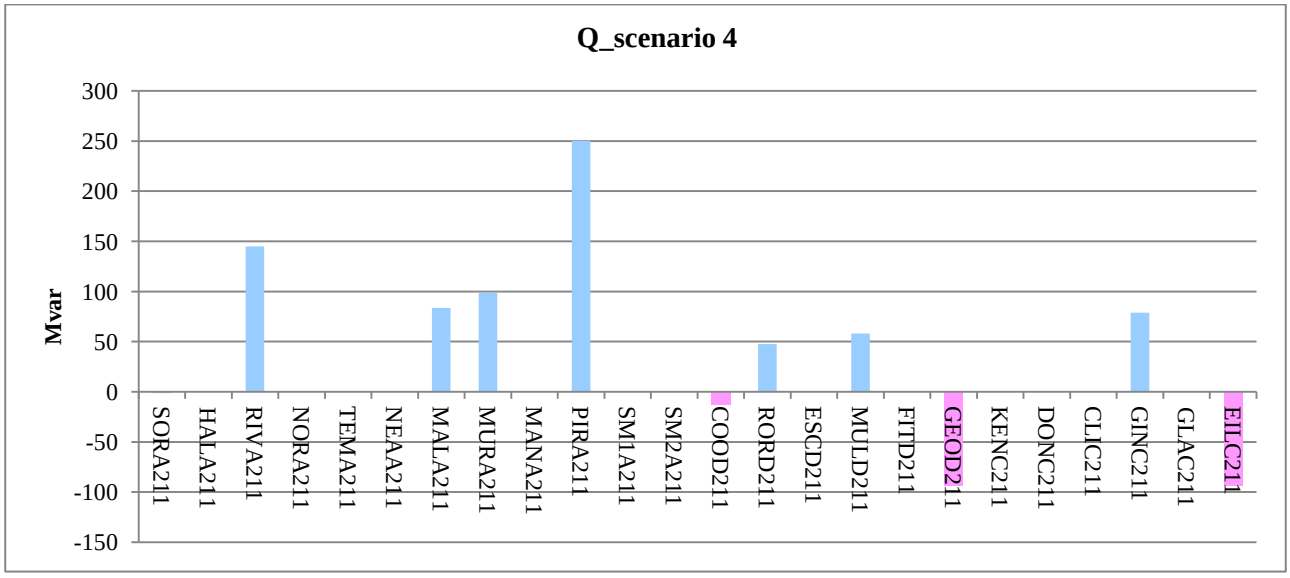

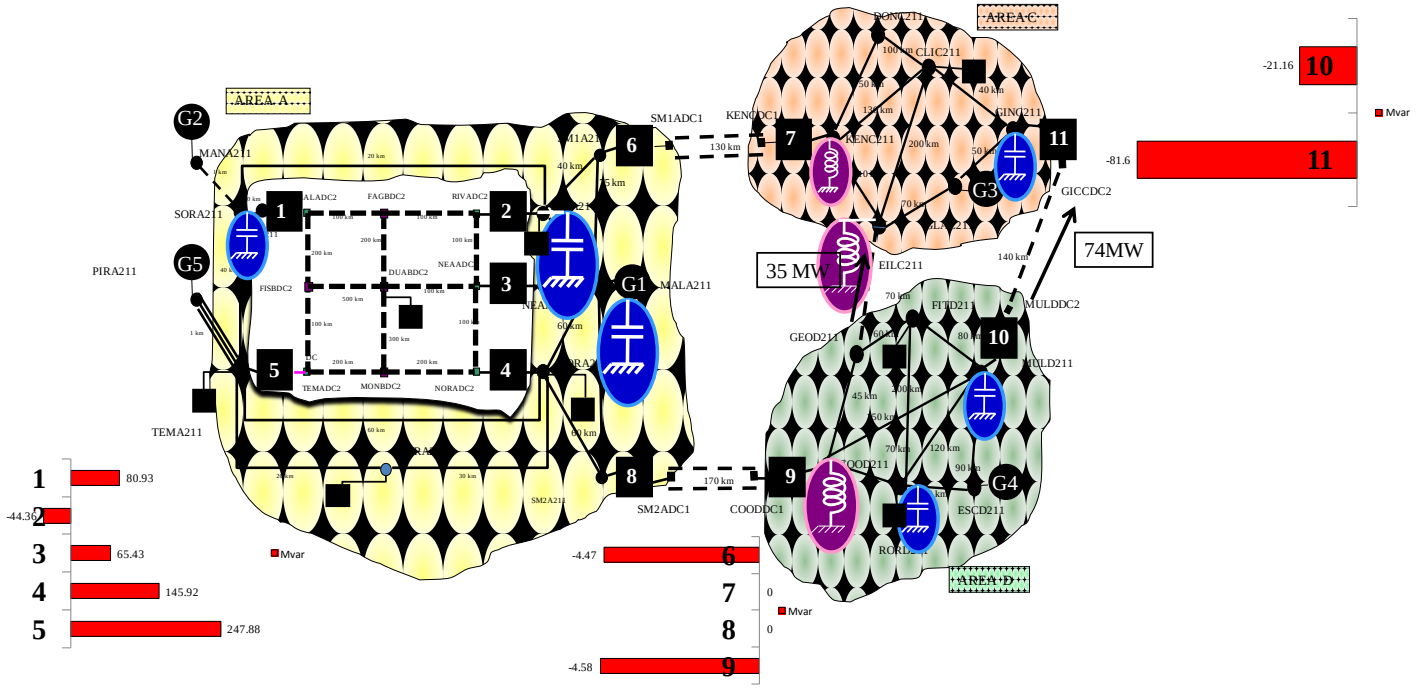

Fig. 7.80: Var use for SCENARIO 5

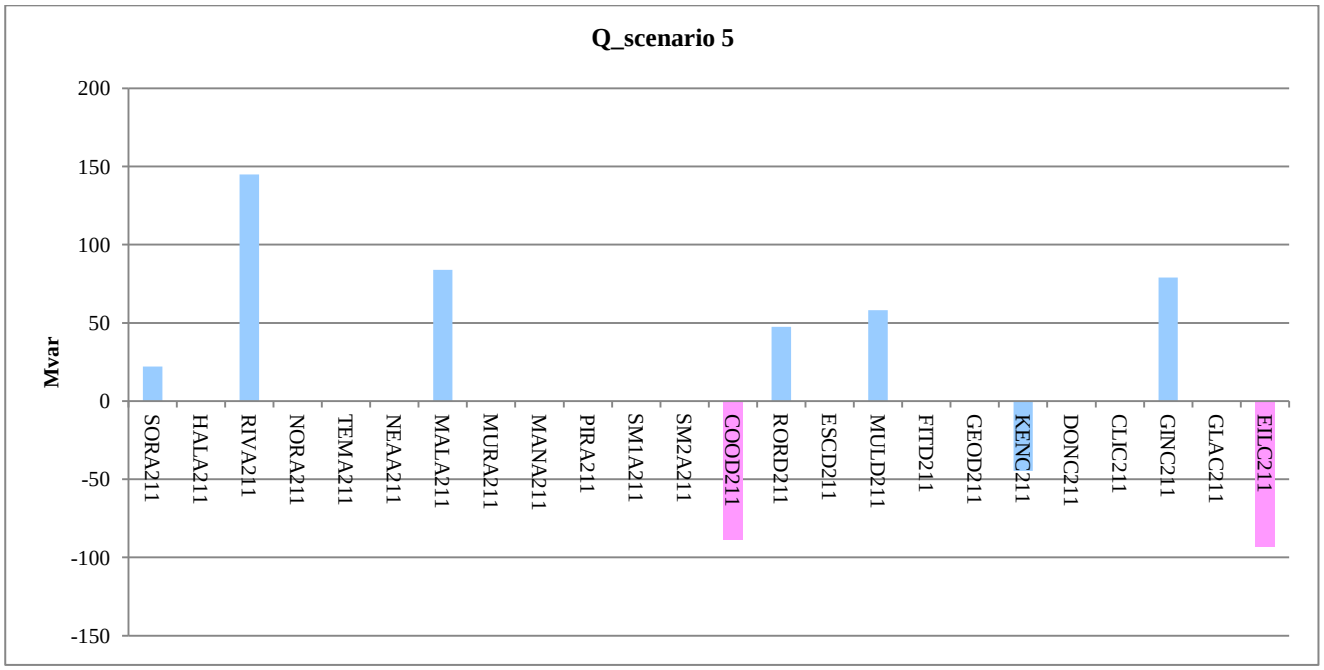

CHAPTER 8
IRISH GRID: SIMULATION RESULTS

The analysis conducted on the test grid have put in evidence what can be the behaviour of a grid to the reactive problem in different scenarios. Now we will look at a real grid, which is the Irish Grid, shown in Fig. 8.9. Considering only the onshore grid, it results that the grid not need to install reactive. For this grid six scenario have been considered, describing the whole year. in particular, the variation of the offshore wind generation has been point out in Fig. 8.1 , comparing it to the demand.

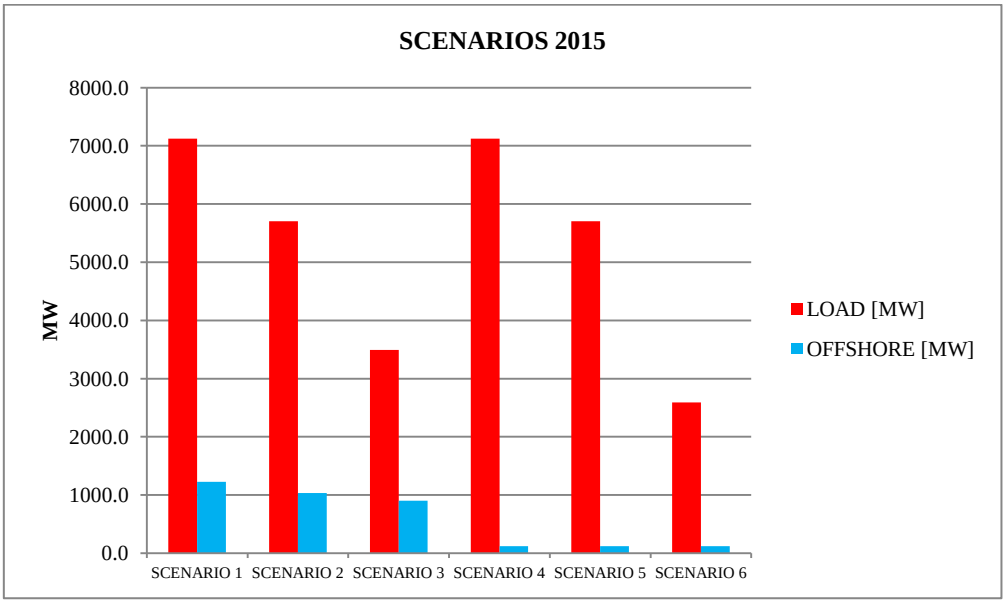

Fig. 8.1: Scenarios for year 2015: load and offshore wind

The offshore wind generation has considered decreasing while the load represents the winter peak for scenario 1and 4. Scenario 2 and 5 are the summer peaks, whilst scenario 3 and 6 are summer valley. The other types of generation are taken into account in Table 8.1, from which it can be seen that the first three scenarios are characterized by quite high wind, whereas the other are with low wind, it has been assumed a 10 % of the wind of the scenario 1, requiring the conventional generation supply wholly the demand.

	LOAD [MW]	OFFSHORE [MW]	ONSHORE [MW]	THERMIC [MW]
SCENARIO 1	7125.4	1224.2	4335.0	1566.2
SCENARIO 2	5705.9	1030.8	2610.8	2064.3
SCENARIO 3	3494.9	901.0	2182.2	411.7
SCENARIO 4	7125.4	122.4	433.5	6569.5
SCENARIO 5	5705.9	122.4	433.5	5150.0
SCENARIO 6	2587.7	122.4	433.5	2031.8

Table. 8.1: Six scenarios for 2015

Graphically, the correspondent generation is shown in Fig,8.2:

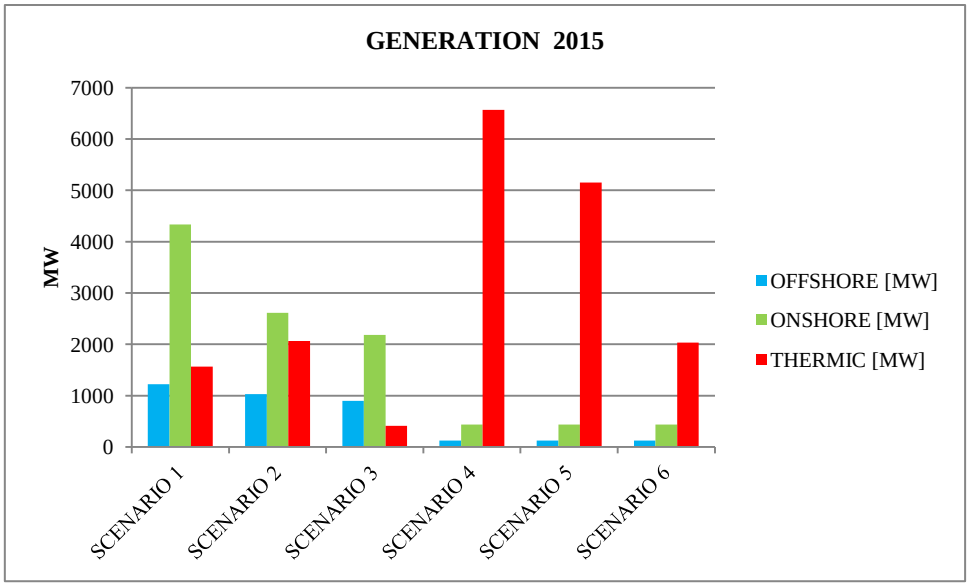

Fig. 8.2: Generation type for the different scenario

We will consider two of these six scenario and precisely those with an opposite generation condition and same demand: scenario 1 and 4. For the two of them let's report the starting point of generation, for the different typology and the relative load. The objective function is made of the gain cost, Fig 8.3, coming from the export toward the close country and the var cost installation, Fig 8.4. In this case the redipstching costs are equal to zero since the program has modified the generation in order that the increase costs are balanced by the decrease costs.

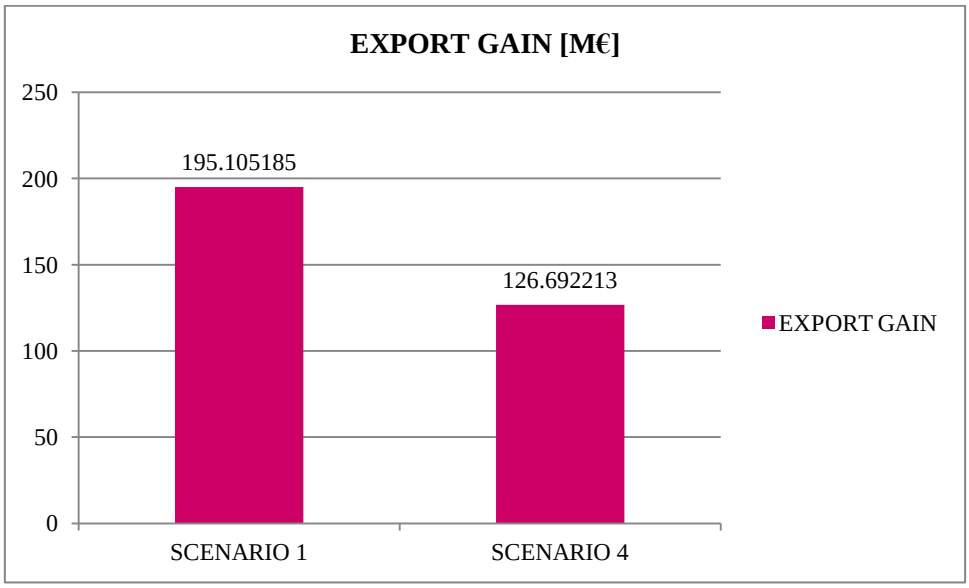

Fig. 8.3: Load/Generation starting point for scenario 4

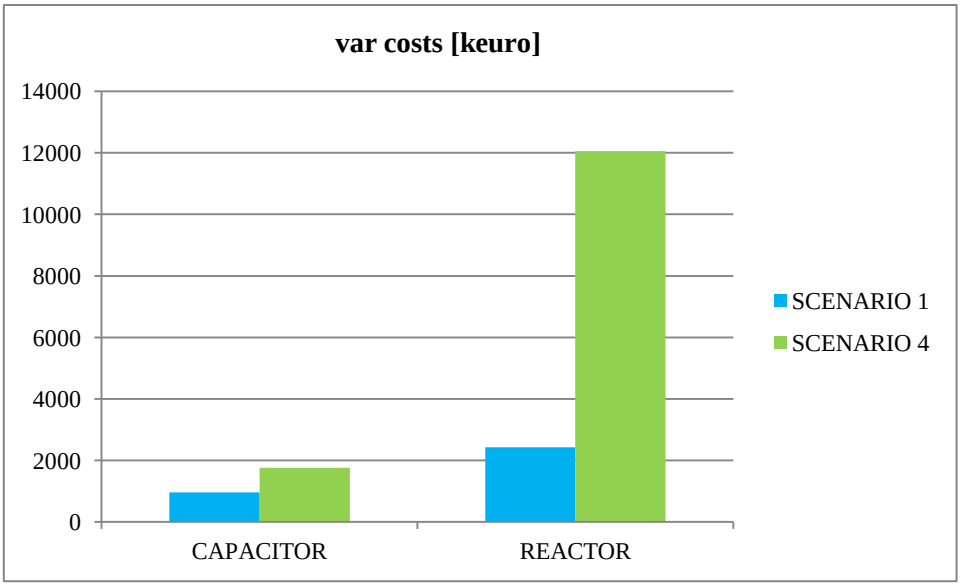

Fig. 8.4: Load/Generation starting point for scenario 4

What results in term of modification of the generation and of export is plotted in Fig. 8.5.

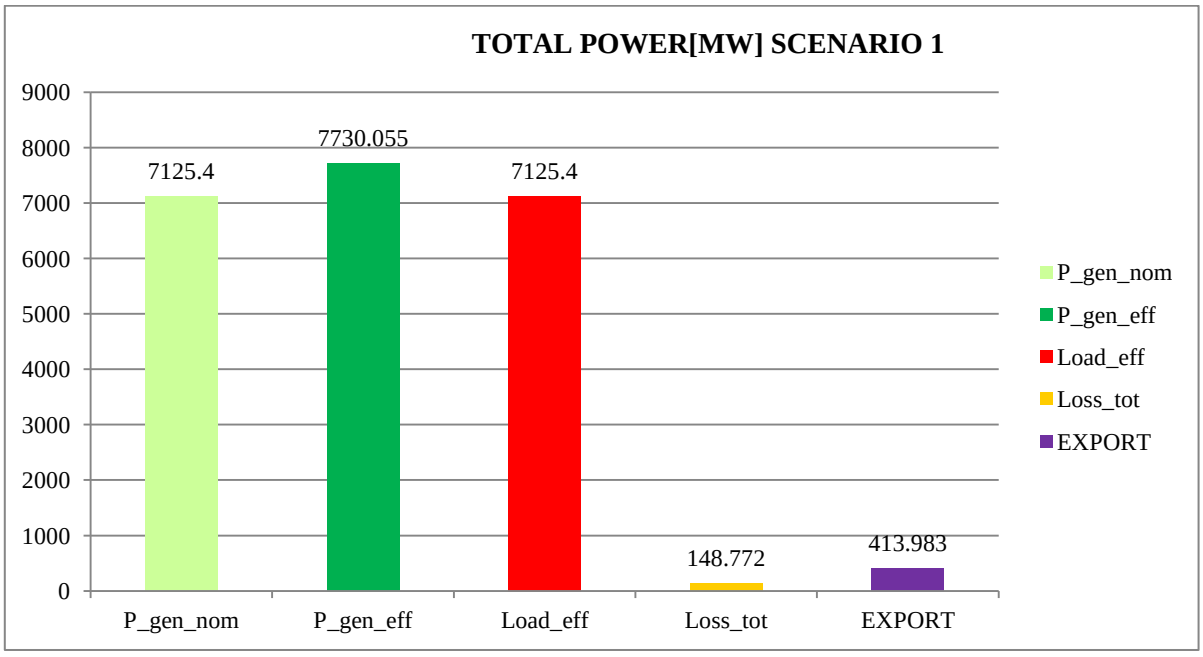

Fig. 8.5: Power Balance for scenario 1

Zooming on the generated power, Fig. 8.6, we want to put on evidence how each generation type has been modified to cope with the losses and to supply the demand.

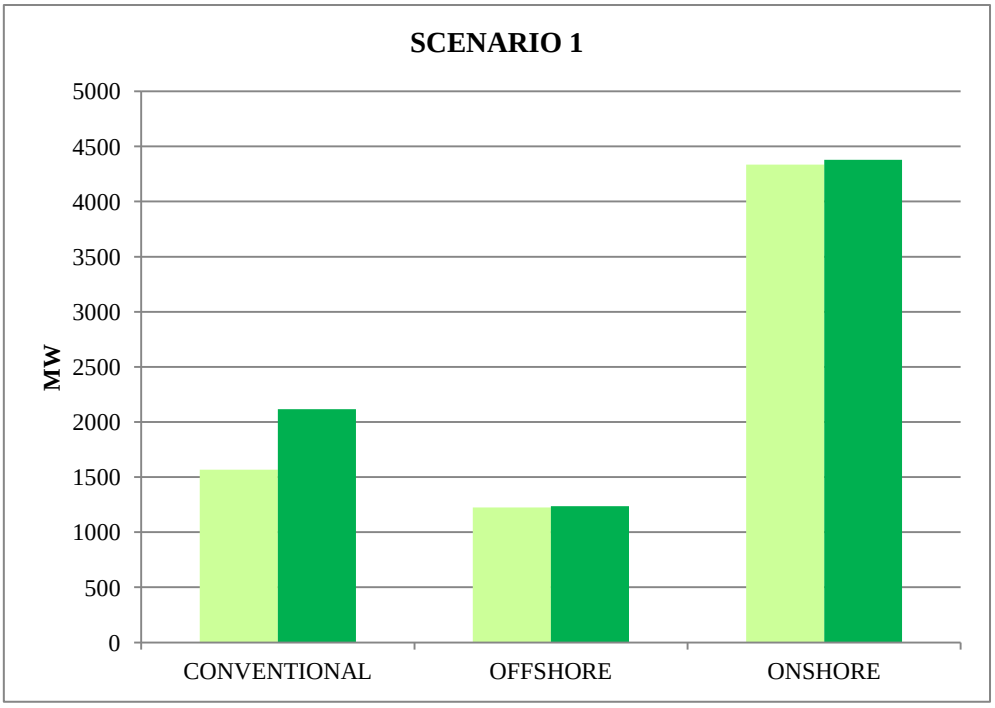

Fig. 8.6: Generation type for scenario 1 before and after optimization

The same results have been shown in Fig 8.7 and Fig. 8.8, for the scenario 4.

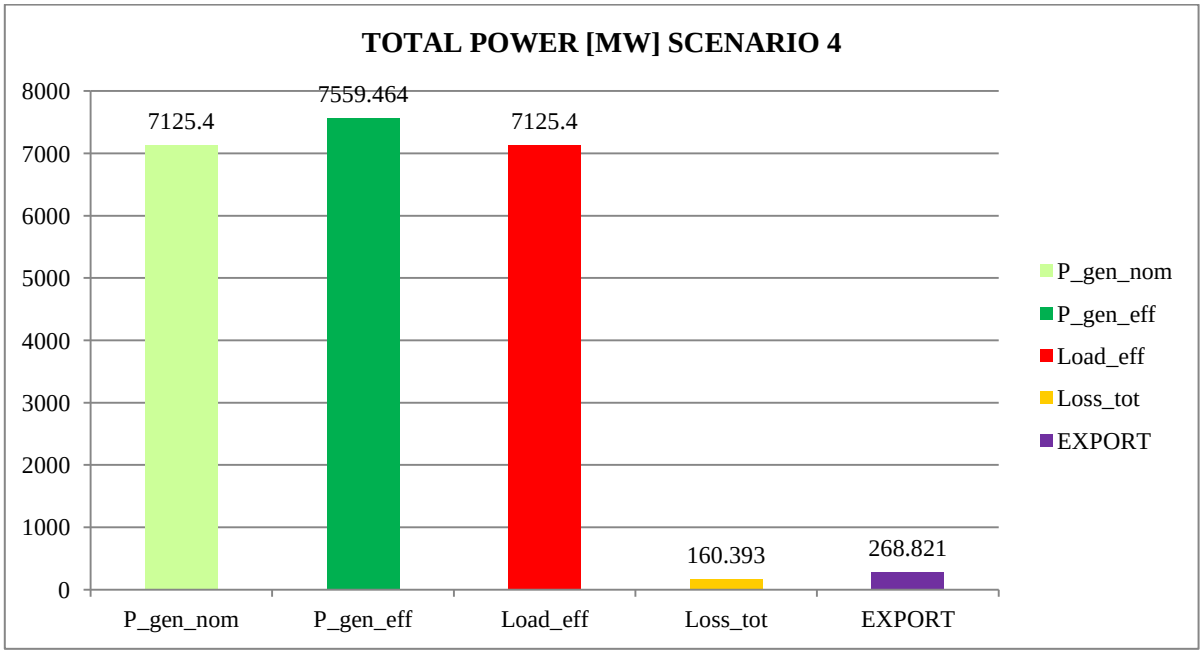

Fig. 8.7 : Power Balance for scenario 4

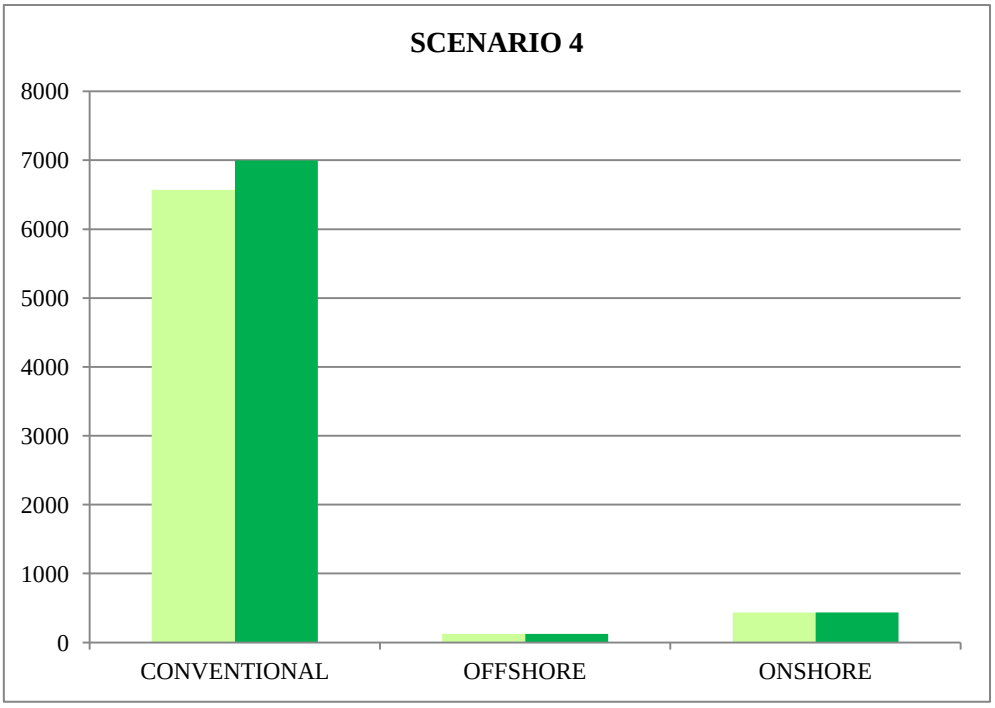

Fig. 8.8: Generation type for scenario 4 before and after optimization

The results are shown in Fig 8.10- 8.13 where we can notice a strongly increase of the reactors installed for the scenario 4, since the major generation source is the conventional while the wind is kept low. The result show hoe the program install the most of the reactive support in that area where there is a plenty of cables.

CHAPTER 9
CONCLUSION AND FUTURE WORKS

The analysis on the reactive problem for a mixed AC/DC topology of grid is a issue with which this thesis has tried to deal, though there are numerous aspects that would need of further development.

At now, an AC optimal power flow which is able to manage a general purpose transmission grid has been implemented and a continuous approach has been considered in modeling the var support. The algorithm has been successfully applied on a test system as a single as well multiple load/generation scenarios and a preliminary investigation has been also performed on an Irish transmission System of 2015 using ESPAUT results. Form a mathematical point of view, the computational speed has been in the range of 10 min for test system and 30 min for ITS system. The algorithm is very effective for a technical and economically estimation of the var resources needs and the mutual interaction between different technologies.

However, some weaknesses have been found in the SOLVER when dealing with multiple scenarios for both test and real system. Therefore, further investigation have to be conducted on this aspect.

The first step is to enable the present algorithm to deal with discrete variable; this is aiming at give a more realistic description of the standard size of the var sources available. This would mean to have a MINLP model and, in such a kind of analysis, a various range of optimal option solutions. Moreover, the solver robustness is a key point and to be able to test several solvers, it is worth to investigate a polynomial approximation of the trigonometric functions.

Referring to the constraints, it is paramount to implement the contingency analysis by examining a deterministic list of transmission connections and var sources.

An important model enhancement is the implementation of the storage devices, in particular to evaluate the impact when larger and larger variables resources will penetrate into the transmission grid.

APPENDIX A

GAMS/LINDOGlobal

The maximum size for this problem is 3000 variables and 2000 constraints. This solver finds guaranteed optimal solutions to general nonlinear problems with continuous and/or discrete variables in 80% of cases. Its procedure (GOP) employs branch-and-cut methods to break an NLP model down a list of subproblems. Each subproblem is analyzed and either

- is shown to not have a feasible or optimal solution, or,
- an optimal solution to the subproblem is found, or,
- the suproblem is further split into two or more subproblems which are then placed on the list

LINDOGlobal supports most nonlinear functions(cos, sin, abs)in global mode, in fact it can automatically linearize a number of nonlinear relationships, through the addition of constraints and integer variables, so the transformed linearized model is mathematically equivalent to the original nonlinear model. The drawback is these. GAMS/LINDOGlobal finds guaranteed globally optimal solutions to general nonlinear problems with continuous and/or discrete variables. Most mathematical functions are supported, including functions that are non-smooth, such as absolute value. Trigonometric function are Nonlinear solvers employing methods like successive linear programming (SLP) or generalized reduced gradient (GRG) return a local optimal solution to an NLP problem, as has been described in chapter 4. However, many practical nonlinear models are non-convex and have more than one local optimal solution. In some applications, the user may want to find a global optimal solution. The LINDOglobal optimization procedure (GOP) employs branch-and-cut methods to break an NLP model down into a list of sub-problems. Each sub-problem is analyzed and either a) is shown to not have a feasible or optimal solution, or b) an optimal solution to the sub-problem is found, e.g., because the sub-problem is shown to be convex, or c) the sub-problem is further split into two or more sub-problems which are then placed on the list. Given appropriate tolerances, after a finite, though possibly large number of steps a solution provably global optimal to tolerances is returned. This solver can automatically linearize a number of nonlinear relationships, such as max(x,y), through the addition of constraints and integer variables, so the transformed linearized model is mathematically equivalent to the original nonlinear model. Keep in mind, however, that each of these strategies will require additional computation time. Thus, formulating models, so they are convex and contain a single extremum, is desirable.In order to decrease required computing power and time it is also possible to disable the global solver and use GAMS/LINDOGlobal like a regular nonlinear solver. LINDOGlobal 2 GAMS/LINDOGlobal has a multistart feature that restarts the standard (non-global) nonlinear solver from a number of intelligently generated points. This allows the solver to _nd a number of locally optimal points and report the best one found. This alternative can be used when global optimization is costly. A user adjustable parameter controls the maximum number of multistarts to be performed.

BARON

(12)The Branch-And-Reduce Optimization Navigator (BARON) is a GAMS solver for the global solution of nonlinear (NLP) and mixed-integer nonlinear programs (MINLP).While traditional NLP and MINLP algorithms are guaranteed to converge only under certain convexity assumptions, BARON implements deterministic global optimization algorithms of the branch-and-bound type that are guaranteed to provide global optima under fairly general assumptions. These include the availability of finite lower and upper bounds on the variables and their expressions in the NLP or MINLP to be solved. BARON implements algorithms of the branch-and-bound type enhanced with a variety of constraint propagation and duality techniques for reducing ranges of variables in the course of the algorithm.

GAMS/BARON can handle nonlinear functions that involve exponential, logarithm and absolute value. Currently, there is no support for other functions, including the trigonometric functions sin(x), cos(x).

APPENDIX B

To calculate the per unit value of the circuital parameters, a power reference A_{ref} has been chosen as 100 MVA; the resulting p.u. value for indistinguishably R,X or C is obtained by the following expression:

$$t = \frac{T \cdot L}{Z_{ref}} = \frac{T \cdot L \cdot A_{ref}}{{V_{nom}}^2}$$

Where T is the general variable L is the length of the line and V_{nom} its reference voltage. The p.u. unite value will be referred to not capital letters.

To implement the power flow equations, we need to calculate the admittance matrix of the network, stargin from the admittance for the single links Y_s:

$$\bar{Y} = \frac{1}{\bar{Z}} = \frac{1}{r + jx} \cdot \frac{r - jx}{r - jx} = \frac{r - jx}{r^2 + x^2} = \frac{r}{r^2 + x^2} - j\frac{x}{r^2 + x^2}$$

Where the real (r) and imaginary parts (i) are respectively:

$$Y_{tt\_r} = Re(Y) = \frac{r}{r^2 + x^2}$$

$$Y_{tt\_i} = Im(Y) + \frac{B_c}{2} = \frac{-x}{r^2 + x^2} + \frac{B_c}{2}$$

These are the parameters that will be used inside the power flow equation in the case of link.

HVAC TRANSMISSION LINE:TRANSFORMER

Transformers have been modeled only by the inductive series parameters and by the tap for OLTC transformers or off-nominal turns ratio τ. Furthermore, the losses and magnetizing admittance of the two-winding converter transformers are ignored. This turns ratio τ has been considered as a constant and appears into the initial data, if any transformer is in the network. The modification of the real and imaginary part of the admittance parameter is:

$$Y_{ff\_r} = \left(\frac{r}{r^2 + x^2}\right) : \tau^2$$

$$Y_{ff\_i} = \left(\frac{-x}{r^2 + x^2} + \frac{b}{2}\right) : \tau^2$$

To take into account phase shift transformer (PST) ,the shift angle θ_{shift} is introduced into the parameters:

$$Y_{ft\_r} = -\frac{r}{r^2 + x^2} \cdot cos(\theta_{\text{shift}}) - \frac{-x}{r^2 + x^2}\frac{1}{\tau} \cdot sin(\theta_{\text{shift}})$$

$$Y_{ft\_i} = \frac{r}{r^2 + x^2}\frac{1}{\tau} \cdot sin(\theta_{\text{shift}}) - \frac{-x}{r^2 + x^2} \cdot cos(\theta_{\text{shift}})$$

$$Y_{tf\_r} = -\frac{r}{r^2 + x^2} \cdot cos(\theta_{\text{shift}}) + \frac{-x}{r^2 + x^2}\frac{1}{\tau} \cdot sin(\theta_{\text{shift}})$$

$$Y_{tf\_i} = -\frac{r}{r^2 + x^2}\frac{1}{\tau} \cdot sin(\theta_{\text{shift}}) - \frac{-x}{r^2 + x^2} \cdot cos(\theta_{\text{shift}})$$

This device allows to control the real power flow. In our model, if any, it will be modelled ad fixed.

Considering each branch *k* of the grid, as depicted in fig.6.1, E_{fk} and E_{tk} are respectively the voltages at the extreme bus, "from" bus and at "to" bus.

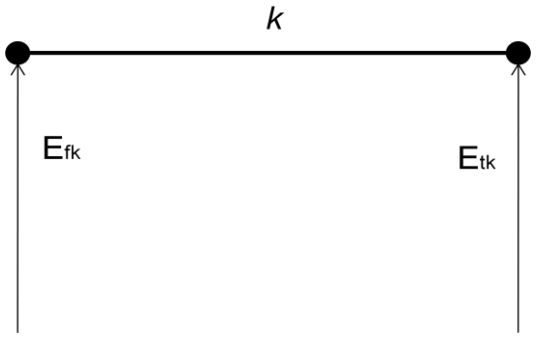

Fig. 11: Branch element

The relationship between the voltages and the current injection at the extreme busses is expressed in matrix form as:

$$\begin{bmatrix} I_{fk} \\ I_{tk} \end{bmatrix} = Y_{ftk} \cdot \begin{bmatrix} E_{fk} \\ E_{tk} \end{bmatrix} = \begin{bmatrix} Y_{ff} & Y_{ft} \\ Y_{tf} & Y_{tt} \end{bmatrix} \cdot \begin{bmatrix} E_{fk} \\ E_{tk} \end{bmatrix}$$

Explaining the matrix terminals for one general branch, this can be also a transformer, results:

$$Y_{ftk} = \begin{bmatrix} Y_{ff} & Y_{ft} \\ Y_{tf} & Y_{tt} \end{bmatrix} = \begin{bmatrix} \left(Y_s + j\frac{B_c}{2}\right)\frac{1}{\tau^2} & -Y_s\frac{1}{\tau e^{j\theta}_{\text{shift}}} \\ -Y_s\frac{1}{\tau e^{-j\theta}_{\text{shift}}} & \left(Y_s + j\frac{B_c}{2}\right) \end{bmatrix}$$

ADMITTANCE MATRIX

The admittance matrix let have the injection of current into each bus of the grid. The real part of the diagonal element for all the bus is the sum of all the admittance parameter for that bus k:

$$Y_{kkr}(fbus, fbus) = Y_{k,shr} + \sum_{(f,t,c)\in T: f=k} Y_{ffr} + \sum_{(f,t,c)\in B: t=k} Y_{ttr}$$

While the imaginary part:

$$Y_{kki}(fbus, fbus) = Y_{k,shi} + \sum_{(f,t,c)\in T: f=k} Y_{ffi} + \sum_{(f,t,c)\in B: t=k} Y_{tti}$$

Where the real part of the off diagonal element for all the bus is:

$$Y_{kmr}(fbus, tbus) = \sum_{(f,t,c)\in B: f=k, t=m} Y_{ftr} + \sum_{(f,t,c)\in B: f=k, t=m} Y_{tfr}$$

And the imaginary part:

$$Y_{kmi}(fbus, tbus) = \sum_{(f,t,c)\in B: f=k, t=m} Y_{fti} + \sum_{(f,t,c)\in B: f=k, t=m} Y_{tfi}$$

Bibliography

1. **J. Moccia, A.Arapogianni.** *Pure Power:Wind energy targets for 2020 and 2030.* EWEA 2011.

2. **P. Bresesti, Member, IEEE, Wil L. Kling, Member, IEEE, R. Vailati.** *Transmission Expansion Issues for Offshore Wind Farms Integration in Europe.* s.l. : IEEE, 2008.

3. **Eirgrid.** *Eirgrid plc Annual Report: Securing Irelnd's Electricity Supply* . 2010.

4. **M. Norton, A. Mansoldo, A. Rivera.** *Offshore grid Study :Analusis of the appropriate Architecture of an Irish Offshore Network.* 2011.

5. **ABB.** *Enabling the power wind -HVDC Light for large-scale offshore wind integration.*

6. **A. sode-Yome, N. Mithulananthan.** Comparison of shunt capaccitor, SVC and STATCOM in static voltage stability margin enhancement. *International Journal of electrical engineering Education 41/2.*

7. **W. Zhang, F. Li, L. M. Tolbert.** *Reviwe or Reactive Power Planning: Objectives, Constaints and Algorithms.* 2007.

8. **D. Chattopadhyay, B Chakrabarti.** *Voltage stability constrained Var planning:Model simplification using statistical approximation.* 2002.

9. **W. Zhang, L.M. Tolbert.** *Servey of Reacive PowerPlanning Methods.* s.l. : IEEE, 2005. p. 11.

10. **C. Barker, C.Davidson, J.Gold.** *HVDC Connecting to the future.* s.l. : Alstom Grid, 2010.

11. *EirGrid Grid Code.* March 2011.

12. **N. Sahinidis, M. Tawarmalani.** *Baron.* 2011.